FINAL REPORT

North Carolina Department of Transportation
Research Project No. 2011-06

Durability of Lightweight Concrete Bridge Decks – Field Evaluation

By

Tara Cavalline, Ph.D., P.E.
Assistant Professor

Amy Kitts, P.E.
Faculty Associate

Jeremy Calamusa
Graduate Research Assistant

Department of Engineering Technology and Construction Management
University of North Carolina at Charlotte
9201 University City Boulevard
Charlotte, NC 28223

February 15, 2013

Technical Report Documentation Page

1. Report No. FHWA/NC/2011-06	2. Government Accession No.	3. Recipient's Catalog No.
4. Title and Subtitle Durability of Lightweight Concrete Bridge Decks – Field Evaluation		5. Report Date February 15, 2013 6. Performing Organization Code
7. Author(s) Tara L. Cavalline, Ph.D., P.E., Amy M. Kitts, P.E., Jeremy Calamusa		8. Performing Organization Report No.
9. Performing Organization Name and Address Department of Engineering Technology and Construction Management University of North Carolina at Charlotte 9201 University City Blvd. Charlotte, NC 28223		Work Unit No. (TRAIS) Contract or Grant No.
Sponsoring Agency Name and Address North Carolina Department of Transportation Research and Analysis Group 1 South Wilmington Street Raleigh, North Carolina 27601		Type of Report and Period Covered Final Report August 15, 2010 – October 31, 2012 Sponsoring Agency Code FHWA/NC/2011-06
Supplementary Notes:		

Abstract

The North Carolina Department of Transportation (NCDOT) has constructed a number of concrete bridge decks using lightweight aggregate, with construction of the first lightweight concrete bridge deck completed approximately 40 years ago. Use of lightweight concrete in bridge decks can significantly reduce the deadload of the structure, allowing for longer spans and reduced sizes of other structural members. Some research has suggested that use of lightweight concrete in bridge decks can offer advantages in addition to those directly related to the reduced weight. These possible advantages included reduced cracking tendency and lower permeability. If this is true, enhanced durability performance could result in lightweight concrete bridge decks being a more economical choice than normalweight concrete bridge decks for some applications. In this study, field evaluations were performed on bridge decks constructed of both normalweight and lightweight concrete. For each lightweight concrete bridge deck selected for inclusion in this study, a companion normalweight bridge deck of similar age, traffic loading, and environmental exposure was selected. Field evaluations included visual surveys and several field tests. Using the results of the field evaluations and testing, along with laboratory testing or concrete core samples and powder samples, the field performance of the lightweight concrete bridge decks was evaluated and compared to the performance of the normalweight concrete bridge decks.

Although some differences in the performance of lightweight and normalweight concrete bridge decks were observed in field and laboratory tests, a distinct difference between the overall durability performance of lightweight bridge decks and normalweight bridge decks included in this study was not readily evident. This finding differs from those of a number of studies that have indicated that lightweight concrete can provide enhanced durability performance, and therefore, additional laboratory-based studies of lightweight and normalweight concrete bridge deck mixtures using local materials are recommended. Damages induced by factors such as structural characteristics and external loads may have played a significant role in observed distresses, as well as in results of field and laboratory tests. Additionally, it is possible that that there has not been ample time for distinct differences in performance between lightweight and normalweight concrete decks included in this study to become evident during field observations, or measurable during field or laboratory tests. Regional trends in performance were observed for some durability tests, however, and this information could be utilized by NCDOT.

Key Words *Concrete, bridge decks, lightweight concrete, portland cement, lightweight aggregates, durability*	Distribution Statement		
Security Classif. (of this report) Unclassified	Security Classif. (of this page) Unclassified	No. of Pages 242	Price

Form DOT F 1700.7 (8-72) **Reproduction of completed page authorized**

DISCLAIMER

The contents of this report reflect the views of the author(s) and not necessarily the views of the University. The author(s) are responsible for the facts and the accuracy of the data presented herein. The contents do not necessarily reflect the official views or policies of either the North Carolina Department of Transportation or the Federal Highway Administration at the time of publication. This report does not constitute a standard, specification, or regulation.

ACKNOWLEDGMENTS

The research personnel involved in this study would like to express their appreciation to the following for their guidance and assistance with this research project:

- The NCDOT personnel serving on the Technical Advisory Committee for this research study. In particular, we would like to thank Mr. Daniel D. Holderman, P.E., Mr. V. Owen Cordle, P.E., and Mr. Henry Black, P.E. for assistance in selecting bridges for inclusion in this study, input on field and laboratory test methods, and obtaining background information useful in the evaluation.

- NCDOT Research and Development personnel, particularly Dr. Mrinmay Biswas, P.E., Mr. Neal Galehouse, P.E., and Mr. Mustan Kadibhai, P.E. for support for the project.

- Mr. Bill Moyers, P.E. of Volkert Engineering for coordinating field services including traffic control and sample removal.

- Volkert Engineering personnel, especially Mr. Ricky Williams, Mr. Jerry Linder, Mr. Roger Bowers, and Mr. Richard Hinton for their assistance with field services.

- Mr. Devin Secore, Mr. Michael Greenwood, and Mr. Josh Ramsey, UNC Charlotte Undergraduate Research Assistants

- Mr. Mario Paredes, P.E. of Florida Department of Transportation, Dr. Tyson Rupnow, P.E. of the Louisiana Transportation Research Center, and Dr. Pratanu Ghosh and Ms. Shannon Hanson of the University of Utah for input on the surface resistivity meter.

- Mr. Bill Lindsey, Laboratory Manager, and Mr. Mike Moss, Research Operations Manager at UNC Charlotte College of Engineering.

- Dr. Brett Tempest and Dr. Janos Gergely, UNC Charlotte Department of Civil Engineering, for insight regarding chloride content and diffusion coefficient testing, and for allowing us to use analysis programs developed as part of NCDOT Project HWY-2004-12, "Concrete Diffusion Coefficients and Existing Chloride Exposure in North Carolina," for this work.

- Dr. Thomas Nicholas II, UNC Charlotte Department of Engineering Technology and Construction Management, for input regarding bridge design and construction.

- Dr. John Diemer, UNC Charlotte Department of Geography and Earth Sciences, for insight on natural aggregates observed during petrographic analysis.

EXECUTIVE SUMMARY

Lightweight aggregate is commonly manufactured by heating clay, shale, slate, or slag in a kiln, causing expansion of trapped gasses and subsequent formation of a porous void system within the aggregate particles. In lightweight concrete mixtures, normalweight aggregate is replaced with lightweight aggregate. Structural lightweight concrete mixtures typically include lightweight coarse aggregate with either normalweight or lightweight fine aggregate. Most lightweight concrete used for structural purposes has an equilibrium density between 105 and 120 pounds per cubic foot, which is up to 30% lighter than normalweight concrete. The North Carolina Department of Transportation (NCDOT) has constructed a number of concrete bridge decks using lightweight aggregate, with construction of the first lightweight concrete bridge deck completed approximately 40 years ago.

Use of lightweight concrete in bridge decks can significantly reduce the deadload of the structure, allowing for longer spans and reduced sizes of other structural members. Some research has suggested that use of lightweight concrete in bridge decks can offer advantages in addition to those directly related to the reduced weight. These possible advantages include reduced cracking tendency and lower permeability. If this is true, enhanced durability performance could result in lightweight concrete bridge decks being a more economical choice than normalweight concrete bridge decks for some applications.

The purpose of this study was to evaluate the field performance of lightweight concrete bridge decks, comparing to normalweight concrete in the same structure or environment. Field evaluations were performed on bridge decks constructed of both normalweight and lightweight concrete. For each lightweight concrete bridge deck selected for inclusion in this study, a companion normalweight bridge deck of similar age, traffic loading, and environmental exposure was selected. Field evaluations included visual surveys and several field tests. Using the results of the field evaluations and testing, along with laboratory testing or concrete core samples and powder samples, the field performance of the lightweight concrete bridge decks was evaluated and compared to the performance of the normalweight concrete bridge decks.

Although some differences in the performance of lightweight and normalweight concrete bridge decks were observed in field and laboratory tests, a distinct difference between the overall durability performance of lightweight bridge decks and normalweight bridge decks included in this study was not readily evident. This finding differs from those of a number of studies that have indicated that lightweight concrete can provide enhanced durability performance, and therefore, additional laboratory-based studies of lightweight and normalweight concrete bridge deck mixtures using local materials are recommended. Damages induced by factors such as structural characteristics and external loads may have played a significant role in observed distresses, as well as in the results of field and laboratory tests. Additionally, it is possible that that there has not been ample time for distinct differences in performance between lightweight and normalweight concrete decks included in this study to become evident during field observations, or measurable during field or laboratory tests. Regional trends in performance were observed for some durability tests, however, and this information could be utilized by NCDOT.

Some findings of this study could be used to assist NCDOT in making decisions regarding use of lightweight concrete for bridge decks in certain regions of North Carolina. Information on surface chloride contents and diffusion of chlorides into bridge decks included in this study can be used to assist with decisions regarding use of deicers, and potentially, with maintenance and repair decisions. Several bridge decks had some locations where chloride contents exceeded the replacement level and/or the corrosion threshold, and this information could be useful in planning for repair and/or replacement of these decks. As the role of conductivity (and its inverse, surface resistivity) in durability performance becomes better understood, surface resistivity measurements obtained during this study may provide insight into durability performance of North Carolina bridge deck mixtures. Additional field and laboratory-based work is suggested to help NCDOT with decisions regarding bridge deck mixtures and test methods that can provide insight into the durability performance of concrete.

TABLE OF CONTENTS

DISCLAIMER iii
ACKNOWLEDGEMENTS iv
EXECUTIVE SUMMARY v
LIST OF TABLES viii
LIST OF FIGURES xi
LIST OF ABBREVIATIONS xvii

1. INTRODUCTION AND RESEARCH OBJECTIVES 1
    1.1 Introduction 1
    1.2 Research Objectives 1

2. LITERATURE REVIEW AND BACKGROUND INFORMATION 2
    2.1 Literature Review 2
        2.1.1 Durability of Concrete Bridge Decks 2
        2.1.2 Cracking of Concrete Bridge Decks 3
            2.1.2.1 Bridge Design Factors Related to Cracking 4
            2.1.2.2 Mixture Design Factors Related to Cracking 5
            2.1.2.3 Material Characteristics Related to Cracking
            2.1.2.4 Placing, Finishing, and Curing Practices That Contribute to Cracking 6
        2.1.3 Background Information on Selected Concrete Characteristics and Test Methods 6
            2.1.3.1 Surface Resistivity 6
            2.1.3.2 Sorptivity and Permeability 7
            2.1.3.3 Dynamic Modulus of Elasticity 9
    2.2 Background and Supporting Information Provided by NCDOT 9
        2.2.1 Inspection Reports and Drawings 9
    2.2.2 Concrete Mixtures 9

3. PROCEDURES 11
    3.1 Identification of Bridge Decks 11
    3.2 Field Evaluations and Testing 13
        3.2.1 Visual Survey 13
        3.2.2 Location Selection and Removal of Cores and Powder Samples 13
        3.2.3 Air and Water Permeability Tests 15
        3.2.4 Surface Resistivity Tests 16
        3.2.5 Rebound Hammer Tests 17
    3.3 Laboratory Testing 17
        3.3.1 Density and Moisture Content 18
        3.3.2 Compressive Strength 18
        3.3.3 Dynamic Modulus 18
        3.3.4 Sorptivity 19
        3.3.5 Rapid Chloride Test (RCT) 20
        3.3.6 Rapid Chloride Permeability Test (RCPT) 21
        3.3.7 Petrographic Examinations 23

4. RESULTS OF FIELD SURVEY AND FIELD TESTING 25
    4.1 Visual Survey 25
    4.2 Air and Water Permeability Tests 30
    4.3 Surface Resistivity Tests 34
    4.4 Rebound Hammer Tests 38

5. RESULTS OF LABORATORY TESTING 40
5.1 Unit Weight and Moisture Content 40
5.2 Compressive Strength 41
5.3 Dynamic Modulus 42
5.4 Sorptivity 43
5.5 Rapid Chloride Test (RCT) 52
5.6 Rapid Chloride Permeability Test (RCPT) 57
5.7 Statistical Analysis of Results 62
5.8 Petrographic Examinations 64

6. FINDINGS AND CONCLUSIONS 66

7. RECOMMENDATIONS 70

8. IMPLEMENTATION AND TECHNOLOGY TRANSFER PLAN 72

9. REFERENCES 75

APPENDIX A – Visual Survey Results 80
APPENDIX B – Air and Water Permeability Test Data and Results 97
APPENDIX C – Surface Resistivity Test Data and Results 114
APPENDIX D – Macroscopic Observations of Concrete Core Samples 131
APPENDIX E – Compressive Strength Test Data and Results 140
APPENDIX F – Dynamic Modulus Test Data and Results 142
APPENDIX G – Sorptivity Test Data and Results 144
APPENDIX H – Rapid Chloride Test (RCT) Data and Results 161
APPENDIX I – Petrographic Examination Results 194

LIST OF TABLES

Table 3-1:	Bridge decks included in this study.	11
Table 3-2:	Superstructures of bridges included in this study.	12
Table 4-1:	Values for air calculated AER and WAR for concrete of varying protective quality for embedded reinforcement (from NDT James Instruments 2007 and Figg 1989).	30
Table 4-2:	Average Air Exclusion Rates (AER) and average Water Absorption Rates (WAR).	31
Table 4-3:	Average temperature-corrected surface resistivity readings by test location.	35
Table 4-4:	Average corrected surface resistivity readings.	36
Table 4-5:	Average rebound numbers for test locations.	39
Table 5-1:	Average moisture contents and average apparent densities.	40
Table 5-2:	Average adjusted compressive strengths.	41
Table 5-3:	Dynamic modulus test results.	43
Table 5-4:	Average initial absorption and average secondary absorption rates for ASTM C1585 capillary suction tests and ponding tests.	46
Table 5-5:	Chloride contents exceeding corrosion threshold and replacement level at 2 in depth.	53
Table 5-6:	Chloride contents exceeding corrosion threshold and replacement level at 1 in depth.	54
Table 5-7:	Surface chloride concentrations and diffusion coefficients.	55
Table 5-8:	Chloride ion penetrability based on charge passed (according to ASTM C1202).	57
Table 5-9:	Description of RCPT test specimens and test results.	59
Table 5-10:	Average total charge passed (coulombs) for RCPT tests.	60
Table 5-11:	Results of Wilcoxon matched pairs tests.	63
Table B-1:	Air permeability and water permeability test results for bridge deck 1N.	98
Table B-2:	Air permeability and water permeability test results for bridge deck 1L.	99
Table B-3:	Air permeability and water permeability test results for bridge deck 2N.	100
Table B-4:	Air permeability and water permeability test results for bridge deck 2L.	101
Table B-5:	Air permeability and water permeability test results for bridge deck 3N.	102
Table B-6:	Air permeability and water permeability test results for bridge deck 3L.	103
Table B-7:	Air permeability and water permeability test results for bridge deck 5N.	104
Table B-8:	Air permeability and water permeability test results for bridge deck 5L.	105
Table B-9:	Air permeability and water permeability test results for bridge deck 6N.	106
Table B-10:	Air permeability and water permeability test results for bridge deck 6L.	107
Table B-11:	Air permeability and water permeability test results for bridge deck 7N.	108
Table B-12:	Air permeability and water permeability test results for bridge deck 7L.	109
Table B-13:	Air permeability and water permeability test results for bridge deck 8N.	110
Table B-14:	Air permeability and water permeability test results for bridge deck 8L.	111
Table B-15:	Air permeability and water permeability test results for bridge deck 9N.	112
Table B-16:	Air permeability and water permeability test results for bridge deck 9L.	113
Table C-1:	Surface resistivity test results for bridge deck 1N.	115
Table C-2:	Surface resistivity test results for bridge deck 1L.	116
Table C-3:	Surface resistivity test results for bridge deck 2N.	117
Table C-4:	Surface resistivity test results for bridge deck 2L.	118
Table C-5:	Surface resistivity test results for bridge deck 3N.	119
Table C-6:	Surface resistivity test results for bridge deck 3L.	120
Table C-7:	Surface resistivity test results for bridge deck 5N.	121
Table C-8:	Surface resistivity test results for bridge deck 5L.	122
Table C-9:	Surface resistivity test results for bridge deck 6N.	123
Table C-10:	Surface resistivity test results for bridge deck 6L.	124
Table C-11:	Surface resistivity test results for bridge deck 7N.	125
Table C-12:	Surface resistivity test results for bridge deck 7L.	126
Table C-13:	Surface resistivity test results for bridge deck 8N.	127

LIST OF TABLES (CON'T)

Table C-14:	Surface resistivity test results for bridge deck 8L.	128
Table C-15:	Surface resistivity test results for bridge deck 9N.	129
Table C-16:	Surface resistivity test results for bridge deck 9L.	130
Table D-1:	Macroscopic observations of concrete core samples from bridge deck 1N.	132
Table D-2:	Macroscopic observations of concrete core samples from bridge deck 1L.	132
Table D-3:	Macroscopic observations of concrete core samples from bridge deck 2N.	133
Table D-4:	Macroscopic observations of concrete core samples from bridge deck 2L.	133
Table D-5:	Macroscopic observations of concrete core samples from bridge deck 3N.	134
Table D-6:	Macroscopic observations of concrete core samples from bridge deck 3L.	134
Table D-7:	Macroscopic observations of concrete core samples from bridge deck 5N.	135
Table D-8:	Macroscopic observations of concrete core samples from bridge deck 5L.	135
Table D-9:	Macroscopic observations of concrete core samples from bridge deck 6N.	136
Table D-10:	Macroscopic observations of concrete core samples from bridge deck 6L.	136
Table D-11:	Macroscopic observations of concrete core samples from bridge deck 7N.	137
Table D-12:	Macroscopic observations of concrete core samples from bridge deck 7L.	137
Table D-13:	Macroscopic observations of concrete core samples from bridge deck 8N.	138
Table D-14:	Macroscopic observations of concrete core samples from bridge deck 8L.	138
Table D-15:	Macroscopic observations of concrete core samples from bridge deck 9N.	139
Table D-16:	Macroscopic observations of concrete core samples from bridge deck 9L.	139
Table E-1:	Compressive strength test data and results	141
Table F-1:	Dynamic modulus test data and results.	143
Table H-1:	Summary RCT test results for bridge deck 1N.	162
Table H-2:	RCT test results by location for bridge deck 1N.	163
Table H-3:	Summary RCT test results for bridge deck 1L.	164
Table H-4:	RCT test results by location for bridge deck 1L.	165
Table H-5:	Summary RCT test results for bridge deck 2N.	166
Table H-6:	RCT test results by location for bridge deck 2N.	167
Table H-7:	Summary RCT test results for bridge deck 2L.	168
Table H-8:	RCT test results by location for bridge deck 2L.	169
Table H-9:	Summary RCT test results for bridge deck 3N.	170
Table H-10:	RCT test results by location for bridge deck 3N.	171
Table H-11:	Summary RCT test results for bridge deck 3L.	172
Table H-12:	RCT test results by location for bridge deck 3L.	173
Table H-13:	Summary RCT test results for bridge deck 5N.	174
Table H-14:	RCT test results by location for bridge deck 5N.	175
Table H-15:	Summary RCT test results for bridge deck 5L.	176
Table H-16:	RCT test results by location for bridge deck 5L.	177
Table H-17:	Summary RCT test results for bridge deck 6N.	178
Table H-18:	RCT test results by location for bridge deck 6N.	179
Table H-19:	Summary RCT test results for bridge deck 6L.	180
Table H-20:	RCT test results by location for bridge deck 6L.	181
Table H-21:	Summary RCT test results for bridge deck 7N.	182
Table H-22:	RCT test results by location for bridge deck 7N.	183
Table H-23:	Summary RCT test results for bridge deck 7L.	184
Table H-24:	RCT test results by location for bridge deck 7L.	185
Table H-25:	Summary RCT test results for bridge deck 8N.	186
Table H-26:	RCT test results by location for bridge deck 8N.	187
Table H-27:	Summary RCT test results for bridge deck 8L.	188
Table H-28:	RCT test results by location for bridge deck 8L.	189
Table H-29:	Summary RCT test results for bridge deck 9N.	190
Table H-30:	RCT test results by location for bridge deck 9N.	191

LIST OF TABLES (CON'T)

Table H-31: Summary RCT test results for bridge deck 9L. 192
Table H-32: RCT test results by location for bridge deck 9L. 193

LIST OF FIGURES

Figure 2-1:	Wenner meter.	6
Figure 3-1:	Typical sampling and testing location plan.	14
Figure 3-2:	Typical sampling and testing location plan for shorter bridges.	14
Figure 3-3:	Air and water permeability test configuration.	15
Figure 3-4:	Surface resistivity testing.	17
Figure 3-5:	Concrete cores as wrapped for transport to UNC Charlotte and subsequent storage until testing.	17
Figure 3-6:	Concrete powder samples in sealed jars.	18
Figure 3-7:	ASTM C1585 sorptivity testing.	19
Figure 3-8:	Ponding sorptivity testing.	20
Figure 3-9:	Rapid Chloride Test (RCT).	21
Figure 3-10:	Vacuum saturation of rapid chloride permeability test specimens.	22
Figure 3-11:	Rapid chloride permeability testing (RCPT).	23
Figure 4-1:	Typical pattern cracking denoted as low severity.	25
Figure 4-2:	Typical pattern cracking denoted as moderate severity.	26
Figure 4-3:	Typical transverse cracking on bridge deck 7N.	26
Figure 4-4:	Cracks extending perpendicular to expansion joint on bridge deck 9L.	27
Figure 4-5:	Typical longitudinal cracking on bridge deck 8N.	28
Figure 4-6:	Typical moderate severity pattern cracking on bridge deck 6N.	28
Figure 4-7:	Typical low severity pattern cracking on bridge deck 1N.	29
Figure 4-8:	Typical relatively short longitudinal crack on bridge deck 5L.	29
Figure 4-9:	Air permeability test results.	32
Figure 4-10:	Water permeability test results.	32
Figure 4-11:	Range and summary statistics of air permeability tests for normalweight and lightweight concrete bridge decks.	33
Figure 4-12:	Range and summary statistics of water permeability tests for normalweight and lightweight concrete bridge decks.	34
Figure 4-13:	Average temperature-corrected surface resistivity readings.	34
Figure 4-14:	Range and summary statistics of average temperature-corrected surface resistivity tests for normalweight and lightweight concrete bridge decks.	34
Figure 5-1:	Results from typical ASTM C1585 absorption test, showing initial absorption (first line segment) and secondary absorption (second line segment).	44
Figure 5-2:	Results from typical ponding sorptivity test (per Bentz et al. 2002), showing initial absorption (first line segment) and secondary absorption (second line segment).	45
Figure 5-3:	Initial absorption, ASTM C1585 capillary suction test.	47
Figure 5-4:	Secondary absorption, ASTM C1585 capillary suction test.	47
Figure 5-5:	Initial absorption, ponding test (Bentz et al. 2002).	48
Figure 5-6:	Secondary absorption, ponding test (Bentz et al. 2002).	48
Figure 5-7:	Range and summary statistics of average initial absorption rates (ASTM C1585 capillary suction) for normalweight and lightweight concrete bridge decks.	49
Figure 5-8:	Range and summary statistics of average secondary absorption rates (ASTM C1585 capillary suction) for normalweight and lightweight concrete bridge decks.	50
Figure 5-9:	Range and summary statistics of average initial absorption rates (ponding test developed by Bentz et al. (2002)) for normalweight and lightweight concrete bridge decks.	51
Figure 5-10:	Range and summary statistics of average secondary absorption rates (ponding test developed by Bentz et al. (2002)) for normalweight and lightweight concrete bridge decks.	51
Figure 5-11:	Surface chloride concentrations for normalweight and lightweight concrete bridge decks.	56

LIST OF FIGURES (CON'T)

Figure 5-12:	Apparent diffusion coefficients for normalweight and lightweight concrete bridge decks.	56
Figure 5-13:	Range and summary statistics of apparent diffusion coefficients for normalweight and lightweight concrete bridge decks.	56
Figure 5-14:	Average total charge passed for RCPT for normalweight and lightweight concrete bridge decks.	61
Figure 5-15:	Range and summary statistics of average charge passed (coulomb values) for normalweight and lightweight concrete bridge decks.	62
Figure A-1:	Visual survey results for bridge deck 1N.	81
Figure A-2:	Visual survey results for bridge deck 1L.	82
Figure A-3:	Visual survey results for bridge deck 2N.	83
Figure A-4:	Visual survey results for bridge deck 2L.	84
Figure A-5:	Visual survey results for bridge deck 3N.	85
Figure A-6:	Visual survey results for bridge deck 3L.	86
Figure A-7:	Visual survey results for bridge deck 5N.	87
Figure A-8:	Visual survey results for bridge deck 5L.	88
Figure A-9:	Visual survey results for bridge deck 6N.	89
Figure A-10:	Visual survey results for bridge deck 6L.	90
Figure A-11:	Visual survey results for bridge deck 7N.	91
Figure A-12:	Visual survey results for bridge deck 7L.	92
Figure A-13:	Visual survey results for bridge deck 8N.	93
Figure A-14:	Visual survey results for bridge deck 8L.	94
Figure A-15:	Visual survey results for bridge deck 9N.	95
Figure A-16:	Visual survey results for bridge deck 9L.	96
Figure G-1:	Results of ASTM C1585 capillary suction test for specimen prepared from bridge deck 1N, core C-7.	145
Figure G-2:	Results of ASTM C1585 capillary suction test for specimen prepared from bridge deck 1N, core C-8.	145
Figure G-3:	Results of ASTM C1585 capillary suction test for specimen prepared from bridge deck 1L, core C-3B.	145
Figure G-4:	Results of ASTM C1585 capillary suction test for specimen prepared from bridge deck 1L, core C-4.	145
Figure G-5:	Results of ASTM C1585 capillary suction test for specimen prepared from bridge deck 2N, core C-4.	146
Figure G-6:	Results of ASTM C1585 capillary suction test for specimen prepared from bridge deck 2N, core C-5.	146
Figure G-7:	Results of ASTM C1585 capillary suction test for specimen prepared from bridge deck 2L, core C-5.	146
Figure G-8:	Results of ASTM C1585 capillary suction test for specimen prepared from bridge deck 2L, core C-7.	146
Figure G-9:	Results of ASTM C1585 capillary suction test for specimen prepared from bridge deck 3N, core C-5.	146
Figure G-10:	Results of ASTM C1585 capillary suction test for specimen prepared from bridge deck 3N, core C-8.	147
Figure G-11:	Results of ASTM C1585 capillary suction test for specimen prepared from bridge deck 3L, core C-1.	147
Figure G-12:	Results of ASTM C1585 capillary suction test for specimen prepared from bridge deck 3L, core C-3.	147
Figure G-13:	Results of ASTM C1585 capillary suction test for specimen prepared from bridge deck 5N, core C-5.	148

LIST OF FIGURES (CON'T)

Figure G-14: Results of ASTM C1585 capillary suction test for specimen prepared from bridge deck 5N, core C-7. 148
Figure G-15: Results of ASTM C1585 capillary suction test for specimen prepared from bridge deck 5L, core C-3. 148
Figure G-16: Results of ASTM C1585 capillary suction test for specimen prepared from bridge deck 5L, core C-6. 148
Figure G-17: Results of ASTM C1585 capillary suction test for specimen prepared from bridge deck 6N, core C-4A. 149
Figure G-18: Results of ASTM C1585 capillary suction test for specimen prepared from bridge deck 6N, core C-6A. 149
Figure G-19: Results of ASTM C1585 capillary suction test for specimen prepared from bridge deck 6L, core C-5. 149
Figure G-20: Results of ASTM C1585 capillary suction test for specimen prepared from bridge deck 6L, core C-8. 149
Figure G-21: Results of ASTM C1585 capillary suction test for specimen prepared from bridge deck 7N, core C-2. 150
Figure G-22: Results of ASTM C1585 capillary suction test for specimen prepared from bridge deck 7N, core C-7. 150
Figure G-23: Results of ASTM C1585 capillary suction test for specimen prepared from bridge deck 7L, core C-3. 150
Figure G-24: Results of ASTM C1585 capillary suction test for specimen prepared from bridge deck 7L, core C-6. 150
Figure G-25: Results of ASTM C1585 capillary suction test for specimen prepared from bridge deck 8N, core C-4. 151
Figure G-26: Results of ASTM C1585 capillary suction test for specimen prepared from bridge deck 8N, core C-6. 151
Figure G-27: Results of ASTM C1585 capillary suction test for specimen prepared from bridge deck 8L, core C-3. 151
Figure G -28: Results of ASTM C1585 capillary suction test for specimen prepared from bridge deck 8L, core C-7. 151
Figure G-29: Results of ASTM C1585 capillary suction test for specimen prepared from bridge deck 9N, core C-1. 152
Figure G-30: Results of ASTM C1585 capillary suction test for specimen prepared from bridge deck 9N, core C-2. 152
Figure G-31: Results of ASTM C1585 capillary suction test for specimen prepared from bridge deck 9L, core C-1. 152
Figure G-32: Results of ASTM C1585 capillary suction test for specimen prepared from bridge deck 9L, core C-2. 152
Figure G-33: Results of ponding test (per Bentz et al. 2002) for specimen prepared from bridge deck 1N, core C-7. 153
Figure G-34: Results of ponding test (per Bentz et al. 2002) for specimen prepared from bridge deck 1N, core C-8. 153
Figure G-35: Results of ponding test (per Bentz et al. 2002) for specimen prepared from bridge deck 1L, core C-3B. 153
Figure G-36: Results of ponding test (per Bentz et al. 2002) for specimen prepared from bridge deck 1L, core C-4. 153
Figure G-37: Results of ponding test (per Bentz et al. 2002) for specimen prepared from bridge deck 2N, core C-4. 154
Figure G-38: Results of ponding test (per Bentz et al. 2002) for specimen prepared from bridge deck 2N, core C-5. 154

LIST OF FIGURES (CON'T)

Figure G-39: Results of ponding test (per Bentz et al. 2002) for specimen prepared from bridge deck 2L, core C-5. 154
Figure G-40: Results of ponding test (per Bentz et al. 2002) for specimen prepared from bridge deck 2L, core C-7. 154
Figure G-41: Results of ponding test (per Bentz et al. 2002) for specimen prepared from bridge deck 3N, core C-6. 155
Figure G-42: Results of ponding test (per Bentz et al. 2002) for specimen prepared from bridge deck 3N, core C-8. 155
Figure G-43: Results of ponding test (per Bentz et al. 2002) for specimen prepared from bridge deck 3L, core C-1. 155
Figure G-44: Results of ponding test (per Bentz et al. 2002) for specimen prepared from bridge deck 3L, core C-3. 155
Figure G-45: Results of ponding test (per Bentz et al. 2002) for specimen prepared from bridge deck 5N, core C-5. 156
Figure G-46: Results of ponding test (per Bentz et al. 2002) for specimen prepared from bridge deck 5N, core C-7. 156
Figure G-47: Results of ponding test (per Bentz et al. 2002) for specimen prepared from bridge deck 5L, core C-3. 156
Figure G-48: Results of ponding test (per Bentz et al. 2002) for specimen prepared from bridge deck 5L, core C-6. 156
Figure G-49: Results of ponding test (per Bentz et al. 2002) for specimen prepared from bridge deck 6N, core C-4A. 157
Figure G-50: Results of ponding test (per Bentz et al. 2002) for specimen prepared from bridge deck 6N, core C-6A. 157
Figure G-51: Results of ponding test (per Bentz et al. 2002) for specimen prepared from bridge deck 6L, core C-5. 157
Figure G-52: Results of ponding test (per Bentz et al. 2002) for specimen prepared from bridge deck 6L, core C-8. 157
Figure G-53: Results of ponding test (per Bentz et al. 2002) for specimen prepared from bridge deck 7N, core C-2. 158
Figure G-54: Results of ponding test (per Bentz et al. 2002) for specimen prepared from bridge deck 7N, core C-7. 158
Figure G-55: Results of ponding test (per Bentz et al. 2002) for specimen prepared from bridge deck 7L, core C-3. 158
Figure G-56: Results of ponding test (per Bentz et al. 2002) for specimen prepared from bridge deck 7L, core C-6. 158
Figure G-57: Results of ponding test (per Bentz et al. 2002) for specimen prepared from bridge deck 8N, core C-4. 159
Figure G-58: Results of ponding test (per Bentz et al. 2002) for specimen prepared from bridge deck 8N, core C-6. 159
Figure G-59: Results of ponding test (per Bentz et al. 2002) for specimen prepared from bridge deck 8L, core C-3. 159
Figure G-60: Results of ponding test (per Bentz et al. 2002) for specimen prepared from bridge deck 8L, core C-7. 159
Figure G-61: Results of ponding test (per Bentz et al. 2002) for specimen prepared from bridge deck 9N, core C-1. 160
Figure G-62: Results of ponding test (per Bentz et al. 2002) for specimen prepared from bridge deck 9N, core C-2. 160
Figure G-63: Results of ponding test (per Bentz et al. 2002) for specimen prepared from bridge deck 9L, core C-1. 160

LIST OF FIGURES (CON'T)

Figure G-64: Results of ponding test (per Bentz et al. 2002) for specimen prepared from bridge deck 9L, core C-2. 160
Figure I-1: Scanned image of polished surface prepared from bridge deck 1N, core C-5. 195
Figure I-2: Scanned image of polished surface prepared from bridge deck 1L, core C-7B. 195
Figure I-3: Scanned image of polished surface prepared from bridge deck 2N, core C-6. 196
Figure I-4: Scanned image of polished surface prepared from bridge deck 2N, core C-7. 196
Figure I-5: Scanned image of polished surface prepared from bridge deck 2L, core C-3. 197
Figure I-6: Scanned image of polished surface prepared from bridge deck 2L, core C-4. 197
Figure I-7: Scanned image of polished surface prepared from bridge deck 3N, core C-2. 198
Figure I-8: Scanned image of polished surface prepared from bridge deck 3N, core C-3. 198
Figure I-9: Scanned image of polished surface prepared from bridge deck 3L, core C-6. 199
Figure I-10: Scanned image of polished surface prepared from bridge deck 5N, core C-3. 199
Figure I-11: Scanned image of polished surface prepared from bridge deck 5N, core C-8. 200
Figure I-12: Scanned image of polished surface prepared from bridge deck 5L, core C-8. 200
Figure I-13: Scanned image of polished surface prepared from bridge deck 6N, core C-3. 201
Figure I-14: Scanned image of polished surface prepared from bridge deck 6N, core C-6B. 201
Figure I-15: Scanned image of polished surface prepared from bridge deck 6L, core C-1. 202
Figure I-16: Scanned image of polished surface prepared from bridge deck 6L, core C-3. 202
Figure I-17: Scanned image of polished surface prepared from bridge deck 7N, core C-6. 203
Figure I-18: Scanned image of polished surface prepared from bridge deck 7N, core C-8. 203
Figure I-19: Scanned image of polished surface prepared from bridge deck 7L, core C-5A. 204
Figure I-20: Scanned image of polished surface prepared from bridge deck 7L, core C-7A. 204
Figure I-21: Scanned image of polished surface prepared from bridge deck 8N, core C-2. 205
Figure I-22: Scanned image of polished surface prepared from bridge deck 8N, core C-7. 205
Figure I-23: Scanned image of polished surface prepared from bridge deck 8L, core C-4. 206
Figure I-24: Scanned image of polished surface prepared from bridge deck 8L, core C-8. 206
Figure I-25: Scanned image of polished surface prepared from bridge deck 9N, core C-3. 207
Figure I-26: Scanned image of polished surface prepared from bridge deck 9N, core C-5. 207
Figure I-27: Scanned image of polished surface prepared from bridge deck 9L, core C-5. 208
Figure I-28: Scanned image of polished surface prepared from bridge deck 9L, core C-8. 208
Figure I-29: Photomicrograph of polished surface prepared from bridge deck 1L, core C-7B, taken at a magnification of 25x. White secondary deposits are present in some entrained air voids. 209
Figure I-30: Photomicrograph of polished surface prepared from bridge deck 1N, core C-5, taken at a magnification of 20x. White secondary deposits are present in some entrained air voids near microcrack. 209
Figure I-31: Photomicrograph of polished surface prepared from bridge deck 2L, core C-4, taken at a magnification of 10x. Localized areas of very high entrained air content can be seen at lower left of image. 210
Figure I-32: Photomicrograph of polished surface prepared from bridge deck 5L, core C-8, taken at a magnification of 7x. Microcrack extends from groove, through lightweight aggregate, into mortar. 210
Figure I-33: Photomicrograph of polished surface prepared from bridge deck 5N, core C-7, taken at a magnification of 7x. Microcrack extends from groove, through normalweight aggregate, into mortar. 211
Figure I-34: Photomicrograph of polished surface prepared from bridge deck 6L, core C-6A, taken at a magnification of 7x. A number of irregularly shaped water voids are present. 211
Figure I-35: Photomicrograph of polished surface prepared from bridge deck 6L, core C-1, taken at a magnification of 15x. White secondary deposits are present, lining some entrained air voids. 212

LIST OF FIGURES (CON'T)

Figure I-36: Photomicrograph of polished surface prepared from bridge deck 7L, core C-5A, taken at a magnification of 10x. White secondary deposits are present, lining some entrained air voids and in some voids in lightweight aggregate. 212
Figure I-37: Photomicrograph of polished surface prepared from bridge deck 8N, core C-7, taken at a magnification of 15x. Macrocrack extending from top surface through coarse aggregate. 213
Figure I-38: Photomicrograph of polished surface prepared from bridge deck 9N, core C-5, taken at a magnification of 10x. Microcrack from top surface propagates around coarse aggregate perimeter and through coarse aggregate. 213
Figure I-39: Datasheet for petrographic examination of sample 1N C-5. 214
Figure I-40: Datasheet for petrographic examination of sample 1L C-7B. 215
Figure I-41: Datasheet for petrographic examination of sample 2N C-6. 216
Figure I-42: Datasheet for petrographic examination of sample 2N C-7. 217
Figure I-43: Datasheet for petrographic examination of sample 2L C-3. 218
Figure I-44: Datasheet for petrographic examination of sample 2L C-4. 219
Figure I-45: Datasheet for petrographic examination of sample 3N C-2. 220
Figure I-46: Datasheet for petrographic examination of sample 3N C-3. 221
Figure I-47: Datasheet for petrographic examination of sample 3L C-6. 222
Figure I-48: Datasheet for petrographic examination of sample 5N C-3. 223
Figure I-49: Datasheet for petrographic examination of sample 5N C-8. 224
Figure I-50: Datasheet for petrographic examination of sample 5L C-5. 225
Figure I-51: Datasheet for petrographic examination of sample 5L C-8. 226
Figure I-52: Datasheet for petrographic examination of sample 6N C-3. 227
Figure I-53: Datasheet for petrographic examination of sample 6N C-6B. 228
Figure I-54: Datasheet for petrographic examination of sample 6L C-1. 229
Figure I-55: Datasheet for petrographic examination of sample 6L C-6A. 230
Figure I-56: Datasheet for petrographic examination of sample 7N C-6. 231
Figure I-57: Datasheet for petrographic examination of sample 7N C-8. 232
Figure I-58: Datasheet for petrographic examination of sample 7L C-5A. 233
Figure I-59: Datasheet for petrographic examination of sample 7L C-7A. 234
Figure I-60: Datasheet for petrographic examination of sample 8N C-2. 235
Figure I-61: Datasheet for petrographic examination of sample 8N C-7. 236
Figure I-62: Datasheet for petrographic examination of sample 8L C-4. 237
Figure I-63: Datasheet for petrographic examination of sample 8L C-8. 238
Figure I-64: Datasheet for petrographic examination of sample 9N C-3. 239
Figure I-65: Datasheet for petrographic examination of sample 9N C-5. 240
Figure I-66: Datasheet for petrographic examination of sample 9L C-5. 241
Figure I-67: Datasheet for petrographic examination of sample 9L C-8. 242

LIST OF ABBREVIATIONS

AASHTO	American Association of State Highway and Transportation Officials
AER	air exclusion rating
ACI	American Concrete Institute
ASTM	American Society for Testing and Materials
C	Coulomb
ºC	degrees Celcius
cf	cubic feet
con't	continued
DOT	Department of Transportation
ºF	degrees Fahrenheit
FHWA	Federal Highway Administration
ft	foot
Hg	mercury
hr	hour
in	inch
K	Kelvin
kg	kilogram
lb	pound
m	meter
min	minute
mL	milliliter
mm	millimeter
MPa	megapascal
NCDOT	North Carolina Department of Transportation
oz	ounce
Pa	Pascal
PCC	portland cement concrete
pcy	pounds per cubic yard
psi	pounds per square inch
ρ	resistivity
sec	second
sf	square feet
SSD	saturated surface dry
V	volume
WAR	water absorption rate
w/c	water to cementitious material ratio
wt	weight

1.0 INTRODUCTION AND RESEARCH OBJECTIVES

1.1 Introduction

In lightweight aggregate concrete, lightweight aggregates are used as replacements for either coarse aggregate, fine aggregate, or both. Structural lightweight concrete typically has a density between 85 and 120 pounds per cubic foot, and is utilized for structural purposes. Lightweight aggregates are highly porous, comprised of either natural or manufactured material. Typically, lightweight aggregates used in structural applications in North Carolina are manufactured from slate material that has been expanded by heating at high temperatures.

In bridge structures, lightweight concrete can provide several advantages over normalweight concrete. These advantages are primarily linked to the reduced deadload of the structural components. The unit weight of lightweight concrete is approximately 30% less than that of normalweight concrete, and therefore substructures can often be reduced and span lengths can be increased. Other advantages can include reduction in formwork costs as well as a possible increase in productivity due to handling of lighter materials.

Additionally, in some studies lightweight aggregate has been shown to contribute to internal curing of concrete. Saturated lightweight aggregate particles provide a reservoir of water available for hydration purposes long after traditional curing measures have been discontinued. Internal curing can result in concrete with lower permeability and reduced cracking, and therefore, enhanced durability performance.

However, lightweight concrete is typically more expensive than normalweight concrete. This higher cost is due to the cost of the lightweight aggregate as well as the increased cement content that must sometimes be utilized. The additional cost associated with its use must be justified. Some practitioners do not feel that it has been conclusively shown that lightweight aggregate concrete bridge decks exhibit better durability performance than normalweight concrete bridge decks. If this is the case, the benefits obtained from the additional cost of lightweight concrete are primarily realized in the use of reduced loads in the structural design.

If enhanced durability performance of lightweight concrete bridge decks can be confirmed, cost/benefit analysis of lightweight aggregate concrete bridge decks would include both a longer service life and reduced maintenance and repair costs. In some situations, this could indicate that lightweight concrete bridge decks are a more economical choice than normalweight concrete bridge decks. Alternatively, if enhanced durability performance is not confirmed, the additional cost of lightweight concrete bridge decks may not be justified.

1.2 Research Objectives

The purpose of this research was to provide NCDOT information that will prove to be useful in making decisions regarding:

- whether to use lightweight concrete or normalweight concrete bridge decks for certain applications,
- maintenance and repair, and
- possible changes to design and construction methods and/or specifications.

The objective of this research was to evaluate the field performance of lightweight concrete bridge decks, comparing to normalweight concrete in the same structure or environment where possible. This study included field evaluations of normalweight and lightweight concrete bridge decks in North Carolina. Bridge decks included in this study were selected in pairs: for each lightweight concrete bridge deck selected for inclusion in this study, a companion normalweight bridge deck of similar age, traffic loading, and environmental exposure was selected.

Field evaluations included visual surveys and field tests (surface resistivity, air and water permeability and rebound hammer testing). Drilled cores and powder samples were also removed from the concrete decks and returned to UNC Charlotte's laboratory for testing. Laboratory tests included compressive strength, dynamic modulus, sorptivity, chloride content, chloride permeability, and surface resistivity. Petrographic examinations were also performed on portions of selected cores. Using the results of the field evaluations and testing, along with laboratory testing of concrete core samples and powder samples, the field performance of the lightweight concrete bridge decks was evaluated and compared to the performance of the normalweight concrete bridge decks.

2. LITERATURE REVIEW AND BACKGROUND INFORMATION

2.1 Literature Review

2.1.1 Durability of Concrete Bridge Decks

Concrete structures should be able to perform satisfactorily over an expected service life, and structures that maintain their required strength and serviceability are deemed durable (Neville 1995). Reduced maintenance costs and longer service life are direct benefits of a durable structure. For bridges, the durability performance of the bridge deck is important, as it provides the wearing surface for traffic and can influence the durability performance of other structural components. Since many bridge decks are comprised primarily (or solely) of reinforced concrete, the durability of the concrete comprising a deck is of great interest to stakeholders.

Durability of concrete is defined by the American Concrete Institute in ACI 116R (2000) as concrete's ability to resist weathering action, chemical attack, abrasion, and other conditions of service. Permeability of concrete is believed to be the most important characteristic of concrete that affects its durability (Chini et al. 2003). As stated by Neville (1995), "all the adverse influences of durability involve the transport of fluids through the concrete." Fluids moving through concrete can transport aggressive agents such as acids, sulfates, and chlorides. Each of these agents propels chemical reactions that can degrade concrete.

For reinforced concrete bridges, one of the major forms of environmental attack is chloride ingress, which leads to corrosion of the reinforcing steel. Chloride ions present in concrete promote corrosion of reinforcing steel. Once corrosion has initiated, cracks in concrete propagate due to tension stresses produced by corrosion products, as the corrosion products occupy a larger volume when compared to the volume of a non-corroding rebar (Presuel-Moreno et al. 2010). Damage due to corrosion causes reduction in strength, serviceability, and aesthetics of the structure (Chini et al. 2003).

Controlling and reducing cracks in concrete bridge decks is also paramount to durability performance. Cracks provide a means for accelerated ingress of chlorides and other aggressive contaminants, causing corrosion of the reinforcing steel and other degradation of the concrete. Alkali-silica reactions can be exacerbated by cracking, as moisture gradients promote migration of alkali ions (Neville 1995). Surface scaling and spalling due to freeze-thaw action is also worsened by presence of cracks (Reinhardt 2008).

Recent research suggests that lightweight concrete can provide substantial advantages over normalweight concrete in a number of applications, including bridge decks. It has been suggested that these advantages extend beyond reduced self-weight, and include enhanced durability performance associated with reduced permeability and reduced cracking tendency (Delatte et al. 2007). The improved contact zone between aggregate and cement paste, internal curing effects, and the reduced modulus of elasticity are touted as possible contributors to the enhanced durability performance of lightweight concrete (Wolf 2008, Vaysburd 1996, Ramirez et al. 2000, and others). Some research has shown that lightweight concrete can have lower levels of microcracking as well as higher resistance to weathering and corrosion (Reinhardt 2008). Microscale characteristics of the contact zone between lightweight aggregate and cement paste has been linked to improved durability performance of lightweight concrete bridges (Vaysburd 1996).

The Indiana Department of Transportation conducted an extensive laboratory study on lightweight concrete mix designs specified for Indiana bridge decks, focusing on both durability performance and mechanical properties. Mixtures were prepared in the laboratory, but hardened concrete core samples removed from existing bridge decks were not included in the research. A key recommendation of this study was that in order to ensure adequate durability performance, lightweight concrete should be allowed to dry before being subjected to free-thaw cycles (Ramirez et al. 2000).

The Virginia Department of Transportation performed a study that included laboratory testing of the durability of lightweight concrete, with laboratory test specimens cast from concrete mixtures identical to those specified for bridges in the state. The findings included that "properly air-entrained lightweight concrete made with high quality lightweight aggregates provides satisfactory resistance to freezing and thawing" (Ozyildirim 2008).

The results of laboratory studies have been utilized in service life prediction models to assess the potential for lightweight concrete to extend the service life of bridge decks beyond that of normalweight bridge decks. Cusson et al. (2010) indicated that the improved internal curing of lightweight concrete extended the predicted service life of each of the three bridge decks included in the case study by more than 20 years. The longer service life predicted was due to significant reductions in chloride penetration, early-age shrinkage cracking, and chloride diffusion. In a comparable study by Thomas et al. (2006), similar results were obtained. Use of lightweight aggregate in concrete resulted in significant reduction in permeability and chloride diffusion coefficients, leading to longer service life predictions.

Use of lightweight concrete in bridge decks has, however, caused some durability concerns for practitioners. These concerns include reduced resistance to salt scaling and lower abrasion resistance (Ozyildirim 2008). Although a number of publications exist providing the results of laboratory-based studies on the durability performance of lightweight concrete, far fewer studies of durability performance studies of lightweight concrete in field settings exist in the literature. Lightweight aggregate manufacturers and others have documented the field performance of lightweight concrete in some bridge deck applications, including those in severe climates in the United States (Wolf 2008) and abroad (Harmon 2005). However, only a few comprehensive field studies of the durability performance of lightweight concrete bridge decks have been performed. Information on these studies is presented in the following paragraphs.

A study by Delatte et al. (2007) for the Ohio Department of Transportation included field evaluation and laboratory testing of 116 Ohio bridge decks. While both lightweight and normal weight decks were included, the main focus of this study was to correlate concrete mixture designs to bridge deck cracking. Field evaluations of bridge decks were correlated to concrete mixture characteristics and material properties in order to determine which parameters had the greatest effect on bridge deck cracking. The results showed a strong correlation between bridge deck cracking and aggregate gradation. The improved internal curing of the lightweight decks (due to the use of saturated lightweight aggregate) did show some correlation to reduced cracking but not as much correlation as aggregate gradation.

The Federal Highway Administration (FHWA) sponsored a study entitled "Compilation and Evaluation of Results from High-Performance Concrete Projects," which included field evaluation and laboratory testing of bridge decks. The initial phase of this study included compilation of data on a number of high-performance concrete (HPC) field applications. While 19 bridges in 14 states were chosen (including Highway 401 Bridge in Wake County, North Carolina), an emphasis was not placed on lightweight concrete decks. A key recommendation of this report was that more research should be conducted concerning air voids and freeze thaw performance (Russell et al. 2006).

In summary, the findings of a number of laboratory-based studies indicate that lightweight concrete can provide enhanced durability performance. However, only a few studies of the durability of lightweight concrete bridge decks in field conditions have been conducted. Of the field-based studies of lightweight concrete bridge deck performance that have been performed, none include the same environmental conditions and local materials commonly used in North Carolina.

2.1.2 Cracking of Concrete Bridge Decks

Control of cracking on bridge decks is imperative, as cracks provide a means for infiltration of solutions that promote corrosion into the concrete, leading to deterioration of the reinforcing steel or other structural components. Cracks occur when tensile stresses in the concrete exceed its tensile strength. This can occur while the concrete is in either a plastic or hardened state, and can be the result of a variety of causes. Although cracks can form in response to external loading, they are more often the result of volumetric instability inside the concrete, caused by thermal, moisture, and chemical effects (TRB 2006). Volume changes cause internal stresses, resulting in cracking. The potential for volumetric instability in concrete is affected by mixture proportions, material constituents, and environmental factors.

As outlined in "Control of Cracking in Concrete: State of the Art," Transportation Research Circular E-C107 prepared by the Transportation Research Board (TRB 2006), factors that are generally accepted to be influential in bridge deck cracking include:

- Bridge design
- Concrete mixture design
- Materials used in the concrete mixture
- Placing, finishing, and curing practices

These factors contribute to restraint, thermal stresses, and shrinkage stresses responsible for initiating and propagating cracks. In addition to the factors listed above, environmental influences such as temperature and humidity also contribute to the development of stresses (TRB 2006). Most bridge deck cracks initiate in early ages (Darwin et al. 2004). These early cracks propagate over time, and additional cracks form for various reasons.

Cracking that occurs prior to setting is typically due to plastic shrinkage and settlement. Cracking that initiates in the hardened state can be due to a number of factors, including superstructure design characteristics, concrete mixture design, material characteristics, and construction placement, finishing, and curing techniques. Environmental conditions present during the construction of the bridge deck, as well as those occurring over the lifetime of the bridge deck, also influence crack initiation and propagation.

2.1.2.1 Bridge Design Factors Related to Cracking

A number of factors related to bridge design can contribute to bridge deck cracking. Restraint is typically caused by end conditions and the composite action between the bridge deck and the supporting members of the superstructure. The fixity conditions at abutments can influence cracking in the end spans of bridge decks. Bridge decks with fixed ends at the abutments tend to exhibit more cracking near the fixed ends due to restraint. These cracks are often longitudinal cracks, not transverse cracks (Darwin et al. 2004). Restraint can also be provided by stay-in-place forms (Saadeghvaziri and Hadidi 2005).

The type of girder used in a bridge superstructure has been shown to influence cracking. Bridge decks of steel girder bridges often exhibit more cracking than bridge decks supported by other types of girders (Darwin et al. 2004). This has been attributed to the fact that steel girders conduct heat faster than concrete girders, causing higher thermal stresses. It has also been reported that the decks of continuous steel girder bridges also have exhibited more cracking than the decks of non-continuous steel girder bridges (Hadidi and Saadeghvaziri 2005).

The role of the rigidity of the superstructure in crack formation and propagation has been studied by a number of researchers, and it is well documented that the relative stiffnesses of components of the superstructure influence cracks. Thicker bridge decks tend to have less cracking (TRB 2006), although the relative stiffnesses of the bridge deck and the girders is an important factor in the propensity for a deck to experience cracking (Hadidi and Saadeghvaziri 2005). It has been suggested that cracking can be reduced by reducing the ratio of the cross-sectional area of the girders to that of the deck (Hadidi and Saadeghvaziri 2005). Research by Saadeghvaziri and Hadidi (2005) indicated that superstructures that are more flexible have less cracking than more rigid superstructures. However, a study by Perfetti et al. (1985) found that vibrational frequency of the superstructure did not correlate to transverse cracking of bridge decks.

Reinforcing steel characteristics (including bar size, spacing, and other details) can affect bridge deck cracking. Larger bar sizes have been associated with greater cracking potential, but other factors including longitudinal/transverse relative bar placements, splicing details, and epoxy coatings are also contributing factors (Hadidi and Saadeghvaziri 2005). Concrete cover over the reinforcing steel has also been shown to influence transverse bridge deck cracking. Generally, an increase in thickness of concrete cover results in lower cracking tendency, although "excessive" cover thicknesses have been linked to an increase in settlement cracks at reinforcing steel (Hadidi and Saadeghvaziri 2005).

Research into the relationship of traffic to bridge deck cracking has provided mixed findings. Hadidi and Saadeghvaziri (2005) discuss the work of several researchers that found no relationship between traffic and bridge

deck cracking tendency. However, a study by McKeel (1985) concluded that "bridges that carry fewer trucks at lower speeds exhibit less cracking than those that carry large number of trucks at higher speeds."

2.1.2.2 Mixture Design Factors Related to Cracking

The characteristics of concrete mixtures used in bridge decks can be associated with cracking potential. Although concrete relies on its strength to resist cracking, for bridge decks, higher compressive strength does not necessarily correlate to more resistance to cracking (Darwin et al. 2004). This is often attributed to the higher modulus of elasticity that accompanies early age strength gain, as well as the increased paste volume and hydration temperatures associated with higher cement contents (Hadidi and Saadeghvaziri 2005). Concrete mixtures with higher cement contents can exhibit increased cracking due to the tendency for a greater heat of hydration, higher modulus of elasticity developed at an early age, and increased drying shrinkage (Hadidi and Saadeghvaziri 2005).

It is generally accepted that concrete mixtures with high (>0.45) water-to-cement ratios (w/c) tend to have higher porosity, which leads to significant drying shrinkage and the increased ability of chlorides to ingress towards the reinforcing steel (TRB 2006). However, the increased autogenous shrinkage associated with low (less than 0.40) w/c ratios results in increased cracking (TRB 2006). Weiss (1999) cites five factors that cause an increase in cracking potential with higher strength concrete mixtures. These five factors are early-age autogenous shrinkage, higher material stiffness, increased brittleness, reduced creep, and increased shrinkage rate. TRB (2006) indicates that "best results have been achieved with the w/c is targeted in the range of 0.38 to 0.44."

Concrete mixtures with higher aggregate content (and correspondingly, lower paste content) exhibit a reduced tendency to crack. This is due to reduction in the paste fraction (lowering shrinkage potential) along with an increase in the proportion of the mixture least susceptible to thermal stresses (TRB 2006). Delatte et al. (2007) found that replacing a small maximum size coarse aggregate material with an optimized coarse aggregate gradation reduced cracking potential.

2.1.2.3 Material Characteristics Related to Cracking

Temperature rise due to hydration of cement at early ages, along with subsequent cooling, can be responsible for the development of residual stresses within the concrete (TRB 2006). Temperature rise is controlled by a number of factors, including the type of cement used, its chemical composition, and its fineness. Thermal cracks often appear within a few days of concrete placement, while drying shrinkage cracks often take longer (a year or longer) to appear (TRB 2006).

The type of cement used can influence concrete cracking as well. Type II cement has been shown to provide greater resistance to cracking due to lower early age temperature rise, lower thermal gradients and reduced shrinkage (Hadidi and Saadeghvaziri 2005). During the past two decades, cement has become finer, which can also result in greater shrinkage of the concrete (Chariton and Weiss 2002).

When supplementary cementitious materials (SCMs) such as fly ash are utilized to replace a portion of Portland cement, concrete has a reduced tendency to crack. This is due to lower early age temperatures and slower development of strength and elastic modulus (TRB 2006). Silica fume has been utilized in bridge deck concrete to reduce permeability, but has also been associated with early age cracking (Delatte et al. 2007).

Since volume changes are largely attributable to the paste fraction, it is generally accepted that concrete mixtures that incorporate larger aggregate sizes experience less cracking (TRB 2006). The absorption of aggregates used in concrete "is closely related to its porosity, and the porosity influences the stiffness and compressibility (TRB 2006)." As aggregates with high absorptions tend to be more compressible, they tend to be subject to more volume changes due to shrinkage, with coarse aggregates tending to be more influential on the overall drying shrinkage than fine aggregates (TRB 2006). The high absorption of lightweight aggregates, however, can be used to reduce cracking due to internal curing (Delatte et al. 2007). Delatte et al. (2007) also found that use of lightweight fine aggregate reduced shrinkage, and are therefore associated with lower cracking potential. Hadidi and Saadeghvaziri (2005) summarize that "in general, concrete mixes with good quality, clean, low shrinkage aggregate with high aggregate to paste ratio have been observed to perform better."

2.1.2.4 Placing, Finishing, and Curing Practices that Contribute to Cracking

A number of practices employed during construction of a bridge deck have been implicated as a cause of (or as a contributor to) cracking of concrete. Evaporative effects caused by wind and low humidity have long been known to be a key cause of plastic shrinkage cracks, and proper curing techniques are essential to prevention of this type of cracking. Pumped concrete tends to have a higher slump, and therefore, settlement cracking increases (Darwin et al. 2004).

Early-age thermal stresses are often influenced by ambient temperatures during placement and shortly thereafter (Hadidi and Saadeghvaziri 2005). Construction sequencing, including pour sequencing, can influence cracking (Hadidi and Saadeghvaziri 2005), as do vibration techniques (Issa 1999). The weight and vibration of construction equipment, as well as deflection of formwork has also been shown to increase cracking (Issa 1999).

2.1.3 Background Information on Selected Concrete Characteristics and Test Methods

2.1.3.1 Surface Resistivity

The Rapid chloride permeability test (RCPT) has been around for approximately 20 years and is widely used to assess the potential for chloride ingress into concrete. However the RCPT test is labor intensive and therefore costly. For this reason, an alternative non-destructive test (NDT) apparatus called the surface resistivity meter has been developed for use in assessing the electrical resistance, and hence relative permeability, of concrete. Concrete electrical resistivity measures the ability of concrete to resist the passage of electrical current, which is passed by the ions in the pore solution of the concrete. Concrete conductivity is fundamentally related to the permeability of fluids and the diffusivity of ions through a porous material. As a result, electrical resistivity can be used as an indirect measure of the ease in which chloride ions can penetrate concrete (Presuel-Moreno et al. 2010).

The surface resistivity test apparatus uses a Wenner 4-probe array and a small alternating current to make instantaneous readings. The Wenner probe was originally developed in order to determine soil resistivity in soil strata, but the technique has been adapted for use in testing of concrete. A current is passed between the two outside contact probes, and the voltage drop between the two inner contact points is measured as shown in Figure 2-1. Results from using the Wenner device are in electrical resistivity (kΩ•cm). The readings are returned by a data acquisition unit as an indication of the concrete's ability to conduct current (Chini et al. 2003).

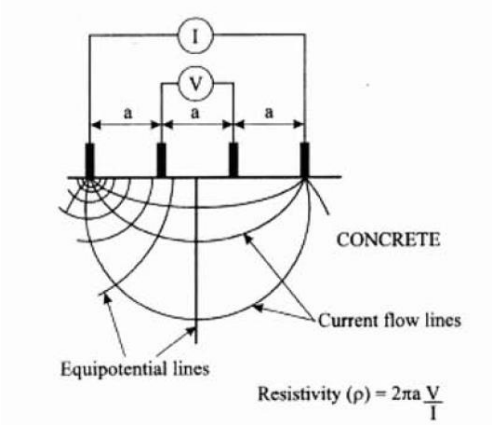

Figure 2-1: Wenner meter (figure from Gowers and Millard 1999).

The main application of the Wenner probe has been in testing cylindrical concrete test specimens in laboratory settings, although Florida Department of Transportation also uses a Wenner surface resistivity probe in the field for assessing the concrete resistivity before the installation of a cathodic protection system so as to estimate needed current (Presuel-Moreno et al. 2010). Some researchers have shown that surface resistivity measurements have been shown to correlate well with rapid chloride permeability measurements across a wide range of permeability values and sample testing ages. Suitable correlations have been found to exist between both 14-day and 28-day surface resistivity values and the 56-day rapid chloride permeability values (Rupnow and Icenogle 2011).

There is considerable interest in determining whether surface resistivity measurements obtained in the field on in-situ structural components can be used to estimate concrete permeability properties (Presuel-Moreno et al. 2010).

Surface resistivity measurements are influenced by a number of environmental factors (primarily temperature and moisture content), as well as the characteristics of the structure or test specimen. Measurements are also influenced by electrode spacing, the geometry of the specimen or structural component being measured, the presence of embedded reinforcing steel, and near-surface layers of concrete that have resistivities differing from that of the bulk concrete (Presuel-Moreno et al. 2010). Use of surface resistivity testing in the field requires particular mindfulness of these factors.

Concrete with a lower degree of saturation will exhibit artificially high surface resistivity values (Presuel-Moreno et al. 2010). Additionally, resistivity increases as temperature increases. A method of correcting surface resistivity measurements made at service temperatures to a standard temperature of 69.8°F (294.15°K) was developed by Elkey and Sellevold of the Norwegian Road Research Laboratory, and has been utilized in the United States (Presuel-Moreno et al. 2010). Some research indicates that the relationship between temperature and surface resistivity is not linear (Cavalline 2012). Additionally, some research has shown that the temperature effect may vary with moisture content (Polder 2001).

Prior to using a Wenner probe surface resistivity meter, spacing of the test probes must be considered. An assumption is made when using the Wenner resistivity technique that the material being measured is homogeneous. However, concrete contains aggregate particles (which normally have a very high resistivity) and cement paste (which has a much lower resistivity). To reduce the influence of aggregates, it has been recommended that the minimum probe spacing be 1.5 times that of the maximum aggregate size (Chini et al. 2003).

Interest in measurement of resistivity, as well as its inverse conductivity, has grown in recent years. As agencies express desire for a rapid test method that can be used to evaluate fluid transport and ion diffusion, researchers have been working to develop and evaluate new test methods to measure the electrical properties of bulk specimens and in-situ concrete. Recent work by Spragg et al. (2011) and others will likely provide additional insight into the uses and limitations of resistivity testing in the near future.

2.1.3.2 Sorptivity and Permeability

Sorptivity is defined as the ability of concrete surface to absorb water by capillary action (Neville 1995). Since concrete deterioration often depends on the migration of fluids (and hence aggressive agents) from the surface, sorptivity is considered a characteristic of concrete useful in prediction of concrete durability (Hooton et al. 1993). According to Hall (1989), "sorptivity data obtained in the laboratory show reasonably systematic variation with mix and curing history," and can be used to evaluate the potential durability performance of one concrete mixture relative to others.

Sorptivity of concrete can be evaluated using test methods that consider pressure induced by a head of water above the concrete surface, as in the ponding method developed by Bentz et al. (2002), or by methods that consider capillary action only (ASTM C1585). Testing can be performed on concrete in-situ, on laboratory cast and cured specimens, or on specimens removed from a structure and returned to a laboratory and conditioned. If field-obtained core specimens are used for sorptivity testing (or if sorptivity testing is perfomed in-situ), the ponding method can provide particularly insightful results, because the test surface is the exposed surface of the concrete.

Initial absorption (within the first few hours) and the secondary absorption (over several days) are both of interest. As the test specimen absorbs water, mass change is recorded. Because sorptivity is a diffusion process, the rate of increase in mass per unit surface area is plotted against the square root of time (Hall 1989). Least-square linear regression is performed in order to fit two line segments to the data, the first for initial absorption and the second for secondary absorption. The initial absorption is often defined as the slope of the best fit line for the 1 minute to 6 hour data, and the secondary absorption is often defined as the slope of the best fit line for the day 1 to day 7 data (Bentz et al. 2002). Initial and secondary sorptivity are typically reported in units of $in/min^{0.5}$ or $mm/min^{0.5}$, and are sometimes referred to as sorptivity coefficients.

Sorptivity test results can be influenced by several factors. The surface layer of concrete is often different than the interior because of a number of reasons, including those related to finishing and aggregate orientation (Figg 1989), as well as abrasion wear, damage from external loads and internal stresses, and damage due to environmental exposure. Often the near-surface portion of concrete is denser than the interior, but this is not always the case with "heavily vibrated high cement content mixes" (Figg 1989). Sorptivity is highly influenced by concrete saturation at the time of testing (DeSousa et al. 1997), and therefore laboratory testing with controlled specimen conditioning is often preferable to in-situ testing (Bentz et al. 2002). Several procedures have been suggested and utilized for specimen conditioning, with the objective of each to obtain a known, uniform relative humidity throughout each specimen (DeSousa et al. 1997, Bentz et al. 2002). Alternatively, DeSousa et al. (1998) present a means for correlating surface humidity to moisture content, and means for accounting for moisture in interpretation of sorptivity values.

Guidelines for assessing sorptivity values have not been established, but values of sorptivity for concrete specimens removed from some existing structures have been published. Bentz et al. (2002) provide early and later age ponding sorptivity values for cores or cast cylinders for concrete mixtures used for pavements in several states. DeSousa et al. (1997) provide sorptivity values for field testing and laboratory testing of cores removed from pavement slabs, a jersey barrier, and a bridge abutment. However, this sorptivity testing was performed using a surface-mounted test apparatus, and results may not be directly comparable to those of Bentz et al. (2002) due to the difference in test methodology. Hooton et al. (1993) present information on the results of sorptivity testing of specimen cast from several laboratory-batched concrete mixtures subjected to different curing conditions.

As discussed previously, permeability has generally been shown to serve as a good indicator of the durability performance of concrete bridge decks. The permeability of concrete is largely affected by water/cement ratio, but also of importance is the "degree of hydration, cement type, content of pozzolanic materials, entrained air, amount of paste, aggregate size, and possible defects such as cracks, pinholes and incomplete compaction (Geiker et al. 1995). Environmental exposure during curing and in service plays a role in the permeability of concrete. Researchers have found that the initial moisture content or degree of saturation of the concrete can have a significant effect on the field water permeability test results (Meletiou et al. 1992). The air permeability of concrete is particularly affected by moisture content. According to Neville (1995), "a change from near saturation to an oven-dried condition has been reported to increase the gas permeability coefficient by nearly 2 orders of magnitude." The difference in permeability of concrete exposed to different curing conditions has been found to become more pronounced in drier exposure conditions (Ewertson and Petersson 1993).

Permeability of concrete to both air and water are of interest, with testing for each not generally standardized (Neville 1995). Air and water permeability can be measured in the laboratory or in the field using several methods. In existing permeability test methods, "dimensions of the sample, the magnitude of the applied pressure, and the application of a confining pressure to the sample surfaces are some of the parameters varied (Geiker et al. 1995). In several popular methods, such as the Figg Method, a hole is drilled into concrete, and the water or air absorption rate from the hole is measured (Hall 1989). The Figg Method (as outlined in ACI 228.2R-98, "Nondestructive Test Methods for Evaluation of Concrete in Structures") is often utilized in laboratory permeability testing, and is also the basis of several commercially available field test kits. Guidance on interpretation of test results is often provided by the manufacturer of the test equipment, although test results from a number of means of permeability testing are presented in literature.

In service conditions, chloride ions often diffuse into concrete along with fluid. Chloride permeability (or penetrability) has been the subject of many research initiatives during the past several decades, with many studies aimed at understanding chloride diffusion theory, establishing test procedures and understanding their limitations, and linking test results to in-situ performance. A number of test methods to evaluate chloride permeability have existed for some time. These include the AASHTO T259 salt ponding test, the bulk diffusion test, and the AASHTO T277 (ASTM C1012) rapid chloride ion permeability test. Review of existing procedures for FHWA by Stanish et al. (2000) concluded that "no one test is a panacea, and different situations may require different tests."

2.1.3.3 Dynamic Modulus of Elasticity

The static modulus of elasticity relates the strain response of a material to applied stresses. The dynamic modulus of elasticity of concrete is "determined by means of vibration of a concrete specimen, only a negligible stress being applied," and therefore creep and microcracking do not affect the measured test results (Neville 1995). For concrete, the ratio of static modulus to the dynamic modulus is always smaller than one (Neville 1995), and several relationships have been developed relating these values over limited ranges using different mixture characteristics. The dynamic modulus of elasticity of concrete is highly sensitive to the cracking present in the specimen, and is therefore useful in evaluating changes in a test specimen due to chemical attack, freeze-thaw stresses, or other mechanisms. Results of dynamic modulus of elasticity testing can be most strongly correlated with compressive strength (Mohammad 2011).

Dynamic modulus testing is most often performed on specimens of a two to one length to diameter ratio, as outlined in ASTM C215. However other researchers have proposed a method for determining the dynamic modulus of elasticity using concrete disks (Leming et al. 1998). A study performed by Dilek (2008) focuses on the dynamic modulus of elasticity of concrete disks exposed to fire, freeze-thaw and rain prior to testing. Dilek proposes the use of a damage index which is a means to quantitatively assess the extent of damage of the concrete, since calculation of dynamic modulus of elasticity of concrete is very sensitive to condition of the specimen. Because of the sensitivity of dynamic modulus testing to the condition of the specimen used, research was also conducted to determine the effect of freeze-thaw cycles on determination of dynamic modulus of elasticity. Bairagi and Dubal (1996) indicate that freeze-thaw exposure lessens the dynamic modulus of elasticity values of concrete specimens.

In studies identified as part of this literature review, laboratory-cast and cured specimens were utilized, and freeze-thaw cycles, temperature changes and fire were also induced in a laboratory. A need exists for further research concerning dynamic modulus of concrete specimens exposed to field conditions.

2.2 Background and Supporting Information Provided by NCDOT

2.2.1 Inspection Reports and Drawings

Inspection reports and drawings for the bridges included in the study were provided to the research team by NCDOT personnel, and were reviewed throughout the study. Typically, the most recent inspection report for each bridge was reviewed prior to visiting the site to perform the field evaluation. For each bridge, information provided on the inspection reports and drawings, such as span lengths, lane widths, shoulder width and other geometric data was used to assist in generation of an Autocad drawing of a portion (or, in some cases, all) of the bridge. Prior to visiting the site, a preliminary sampling location plan was developed and noted on the drawing. This drawing was also used to record distresses observed during the field evaluation, as well as other field notes.

For some bridges, construction drawings were utilized to verify the location of lightweight and normalweight concrete deck sections (on bridges that contained both types of concrete) as well as to confirm geometric dimensions. Information on the construction drawings and field reports was also used to identify the superstructure of the portion of the bridge selected for the field evaluation. Construction drawings were not available for all bridges, and review of drawings was cursory.

2.2.2 Concrete Mixtures

Information pertaining to the concrete mixtures used on the bridge decks included in the study was obtained from NCDOT personnel and reviewed. Typically, information on the mixture proportions, cement composition, placement conditions, and fresh and hardened concrete test results used on the subject bridge decks was not available. Digital records of approved mixture designs were not available for any of the bridge decks included in this study.

A search of paper records by NCDOT personnel yielded approved mixture design submittals for four of the bridges (330354, 240231, 070038, and 070160). For each of these bridge decks, multiple mixture designs were submitted

and approved, and it is unclear which of the mixtures was specifically used for the portion of the deck included in the study. Typically, variations between proposed mixtures for a single project pertained to inclusion (or non-inclusion) of fly ash, or cement type. Additional insight into the mixture designs used in the bridge decks was gained through petrographic examinations. Results of petrographic examinations are presented in Section 5.7, Petrographic Examinations.

3. PROCEDURES

3.1 Identification of Bridge Decks

This Task was completed during August and September 2010. NCDOT personnel developed a preliminary list of candidate bridges and provided it to UNC Charlotte for review. From the preliminary list of candidate bridge decks, UNC Charlotte and NCDOT personnel collaboratively selected eighteen bridge decks for inclusion in the study. For each lightweight concrete bridge deck selected for inclusion in this study, a companion normalweight bridge deck of similar age, traffic loading, and environmental exposure was selected. Therefore, the eighteen selected bridge decks include nine lightweight concrete bridge decks and nine normalweight concrete bridge decks.

Climatic conditions vary across North Carolina, and bridges across the state receive differing exposure to moisture and freeze-thaw cycles. Deicing and anti-icing methods (including application of chloride-based deicers) vary throughout the state, as does the application frequency. Additionally, bridge decks near the coast may experience more chloride exposure due to proximity to (brackish water and seawater) than those inland. Effort was made to select bridges from three different regions of the state: the Mountains, the Piedmont, and the Coast. Regional breakdown of the selected bridge decks is as follows:

- Mountains – 4 bridge decks (2 normalweight, 2 lightweight)
- Piedmont – 4 bridge decks (2 normalweight, 2 lightweight)
- Coastal – 10 bridge decks (5 normalweight, 5 lightweight)

Bridge decks selected for inclusion in this study, along with information on the geographic region of the state, year constructed, traffic information, roadway carried, and feature or intersection crossed, is shown in Table 3-1. To facilitate ease of identification of pairs of decks, each bridge deck was given a Pair/ID designation. For each member of a pair, the normalweight concrete deck was designated as "#N," while the lightweight concrete deck was designated as "#L." In Table 3-1, for "Type of Deck," normalweight concrete decks are also listed as "NWC," while lightweight decks are listed as "LWC." Average daily traffic information (ADT) is also provided.

Table 3-1: Bridge decks included in this study.

Region	Pair/ID	Number	County	Type of Deck	Year Built	ADT	Roadway Carried	Feature or Intersection
Coastal	1N	070160	Bertie	NWC	1998	4,300	US17 NBL	Tributary to Chowan River
	1L	070038	Bertie	LWC	2000	9,400	US17	Chowan River
	2N	150012	Carteret	NWC	1995	1,300	NC12	Thorofare Bay Channel
	2L	150012	Carteret	LWC	1995	1,300	NC12	Thorofare Bay Channel
	3N	150014	Carteret	NWC	1994	6,200	NC101	Intracoastal Waterway
	3L	150014	Carteret	LWC	1994	6,200	NC101	Intracoastal Waterway
	4N	240083	Craven	NWC	1998	21,500	US70 EBL	Trent River
	4L	240231	Craven	LWC	2003	16,000	US17	Neuse River and US70
	5N	270012	Dare	NWC	1990	16,000	US64	Roanoke Sound
	5L	270012	Dare	LWC	1990	16,000	US64	Roanoke Sound
Piedmont	6N	330345	Forsyth	NWC	1998	68,000	I40 BUS	Salem Ave. and Southern RR
	6L	330254	Forsyth	LWC	1999	64,000	I40 BUS	Miller St. and Southern RR
	7N	590541	Mecklenburg	NWC	1989	8,500	NC16 SBL	Catawba River
	7L	590363	Mecklenburg	LWC	1992	8,000	NC16 NBL	Catawba River
Mountains	8N	580160	McDowell	NWC	2000	14,000	I-40 EBL	SR1763 and Muddy Creek
	8L	430120	Haywood	LWC	1999	14,000	US23,74	SR1177 and Eagle Nest Creek
	9N	580153	McDowell	NWC	2000	14,000	I-40 EBL	SR1803
	9L	580146	McDowell	LWC	1996	16,000	I-40 EBL	SR1741

The design characteristics of a bridge, particularly the superstructure, have been shown to influence cracking in bridge decks (Hadidi and Saadeghvaziri 2005, Hadidi and Saadeghvaziri 2005, TRB 2006). The type of superstructure comprising each of the bridges included in the study is shown in Table 3-2. For most pairs of bridges, the type of superstructure is similar. However, for lightweight bridge decks in some locations, it was not possible to find a companion normalweight bridge deck with a similar superstructure, that also closely matched in age, traffic, and geographic region. In the analysis portion of this report, differences in superstructure are considered in the findings where appropriate.

Table 3-2: Superstructures of bridges included in this study.

Region	Pair/ID	Number	Superstructure
Coastal	1N	070160	Reinforced concrete deck on prestressed concrete girders
	1L	070038	Reinforced concrete deck, prestressed concrete panels on prestressed concrete girders (continuous steel plate girdersused in main spans of bridge - not included in study)
	2N	150012	Reinforced concrete deck on prestressed concrete girders
	2L	150012	Reinforced concrete deck on prestressed concrete girders
	3N	150014	Reinforced concrete deck on prestressed concrete girders
	3L	150014	Reinforced concrete deck on prestressed concrete girders
	4N	240083	Reinforced concrete deck on prestressed concrete girders (widened)
	4L	240231	Reinforced concrete deck on continuous steel girders (prestressed concrete girders used in other spans of bridge - not included in study)
	5N	270012	Reinforced concrete deck on prestressed concrete girders
	5L	270012	Reinforced concrete deck on prestressed concrete girders
Piedmont	6N	330345	Reinforced concrete deck on steel plate girders (main spans) (prestressed concrete girders used on some approach spans – not included in study)
	6L	330254	Reinforced concrete deck on steel I-beams
	7N	590541	Reinforced concrete deck (stay-in-place metal forms at approach spans) on plate girders and continuous plate girders (main spans)
	7L	590363	Reinforced concrete deck on continuous steel I-beams (approach spans)(continuous steel girder/floorbeams used in main spans – not included in study)
Mountains	8N	580160	Reinforced concrete deck (stay-in-place metal forms) on prestressed concrete girders
	8L	430120	Reinforced concrete deck (stay-in-place metal forms) on steel I-beams (widened)
	9N	580153	Reinforced concrete deck (stay-in-place metal forms) on prestressed concrete girders
	9L	580146	Reinforced concrete deck (stay-in-place metal forms) on steel I-beams (widened)

Unfortunately after performing field work on bridge decks 4N and 4L, it was determined that 4L was incorrectly identified in NCDOT records as a lightweight concrete bridge deck. It is our understanding that this bridge was initially scheduled to receive a lightweight concrete bridge deck, but changes were made just prior to (or during) construction, and a normalweight concrete bridge deck was constructed instead. In following with the intent of this study (to compare lightweight concrete bridge decks and normalweight concrete bridge decks of similar age, exposure, and traffic loading), results from field and laboratory testing of bridge decks 4N and 4L are not included in this report. Therefore, the regional breakdown of the selected bridge decks as discussed in this report is as follows:

- Mountains – 4 bridge decks (2 normalweight, 2 lightweight)
- Piedmont – 4 bridge decks (2 normalweight, 2 lightweight)
- Coastal – 8 bridge decks (4 normalweight, 4 lightweight)

3.2 Field Evaluations and Testing

For each bridge deck, a sample section was identified for field evaluation and testing. To facilitate completion of fieldwork within the allowable lane closure hours in one working day, sections typically ranged from 140 feet to 280 feet in length. For smaller bridges (less than 100 feet), the sample section included the full length of the bridge deck. Thru-traffic needed to be accommodated during the work, so sample sections typically consisted of the shoulder and right-hand travel lane. When the total bridge length was longer than the sample section, effort was made to ensure that distress visually evident in the sample section was typical of the distress visually evident on other parts of the bridge deck. For some bridges, a portion of the ramp lane was included due to geometric constraints and safety considerations.

Since powder samples could not be collected for rapid chloride (RCT) testing if the surface of the concrete was wet, fieldwork was not performed during wet conditions. Additionally, fieldwork was typically not performed during freezing temperatures, as testing with the surface resistivity meter requires a saturated surface condition. When temperatures approached freezing, warm water was used to saturate the surface of the concrete for surface resistivity testing.

Field evaluations included visual surveys, removal of core samples and powder samples, and several field tests. Visual surveys performed by UNC Charlotte personnel included mapping cracks and other distresses on site plans as well as photographically documenting the condition of the decks within the constraints of the lane closures. Volkert Engineering was retained by NCDOT to assist UNC Charlotte with field evaluations. As part of their work, Volkert Engineering performed a chain drag of each deck to identify delaminations. Volkert Engineering also removed core samples and powder samples in locations selected by UNC Charlotte personnel. Core samples and powder samples were returned to UNC Charlotte laboratories for further testing. Field tests performed by UNC Charlotte personnel on each deck included air and water permeability testing and surface resistivity testing.

3.2.1 Visual Survey

A visual survey was performed on each of the bridge decks included in this study. On each bridge deck, the visual survey was limited to the sample section. Each visual survey was performed by the project PI in order to maintain consistency. The surveys were performed during dry conditions. Visual survey observations were noted on a field sketch that was drawn to scale in AutoCad and printed out prior to visiting the site. Prior to beginning each visual survey, the dimensions of the travel lanes were verified and the sample section length was noted on the field sketch.

Specific distresses identified during the visual survey included longitudinal cracks, transverse cracks, surface cracking, delaminations, and other surface distress. Cracks were only noted if they were visible by viewing the deck in a position bent no lower than the waist. If a crack was observed, the continuation of a crack was added to the field sketch if the observer could follow it by bending no lower than the waist. Delaminations were identified by Volkert personnel who performed a chain drag survey. Areas of delamination were noted on the field sketches by UNC Charlotte personnel. Upon return to UNC Charlotte, the visual observations made on hand-drawn field sketches were transferred into the AutoCad drawing of the sample section.

3.2.2 Location Selection and Removal of Cores and Powder Samples

During field evaluations and testing, thru traffic needed to be maintained at all times. Therefore, locations for removal of cores and powder samples were selected within the sample section, which typically consisted of the right travel lane and shoulder. For each bridge deck, the eight locations were identified and marked with spraypaint. At each of the locations, one or more core samples were removed, along with powder samples for chloride content testing.

On most bridges, the eight sampling and testing locations were laid out along a line oriented diagonally from the start of the sample section towards the opposite corner at the end of the sample section, as shown in Figure 3-1. The first location was typically offset five feet from the first joint and two feet from the right-side barrier. The diagonal line in which the locations were selected was always oriented in the direction of traffic, with the first location nearest the barrier and the last location closest to the open travel lane. This procedure typically resulted in

positioning of one to three sampling locations in the shoulder and five to seven sampling locations in the right travel lane. The eight locations were evenly spaced on each bridge deck. Based on the length of the bridge (or the sample section for larger bridges), the spacing between locations ranged from approximately 20 to 40 feet.

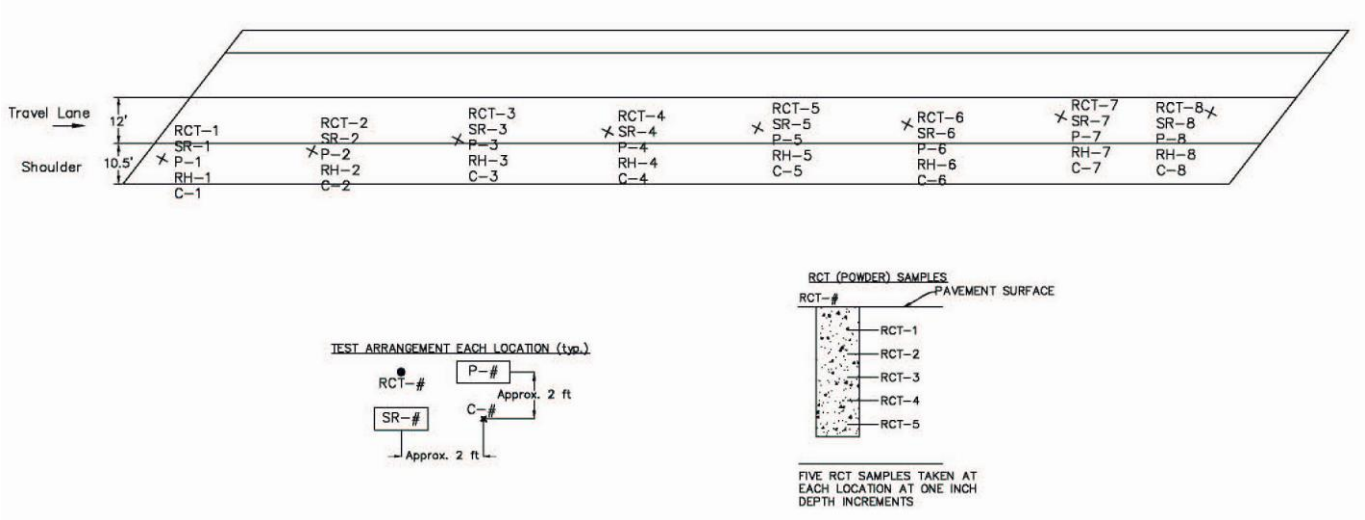

Figure 3-1: Typical sampling and testing location plan.

On smaller bridges, space constraints required a change in the sampling layout and spacing from a single diagonal line to a double diagonal line, as shown in Figure 3-2. This configuration typically resulted in two sampling locations in the shoulder and six locations in the travel lane, allowing adequate space between locations for movement of personnel and equipment during fieldwork activities.

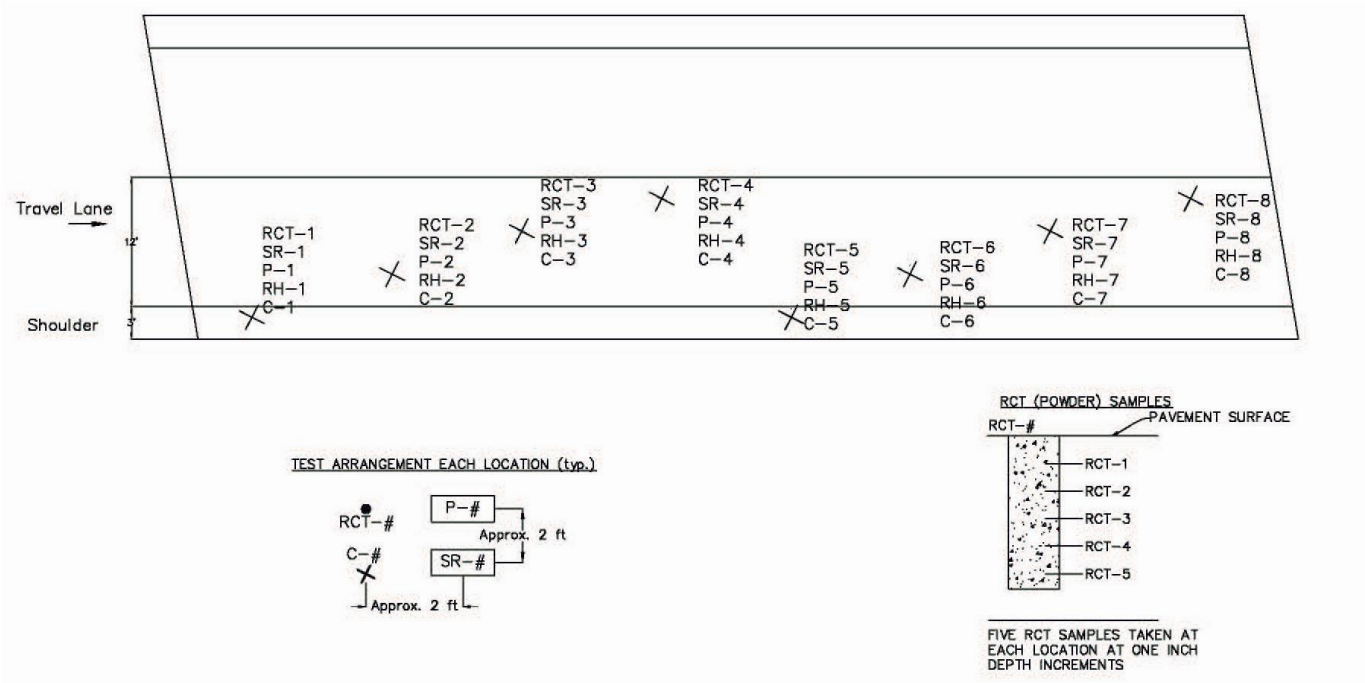

Figure 3-2: Typical sampling and testing location plan for shorter bridges.

Volkert Engineering personnel were responsible for removal of the cores and powder samples from each location. At each location, Volkert personnel used a locating device to identify the top layer of reinforcing steel. Cores were removed in a position that minimized the likelihood of encountering reinforcing steel with the drill bit. The lower layer of reinforcing steel was sometimes offset from the top layer of steel, and was not detected by the locating device. Therefore, whenever possible, drilling was stopped prior to cutting through the lower layer of reinforcing

steel. Cores were removed using a cold steel chisel and a hammer. To preserve the in-situ moisture content, cores were wrapped in plastic wrap and aluminum foil, and sealed in plastic bags for transport to UNC Charlotte's laboratory.

Powder samples of the concrete bridge decks were removed using a rotary hammer drill. At each location, five samples were taken within the upper five in of bridge deck. Additional information on sampling depths is presented in Section 3.3.5, Rapid Chloride Test (RCT). Between each sampling depth, compressed air was used to clean the drill bit and to blow remaining dust out of the hole.

3.2.3 Air and Water Permeability Tests

Field tests to evaluate air and water permeability were performed in general accordance with the Figg method as outlined in ACI 228.2R-98, "Nondestructive Test Methods for Evaluation of Concrete in Structures," using the Poroscope Plus test equipment manufactured by NDT James Instruments. This testing was typically the most time-consuming activity of fieldwork. Although effort was made to perform this test on multiple locations, the duration of the test did not allow multiple locations to be tested during the allowable lane closure times. Due the aforementioned time constraints and equipment problems, air and water permeability testing was typically performed at one to three locations per bridge deck.

Test locations were selected as shown in the test layout in Figure 3-1. At each test location, four 0.394 in (10 mm) diameter and 1.56 in (40 mm) deep holes were drilled, as specified by the equipment manufacturer. The four holes were drilled at the corners of a 3 in (76.2 mm) square. The configuration of the test holes is shown in Figure 3-3. The holes were blown out with compressed air, and a manufacturer-provided test plug was inserted into each hole. Prior to insertion of each plug, a lubrication compound approved by the manufacturer was spread onto the circumferential side of the plug. The lubricant was not put onto the bottom of the plug. After the each plug was inserted, a 0.394 in (10 mm) by 0.787 in (20 mm) void was left at the bottom of each hole. The test plugs were then expanded into the side walls of the hole using plastic screws provided by the equipment manufacturer. A lubricant was applied to the top of each test plug, and a hypodermic needle was inserted into each of the test plugs. The hypodermic needles remained in each test plug for both air and water permeability testing.

Figure 3-3: Air and water permeability test configuration.

At each test location, air permeability testing was performed first. The air tubing from the Poroscope Plus equipment was connected to a hypodermic needle in one of the test plugs, and a hand vacuum pump was used to evacuate the air from the void to vacuum pressure less than 7.98 psi (55 kPa). The Poroscope Plus equipment was then used to measure the time for the pressure in the hole to increase from -7.98 psi (-55 kPa) to -7.25 psi (-50 kPa).

At each test location, this procedure was repeated until the subsequent time readings stabilized to within approximately 2%.

After air permeability readings were taken on each of the four holes, water permeability testing was performed. Air tubing was removed from the Poroscope Plus equipment and the water line was attached to the equipment. The water line was connected from the Poroscope Plus equipment to one of the hypodermic needles, and the water line was attached to the equipment. A large syringe was used to force distilled water through the Poroscope Plus equipment and the water line until the void in the concrete at the bottom of the test hole was full of water, and all air had been removed from both the test hole and the water line. For each test, the Poroscope Plus equipment measures the time it takes for a meniscus in the water tubing to move 1.97 in (50 mm). This reading was recorded as the water permeability reading. At each test location, the water permeability test procedure was also performed until readings stabilized to within approximately 2%. At some locations, test times were exceedingly long (greater than approximately 13 to 15 minutes). For these test locations, the reading just prior to stopping the test was recorded.

3.2.4 Surface Resistivity Tests

Surface resistivity measurements were made on selected locations on the bridge deck surface. The commercially-available surface resistivity meter used for this testing utilizes the Wenner probe method of measurement. A voltage potential is applied to the concrete surface through the two outer pins of the probe, and the resultant potential difference between the inner pins is measured and subsequently converted to kΩ•cm. Additional background information on the Wenner probe method is presented in Section 2.1, Literature Review. Surface resistivity testing is typically performed on cast concrete cylinders, as outlined in AASHTO TP 95-2011, "Standard Method of Test for Surface Resistivity Indication of Concrete's Ability to Resist Chloride Ion Penetration." A test protocol for use of the surface resistivity meter in field applications has not yet been developed into an ASTM or AASHTO standard test method. Therefore, a test protocol developed by other researchers and utilized in similar field applications (Ghosh et al. 2012) was used for this work.

Surface resistivity measurements were taken at eight locations on each bridge deck. To minimize the influence of reinforcing steel on the surface resistivity measurements, in the proximity of each test location, a pachometer device was used to identify several bars in the top mat of reinforcing steel. Locations for surface resistivity testing were positioned between both transverse and longitudinal reinforcing bars, with the surface resistivity meter placed parallel to the direction of travel.

Prior to performing surface resistivity testing on each bridge deck, test locations were conditioned to saturate the near surface concrete and to lower the temperature. Each test location was brushed with a synthetic bristle brush to remove surface debris. Approximately a half gallon of water was poured on the surface of the deck and a wet towel was placed on the wet surface. An additional half gallon (approximately) of water was poured on the towel. An eight to ten pound bag of ice was then placed on the wet towel. Prior to placing the bag of ice on the wet towel, a number of holes were sliced into the underside of the bag to allow the melt water to continue to saturate the towel and deck surface. The bag of melting ice was allowed to remain on the surface of the deck for at least two hours prior to performing the surface resistivity testing.

Once the minimum two-hour conditioning time had elapsed, the bag of ice and wet towel was removed from the test location. Excess water was removed from the surface of the saturated test location using a synthetic bristle brush. A minimum of eight readings were taken at each test location, with readings spaced approximately one in apart. For this work, the four adjustable probes were each spaced 2 in (5.08 cm) apart. A temperature measurement of the concrete deck surface was taken within a few seconds of each surface resistivity measurement. Surface resistivity testing is shown in Figure 3-4, below.

Figure 3-4: Surface resistivity testing.

3.2.5 Rebound Hammer Tests

A rebound hammer was used to determine the rebound number of the concrete at eight test locations on each bridge deck. This testing was performed in general accordance with ASTM C805, "Standard Test Method for Rebound Number of Hardened Concrete." At each test location, ten readings were taken at three areas of the surface, each area spaced several feet apart. Although a brush was used to remove visible debris from the test surface, no additional preparation of the surface was performed prior to testing.

3.3 Laboratory Testing

Concrete cores and powder samples removed from each bridge deck were returned to UNC Charlotte's laboratory for conditioning and testing. Prior to conditioning and testing, each core remained wrapped in plastic wrap and aluminum foil, sealed in the plastic bag it was placed into after removal from the bridge deck (Figure 3-5). Powder samples remained sealed in glass jars, shown in Figure 3-6. The cores and powder samples remained in a controlled laboratory environment until testing.

Figure 3-5: Concrete cores as wrapped for transport to UNC Charlotte and subsequent storage until testing.

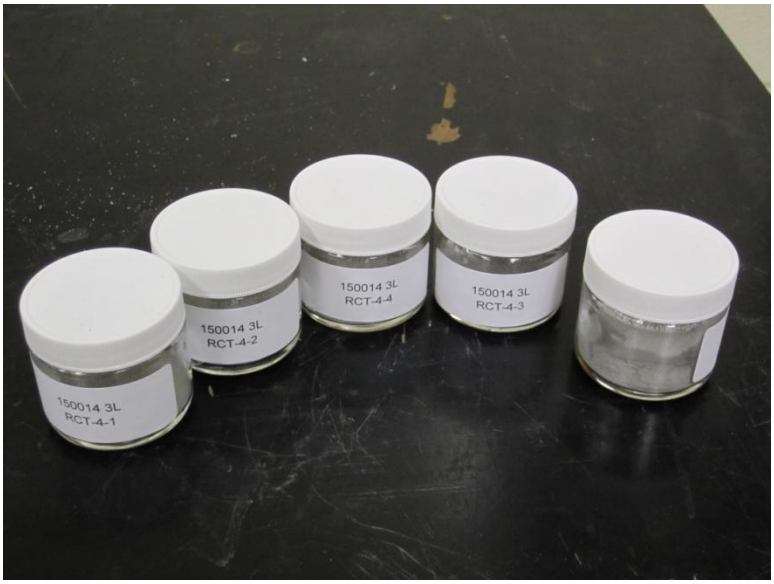

Figure 3-6: Concrete powder samples in sealed jars.

3.3.1 Density and Moisture Content

Selected cores and pieces of cores were tested to obtain values for unit weight and moisture content of each bridge deck. This testing was performed in general accordance with ASTM C642, "Standard Test Method for Density, Absorption, and Voids in Hardened Concrete." The apparent density was calculated for each specimen tested. The boiling procedure was not used in determining the saturated mass.

3.3.2 Compressive Strength

Cores were tested for compressive strength in general accordance with ASTM C42 "Standard Test Method for Obtaining and Testing Drilled Cores and Sawed Beams of Concrete" and ASTM C39 "Standard Test Method for Compressive Strength of Cylindrical Concrete Specimens." The cores selected for testing were typically those that had the largest length to diameter (L/D) ratios and did not contain reinforcing steel. The ends of cylinders were sawcut and a capping compound was applied to specimen not meeting the perpendicularity and planeness requirements of ASTM C39. Compressive strength tests were performed in accordance with ASTM C39, and for cores with L/D ratios less than 1.75, a correction factor was applied as outlined in ASTM C42.

3.3.3 Dynamic Modulus

Testing to determine the dynamic modulus of elasticity of selected cores was performed in general accordance with ASTM C 215 "Standard Test Method for Fundamental Transverse, Longitudinal, and Torsional Resonant Frequencies of Concrete Specimens." Only cores having a length to diameter ratio or two or greater were used for this testing. The ends of the cores were sawcut prior to testing to obtain more plumb specimens, and the mass and dimensions of each specimen was recorded. Prior to and during testing, specimens were stored in a conditioned laboratory setting.

The cores were supported such that free vibration could be achieved. A small steel frame was used to support the hanging specimens. The accelerometer was attached to the dry concrete surface core using beeswax. A frequency counter in LabView software was used to measure the frequency data. Using a steel hammer, each specimen was struck at approximately its midpoint to trigger the data acquisition. For each specimen, the test was repeated two additional times and the average frequency was calculated. If the frequency measurement varied by more than 10%, the test was repeated. The transverse frequency, specimen mass, and specimen dimensions were then used to calculate the dynamic modulus of elasticity.

3.3.4 Sorptivity

Sorptivity is a measure of the rate of absorption of water by concrete. The rate of absorption of concrete will depend on mixture proportions, type of aggregate, air content, the existence of cracks or internal defects, and surface finish characteristics. Since water can transport aggressive agents into concrete, low sorptivity is viewed as a favorable characteristic of concrete when assessing durability performance. For this study, two methods were used to determine the sorptivity of each specimen. First, sorptivity testing was performed in general accordance with ASTM C1585, "Standard Test Method for Measurement of Rate of Absorption of Water by Hydraulic Cement Concretes," in which the rate of absorption through capillary rise (or "suction") is determined. Second, sorptivity testing was performed via the ponding test developed by Bentz et al. (2002). A more detailed background on these tests is presented in Section 2.2.

Specimens for both ASTM C1585 capillary suction tests and ponding tests were prepared using the top 2 in (50.8 mm) of cores. Sorptivity test results have been shown to be influenced by the moisture content of test specimens (DeSousa et al. 1998). Therefore, it is critical that specimens be conditioned to a prescribed moisture content prior to performing sorptivity tests. Specimen conditioning procedures used for both the ASTM C 1585 test and the ponding sorptivity test were the same. The specimens were put into desiccators with a solution of 2.83 oz (80.2 g) of potassium bromide mixed with 3.53 oz (100 g) of water. The desiccators were then placed into an oven set at $122 \pm 35.6^{o}F$ ($50 \pm 2^{o}C$) for three days. The specimens were then placed in airtight containers for a minimum of 15 days at a room temperature, using a separate container for each specimen.

Sorptivity testing in accordance with ASTM C1585 was performed first. Once conditioned, the specimens were removed from the containers and weighed. For each specimen, four diameters were measured and the average was calculated. The circumferential sides of each specimen were sealed with water-resistant duct tape to prevent distilled water from seeping into the circumferential side surfaces of the specimen. Plastic was then draped over the top surface of the specimen (the surface not exposed to the distilled water) and a rubber band was used to secure it in place. Each specimen was then weighed in order to obtain a weight that included the duct tape, plastic, and rubber band.

Each specimen was placed into approximately 0.040 in to 0.118 in (1 to 3 mm) of water, with the submerged test surface sitting on three spherical single-point supports. Specimens were weighed at immersion durations of 1 min, 5 min, 10 min, 20 min, 30 min, 60 min, 2 hr, 3 hr, 4 hr, 5 hr, 6 hr, 1 day, 2 days, 3 days, 4 days, 5 days, and 6 days. Measurements were taken at times that were within the tolerances specified in ASTM C1585. Prior to weighing each specimen at the prescribed time, the specimen was dabbed with a damp paper towel to remove excess distilled water. Each measurement did not take longer than 15 sec, and after weighing, each specimen was immediately replaced on the supports, with the bottom surface submerged in the distilled water. A photograph of specimens prepared for ASTM C1585 sorptivity testing is shown in Figure 3-7.

Figure 3-7: ASTM C1585 sorptivity testing.

Prior to performing the ponding sorptivity testing, specimens were reconditioned in accordance with the same conditioning procedure utilized for the ASTM C1585 sorptivity test. For the ponding test, water resistant duct tape was applied to the circumferential sides of each specimen, with approximately 1 in of tape allowed to extend above the top surface of the specimen. A rubber band was placed around the tape at the top of the core, and a circular hose clamp was then tightened around the rubber band and tape. The rubber band facilitated even distribution of pressure from the hose clamp, creating a barrier for the distilled water added to the reservoir created by the duct tape extended above the top of the core. Specimens prepared for ponding sorptivity testing are shown in Figure 3-8.

Figure 3-8: Ponding sorptivity testing.

At the start of testing, distilled water was placed into a reservoir created by the water-resistant duct tape on the top surface of the core. For each specimen, distilled water was added to a depth of approximately 0.118 in (3 mm) above the surface. Weight measurements were obtained at the same intervals prescribed for the C1585 testing procedure. Prior to weighing each specimen, the water in the reservoir was poured into a waste container, and a damp cloth was used to blot the surface to remove excess distilled water. After the specimen was weighed, new distilled water was added to the reservoir, and the test continued. For the duration of the test, the depth of distilled water was maintained at approximately 0.118 in (3 mm) above the surface of each specimen.

3.3.5 Rapid Chloride Test (RCT)

The Rapid Chloride Test (RCT) by Germann Instruments was used to determine the chloride content of powder samples of concrete removed from eight locations on each bridge deck. Powder samples were obtained using a rotary hammer drill, as discussed in Section 3.2.2. Chloride content tests were performed on five powder samples from each location in order to obtain a profile of the chloride content of the upper five in of the bridge deck. The sample representative of the 1 in (24.4 mm) depth was comprised of powder obtained by drilling at depths between ½ in and 1½ in, the sample representative of the 2 in (50.8 mm) depth was comprised of powder obtained by drilling at depths between 1½ in and 2½ in, and so forth.

The RCT test kit includes an electrode, electrometer, electrode wetting agent, calibration liquids, and test vials filled with 10 mL of proprietary extraction liquid (acid solution). After following the manufacturer prescribed procedure for adding concrete powder samples to the test vials, chloride ions from the concrete powder become incorporated into the solution in the test vial. The voltage reading from a calibrated electrode submerged into the solution can be used to determine the chloride content of each powder sample.

Prior to each day's testing, the electrode was calibrated using manufacturer-provided calibration liquids with chloride concentrations of 0.005%, 0.020%, 0.050%, and 0.500%. To perform the calibration, the electrode was

placed into each of the calibration liquids and the voltage reading (in mV) was allowed to stabilize. The electrode was cleaned between each of the calibration liquids. Voltage readings for each known solution were plotted against chloride content (on a semi-logarithmic scale), and a line of best fit was determined using a spreadsheet program. The equation of this best fit line was then used to correlate voltage readings obtained while testing vials prepared using powder samples obtained from the bridge decks.

After electrode calibration was performed (once for each day's testing), concrete powder samples in the extraction liquid were tested. To perform each test, 0.053 oz (1.5 grams) of powder (measured within a tolerance of ± 2%) was weighed and put into the test vial with the proprietary extraction solution. The test vial was shaken for 5 min. After the vial was shaken for 5 min, the cap was loosened to allow gas to escape and then retightened. As prescribed by the manufacturer, test vials were allowed to sit overnight, allowing adequate contact time between the powder sample and the extraction liquid. The following morning, the electrode was submerged into each vial, the reading was allowed to stabilize, and the measurement was recorded. Between test vials, the electrode was cleaned using distilled water as prescribed by the equipment manufacturer. Using the calibration curve prepared for the day's testing, the mV readings for each vial were converted into chloride content (in percent). The RCT test setup is shown in Figure 3-9.

Figure 3-9: Rapid Chloride Test (RCT).

The chloride content of concrete is often reported as pounds of chloride per cubic yard of concrete. The percent chloride values obtained using the calibration curve were multiplied by a factor of 38.15 (pcy/1% Cl) for normal weight bridge decks, and 34.462 (pcy/1% Cl) for light weight bridge decks to obtain pounds of chloride per cubic yard of concrete. These factors were obtained by assuming concrete unit weights of 141.6 pcy for normalweight concrete and 127.6 pcy for lightweight concrete.

3.3.6 Rapid Chloride Permeability Test (RCPT)

Rapid chloride permeability tests (RCPT) were performed in accordance with ASTM C1202, "Standard Test Method for Electrical Indication of Concrete's Ability to Resist Chloride Ion Penetration." This test is typically performed on specimens prepared from cast cylinders. For this study, RCPT tests were performed on 2 in thick test specimens cut from the 4 in diameter cores removed from the bridge decks.

Identification of the best locations for sawcutting test specimens from the cores proved to be somewhat challenging. Cores typically ranged from 4 in to 7 in in length, and some contained pieces of reinforcing steel, which cannot be present in RCPT test specimens. To provide suitable specimens for all tests performed as part of this work, it was necessary to limit the number of cores allocated for preparation of specimens for each test method. Typically, only two cores could be sawcut to obtain RCPT specimens. Additionally, to minimize the effects of ingressed chlorides

on the test results, the optimal location for test specimens used for RCPT testing would be as low as possible on the core (furthest from the bridge deck surface).

To addresses the aforementioned limitations, a strategy was developed to assist with identification of the locations for sawcutting the RCPT test specimens. For each bridge deck included in the study, a total of four specimens were prepared, removed from at least two different cores. For each bridge deck, two test specimens were cut from locations deemed "low" (below a depth of 4 in) and two test specimen were cut from locations deemed "high" (from below a depth of 1½ in). One exception was bridge deck 2N, where only three specimens were tested. Reinforcing steel placement on this bridge deck resulted in short core lengths, and many of the cores contained some of the top layer of reinforcing steel.

Two RCPT test machines (manufactured by RLS Instruments) were provided by NCDOT for use on this study. Each RCPT test machine could test four specimens at a time; therefore running both RCPT test machines at the same time allowed for eight test specimens to be tested simultaneously. In order to facilitate comparison of the pairs of bridge decks, four specimens from a lightweight concrete bridge deck were tested at the same time as four specimens from the companion normalweight concrete bridge. For example, the four test specimens from bridge deck 1L were tested at the same time as the four test specimens from bridge deck 1N. The specimens from each bridge deck were assigned to terminals on the RCPT test machines in a manner that allowed two specimens from each bridge to be tested on each piece of equipment, with one "high" specimen and one "low" specimen on each machine.

The circumferential sides of each specimen were coated in fast setting epoxy, which was allowed to cure overnight. Prior to testing for chloride ion permeability, test specimens were conditioned using the vacuum saturation procedure specified in ASTM C1202. The vacuum saturation apparatus is shown in Figure 3-10.

Figure 3-10: Vacuum saturation of rapid chloride permeability test specimens.

Specimens were placed in a vacuum desiccator, and an attached vacuum pump was used to decrease the pressure in the desiccator to less than 50 mm Hg (6650 Pa). The specimens were allowed to remain under a vacuum for 3 hr. After 3 hr, de-aerated water was allowed to flow into the desiccator. While the de-aerated water was put into the desiccator, the vacuum pump remained on, and care was taken to not allow air to flow into the desiccator through the water tubing. The de-aired water was added to a depth that fully submerged the specimens, and the stopcock on the water feed line was closed (preventing air from flowing into the desiccator). The vacuum was allowed to run for one hour after the specimens were submerged. At the end of this hour, the vacuum pump was turned off, and air was allowed to flow into the desiccator. The specimens were then allowed to soak in the water for 18 ± 2 hr.

After vacuum saturation, each test specimen was placed between two test cells, and was sealed in place with silicone caulk. Test cells for this test were manufactured from a polymethylmethacrylate (e.g., Plexiglas) material. Each test cell had metal mesh mounted in front of a reservoir capable of holding a chemical reagent in contact with the concrete test specimens. The metal mesh in each test of the test cells facilitated application of a voltage potential across the concrete test specimen, via wires connected from banana plugs on the test cells to the RCPT equipment.

After the caulk had adequately cured, the test specimens, mounted in the test cells, were connected to the RCPT test equipment, with each cell on its own circuit. This test setup is shown in Figure 3-11.

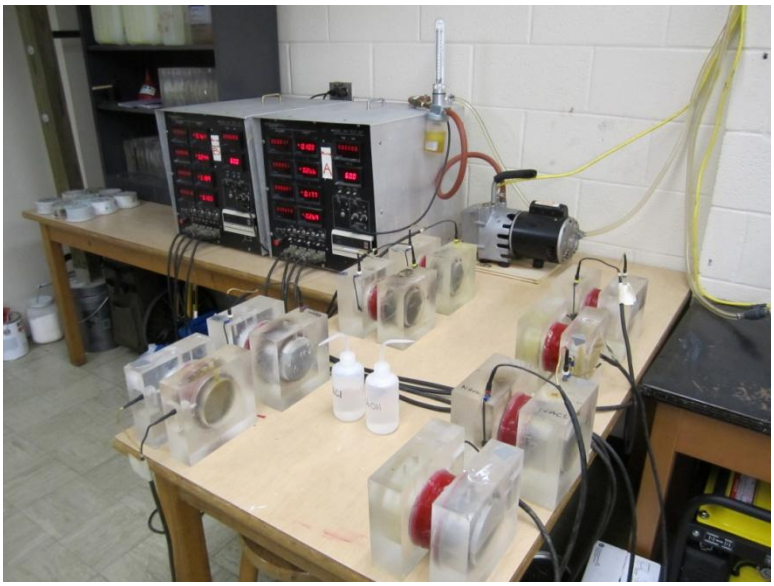

Figure 3-11: Rapid chloride permeability testing (RCPT)

For each specimen, the reservoir of the test cell attached to the positive terminal was filled with a 0.3 N sodium hydroxide solution, and the reservoir of the test cell attached to the negative terminal was filled with a 3% (by mass) sodium chloride solution. Using the RCPT equipment, a 60.0 V potential was applied to each test cell. Instantaneous current readings and total charge passed readings were obtained at 30 min intervals for the duration of the six-hour test.

3.3.7 Petrographic Examinations

From selected cores from each bridge deck, polished surfaces and fractured surfaces were prepared for macroscopic and microscopic observations. For all cores, the upper several inches of the core sample are of primary interest because of the influence of the upper portion of the bridge deck on the integrity and performance of the wearing surface. Compared to concrete lower in the pavement slab, the upper several inches of the concrete pavement tend to exhibit more substantial materials-related distress and cracking. The upper portion of the pavement is subjected to higher stresses from external loads, is often exposed to more moisture, and potentially experiences more freeze-thaw cycles.

In selecting the orientation of the vertical plane for polished samples, an attempt was made to choose the direction that would most likely intersect cracks. Selection of the orientation of the vertical plane for the polished surfaces is summarized as follows:

- If macrocracks are visible on the top surface of the core, the vertical plane for the polished sample was selected perpendicular to the macrocracks.

- If no macrocracks are visible on the top surface of the core, the vertical plane for the polished sample was selected in an orientation perpendicular to grooves, if present.

- If macrocracks and grooves are not present on the top surface of the core, the orientation of the vertical plane for the polished sample was selected at random.

Polished samples were prepared by UNC Charlotte. The samples were sawcut along the vertical plane and polished using progressively finer grit material. Fractured surfaces were prepared by using hand tools and compression testing equipment. No thin-section samples were prepared as part of this work. Fractured and polished surfaces were observed using a stereomicroscope at magnifications ranging from 7x to 45x. Observations were performed in general accordance with ASTM C856, "Petrographic Examination of Hardened Concrete." Photographs were taken of the samples using a camera mounted on the trinocular tube of the stereomicroscope.

Microscopic observations included:

- Observation of the general characteristics of the concrete, including the paste, aggregates, air void system.

- Observation of microcracks present within the paste or aggregates.

- Observation of secondary deposits evident within voids and/or microcracks, or around aggregate perimeters, and if possible, visually identifying secondary deposits such as secondary ettringite.

- Observation of reaction rims present around aggregates.

Microscopic observations were used to provide an opinion regarding the quality of the paste, the quality of paste-aggregate bonds, and the overall quality of the concrete comprising the sample. Microscopic observations, along with macroscopic observations of the polished surface, were used to qualitatively estimate the air void content of each sample, and, if appropriate to qualitatively estimate the amount of secondary deposit infill in the void space. The air contents of samples were not quantitatively determined using the procedure outlined in ASTM C457, "Standard Test Method for Microscopical Determination of Parameters of the Air-Void System in Hardened Concrete," but were instead approximately estimated based on the experience of the observer.

4. RESULTS OF FIELD SURVEY AND FIELD TESTING

4.1 Visual Survey

Observations made during visual surveys of the bridge decks (as outlined in Section 3.2.1, Visual Survey) were recorded on field sketches, and subsequently transferred into AutoCad drawings. These drawings are included in Appendix A – Visual Survey Results. Distresses that were identified and recorded during the visual survey included longitudinal cracks, transverse cracks, pattern (surface) cracking, delaminations, and other surface distress. Distresses are shown on the drawings in the format outlined by the Federal Highway Administration (FHWA) in the Distress Identification Manual for the Long-Term Pavement Performance Program (2003). Cracks are shown on the drawings as lines, while areas of pattern cracking are shown with hatching.

In order to provide additional insight into the condition of the bridge decks, a modification to the procedures outlined in FHWA's Distress Identification Manual was made when denoting pattern cracking on the visual survey field sketches and notes. As part of the FHWA's distress identification procedure, severity levels are not assigned to map cracking (sometimes called "craze cracking") visible in pavements. In an effort to assist with judging the relative condition of bridge decks based on visual distresses, the project team assigned severity levels to observed pattern cracking (low, moderate, and high severity).

Pattern cracking denoted as low severity was typically only faintly visible during the observations, comprised of fine hairline cracks (as "hairline" is defined in ACI 201.1, "Guide for Conducting a Visual Inspection of Concrete in Service"). The cracks were usually networked to some extent, but often, areas of cracks were just beginning to network. Typical pattern cracking denoted as low severity is shown in Figure 4-1. Pattern cracking denoted as moderate severity was easily visible during the visual survey, and the widths of the cracks were larger than what would be considered hairline by ACI 201.1. Typical pattern cracking denoted as moderate severity is shown in Figure 4-2. No pattern cracking observed during this study was judged to be high severity cracking.

Figure 4-1: Typical pattern cracking denoted as low severity.

Figure 4-2: Typical pattern cracking denoted as moderate severity.

As outlined in the literature review presented in Section 2.1, there are many factors that influence cracking of bridge decks. In addition to factors related to concrete mixture design, factors related to placing, curing, and finishing of the bridge deck can play a role in crack formation and propagation. Bridge design factors, such as superstructure type, span lengths, skew angles, and joint details also affect cracking of bridge decks. A description of the superstructures of the bridges included in this study is provided in Table 3-2.

Continuous steel girders have historically been associated with more extensive bridge deck cracking (Darwin et al. 2004). The two bridge decks with continuous span girders (bridge decks 6N and 6L) exhibited some of the more extensive pattern cracking and some transverse cracking, and it is possible that some of this cracking could be the result of stresses present in the deck slab due to the continuous steel girders, rather than from concrete materials-related causes. The most extensive transverse cracking observed on bridge decks included in the study is present on bridge decks 7N and 7L, which are supported by steel plate girders and steel I-beams, respectively. Transverse cracking on bridge deck 7N is shown in Figure 4-3. Transverse cracking on these decks may also be related to structural-related stresses, loads applied too soon after the deck was constructed, or other reasons. These two bridges are also two of the oldest bridges included in the study, and traffic loads could also play a role in the development of transverse cracks.

Figure 4-3: Typical transverse cracking on bridge deck 7N.

Bridge decks with stay-in-place metal forms (bridge decks 8N/8L and 9N/9L) also tended to exhibit more longitudinal and transverse cracking than bridge decks on precast concrete girders and non-continuous steel girders. Stay-in-place metal forms are not typically bonded to the concrete deck, although some restraint due to partial bonding and friction can be expected. It is interesting to note that although all four of these bridges have stay-in-place forms, they are supported by different types of girders, with bridges 8L and 9L on widened steel I-beams, while bridges 8N and 9N have stay-in-place forms on prestressed concrete girders. Some of the cracking observed on the bridge decks 8N, 8L, 9N, and 9L may also be attributable to the superstructure design, rather than from concrete materials-related causes. Other bridge decks exhibiting transverse cracks (albeit to a lesser extent than in bridge decks 6N, 6L, 7N, 7L, 8N, 8L, 9N, and 9L), include bridge decks 1L, 3N, and 5N.

For each bridge deck included in the study, the sample section included one or more expansion joints. Distress observed near expansion joints typically included cracking and/or spalling. Cracks are often oriented perpendicular to the expansion joint, and can likely be attributed to additional restraint due to reinforcing details at the expansion joints. Cracks extending perpendicular from an expansion joint are shown in Figure 4-4. For several bridge decks, such as bridge deck 8L, the most significantly distressed areas were located in the proximity of the expansion joints. Other bridges exhibiting longitudinal cracks oriented perpendicular to joints included bridge deck 1N, 1L, 2L, 3N, 5N, 7L, 7N, 8N, 9L, and 9N.

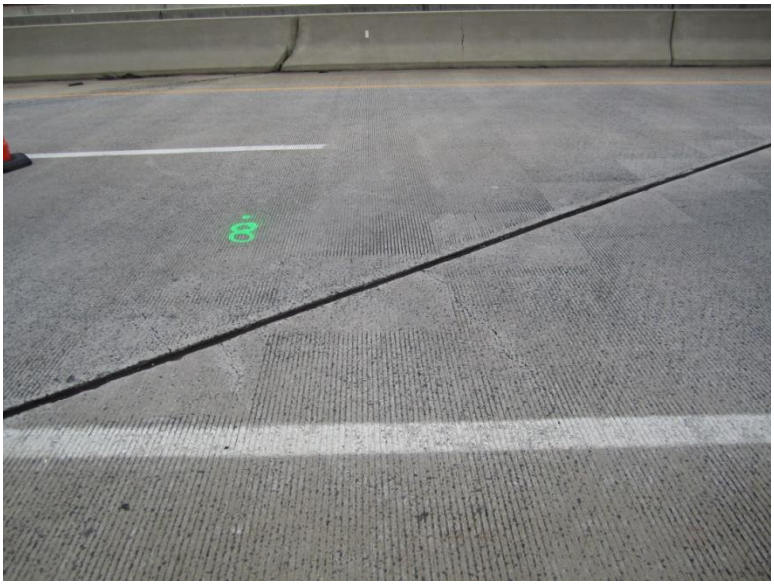

Figure 4-4: Cracks extending perpendicular to expansion joint on bridge deck 9L.

Cracks were also observed in the vicinity of bents. Reinforcing details near expansion joints, as well as issues related to transitions between positive and negative moment regions, can contribute to cracking near supports. Distresses were also observed at joints at abutments. If integral abutments are used in the bridge design, cracking of bridge decks can occur some distance from the end joints.

Longitudinal cracks that are not adjacent to expansion joints were also observed on several bridge decks, including bridge decks 5L, 7N, 8N, and 9N. A typical longitudinal crack is shown in Figure 4-5. Longitudinal cracks on bridge decks can be the result of a lever arm forming due to cantilever action from wheel loads applied to the deck alongside of girders. These could be result of overstress due to oversized loads, or some other overload issue related to detailing of reinforcement. Longitudinal cracks could also have resulted from vehicle impacts into barriers.

Figure 4-5: Typical longitudinal cracking on bridge deck 8N.

Pattern cracking was observed on a number of bridge decks included in the study. As discussed in the literature review presented in Section 2.1, pattern cracking can be attributed to a number of factors, both directly related and unrelated to concrete materials characteristics. The most severe pattern cracking was observed in bridge decks 6N and 6L. These bridge decks, located on I-40 westbound in Winston-Salem, North Carolina, had the highest traffic loading (ADT of 68,000 and 64,000, respectively). This pattern cracking could have initiated due to materials related issues, but may also have been exacerbated due to traffic loads. Typical moderate severity pattern cracking on bridge deck 6N is shown in Figure 4-6.

Figure 4-6: Typical moderate severity pattern cracking on bridge deck 6N.

Pattern cracking was also observed on bridge decks 1N, 1L, 5N, 7N, 7L, and 8L. Typical low severity pattern cracking is shown in Figure 4-7. Of interest are the bridge deck pairs where one bridge deck exhibits pattern cracking and the other bridge deck does not. Bridge decks 5N and 5L are on the same bridge, the bridge on US 64 spanning the Roanoke Sound to provide access to the Outer Banks. Pattern cracking (deemed low severity) was observed over much of the normalweight portion of the bridge deck observed, while no pattern cracking was observed in the lightweight concrete deck. Bridge deck 5L did, however, exhibit a series of relatively short cracks

oriented in the longitudinal direction (shown in Figure 4-8). The cause of these cracks is not readily evident at this time.

Figure 4-7: Typical low severity pattern cracking on bridge deck 1N.

Figure 4-8: Typical relatively short longitudinal crack on bridge deck 5L.

Another pair exhibiting a difference in the presence of pattern cracking was bridge deck pair 8L and 8N. Bridge deck pair 8L and 8N may not be the strongest pairing, as they are on two different roadways in two separate counties. However, the ADT for these two bridge decks is similar, as are the ages. Pattern cracking was present in bridge deck 8L, but not bridge deck 8N.

To summarize, bridge decks included in this study exhibited a wide variety of distresses. Some bridge decks had little to no visible distress, and other bridge decks had a significant amount of linear and pattern cracking. It is important to remember that bridge decks included in this study were typically 10 to 20 years of age at the time of the site visit, which can be up to 1/3 of the design life of the structure. Ultimately, information obtained during visual surveys was useful in evaluating field testing and laboratory testing results. In some instances, poor field and/or laboratory test results was linked to distress that was evident during the visual survey.

4.2 Air and Water Permeability Tests

Air permeability and water permeability tests were performed in the field using the Poroscope Plus test equipment, which measures permeability in general accordance with the Figg Method. The Poroscope Plus readings for air permeability and water permeability readings are in units of seconds. In literature provided with the Poroscope Plus, NDT James Instruments provides an equation for converting air permeability readings into an Air Exclusion Rating (AER), and an equation for converting the water permeability reading into a water absorption rate (WAR). These equations are shown below as Eq. 1 and Eq. 2.

$$AER = \frac{t}{\left[\frac{55V}{59} - V\right] \times \frac{55.5}{100}} = 19.05 \times \frac{t}{V} \qquad \text{(Eq. 1)}$$

$$WAR = \frac{t}{10}\left(\frac{sec}{ml}\right) \times 10^3 \qquad \text{(Eq. 2)}$$

In Eq. 1 and Eq. 2, t is the measured time (seconds) and V is the volume of the apparatus, including the test hole (in mL). For the Poroscope Plus equipment, V is 77.1 mL, so AER = 0.247×t. Literature provided with the Poroscope Plus equipment (NDT James Instruments 2007) "gives the tentative values for air and water permeability times and calculated AER ratings for concrete of varying protective quality for embedded reinforcement." Information from this table is shown in Table 4-1. This table is based upon "tentative ranges" of the representative types of material, as outlined by Figg (1989). The representative types of materials presented by Figg (1989) are also shown in Table 4-1. Color has been added to this table to assist in interpreting results presented subsequently in this section.

Table 4-1: Values for air calculated AER and WAR for concrete of varying protective quality for embedded reinforcement (from NDT James Instruments 2007 and Figg 1989).

Concrete Category	Protective Quality	Air Permeability		Water Permeability	Type of Material (from Figg 1989)
		Time (sec)	AER (s/mL)	WAR (sec/ml)	
0	Poor	<30	<8	<3	Porous mortar
1	Not very good	30-100	8-25	3-10	20 MPa (2900 psi) concrete
2	Fair	100-300	25-75	10-30	30-50 MPa (4350-7250 psi) concrete
3	Good	300-1000	75-250	30-100	Densified, well-cured concrete
4	Excellent	>1000	>250	>100	Polymer-modified concrete

For each bridge deck included in the study, air permeability and water permeability tests were performed at one or more test locations. At each test location, multiple readings were taken as outlined in Section 3.2.3, Air and Water Permeability, and the test results for each test location were averaged. Subsequently, for each bridge deck, the average air permeability and average water permeability readings for all test locations were averaged in order to obtain an average air permeability and average water permeability reading representative of the bridge deck. The average air permeability and average water permeability for each bridge deck were then converted into average AER and average WAR values, and are shown in Table 4-2. The Poroscope Plus equipment stopped working during water permeability testing on bridge deck 6N, so no reading for water permeability was obtained.

Table 4-2: Average Air Exclusion Rates (AER) and average Water Absorption Rates (WAR)

Bridge Deck	Average Air Exclusion Rate, AER (sec/ml)	Average Water Absorption Rate, WAR (10^3 sec/ml)
1N	29.4	44.6
1L	16.8	47.5
2N	9.2	4.3
2L	19.0	68.5
3N	24.8	17.9
3L	8.3	75.9
5N	9.4	3.4
5L	8.5	15.8
6N	6.4	N/A
6L	14.0	12.4
7N	4.4	5.1
7L	3.3	2.9
8N	49.4	7.7
8L	22.5	9.9
9N	22.1	45.3
9L	28.0	7.1

Assessing the air permeability test results, the relative protective quality ratings of AER ranged from "poor" to "fair," with most bridge decks averaging in the "not very good" range. It is likely that if tested during early ages, the concrete comprising the bridge decks would show far better resistance to air permeability. Near-surface cracking of the concrete due to traffic may influence movement of air through the concrete. The results of the field survey (in which macrocracks were observed) and petrographic analysis (in which microcracks were observed) for each bridge deck provide insight into the role of cracking in these results. In particular, bridge decks 6N/6L and 7N/7L exhibited some of the most extensive linear and pattern cracking, and also had some of the lowest values for AER and WAR, exhibiting the least resistance to permeability of air and water. Bridges with the least amount of distress tended to have some of the highest AER and WAR values, showing the greatest resistance to air and water permeability.

A graphical representation of air permeability test results is shown in Figure 4-9. For five of the eight pairs of bridge decks, the AER for the normalweight bridge deck was higher than the AER of the lightweight bridge deck, indicating that the normalweight bridge deck has better resistance to air permeability. For the other three pairs of decks, the AER values indicate that the lightweight concrete bridge deck had lower air permeability. Regional trends in air permeability were not readily evident. Of the four pairs of coastal bridge decks included in the study, three out of four normalweight bridge decks had lower air permeability than their lightweight deck counterparts. For both the piedmont and mountain regions, the results were split between the two pairs of bridge decks, with the normalweight bridge deck having lower air permeability for one pair, and the lightweight bridge deck having lower permeability for the other pair. It is notable that the relative protective quality ratings for the mountain bridge

decks tended to be higher than those for the piedmont bridge decks. This can possibly be attributed to the extensive linear and pattern cracking present in the piedmont bridge decks.

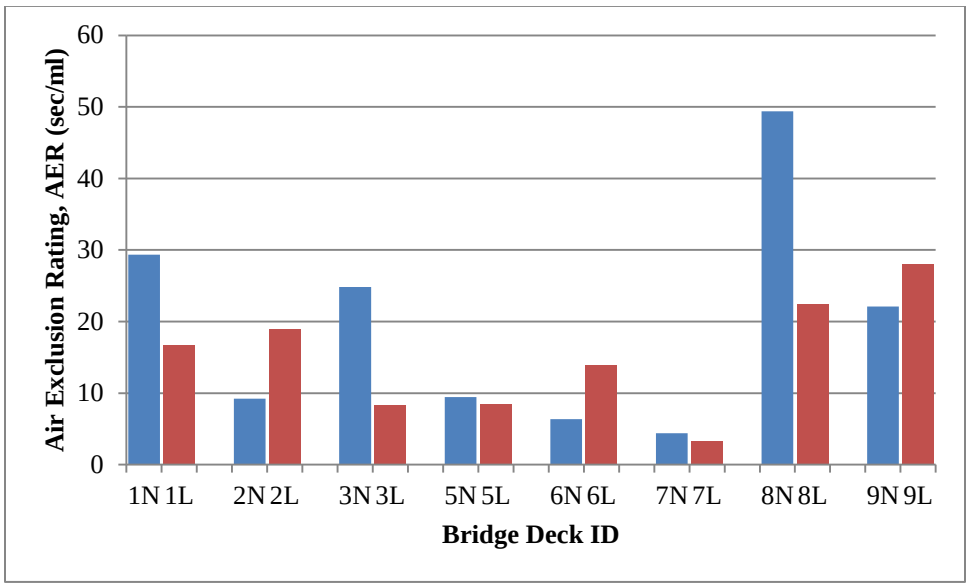

Figure 4-9: Air permeability test results

For water permeability test results, the relative protective quality ratings of WAR ranged from "poor" to "good," as shown in Table 4-2. During water permeability testing on bridge deck 6N, the Poroscope Plus stopped working, and no value was obtained. Therefore, when comparing water permeability test results (via average WAR values) data is available for seven pairs of bridge decks instead of eight pairs of bridge decks. Figure 4-10 shows the water permeability test results graphically. For five of the seven pairs of bridge decks, the WAR for the lightweight bridge decks was higher than that of the normalweight bridge decks, indicating lower water permeability. This is in contrast to the air permeability test results, in which the normalweight concrete decks tended to have lower water permeability.

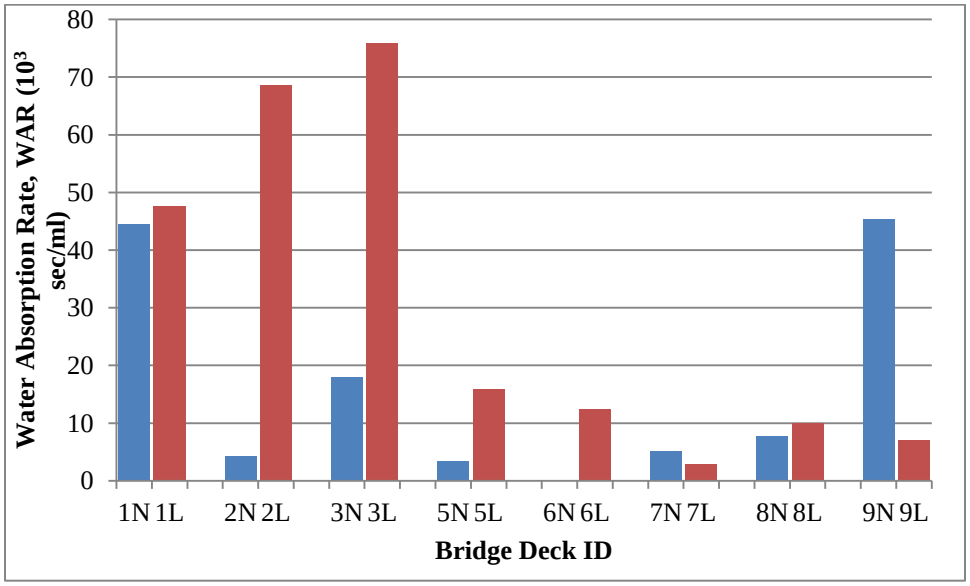

Figure 4-10: Water permeability test results

For coastal bridge deck pairs, it is notable that all four lightweight bridge decks showed lower water permeability, sometimes to a very substantial extent. With the exception of bridge decks 2N and 5N, coastal bridge decks also

generally exhibited the lowest water permeability of all bridge decks in the study. This is again in contrast to the air permeability test results, in which three of the four normalweight bridge decks had lower air permeability than their counterpart coastal lightweight bridge decks.

For piedmont bridge deck pairs, a regional trend cannot be identified due to the lack of data for bridge deck 6N. Although the average WAR values indicate that the water permeability of bridge deck 7N is lower than bridge deck 7L, both decks exhibited relatively high water permeability, rated in the low range of "not very good" and "poor." The average AER values for both bridge deck 7N and bridge deck 7L were also in the "poor" range for protective quality. For mountain bridge deck pairs, a regional trend was not evident.

Statistical analysis was performed by aggregating the air permeability test data for normalweight bridge decks and lightweight bridge decks. A box and whisker plot showing the median, upper quartile, lower quartile, and maximum and minimum values is shown in Figure 4-11. When grouped, the mean AER value for normalweight bridge decks (19.4 sec/mL) is higher than the mean AER value for lightweight bridge decks (15.0 sec/mL), indicating lower air permeability. The median AER values for the normalweight bridge decks and lightweight bridge decks are similar (15.8 for normalweight decks versus 15.4 for lightweight decks). However, AER values for the lightweight bridge decks had a smaller range (difference between minimum and maximum values) than those of the normalweight bridge decks.

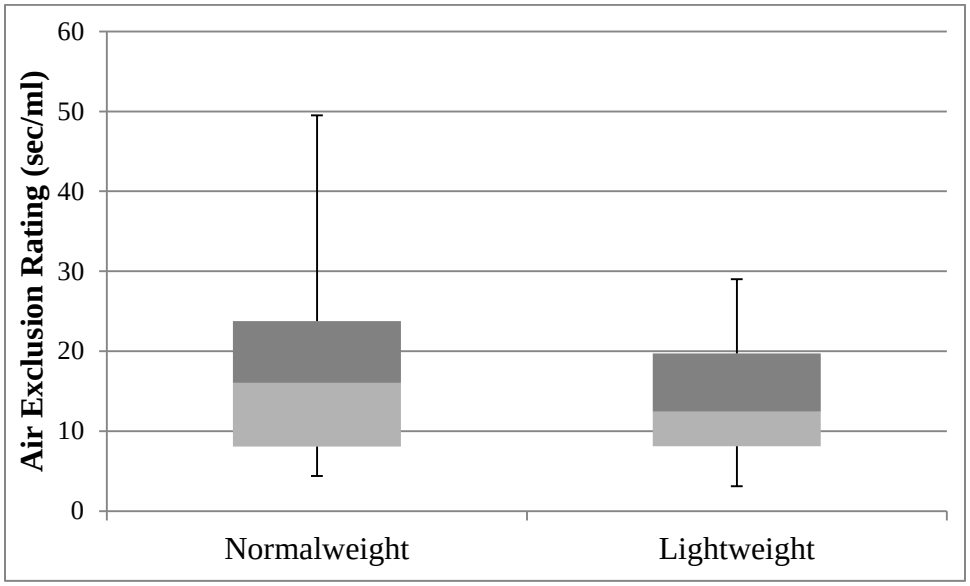

Figure 4-11: Range and summary statistics of air permeability tests for normalweight and lightweight concrete bridge decks.

Statistical analysis was also performed by aggregating the water permeability test data for normalweight bridge decks and lightweight bridge decks. A box and whisker plot showing the median, upper quartile, lower quartile, and maximum and minimum values is shown in Figure 4-12. When grouped, the mean WAR for the lightweight decks is 30.0×10^3 sec/mL, which is much higher than the mean for normalweight concrete decks (18.3×10^3 sec/mL). The median WAR value for the lightweight bridge decks (14.1×10^3 sec/mL) is noticeably higher than that of the normalweight weight bridge decks (7.7×10^3 sec/mL), indicating lower water permeability. However, WAR values for the normalweight bridge decks had a smaller range (difference between minimum and maximum values) than those of the lightweight bridge decks. These results are somewhat reversed from what was observed in the air permeability test results shown in Figure 4-11.

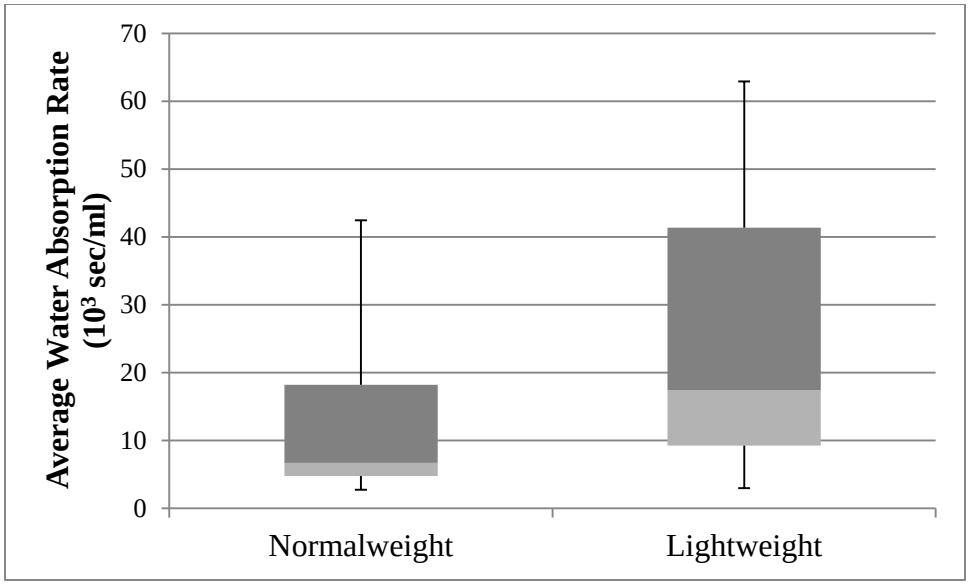

Figure 4-12: Range and summary statistics of water permeability tests for normalweight and lightweight concrete bridge decks.

It is noted that studies performed by (Meletiou et al. 1992) found that the initial moisture content or degree of saturation of the concrete can have a significant effect on the field water permeability test results. In that study, consistent results were obtained when the test section was presaturated prior to testing. However, the operating instructions for the Poroscope Plus used in this study do not call for presaturation of concrete surface prior to water permeability field testing.

4.3 Surface Resistivity Tests

Given the relationship between permeability of fluids and diffusivity of ions through porous material, electrical resistivity measurements of concrete can be used to indirectly measure the concrete's susceptibility to chloride ingress. Higher resistivity readings indicate concrete that will exhibit lower permeability and therefore better durability performance. Surface resistivity testing was performed at eight locations on each bridge deck, as shown in Figure 3-1 and Figure 3-2. At each test location, eight measurements of surface resistivity were made, along with a measurement of the temperature of the concrete surface. For each test location, the eight measurements were taken parallel to each other, within an area spaced approximately 1 in to 1½ in apart along the test area. The presence (or absence) of aggregates near the probes, localized high or low aggregate content, and internal distress (not visible on the surface) may have affected individual readings. For this reason, the eight measurements at each test location were averaged, as were the temperature measurements, to obtain an average surface resistivity and average temperature for the location. Since the dimensions of the bridge deck were large compared to the probe spacing, semi-infinite geometry was assumed, and no correction was applied to the resistivity reading read from the equipment. These data are included in Appendix C.

As discussed in Section 2.1, Literature Review, surface resistivity is sensitive to temperature, with increasing resistance at lower temperatures. To correct the results for temperature, an equation originally developed by Elkey and Sellevold of the Norwegian Road Research Laboratory (as presented in Presuel-Moreno et al. 2010) was utilized. This equation, shown below in Eq. 3, corrects surface resistivity data to 294.15°K, or 69.8°F, and is shown below. In this equation, K = 2889, and $T_{°K standard}$ = 294.15°K.

$$\rho_{normalized} = \rho_{field} \times exp\left[K \times \left(\frac{1}{T_{°K\,standard}} - \frac{1}{T_{°K\,field}}\right)\right] \qquad \text{(Eq. 3)}$$

For each bridge deck, the temperature-corrected surface resistivity results were averaged to provide one temperature-corrected value. Surface resistivity testing is a relatively new technique for characterizing and assessing concrete. Although a number of studies have been performed on concrete cylinders batched and cured in

a controlled laboratory setting, techniques for use of the surface resistivity meter to evaluate concrete in existing structures have not yet been extensively developed. For this reason, for each bridge deck, additional information pertaining to the average surface resistivity reading at each of the eight test locations, including the average, standard deviation, and coefficient of variation, is presented in Table 4-3.

Table 4-3: Average temperature-corrected surface resistivity readings by test location.

		Bridge Deck							
	Test Location	**1N**	**2N**	**3N**	**5N**	**6N**	**7N**	**8N**	**9N**
Average Temperature-Corrected Surface Resistivity (kΩ-cm)	C-1	125	23	180	23	151	50	24	24
	C-2	136	23	188	69	122	31	22	24
	C-3	160	15	192	38	131	37	28	27
	C-4	141	35	234	44	164	68	27	31
	C-5	140	84	248	29	111	64	23	29
	C-6	219	18	220	47	112	13	18	36
	C-7	125	25	171	31	143	25	27	32
	C-8	137	27	172	172		10	22	43
	Average	147.9	31.3	200.6	56.6	133.4	37.3	23.9	30.8
	Standard Dev.	30.8	22.1	29.5	48.7	20.1	21.9	3.4	6.4
	Coefficient of Variation	0.21	0.71	0.15	0.86	0.15	0.59	0.14	0.21

		Bridge Deck							
	Test Location	**1L**	**2L**	**3L**	**5L**	**6L**	**7L**	**8L**	**9L**
Average Temperature-Corrected Surface Resistivity (kΩ-cm)	C-1	98	26	150	59	38	88	16	15
	C-2	131	24	193	144	24	85	10	14
	C-3	73	60	181	135	21	31	9	17
	C-4	90	68	166	70	16	42	8	28
	C-5	78	29	151	122	16	165	10	21
	C-6	59	54	144	76	27	53	11	12
	C-7	43	66	240	100	28	59	13	17
	C-8	79	56	145	70	18	61	12	25
	Average	81.4	47.9	171.3	97.0	23.5	73.0	11.1	18.6
	Standard Dev.	26.4	18.5	33.0	33.0	7.5	41.9	2.5	5.6
	Coefficient of Variation	0.32	0.39	0.19	0.34	0.32	0.57	0.23	0.30

In addition to mixture components and curing conditions, in situ moisture content and aggregate type can affect resistivity. Other researchers have shown that conductivity (and hence its inverse, resistivity) is highly influenced by the pore solution chemistry (Spragg et al. 2011). The presence of chlorides has been shown to decrease surface resistivity (Presuel-Moreno et al. 2010). Therefore, chloride contained in the near-surface concrete at each test location could influence the surface resistivity measurements, influencing the variability shown in Table 4-3. Abrasion by tires may create a more "open" concrete surface. This may result in greater chloride ingress than that experienced along the shoulders. Drainage on most bridge decks typically is routed away from the travel lanes, with water flow directed across the shoulder towards drains along the sides of the bridge decks. This drainage pattern often exposes concrete along the shoulder and edge of the bridge deck to more chloride, creating the potential for more chloride ingress. Therefore, surface resistivity measurements obtained in areas with high near-surface chloride contents could be lower than areas without significant near-surface chloride contents. Using the diagonal sampling pattern for testing locations should have helped to address this variability when the surface resistivity is averaged.

Surface resistivity measurements could also be influenced by localized cracking and characteristics of the near-surface paste, especially at test locations within the wheelpaths. Bridge decks exhibiting the most extensive cracking did not necessarily have the greatest variability in surface resistivity measurements at each test location. The average temperature-corrected surface resistivity value for each bridge deck included in the study is shown in Table 4-4.

Table 4-4: Average corrected surface resistivity readings.

Bridge Deck	**Average Corrected Surface Resistivity Reading (kΩ-cm)**
1N	148
1L	81
2N	31
2L	48
3N	201
3L	171
5N	57
5L	93
6N	186
6L	24
7N	37
7L	73
8N	24
8L	11
9N	31
9L	19

A graphical representation of data presented in Table 4-4 is shown in Figure 4-12. It can be seen that for coastal bridges, two normalweight bridge decks had higher average temperature-corrected surface resistivity readings and two lightweight concrete bridge decks had higher average temperature-corrected surface resistivity readings. Some of the highest surface resistivity readings were obtained at bridge decks 3N/3L, which are both on a bridge over the Intracoastal Waterway near Morehead City. These high readings indicate the potential for better concrete quality including reduced permeability and higher resistance to chloride ingress. Very little distress was observed during visual surveys on bridge decks 3N and 3L.

The greatest difference in temperature-corrected surface resistivity readings was obtained for the two bridges in Winston-Salem, North Carolina, bridge decks 6N and 6L. Bridge deck 6N exhibited far higher resistivity readings than 6L. These bridge decks exhibited extensive cracking which may have influenced the readings, as cracks could have influenced the saturation of the test sites. Since both 6N and 6L had extensive cracking present, the difference in readings may not be explained by the presence of cracks. The potential causes of this wide disparity in surface resistivity are unclear at this time.

For both mountain bridge deck pairs, the normalweight decks showed higher temperature-corrected resistivity than the lightweight bridge decks. However, some of the lowest temperature-corrected resistivity readings were obtained for these four bridge decks. In addition, these four bridge decks were also found to have some of the highest surface chloride concentrations which may have resulted in low resistivity readings. Information on chloride contents is presented in Section 5.5, Rapid Chloride Test (RCT).

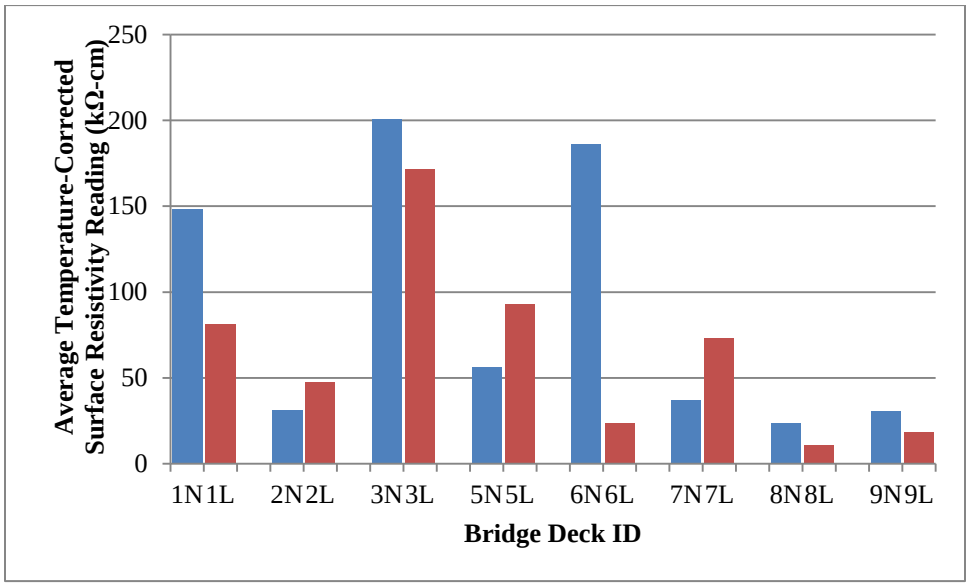

Figure 4-12: Average temperature-corrected surface resistivity readings.

A box and whisker plot showing the summary statistics for average temperature-corrected surface resistivity is shown in Figure 4-13. As shown in Figure 4-13, the readings taken on both normalweight and lightweight decks exhibit similar ranges; however, readings taken on lightweight decks exhibit a much smaller interquartile range indicating less dispersion in the data. The mean temperature-corrected surface resistivity for the normalweight decks (81.9 kΩ-cm) was higher than that of the lightweight decks (65.5 kΩ-cm).

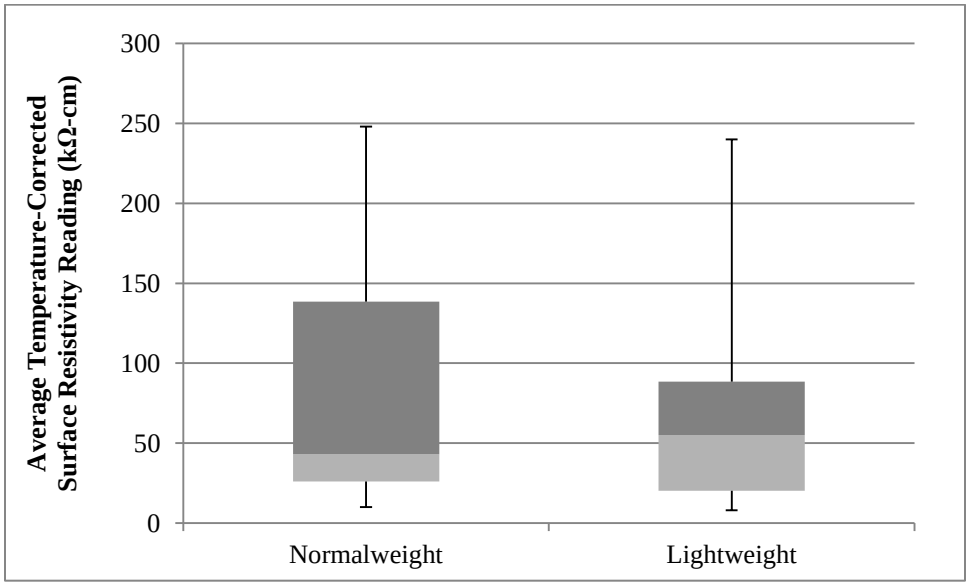

Figure 4-13: Range and summary statistics of average temperature-corrected surface resistivity tests for normalweight and lightweight concrete bridge decks.

The mean and median temperature-corrected surface resistivity readings for the lightweight decks (65.5 kΩ-cm and 55.0 kΩ-cm, respectively) are much closer together than the mean and median temperature-corrected surface resistivity readings for the normalweight decks (81.9 kΩ-cm and 43.0 kΩ-cm, respectively), indicating that the lightweight data is more normally distributed than the data for the normalweight decks. This may be attributable to the fact that all lightweight bridge deck concrete from decks included in this study appeared to contain the same general type of manufactured lightweight aggregate. Normalweight bridge decks were comprised of concrete with a number of different coarse aggregate types from various geographic regions of the state (mountain, piedmont, and coastal). Information on the coarse aggregate types present in each of the normalweight bridge decks is presented in Section 5.7 Petrographic Examinations.

4.4 Rebound Hammer Tests

The limitations of rebound hammer tests are well documented (Neville 1995, Mindess et al. 2003), as the rebound number obtained from testing concrete surfaces is influenced by surface finish, moisture content, temperature, carbonation, and rigidity of the structural member, among other factors. Use of the rebound hammer to provide an assessment of strength is strongly discouraged by a number of researchers, and "while the rebound hammer test is useful within a limited scope, the test is not a strength test and exaggerated claims of its use as a replacement for the compression test should not be accepted (Neville 1995)."

Rebound hammer testing can, however, be used to provide a quick assessment of the uniformity of concrete. As stated by Mindess et al. (2003), "the general view held by many users of the Schmidt rebound hammer is that it is useful in checking the uniformity of concrete and in comparing one concrete against another, but that it can only be used to obtain a rough indication of the concrete strength in absolute terms." Rebound hammer test results obtained from the subject bridge decks were not used to assess the compressive strength of the concrete. The results were, however obtained in order to allow for a general assessment of the uniformity of the concrete, and to identify potential locations where the concrete strength or general condition may differ significantly from the rest of the concrete comprising the bridge deck.

Rebound hammer tests were performed at each of the eight test locations on the bridge decks included in the study. At each test location, three sets of rebound hammer tests were performed, each test spaced several feet apart. The rebound number for each test site was computed as outlined in ASTM C805. For each test location, the three rebound numbers obtained were averaged in order to obtain an average rebound number for the test location. The eight rebound numbers for each bridge deck were tallied, and are presented in Table 4-5.

Table 4-5: Average rebound numbers for test locations.

Bridge Deck	Location								
	C-1	C-2	C-3	C-4	C-5	C-6	C-7	C-8	Average
1N	39.7	41.7	38.5	43.2	34.7	40.9	39.0	43.8	40.2
1L	37.5	34.2	36.5	38.6	38.2	35.6	37.4	37.1	36.9
2N	33.1	31.5	32.7	31.4	33.2	36.0	34.4	35.6	33.5
2L	33.6	33.7	30.6	34.0	33.7	35.8	29.8	31.9	32.9
3N	38.4	40.7	41.1	42.7	40.2	37.3	38.8	39.7	39.9
3L	34.2	35.3	35.3	35.5	33.4	35.3	37.7	35.4	35.3
5N	34.3	44.1	34.6	38.3	39.0	36.3	39.5	38.4	38.1
5L	28.5	34.1	30.9	33.8	38.3	34.0	34.8	36.6	33.9
6N	39.5	35.2	37.2	35.4	35.3	40.5	38.5	38.1	37.5
6L	34.0	31.6	33.9	31.8	31.7	33.2	33.9	33.6	33.0
7N	33.5	40.0	46.7	44.6	39.6	38.8	44.6	45.0	41.6
7L	35.7	36.0	41.6	38.4	38.2	36.2	39.0	40.4	38.2
8N	40.3	42.1	46.8	49.7	48.4	46.0	44.1	43.0	45.1
8L	36.4	36.7	36.9	39.1	44.0	44.9	39.8	44.6	40.3
9N	37.6	33.3	35.8	33.7	39.1	40.7	38.3	39.9	37.3
9L	34.2	34.7	38.2	38.7	39.2	39.5	38.8	38.8	37.8

It can be seen in Table 4-5 that, as expected, the average rebound number at each test location varied across the sample section. For some bridge decks, a few locations had rebound numbers that were somewhat lower than those obtained at other locations. These relatively low rebound numbers may indicate a localized area of distress or different concrete characteristics due to placement, finishing, or other issues. The relatively low rebound numbers may also be the result of some other surface characteristic of the concrete. For example, groove depths on bridge decks included in the study were of varying thickness, and sometimes the depths varied along the length of a sample section. For this reason, this data is viewed as supplemental. Ultimately, during the analysis portion of this study, no test results from other testing were discounted due to low rebound hammer test results.

With the exception of bridge deck pair 9N and 9L, typically the average rebound number for a normalweight concrete bridge deck is higher than the average rebound number for its sister lightweight concrete bridge deck. Again, due to limitations on interpretation of rebound hammer test results discussed above, no distinction in relative strengths of lightweight and normalweight concrete bridge decks is implied with these results.

5. RESULTS OF LABORATORY TESTING

5.1 Unit Weight and Moisture Content

Testing was performed to determine the apparent density and moisture content of representative cores and selected portions of cores. A summary of average apparent densities and average moisture contents is shown in Table 5-1.

Table 5-1: Average moisture contents and average apparent densities.

Bridge Deck	Average Moisture Content (%)	Average Apparent Density (pcf)
1N	4.8	158.0
1L	7.2	134.6
2N	3.7	---
2L	7.1	128.1
3N	4.0	157.9
3L	5.7	---
5N	3.4	155.4
5L	4.8	122.0
6N	3.5	158.6
6L	5.3	126.9
7N	4.3	159.5
7L	4.9	---
8N	4.0	160.0
8L	6.0	129.8
9N	3.9	161.3
9L	5.7	126.0

Since most laboratory tests performed in this study require specific specimen conditioning procedures, moisture contents of the concrete comprising the bridge decks is of interest mainly in evaluation of field testing results. For all pairs of bridge decks, the moisture content of cores removed from lightweight bridge decks was higher than the moisture content of the companion normalweight bridge decks. The difference in moisture content was most pronounced in two of the coastal bridges, 1N/1L and 2N/2L. The greatest difference in moisture content was 3.4% between 2N and 2L, which are both located on the bridge to Cedar Island crossing the Thorofare Bay Channel.

Due to the limited number of test specimens obtained from each bridge deck, ASTM C642 testing to determine apparent density of concrete was only performed on one or two cores (or portions of cores) from each bridge deck. The average apparent density of normalweight concrete specimens was slightly higher than the expected 140 to 145 pcf that is typical for concrete. The average apparent density of lightweight concrete specimens was also slightly higher than the expected range of values for structural lightweight concrete.

5.2 Compressive Strength

Compressive strength test results were obtained for one to three cores per bridge deck. Additional compressive strength test results were desired. However, only a limited number of cores could be obtained from each bridge deck during the allowable lane closure period. The goal of this study was evaluate durability performance, and it was decided that since the number of test specimens was limited, priority assignment of the core specimens should be allotted to other tests (rapid chloride permeability testing, sorptivity testing, etc.) that better assess potential durability performance than compressive strength testing. The presence of steel in a number of cores also limited the number of specimens suitable for compressive strength testing. Although a rebar locator was used to identify the location of the top reinforcing steel, occasionally reinforcing bars (typically the bottom layer), chairs, or welded wire was encountered by the drill bit and was included in the cores. Cores that contained steel were not tested for compressive strength.

When removing cores, care was taken to ensure that the cores did not go through the full thickness of the bridge deck. Care was also taken to avoid cutting through the bottom layer of reinforcing steel. For most cores, drilling was stopped just above the bottom layer of reinforcing steel. For this reason, most cores were not the ASTM C39 optimum length to diameter (L/D) ratio of 2 to 1. ASTM C39 provides a correction factor for various L/D ratios, and the adjusted compressive strength is lower than the measured compressive strength. The correction factor is scaled so that the reduction is greater for shorter test specimen. The results of compressive strength tests, including information on the dimensions of test specimens and the correction factors applied, are included in Appendix E. After the L/D ratio correction factor was applied to each compressive strength result, the average adjusted compressive strength for each bridge deck was computed. These averages are summarized in Table 5-2, below.

Table 5-2: Average adjusted compressive strengths.

Bridge Deck	Average Adjusted Compressive Strength (psi)
1N	4,370
1L	3,950
2N	3,940
2L	4,555
3N	4,415
3L	3,013
5N	3,290
5L	4,850
6N	4,075
6L	4,328
7N	3,953
7L	3,130
8N	4,248
8L	3,893
9N	4,688
9L	6,015

The average adjusted compressive strengths for most bridges ranged from 3,200 psi to approximately 5,000 psi. These values are lower than what may be expected based on the typical design 28-day compressive strength for bridge decks, which is often 4,000 psi to 6,000 psi. However, as these cores are drilled specimens removed from bridge decks that have been in service for many years, they likely contain internal damage that resulted in lower compressive strength test results. Additionally, ASTM C42 emphasizes that "historically, it has been assumed that core strengths are generally 85% of the corresponding standard-cured cylinder strengths." Generally, compressive strength is not viewed as a direct indicator of durability performance. Therefore it is the intent of the authors to provide these adjusted compressive strength results for informational purposes only.

5.3 Dynamic Modulus

Dynamic modulus testing was performed on one to three cores per bridge deck. This testing was performed on the same cores that were used for compressive strength testing, with the non-destructive dynamic modulus testing performed first. As discussed in Section 5.2, Compressive Strength, these cores did not contain reinforcing steel. Prior to dynamic modulus testing the ends of the cores were sawcut to create a more plane sample for both this test as well as for compressive strength tests.

As discussed in Section 5.2, Compressive Strength, when cores were removed, care was taken to ensure that the cores did not go through the full thickness of the bridge deck. Care was also taken to avoid cutting through the bottom layer of reinforcing steel. For most cores, drilling was stopped just above the bottom layer of reinforcing steel. For this reason, most cores were not the optimum length to diameter (L/D) ratio of 2 to 1 for dynamic modulus testing. Unlike ASTM C39 which provides a correction factor to adjust the compressive strength, ASTM C215 "Standard Test Method for Fundamental Transverse, Longitudinal, and Torsional Resonant Frequencies of Concrete Specimens" does not provide adjustment factors. Testing was performed as outlined in Section 3.3.3, Dynamic Modulus. Where more than one core was used for testing per bridge deck, the dynamic modulus values were averaged. These values are summarized in Table 5-3, below. Additional data can be found in Appendix F.

Table 5-3: Dynamic Modulus test results.

Bridge Deck	Dynamic Modulus (ksi)
1N	4,640
1L	3,120
2N	4,590
2L	3,290
3N	4,720
3L	2,440
5N	4,050
5L	3,330
6N	4,630
6L	3,400
7N	4,610
7L	2,690
8N	4,670
8L	3,050
9N	4,710
9L	3,710

As discussed in Section 2.1, Literature Review, experimental determination of dynamic modulus is extremely sensitive to cracking of the specimen. No visible macrocracking was evident in the specimens used for testing, but microcracking present in the test specimens could certainly have impacted the test results. Microcracks were likely present due to in-situ loading of traffic and environmental exposure. The core drilling of the specimens could also have induced microcracks at the surfaces of the specimens.

For all eight pairs of bridge decks, the lightweight concrete bridge deck had a lower dynamic modulus than the normalweight concrete bridge deck. These results are consistent with expectations. Lightweight aggregate typically has a lower modulus of elasticity than natural normalweight aggregates; therefore, lightweight concrete often has a lower dynamic modulus than normalweight concrete. One study found it to be approximately 60% to 70% of normalweight concrete (Lee et al. 1997).

5.4 Sorptivity

Two methods were used to characterize the sorptivity of each specimen. First, sorptivity testing was performed in general accordance with ASTM C1585 on a sawcut surface corresponding to a depth 2 in below the surface of the bridge deck. Testing performed by the method outlined in this standard measures the rate of absorption through capillary rise. Second, a ponding sorptivity test, in which absorption is assisted by gravity, was performed on the top surface of the same specimens. Ponding sorptivity testing was performed in general accordance with the procedure outlined by Bentz et al. (2002). For each bridge deck, two specimens were tested, with both the ASTM C1585 capillary suction test and the ponding test performed on the same specimens. Additional information on these tests is presented in the literature review in Section 2.1.3.2, Sorptivity and Permeability.

For both the ASTM 1585 capillary suction test and the ponding test, the initial absorption and the secondary absorption were determined. Measurements of mass were used to compute the absorption, I, defined by Eq. 4, where I is the absorption in mm, a is the exposed area of the specimen in mm^2, d is the density of water in g/mm^3, and m_t is the change in specimen mass in grams at the time, t.

$$I = \frac{m_t}{a \times d} \qquad \text{(Eq. 4)}$$

Absorption values were plotted against the square root of time. For each test specimen, least-square linear regression was performed in order to fit two line segments to the data. The first line segment was used to fit the data for absorption change between 1 minute and 6 hours. The second line segment was used to fit the data for absorption change between day 1 and day 7. The initial absorption is defined as the slope of the best fit line for the 1 minute to 6 hour data, and the secondary absorption is defined as the slope of the best fit line for the day 1 to day 7 data. Typical plots showing the initial absorption and secondary absorption periods for the ASTM C1585 capillary suction test and the ponding test (along with the best fit lines) are shown in Figure 5-1 and Figure 5-2, respectively. Sorptivity test results, including the initial absorption and secondary absorption computed for each test specimen, are provided in Appendix G.

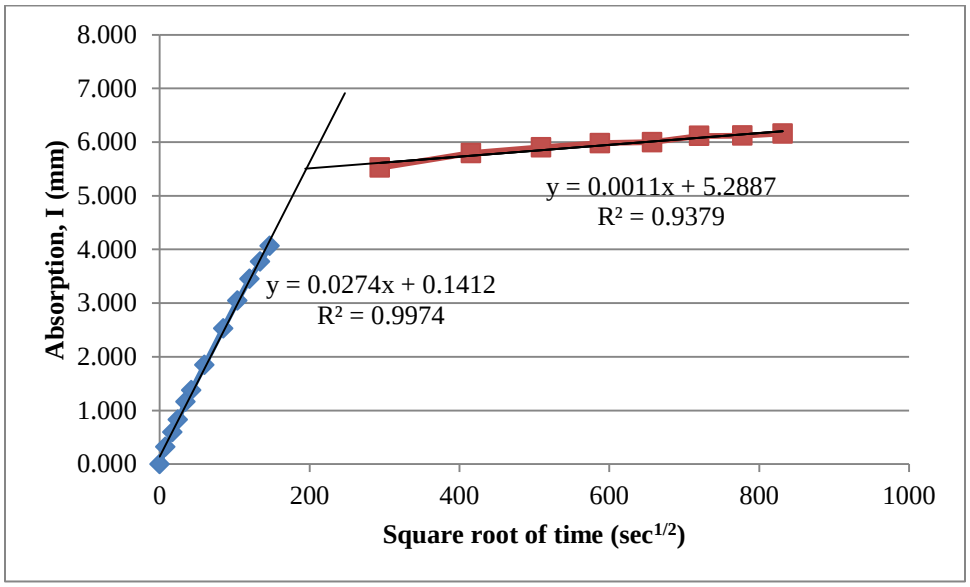

Figure 5-1: Results from typical ASTM C1585 absorption test, showing initial absorption (first line segment) and secondary absorption (second line segment).

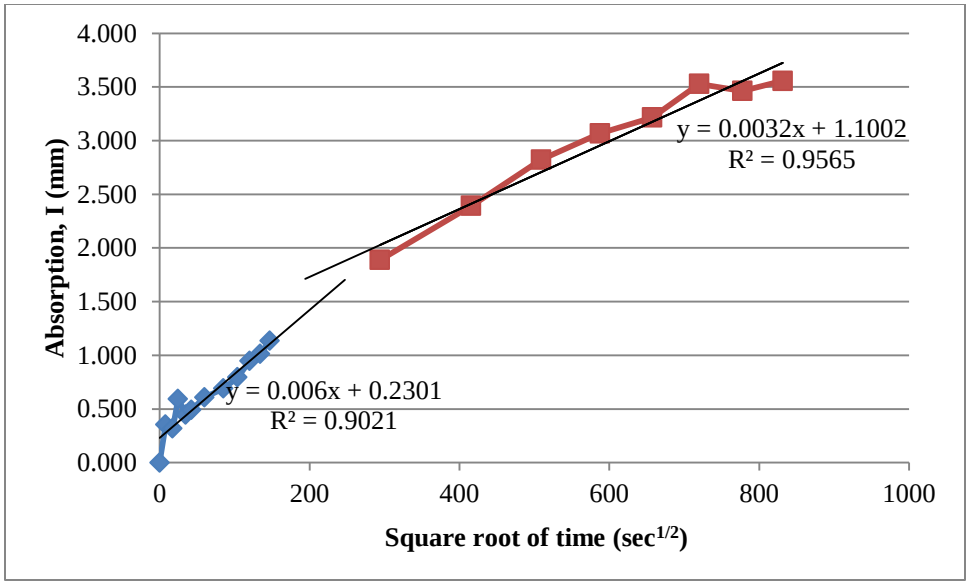

Figure 5-2: Results from typical ponding sorptivity test (per Bentz et al. 2002), showing initial absorption (first line segment) and secondary absorption (second line segment).

As outlined in Section 3.3.4, Sorptivity, the ASTM C1585 capillary suction test was performed on a sawcut surface of a core, with the test surface oriented parallel to the wearing surface of the deck, at a depth of two in. This test surface likely exhibits far less microcracking than the test surface used in the ponding sorptivity test. Additionally, the test surface used in the ASTM C1585 capillary suction test would also not be as "open" from abrasion from traffic. Therefore, it is likely that the C1585 capillary suction sorptivity test results are more indicative of the true material performance (and less sensitive to other environmental or traffic related factors) than the results of the ponding test developed by Bentz et al. (2002).

ASTM C1585 capillary suction test specimens are submerged with the test surface down and the absorption of water is not assisted by gravity. Therefore, the capillary suction test method may not reflect actual field conditions as well as the ponding sorptivity test. The test surface used in the ponding sorptivity test is the top end of the core, and therefore the actual wearing surface of the bridge decks. As such, the ponding sorptivity test results for this project are influenced by the damage present at and near the surface of the bridge deck. Macrocracks and microcracks present in the bridge decks likely increase the rate of absorption, and increased surface wear would likely also increase absorption. The depth of grooves present on the surface would also influence the absorption, as deeper grooves would provide more surface area on the test specimen.

Manufactured lightweight coarse aggregates typically have significantly higher absorption (often greater than 5%) than normalweight coarse aggregates. The results of sorptivity testing, particularly initial absorption, could be significantly influenced by the absorption of the lightweight aggregates. Exposed lightweight aggregate surfaces would likely allow for greater initial absorptions and possibly greater secondary absorptions as well. For both capillary suction and ponding sorptivity tests, the amount of exposed coarse aggregate could significantly affect the test results. For lightweight concrete, higher aggregate contents could also result in higher absorption rates.

A summary of the average initial absorption and the average secondary absorption rates for both the ASTM C1585 capillary suction test and the ponding test are shown below in Table 5-4.

Table 5-4: Average initial absorption and average secondary absorption rates for ASTM C1585 capillary suction tests and ponding tests.

	Capillary Suction Test (ASTM C1585)		Ponding Test (Bentz et al. 2002)	
Bridge Deck	**Initial Absorption, I (mm)**	**Secondary Absorption, I (mm)**	**Initial Absorption, I (mm)**	**Secondary Absorption, I (mm)**
1N	0.0110	0.0012	0.0021	0.0009
1L	0.0144	0.0030	0.0033	0.0017
2N	0.0161	0.0004	0.0033	0.0022
2L	0.0122	0.0038	0.0040	0.0021
3N	0.0152	0.0010	0.0021	0.0012
3L	0.0110	0.0034	0.0022	0.0007
5N	0.0125	0.0021	0.0019	0.0005
5L	0.0115	0.0011	0.0022	0.0009
6N	0.0180	0.0008	0.0018	0.0006
6L	0.0259	0.0011	0.0031	0.0006
7N	0.0277	0.0005	0.0036	0.0034
7L	0.0183	0.0009	0.0035	0.0027
8N	0.0155	0.0010	0.0025	0.0019
8L	0.0256	0.0009	0.0025	0.0011
9N	0.0152	0.0007	0.0053	0.0030
9L	0.0205	0.0007	0.0032	0.0019

ASTM C1585 capillary suction test results are displayed graphically in Figure 5-3 and Figure 5-4. Figure 5-3 shows the average initial absorption rates, and Figure 5-4 shows the average secondary absorption rates.

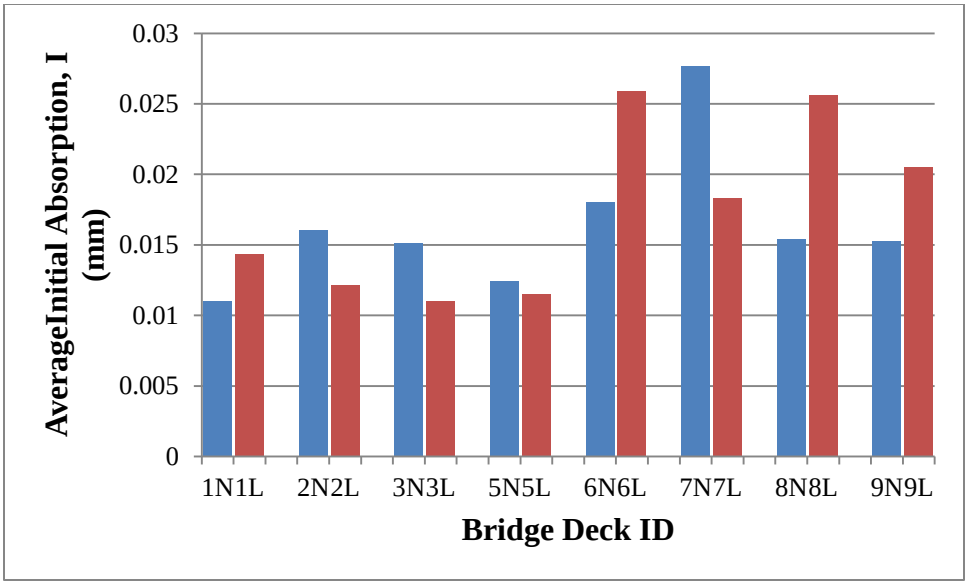

Figure 5-3: Initial absorption, ASTM C1585 capillary suction test.

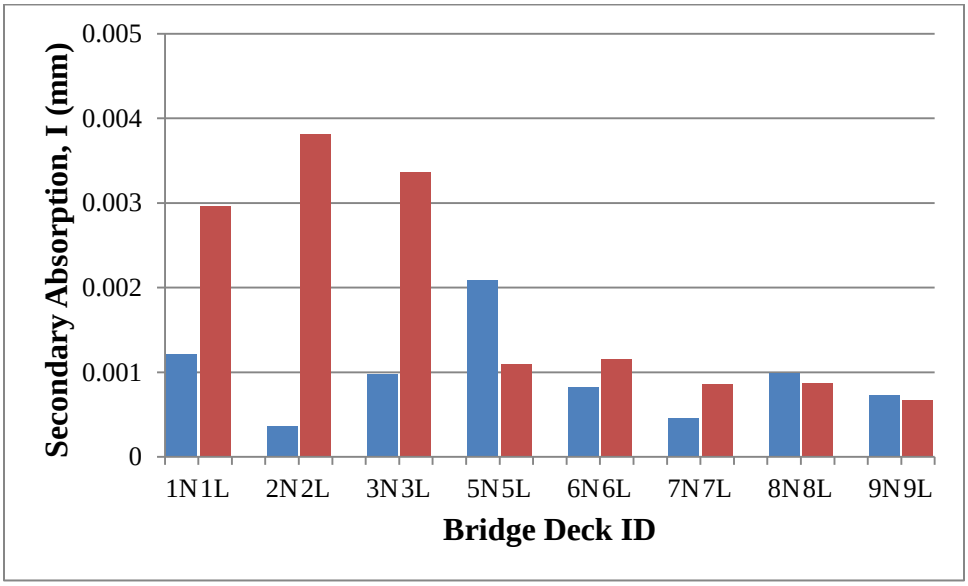

Figure 5-4: Secondary absorption, ASTM C1585 capillary suction test.

For coastal bridge deck pairs, three of four normalweight bridge decks had higher average initial absorptions than their companion lightweight bridge decks. It is noted, however, that the difference between the average initial absorptions of the coastal bridges is less than the differences in average initial absorptions obtained for bridge deck pairs in the piedmont and mountain regions. For mountain bridge deck pairs, both lightweight bridge decks had higher average initial absorptions than the normalweight bridge decks. For piedmont bridge deck pairs, the results were split, with one normalweight bridge deck and one lightweight bridge deck having higher average initial absorption than the companion deck.

Average secondary absorptions for lightweight bridge decks tended to be larger than those of the companion normalweight decks. For five of the eight pairs of decks, the lightweight deck exhibited higher average secondary absorptions. The difference in average secondary absorptions was most evident in three of the four coastal bridge deck pairs, 1N/1L, 2N/2L, and 3N/3L. For the fourth coastal bridge deck pair (a bridge near the Outer Banks), the lightweight deck had significantly lower average secondary absorption than the normalweight portion of the deck.

Bridge deck pairs in the piedmont and the mountains exhibited far less disparity between the average secondary absorptions of normalweight and lightweight concrete bridge decks. For the piedmont bridge deck pairs, the lightweight bridge decks had slightly higher average secondary absorptions than the normalweight bridge decks.

For the mountain bridge deck pairs, the normalweight decks exhibited slightly higher average secondary absorption values than the lightweight bridge decks, but the difference was very small.

Box and whisker plots showing summary statistics for average initial absorption rates and average secondary absorption rates for the ASTM C1585 tests are shown in Figure 5-5 and Figure 5-6, respectively. As can be seen in Figure 5-5, the average initial absorption rates for both normalweight and lightweight decks exhibit similar ranges and similar median values (0.015 mm for normalweight bridge decks and 0.016 mm for lightweight bridge decks). The mean values for the average initial absorption value for normalweight concrete bridge decks (0.016 mm) and lightweight concrete bridge decks (0.017 mm) were almost identical. The average initial absorption rates for normalweight decks have a much smaller interquartile range indicating less dispersion in the data than the data for the lightweight decks.

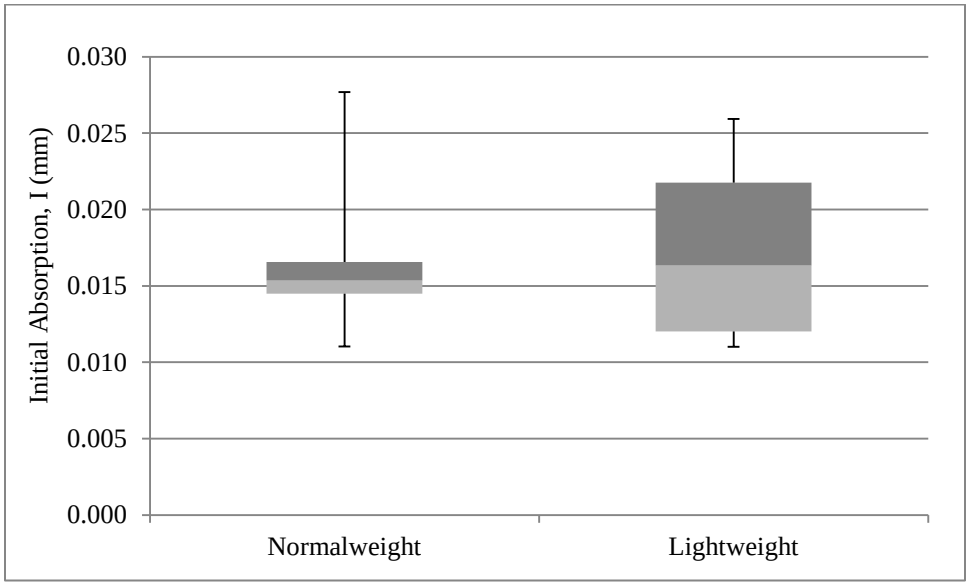

Figure 5-5 Range and summary statistics of average initial absorption rates (ASTM C1585 capillary suction) for normalweight and lightweight concrete bridge decks.

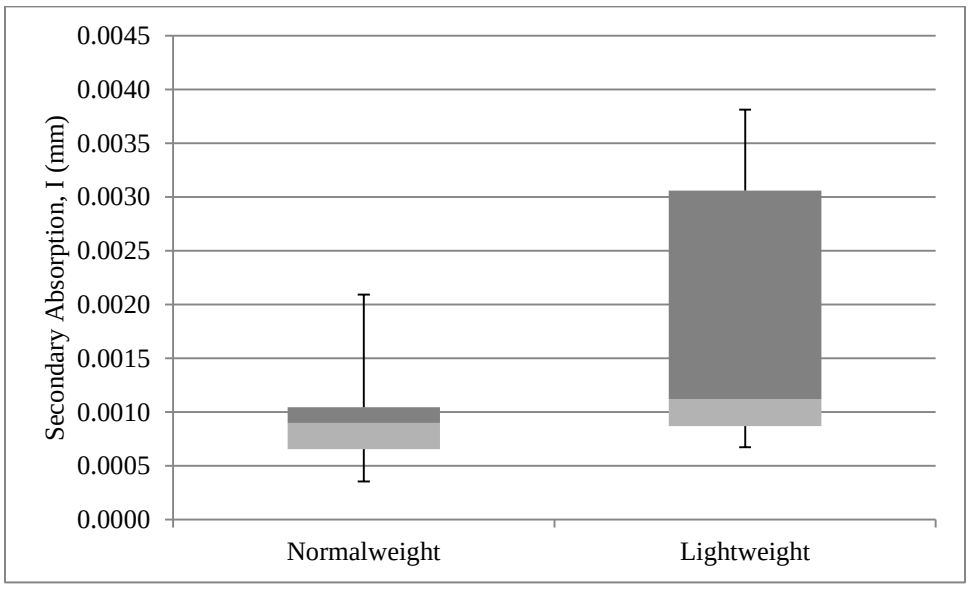

Figure 5-6 Range and summary statistics of average secondary absorption rates (ASTM C1585 capillary suction) for normalweight and lightweight concrete bridge decks.

The box and whisker plot for average secondary absorption for the capillary suction test (Figure 5-6) again shows that the normalweight and lightweight decks had similar median values. It is noted, however, that the mean for the average secondary absorption of the normalweight concrete bridge decks (0.00095 mm) is almost half that of the lightweight bridge decks (0.00185 mm). The lightweight decks included in the study had a wider range of average secondary absorption values, and a substantially larger interquartile range.

The average initial absorption and secondary absorption values computed from the results of ponding sorptivity tests are shown graphically in Figure 5-7 and Figure 5-8, respectively. For coastal bridge deck pairs, the lightweight bridge decks again exhibited greater average initial absorption values, although for two pairs, there was very little difference. For piedmont bridge decks, very little difference was observed between the average initial absorption rates for the bridge decks near Charlotte, North Carolina, 7N and 7L, which exhibited the most severe transverse cracking of the bridges included in the study. The other pair of piedmont bridge decks, 6N and 6L in Winston-Salem, North Carolina, had some of the most extensive pattern (surface) cracking observed in the study. For these two bridge decks, the lightweight bridge deck had a higher average initial absorption value. For mountain bridge deck pairs, 8N and 8L both had the same average initial absorption value, while bridge deck 9N had a higher average initial absorption value than bridge deck 9L.

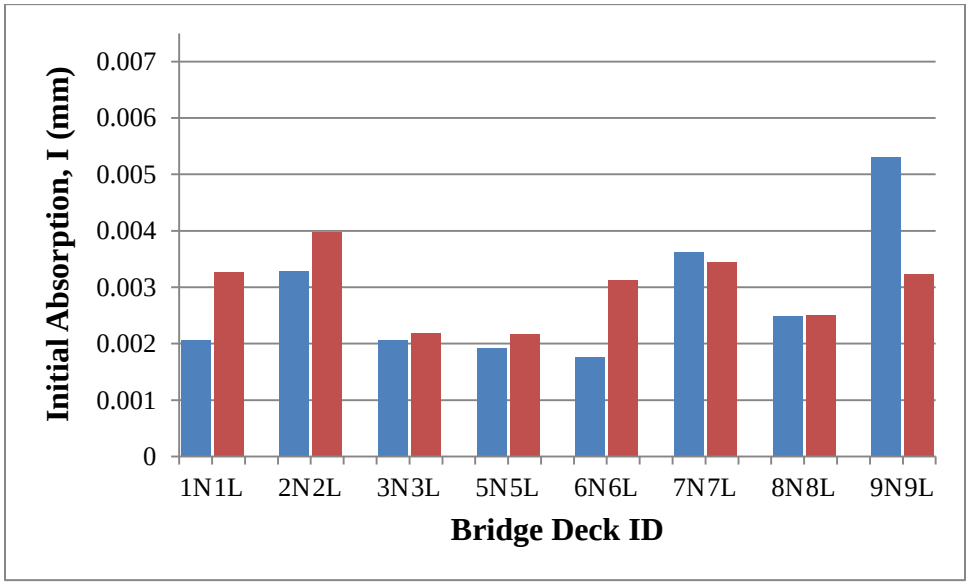

Figure 5-7: Initial absorption, ponding test (Bentz et al. 2002).

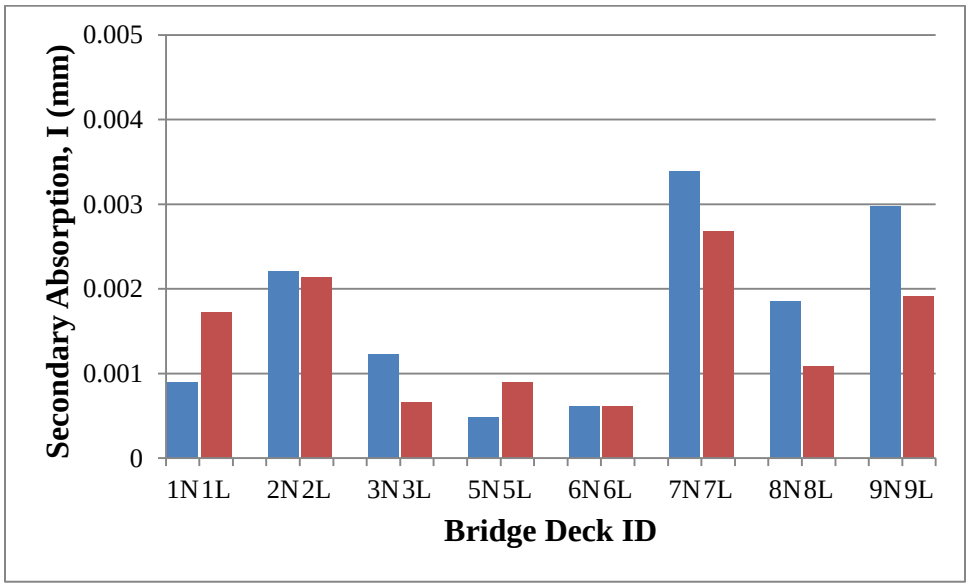

Figure 5-8: Secondary absorption, ponding test (Bentz et al. 2002).

As can be seen in Figure 5-8, the average secondary absorption values from the ponding sorptivity tests were significantly different than the secondary absorption values from the ASTM C1585 capillary suction sorptivity tests (as shown in Figure 5-4). In the capillary suction sorptivity test, specimens from bridge decks from the piedmont and mountain regions had some of the lower average secondary absorption values of all bridge decks included in the study. Conversely, in the ponding suction tests, both bridge deck pairs in the mountains, as well as one pair in the piedmont region (7N and 7L), exhibited some of the highest average secondary absorption rates. For each of these pairs of bridge decks, the normalweight decks had higher average secondary absorption rates than the lightweight bridge decks.

For two of the coastal bridge deck pairs, the average secondary absorption rates for the normalweight bridge decks were higher than the average secondary absorption rates for the lightweight bridge decks. The lightweight bridge decks had lower average secondary absorption rates than the normalweight bridge decks for the other two coastal bridge deck pairs. The average secondary absorption rates for the normalweight deck and lightweight deck in two bridge deck pairs, 2N/2L and 6N/6L, were the nearly the same.

Box and whisker plots showing summary statistics for average initial absorption rates and average secondary absorption rates for the ponding sorptivity tests are shown in Figure 5-9 and Figure 5-10, respectively. As can be seen in Figure 5-9, the initial absorption rates for the normalweight bridge decks have a larger range and somewhat larger interquartile range than the lightweight bridge decks. The median value for average initial absorption of the normalweight bridge decks is somewhat lower than the lightweight bridge decks, but it is noted that the means are relatively close (0.00281 mm for normalweight decks and 0.00299 mm for lightweight decks).

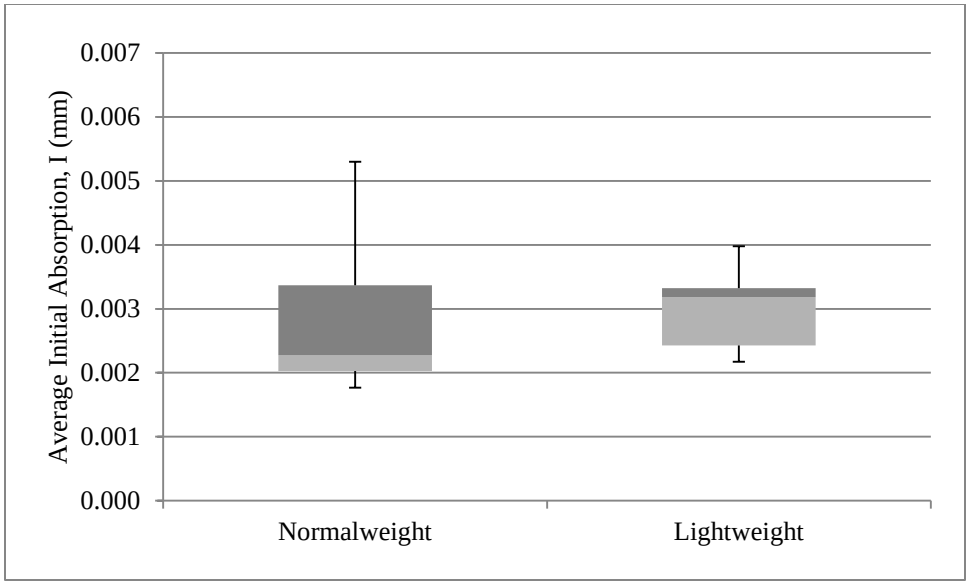

Figure 5-9 Range and summary statistics of average initial absorption rates (ponding test developed by Bentz et al. (2002)) for normalweight and lightweight concrete bridge decks.

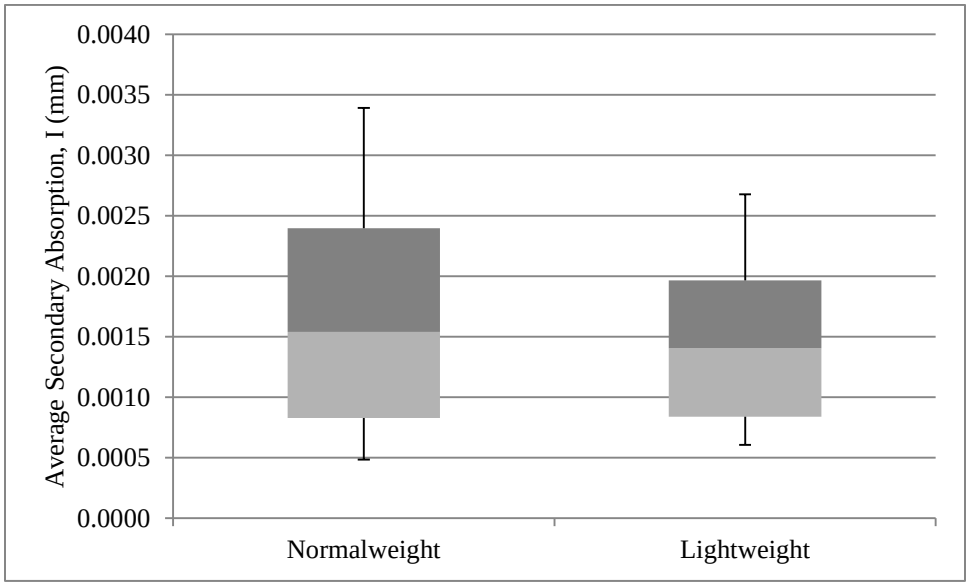

Figure 5-10 Range and summary statistics of average secondary absorption rates (ponding test developed by Bentz et al. (2002)) for normalweight and lightweight concrete bridge decks.

The box and whisker plot of average secondary absorption values for the ponding sorptivity test indicates that again the normalweight bridge decks had a greater range and interquartile range. The mean and median values for normalweight bridge decks (0.00170 mm and 0.00154 mm, respectively) and for lightweight bridge decks (0.00146 mm and 0.00140mm, respectively) were relatively close.

Overall, it would be of interest to link these sorptivity test results to predicted durability performance. For both the ASTM C1585 capillary suction test and the ponding sorptivity test, very limited test data is available from other studies. Most published data on sorptivity is from laboratory-based studies. Of note, Bentz et al. (2002) performed ponding sorptivity tests on test specimens prepared from normalweight concrete pavement slabs cast as part of work performed for Missouri DOT. Initial and secondary absorption rates from ponding tests performed as part of this work were lower than those obtained by Bentz et al. on specimens from pavement slabs.

5.5 Rapid Chloride Test (RCT)

Rapid chloride testing (RCT) was performed to determine the chloride content of the concrete powder samples removed from each bridge deck. For each powder sample, millivolt readings from the RCT equipment were converted into chloride contents as outlined in Section 3.3.5. RCT data and computed chloride contents is provided in Appendix H, with data arranged by both depth and test location.

Diffusion of chlorides into concrete can be affected by a number of factors, including cracking, surface condition, drainage, and road salt application techniques. These factors can each differ depending on location. On a bridge deck, cracking may be more prolific in the travel lanes (particularly in the wheelpaths). Abrasion by tires may create a more "open" concrete surface. This may result in greater chloride ingress than that experienced along the shoulders. However, drainage on most bridge decks is away from the travel lanes, with water flow directed across the shoulder towards drains along the sides of the bridge decks. This drainage pattern often exposes concrete along in the shoulder and edge of the bridge deck to more chloride, creating the potential for more chloride ingress. To address this variability, powder samples were taken along a diagonal line spanning from the shoulder across one or more lanes of traffic.

The concept of corrosion threshold is used to assist in determining an estimated value for the chloride concentration that will initiate depassivation of the reinforcing steel, and hence support the initiation of corrosion. Although test methods can be used to determine the corrosion threshold values for specific materials, a specific value is often identified by an agency as the corrosion threshold to be used for assessment purposes. The chloride threshold for bridge decks used by NCDOT is 1.4 pcy. Another chloride threshold used in assessment of bridge decks is the replacement level. FHWA recommends that concrete bridge decks be replaced when the chloride concentrations reach 2 pcy.

In the data presented in Appendix H, test results exceeding the corrosion threshold (greater than 1.4 pcy but less than 2.0 pcy) are formatted in yellow, while test results exceeding the replacement level (greater than 2.0 pcy) are formatted in red. In order to assist with assessment the relative durability performance of lightweight concrete bridge decks as compared to similar normalweight concrete bridge decks, the number of test results where the replacement level and/or the corrosion threshold were tallied for certain depths. Of particular interest are the test results at the 2 in depth, as this is roughly the level of the top layer of reinforcing steel in many bridge decks. This information is presented in Table 5-5.

Table 5-5: Chloride contents exceeding corrosion threshold and replacement level at 2 in depth.

Bridge Deck	Number of test locations	Number of test locations where corrosion threshold has been exceeded at 2 in depth	Number of test locations where replacement level has been exceeded at 2 in depth
1N	8	0	0
1L	8	0	0
2N	8	0	0
2L	8	0	0
3N	8	0	0
3L	8	0	0
5N	8	0	0
5L	8	0	0
6N	8	0	0
6L	8	4	0
7N	8	2	0
7L	8	2	0
8N	8	6	2
8L	8	5	2
9N	8	4	1
9L	8	5	4

Review of this data indicates that some bridge decks have areas where the chloride content exceeds the 2 pcy replacement level at a depth of 2 in below the surface, the approximate level of the top layer of reinforcing steel. These bridges were in the mountains, where road salting is likely more frequent than some other areas of the state, particularly in urban areas. One lightweight concrete bridge deck (9L) had 4 locations exceeding the replacement level at a depth of 2 in, while its sister deck (9N) had only 1 location exceeding the replacement level at a depth of 2 in. For this pair bridge decks, the number of locations where the corrosion threshold was exceeded at a depth of 2 in was similar (4 locations for 9N versus 5 locations for 9L). The other pair of bridge decks in the mountains (8L and 8N), had similar numbers of locations where the replacement level was exceeded (2 locations for both 8L and 8N), as well as the number of locations where the corrosion threshold was exceeded.

No bridge decks included in this study from the piedmont region had chloride contents that exceeded the replacement level at a depth of 2 in. Bridge decks 7N and 7L each had two test locations where the corrosion threshold was exceeded at 2 in. However, when comparing bridge decks 6N and 6L, a noticeable difference is present in that the corrosion threshold was exceeded at a 2 in depth at 4 locations on bridge deck 6L, but at no locations on bridge deck 6N. Test results for coastal bridge decks included in this study (1N/1L, 2N/2L, 3N/3L, 5N/5L) indicated that the corrosion threshold and replacement level were not exceeded at the 2 in depth for any of these bridge decks.

To assist with analysis, review of the chloride content data at the 1 in depth was also performed. This information is presented in Table 5-6.

Table 5-6: Chloride contents exceeding corrosion threshold and replacement level at 1 in depth.

Bridge Deck	Number of test locations	Number of test locations where corrosion threshold has been exceeded at 1" depth	Number of test locations where replacement level has been exceeded at 1" depth
1N	8	0	0
1L	8	0	0
2N	8	8	3
2L	8	1	0
3N	8	0	0
3L	8	0	0
5N	8	1	0
5L	8	2	0
6N	8	2	1
6L	8	8	7
7N	8	8	3
7L	8	7	5
8N	8	8	8
8L	8	7	2
9N	8	8	7
9L	8	8	8

The corrosion threshold and replacement level were exceeded at all test locations at the 1 in depth for bridges decks 8N and 9L, and at all but one location on bridge deck 9N. Bridge deck 8L showed better performance than the other bridge decks in the mountain region, with the replacement levels reached at only 2 test locations at the 1 in depth. One notable difference, however, is that bridge deck 8L is located along US23/74 in Haywood County, while bridge decks 8N, 9L, and 9N are all located along I-40 in McDowell County.

For the Piedmont region bridge decks included in the study, the normalweight concrete bridge decks had fewer instances where the replacement level was exceeded at 1 in. Bridge deck 6N had significantly fewer locations where the corrosion threshold was exceeded than bridge deck 6L. For coastal bridges, this trend was reversed for bridge decks 2N and 2L, where the normalweight bridge deck (2N) had significantly more locations where the corrosion threshold and replacement level were exceeded at the 1 in depth than the lightweight bridge deck (2L). Results for 5N and 5L were similar, with 1 and 2 locations where the corrosion threshold was exceeded at the 1 in depth. No test results at the 1 in depth exceeded either the corrosion threshold or the replacement threshold for bridge decks 1N, 1L, 3N, or 2L.

Powder samples were collected from each bridge deck in a manner that spread the sampling locations out from the shoulder progressively across the lanes of traffic. Almost all decks drained towards the shoulder, and therefore if ponding occurs, it would most likely be at the near-edge sampling locations (hole 1). Review of data from individual holes indicates that the chloride content values for the sampling locations closest to the side of the bridge tended to have the highest chloride contents, most noticeably within the upper two in.

For each bridge deck, chloride contents computed at each test location were used to compute a diffusion coefficient characteristic of the bridge deck. Diffusion coefficients were computed using a MathCad worksheet developed by Gergely et al. (2006) as part of their previous research for NCDOT, "Concrete Diffusion Coefficients and Existing Chloride Exposure in North Carolina," NCDOT Research Project No. HWY-2004-12. The MathCad worksheet utilizes a cumulative minimization of the squared sum of error method to find solutions to Fick's second law, which describes the diffusion of chlorides into concrete. This equation is shown as Eq. 5, where C is the concentration of chlorides, C_0 is the surface concentration of chlorides, D_c is the diffusion coefficient (in^2/year), t is time in years, and *erf* is the error function.

$$C(x,t) = C_0\left\{1 - erf\left(\frac{x}{2\sqrt{D_c \times t}}\right)\right\} \qquad \text{(Eq. 5)}$$

To obtain the representative diffusion coefficient and surface concentration for each bridge deck, the data for all eight holes was included in the cumulative minimization of the squared sum of error method utilized in the MathCad program. According to work by Tempest (2006), this method of determining a representative diffusion coefficient and surface concentration value for a bridge deck may be more representative than computing values for each individual hole and then averaging. Diffusion coefficients and surface chloride concentrations computed for each bridge deck are shown in Table 5-7. These values are shown graphically in Figure 5-11 and Figure 5-12.

Table 5-7: Surface chloride concentrations and diffusion coefficients.

Bridge Deck	**Surface Chloride Concentration, C_s (lb/yd)**	**Apparent Diffusion Coefficient D_a (in^2/year)**
1N	0.305	0.759
1L	0.611	0.318
2N	3.748	0.072
2L	3.906	0.027
3N	0.279	0.238
3L	0.279	0.116
5N	1.299	0.034
5L	2.456	0.022
6N	2.546	0.070
6L	8.106	0.078
7N	2.811	0.157
7L	2.913	0.163
8N	12.654	0.088
8L	8.507	0.114
9N	9.168	0.101
9L	7.010	0.113

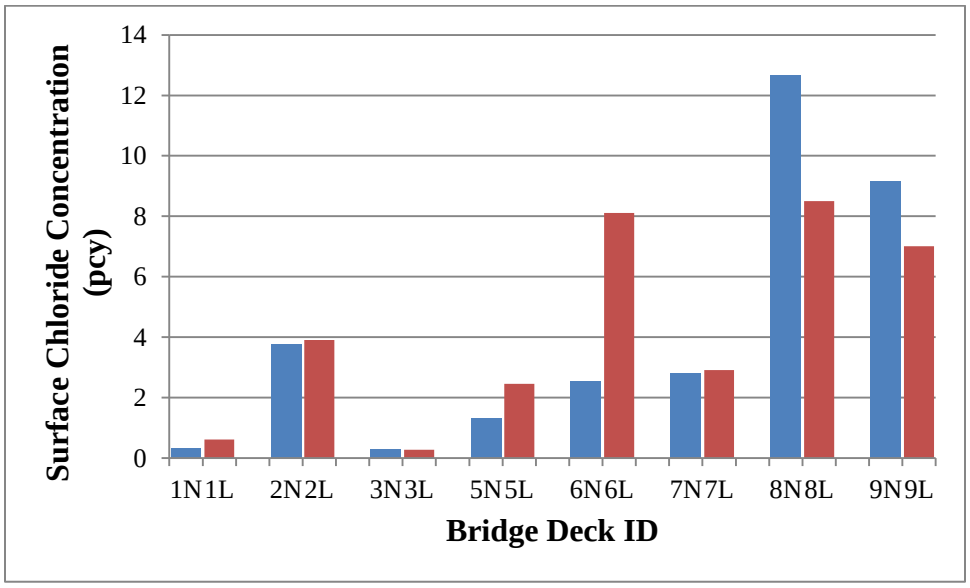

Figure 5-11: Surface chloride concentrations for normalweight and lightweight concrete bridge decks.

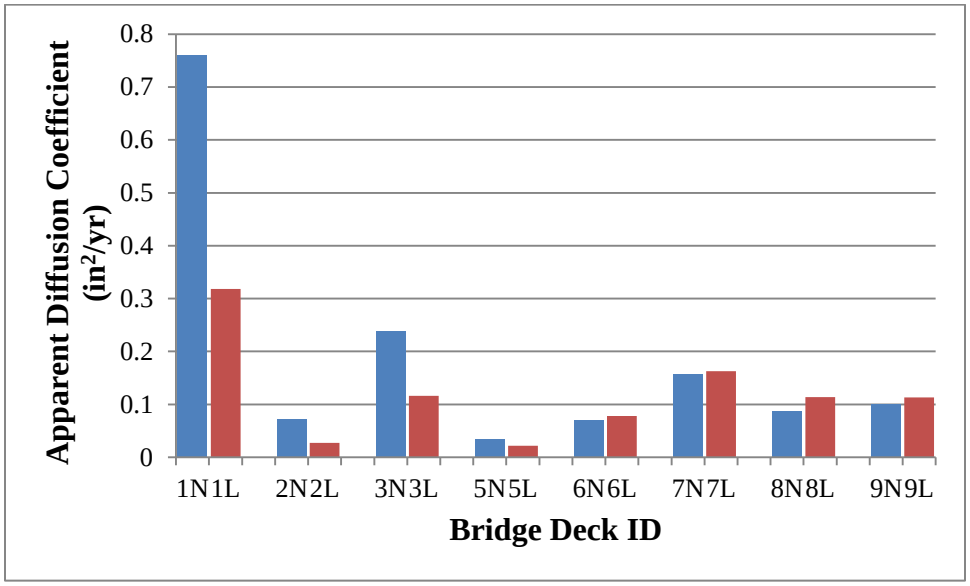

Figure 5-12: Apparent diffusion coefficients for normalweight and lightweight concrete bridge decks.

With the exception of bridge decks 2L and 2N (which are on the same bridge over the Thorofare Bay Channel, leading to Cedar Island) surface concentrations of chlorides tended to be highest on bridge decks in the mountain and the Piedmont regions. This can be seen in Figure 5-12. It is also evident that for the bridges in the coastal region, the normalweight concrete decks had higher diffusion coefficients. However, for the piedmont and mountain regions, the lightweight concrete bridge decks had higher diffusion coefficients.

Age plays an important role in diffusivity. Time is included in the mathematical functions governing diffusion, based on Fick's second law. Additionally, cracks that occur over time will increase the rate of ingress of chlorides. One of the criteria used to assist in identifying bridge deck pairs included in this study was that they should be of similar age. Most bridge deck pairs were constructed either the same year, or had the construction dates within one year of each other. It is noted, however, that three pairs of bridges, had construction dates that differed by two years (bridge decks 1L and 1N), three years (bridge decks 7L and 7N), four years (bridge decks 9L and 9N). This

may help in explaining the relative difference in diffusion coefficients for 1N and 1L, although the diffusion coefficients for 7L and 7N, as well as for 9L and 9N, are relatively close.

Statistical analysis was performed by aggregating the apparent diffusion coefficient data for normalweight bridge decks and lightweight bridge decks. A box and whisker plot showing the median, upper quartile, lower quartile, and maximum and minimum values is shown in Figure 5-13. Apparent diffusion coefficients for the lightweight bridge decks had a smaller range than those of the normalweight bridge decks. The apparent diffusion coefficient for bridge deck 1N was much greater than that of the other normalweight bridge decks, which is also evident in Figure 5-13.

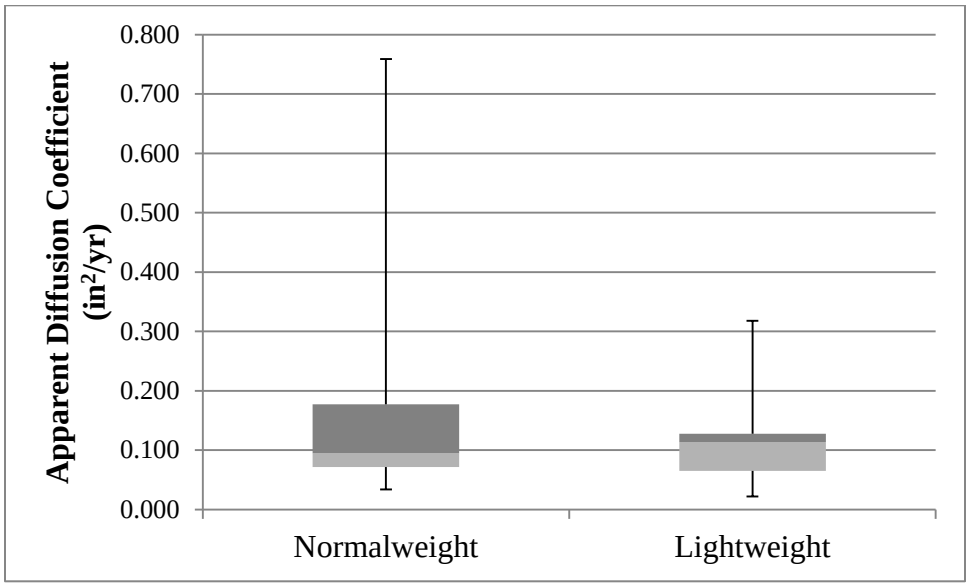

Figure 5-13: Range and summary statistics of apparent diffusion coefficients for normalweight and lightweight concrete bridge decks.

The mean apparent diffusion coefficient for normalweight bridge decks was significantly higher (0.190 in^2/year) than that of the lightweight bridge decks (0.119 in^2/year). This difference is reduced, however, if the apparent diffusion coefficient for bridge deck 1N is removed from the dataset. When bridge deck 1N is removed from the dataset, the mean apparent diffusion coefficient for the normalweight bridge decks is reduced to 0.109 in^2/year.

5.6 Rapid Chloride Permeability Test (RCPT)

Rapid chloride permeability tests (RCPT) were performed on four specimens from each bridge deck. The 2 in thick slices of cores used were obtained at positions in cores that corresponded to depths outlined in Section 3.3.6, Rapid Chloride Permeability Test (RCPT). According to ASTM C1202, chloride ion penetrability is assessed as shown in Table 5-8. Typically, good quality concrete mixtures with low water-cement ratios (resulting in dense microstructures and low permeability concrete) have lower charge passed (coulomb) values and better withstand chloride ingress.

Table 5-8: Chloride ion penetrability based on charge passed (according to ASTM C1202).

Charge passed (Coulombs)	Chloride Ion Penetrability
>4,000	High
2,000 to 4,000	Moderate
1,000 to 2,000	Low
100 to 1,000	Very Low
<100	Negligible

RCPT test results from this study can be compared to the relative penetrability ratings shown in Table 5-8. It is important to remember, however, that the RCPT test is typically performed on cast concrete cylinders. Test specimens used for this study were comprised of concrete that had been in service for a number of years, which have been subjected to traffic loading and other in-situ stresses. Therefore, the test specimens likely contained microcracks that may have affected the results, increasing the charge passed values to some extent. Additionally, the test specimen for this study had also been exposed to chlorides, which would also increase the coulomb values obtained in the RCPT.

The results of RCPT tests for each bridge deck are provided in Table 5-9. Also included in this table is information on the depth at which the specimens were cut from the cores. As outlined in Section 3.3.6, Rapid Chloride Permeability Test (RCPT), the limited number of cores that could be removed from each deck allowed only two to three cores to be available for each test. The presence of reinforcing steel in a number of cores limited the depth at which the 2 in thick specimen could be removed. Effort was also made to obtain specimen from as low as possible on the core (furthest from the bridge deck surface) to minimize the effects of ingressed chlorides on the test results. For each bridge, an attempt was made to cut two test specimen from locations deemed "low" (below a depth of 4 in) and two test specimen were cut from locations deemed "high" (from below a depth of 1½ in). An exception to this was bridge deck 2N, where reinforcing steel placement resulted in short core lengths, many of which contained reinforcing steel. For bridge deck 2N, only three specimens were tested.

Review of Table 5-9 indicates that specimens removed from shallower depths did not always have coulomb values higher than the specimens from the same bridge deck that were removed from deeper depths. Additional work would need to be performed to evaluate the effect of specimen depth on coulomb values. For this study, the average values of specimen depth were tabulated, averaged for each bridge deck, and used in further evaluation of the results.

Table 5-9: Description of RCPT test specimens and test results.

Bridge Deck	Specimen ID	Depth of Top of Specimen (in.)	Depth of Bottom of Specimen (in.)	Average Specimen Depth (in.)	Specimen Depth High/Low	Charge Passed (Coulombs)	Average Charge Passed (Coulombs)	Average Depth For all Specimens from Deck
1N	1N C2 1.5-3.5	1.5	3.5	2.5	H	3,457	3,637	3.50
	1N C4 2.5-4.5	2.5	4.5	3.5	H	3,471		
	1N C7 3.0-5.0	3	5	4	L	4,107		
	1N C8 3.0-5.0	3	5	4	L	3,512		
1L	1L C2 1.25-3.25	1.25	3.25	2.25	H	3,405	3,330	3.38
	1L C8 1.5-3.5	1.5	3.5	2.5	H	3,238		
	1L C2 3.25-5.25	3.25	5.25	4.25	L	3,481		
	1L C8 3.5-5.5	3.5	5.5	4.5	L	3,197		
2N	2N C1 0.75-2.75	0.75	2.75	1.75	H	12,470	10,823	2.17
	2N C8A 1.25-3.25	1.25	3.25	2.25	H	13,184		
	2N C2 1.5-3.5	1.5	3.5	2.5	H	6,816		
2L	2L C8 1.5-3.5	1.5	3.5	2.5	H	2,113	2,476	4.81
	2L C8 1.5-3.5	1.5	3.5	2.5	H	2,382		
	2L C6 5.75-7.75	5.75	7.75	6.75	L	3,181		
	2L C6 6.5-8.5	6.5	8.5	7.5	L	2,229		
3N	3N C7 1.25-3.25	1.25	3.25	2.25	H	3,038	3,118	3.00
	3N C7 3.25-5.25	1.75	3.75	2.75	H	2,609		
	3N C5 3.25-5.25	1.75	3.75	2.75	H	3,477		
	3N C6 1.75-3.75	3.25	5.25	4.25	L	3,346		
3L	3L C4 0.5-2.5	0.5	2.5	1.5	H	2,044	2,423	3.88
	3L C4 1.25-3.25	1.25	3.25	2.25	H	3,233		
	3L C2 4.5-6.5	4.5	6.5	5.5	L	2,530		
	3L C1 5.25-7.25	5.25	7.25	6.25	L	1,884		
5N	5N C5 1.0-3.0	1	3	2	H	3,452	5,105	2.88
	5N C6 1.0-3.0	1	3	2	H	9,539		
	5N C1 3.0-5.0	3	5	4	L	3,532		
	5N C1 2.5-4.5	2.5	4.5	3.5	L	3,898		
5L	5L C2 1.75-3.75	1.75	3.75	2.75	H	2,233	3,841	4.00
	5L C8 3.0-5.0	3	5	4	L	4,353		
	5L C5 3.5-5.5	3.5	5.5	4.5	L	4,037		
	5L C6 3.75-5.75	3.75	5.75	4.75	L	4,739		
6N	6N C2 1.0-3.0	1	3	2	H	5,404	4,785	3.50
	6N C5 1.5-3.5	1.5	3.5	2.5	H	4,255		
	6N C2 3.0-5.0	3	5	4	L	5,642		
	6N C5 4.5-6.5	4.5	6.5	5.5	L	3,839		
6L	6L C4 1.0-3.0	1	3	2	H	14,157	11,681	3.00
	6L C7 1.0-3.0	1	3	2	H	9,968		
	6L C4 3.0-5.0	3	5	4	L	10,799		
	6L C7 3.0-5.0	3	5	4	L	11,798		
7N	7N C4 1.0-3.0	1	3	2	H	10,072	10,525	4.25
	7N C4 3.0-5.0	3	5	4	H	14,711		
	7N C5 3.5-5.5	3.5	5.5	4.5	L	9,868		
	7N C5 5.5-7.5	5.5	7.5	6.5	L	7,449		
7L	7L C4 1.0-3.0	1	3	2	H	9,618	11,701	3.94
	7L C2 2.25-4.25	2.25	4.25	3.25	H	14,717		
	7L C3 3.0-5.0	3	5	4	L	8,419		
	7L C6 5.5-7.5	5.5	7.5	6.5	L	14,049		
8N	8N C5 1.0-3.0	1	3	2	H	10,224	11,440	3.06
	8N C1 1.0-3.0	1	3	2	H	10,724		
	8N C6 3.0-5.0	3	5	4	L	9,761		
	8N C5 3.25-5.25	3.25	5.25	4.25	L	15,052		
8L	8L C2 2.25-4.25	2.25	4.25	3.25	H	6,361	7,891	4.25
	8L C6 2.25-4.25	2.25	4.25	3.25	H	9,197		
	8L C2 4.25-6.25	4.25	6.25	5.25	L	7,104		
	8L C6 4.25-6.25	4.25	6.25	5.25	L	8,901		
9N	9N C4 2.5-4.5	2.5	4.5	3.5	H	9,582	8,830	5.00
	9N C7 3.5-5.5	3.5	5.5	4.5	H	9,727		
	9N C4 4.5-6.5	4.5	6.5	5.5	L	8,172		
	9N C7 5.5-7.5	5.5	7.5	6.5	L	7,840		
9L	9L C7A 1.0-3.0	1	3	2	H	9,943	9,240	5.50
	9L C4 5.25-7.25	5.25	7.25	6.25	L	7,752		
	9L C1 5.75-7.75	5.75	7.75	6.75	L	7,185		
	9L C2 6.0-8.0	6	8	7	L	12,080		

The results of the RCPT for the specimen for each bridge deck were averaged in order to obtain a representative RCPT value for each bridge deck, shown in Table 5-10. The average depth from which each of the four specimens was obtained is also shown in Table 5-10.

Table 5-10: Average total charge passed (coulombs) for RCPT tests.

Bridge Deck	Average Total Charge Passed (Coulombs)	Average Depth of Test Specimen (in)
1N	3,637	3.50
1L	3,330	3.38
2N	10,823	2.17
2L	2,476	4.81
3N	3,118	3.00
3L	2,423	3.88
5N	5,105	2.88
5L	3,841	4.00
6N	4,785	3.50
6L	11,681	3.00
7N	10,525	4.25
7L	11,701	3.94
8N	11,440	3.06
8L	7,891	4.25
9N	8,830	5.00
9L	9,240	5.50

It is evident that the average coulomb values for all bridge decks were relatively higher than what would be typically expected from tests performed on specimens prepared from cast cylinders of bridge deck concrete mixtures. Due to the critical role a bridge deck plays in protection of the bridge superstructure as well as its role in carrying traffic, bridge deck concrete mixtures are often relatively high strength mixtures with low water-cement ratios. Testing of cast cylinders of bridge deck mixtures typically results in coulomb values in the very low, low, and possibly moderate range of values (as shown in Table 5-8). Test specimens used for this study were obtained from cores removed from decks which had experienced years of environmental exposure and traffic loading. Therefore, RCPT coulomb values for these "damaged" test specimens would expectedly be higher than those of other "undamaged" specimens of similar mixture proportions.

For coastal bridges, the coulomb values tended to be within the moderate range of chloride ion penetrability, which could be considered respectable given the age (and hence, relative condition) of the test specimen used for testing. Lightweight concrete bridge decks tended to show better performance, having average coulomb values lower than their counterpart normalweight concrete bridge decks. This was particularly evident when comparing the results from bridge deck 2N and 2L, both of which are on the bridge to Cedar Island, spanning over the Thorofare Bay Channel. The normalweight portion of this bridge deck has some of the highest coulomb values, indicating high susceptibility to chloride ingress, of all decks included in this study. It is noted that only three specimens from this

bridge were tested. Additionally, each of these test specimens were obtained from locations on the cores that were relatively close to the deck surface.

A graphical comparison of coulomb values for bridge deck pairs is shown in Figure 5-14. Most of the average coulomb values for piedmont and mountain region bridge decks were relatively higher than those on the coastal bridges. For piedmont bridge decks, the lightweight concrete bridge decks had higher coulomb values than the normalweight concrete bridge decks. Mountain bridge decks had mixed results, with one of the normalweight bridge decks (9N) and one of the lightweight bridge decks (8L) having better resistance to chloride penetration than their counterpart decks.

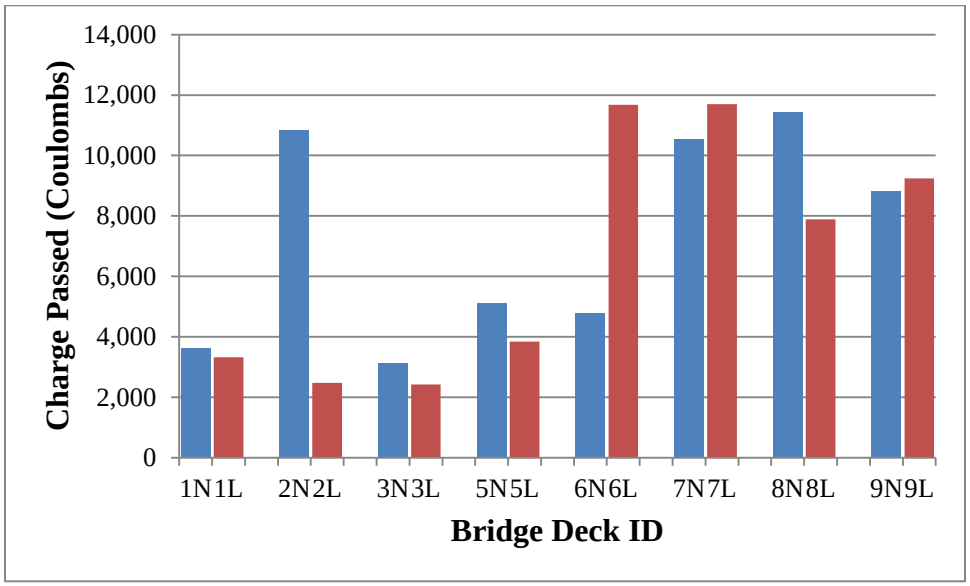

Figure 5-14: Average total charge passed for RCPT for normalweight and lightweight concrete bridge decks.

Statistical analysis was performed on the RCPT average coulomb values for normalweight bridge decks and lightweight bridge decks. A box and whisker plot showing the median, upper quartile, lower quartile, and maximum and minimum values is shown in Figure 5-15. When grouped, the mean coulomb value for the lightweight bridge decks (6,573 coulombs) was lower than the mean coulomb value for the normalweight bridge decks (7,283 coulombs), indicating a greater resistance to chloride ion penetration.

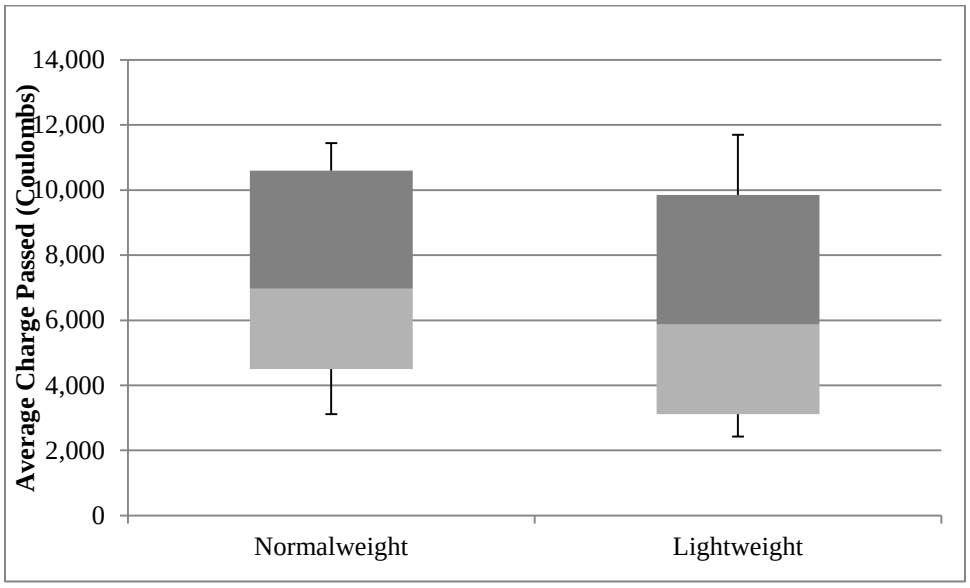

Figure 5-15: Range and summary statistics of average charge passed (coulomb values) for normalweight and lightweight concrete bridge decks.

Similar to the mean coulomb values, the median value for the lightweight bridge decks was lower than the median value for the normalweight bridge decks. The range of values for the results could be considered similar between the normalweight and lightweight decks. It is of note that when aggregated, the average depth from which all normalweight specimens were obtained was 3.52 in, while the average depth from which all lightweight specimens were obtained was 4.05 in.

5.7 Statistical Analysis of Results

To assist in comparing the performance of normalweight and lightweight concrete bridge decks, a statistical analysis technique, the Wilcoxon matched pairs test, was performed using key results from each field and laboratory test. The Wilcoxon matched pairs test is a non-parametric hypothesis test used to evaluate whether the means of two conditions within a matched groups study are significantly different. In performing the Wilcoxon matched pairs test, it is assumed that each pair of observations represents a random sample from a population, and each pair is independent of every other pair of observations. To perform the Wilcoxon Matched Pairs test, data does not necessarily need to be collected from a normal distribution. Therefore, for sample sizes with unknown distributions, the Wilcoxon matched pairs test is more sensitive than the Student's t-test. This was particularly useful, as the test results from the relatively small dataset of 16 bridges (8 normalweight, 8 lightweight), did not exhibit a normal distribution for some test results. However, it is noted that the Wilcoxon matched pairs test, like many statistical tests, is more powerful when used with larger samples.

For the Wilcoxon matched pairs test, the null hypothesis (in this case, the difference in means is equal to zero, or the mean of test results for lightweight concrete is equal to the mean of the test results for normalweight concrete) is rejected if the p-value is less than 0.05. If the p-value is greater than 0.05 then the null hypothesis is not rejected, and it cannot be said that the mean of the test result for the lightweight concrete decks was different than the mean of the test result for the normalweight concrete decks at the level of statistical significance.

Results of the Wilcoxon matched pairs tests for key performance parameters are shown in Table 5-10. In all instances, except for dynamic modulus, the data does not demonstrate a statistically significant difference in performance (at α=0.05) between normalweight decks and lightweight decks. As discussed in Section 5.3, Dynamic Modulus, it is expected that the mean dynamic modulus of lightweight concrete decks would be

significantly different than the mean dynamic modulus of normalweight concrete decks, since dynamic modulus is dependent on the density of the concrete (and hence the density of aggregates).

Table 5-10: Results of Wilcoxon matched pairs tests.

Performance Characteristic	**p-value**	**Result (at α=0.05)**	
Dynamic Modulus	0.012	accept	Statistically significant difference between performance of lightweight and normalweight concrete decks
Secondary Sorptivity - Suction	0.161	reject	Performance of lightweight and normalweight concrete decks not statistically different at α=0.05
Water Permeability (WAR)	0.204	reject	
Secondary Sorptivity - Ponding	0.310	reject	
Initial Sorptivity - Ponding	0.327	reject	
Diffusion Coefficient	0.362	reject	
Air Permeability (AER)	0.400	reject	
RCPT	0.484	reject	
Surface Resistivity	0.575	reject	
Surface Chloride Concentration	0.612	reject	
Initial Sorptivity - Suction	0.674	reject	

5.8 Petrographic Examinations

Petrographic examinations were performed on polished surfaces and fractured surfaces of the upper portions of selected cores. As outlined in Section 3.3.7, Petrographic Examinations, observations were made with a stereomicroscope at magnifications ranging from 7x to 45x. A scanning electron microscope (SEM), which can be used for examinations at higher magnifications, was not used as part of this work. During petrographic examinations, observations regarding the general characteristics of the concrete, including the paste, aggregates, and air void system, were made. Observations on air content, microcracks, secondary deposits, and the presence of secondary cementitious materials such as fly ash were also recorded. Datasheets outlining the macroscopic and microscopic observations of polished samples are included in Appendix I. A summary of the results of our petrographic observations is included in this section.

As part of this work, NCDOT requested that UNC Charlotte provide an opinion regarding the durability performance of decks that contain fly ash. NCDOT personnel indicated that fly ash is likely present in bridge decks constructed after June 2000 in Divisions 5, 7, 9, 10, 11, 12, 13, 14, (some mountain and piedmont areas) and bridges east of US 17 (coastal bridges). In current NCDOT Standard Specifications, dosing for Class F Fly Ash is 20% by weight of required cement content with 1.2 lb Class F fly ash per lb of cement replaced. Based this information, the following summary is provided regarding fly ash in the bridge decks included in this study.

- Fly ash should be present in bridge deck 4L, which has a 2003 construction date.
    - Mixture submittals were not available for this bridge deck.
    - Visual observations of samples prepared from this bridge deck indicate that fly ash is likely present. Dark particles that may be fly ash were observed in the paste matrix, and cenospheres were observed after acid etching of the samples. Additional analysis (using SEM or other techniques) could be used to confirm the presence of fly ash.

- Fly ash could be present in bridge decks 1L, 8N, and 9N, which each have a construction date of 2000.
    - It is unclear which of these decks were constructed before/after the June 2000 requirement.
    - Visual observations of samples prepared from bridge deck 1L indicate that fly ash is present, which is consistent with the mixture submittal for this bridge. Dark particles that may be fly ash were observed in the paste matrix, and cenospheres were observed after acid etching of the samples. Additional analysis (using SEM or other techniques) could be used to confirm the presence of fly ash.
    - Mixture submittals were not available for bridge decks 8N and 9N. Because these bridges are located in McDowell County (Division 13) it is possible that fly ash was included in these mixtures. Although observations made during petrographic examinations of samples from these bridge decks did not confirm the presence of fly ash, it may be present. Dark particles that may be fly ash were observed in the paste matrix, but cenospheres were not observed after acid etching of the samples. Additional analysis (using SEM or other techniques) could be used to confirm the presence of fly ash.

- The remaining bridges included in this study (1N, 2N/2L, 3N/3L, 4N, 5N/5L, 6N, 6L, 7N, 7L, 8L, and 9L) have pre-2000 construction dates, and may or may not contain fly ash in the decks.
    - Mixture submittals were not available for these bridge decks.
    - Bridge deck 1N appears to include fly ash, as dark particles that may be fly ash were observed in the paste matrix, and cenospheres were observed after acid etching of the samples. Additional analysis (using SEM or other techniques) could be used to confirm the presence of fly ash.
    - Observations made during petrographic examinations of samples from bridge decks 3N, 3L, 4N, 5N, 5L, 6N, 6L, 7N, 7L, and 9L did not confirm the presence of fly ash. Dark particles that may be fly ash were observed, but cenospheres were not observed after acid etching of the samples. Additional analysis (using SEM or other techniques) could be used to determine whether fly ash was used in these mixtures.
    - Observations made during petrographic examinations of samples from bridge deck 8L indicated less evidence of the presence of fly ash. Fewer dark particles were present in the paste indicating that fly ash may or may not have been included in the mix. Cenospheres were not observed after

acid etching of the samples. Additional analysis (using SEM or other techniques) could be used to confirm the presence or absence of fly ash.

The presence (or absence) of microcracks and secondary deposit material was of specific interest during petrographic observations. Microcracks may be the result of a number of materials-related and stress-related causes, as discussed in the literature review. Microcracks allow for the ingress of moisture and aggressive agents, and could have influenced the results of other field and laboratory tests. Secondary deposits can be crystalline material from a number of internal sources (secondary ettringite) or external sources (salts), and can infill entrained air voids, resulting in reduced freeze-thaw durability of concrete.

In this study, the performance of bridge decks pairs was compared. For this reason, information observed differences in microcracking and secondary deposits present may supplement test results. Key differences in performance between samples from bridge deck pairs, along with other petrographic observations of note, are provided below. Photomicrographs from some petrographic specimens are included in Appendix I.

Bridge deck pair 1N/1L
More microcracks were observed the sample from 1N than from the sample from 1L. Microcracks present in samples from 1N appear to extend significantly deeper into the sample. The sample from 1L that was observed also contained a significant number of entrapped air voids.

Bridge deck pair 2N/2L
Samples from both bridge decks 2N and 2L contain a relatively high air content. In a number of areas, air voids have coalesced, resulting in high air content in many localized areas. This high air content may have been a key contributor to the relatively poor performance of these bridge decks in some tests. Samples from bridge deck 2L contained more microcracks than samples from bridge deck 2N, which may be due to the fact that localized areas of high air content appear to be more prevalent in samples from bridge deck 2L.

Bridge deck pair 3N/3L
A similar extent of microcracking was observed in samples from both 3N and 3L.

Bridge deck pair 5N/5L
A similar extent of microcracking was observed in samples from both 5N and 5L. Samples from 5N were judged to have higher entrained air contents than samples from 5L.

Bridge deck pair 6N/6L
An inordinate number of water voids is present in samples from 6L, and some segregation is evident in one sample from 6L. This inordinate number of air voids may have contributed to relatively poor performance of specimens from bridge deck 6L in some tests. Samples from both 6N and 6L contained a number of microcracks, with samples from 6N appearing to contain more microcracks than samples from 6L. More secondary deposits were observed in air and water voids in samples from 6L than in 6N, however, possibly showing additional ingress of water and some deleterious substances (such as salts).

Bridge deck pair 7N/7L
A similar extent of microcracking was observed in samples from 7N and 7L. However, more secondary deposits were observed in samples from 7L than in samples from 7N, possibly showing additional ingress of water and some deleterious substances (such as salts).

Bridge deck pair 8N/8L
A similar extent of microcracking was observed in samples from 8N and 8L.

Bridge deck pair 9N/9L
The extent of microcracking observed in samples from 9N was judged to be greater than the extent of microcracking observed in samples from 9L. However, more secondary deposits were observed in samples from 9L than in samples from 9N, possibly showing additional ingress of water and some deleterious substances (such as salts).

6. FINDINGS AND CONCLUSIONS

The purpose of this research was to provide NCDOT information that will prove to be useful in making decisions regarding 1) use lightweight concrete or normalweight concrete bridge decks for certain applications, 2) maintenance and repair, and 3) possible changes to design and construction methods and/or specifications. Although some differences in the performance of lightweight and normalweight concrete bridge decks were observed in field and laboratory tests, a distinct difference between the overall durability performance of lightweight bridge decks and normalweight bridge decks included in this study was not readily evident. This finding differs from those of a number of studies that have indicated that lightweight concrete can provide enhanced durability performance, and additional laboratory-based studies of lightweight and normalweight concrete bridge deck mixtures using local materials are recommended.

Damages induced by factors such as structural characteristics and external loads may have played a significant role in observed distresses, as well as in the results of a number of field and laboratory tests. Additionally, it is possible that that there has not been ample time for distinct differences in performance between lightweight and normalweight concrete decks included in this study to become evident during field observations, or measurable during field or laboratory tests. Regional trends in performance were observed for some durability tests, however, and this information could be utilized by NCDOT.

Based on the results of our visual surveys, structural characteristics of some bridges may have influenced the cracking observed on both lightweight and normalweight bridge decks. Bridge decks with continuous steel girders exhibited some of the more extensive pattern cracking and some transverse cracking. The most extensive transverse cracking observed on bridge decks included in the study is present on two bridge decks which are supported by steel plate girders and steel I-beams, respectively. Transverse cracking on these decks may also be related to structural-related stresses, loads applied too soon after the deck was constructed, or other reasons. Bridge decks with stay-in-place metal forms also tended to exhibit more longitudinal and transverse cracking than bridge decks on precast concrete girders and non-continuous steel girders. Cracking perpendicular to expansion joints was likely related to additional restraint from near-joint reinforcement, rather than materials-related causes. On some bridges, cracks were observed in the vicinity of bents. Reinforcing details near expansion joints, as well as issues related to transitions between positive and negative moment regions, could have contributed to this cracking. Integral abutments could have also contributed to some cracking.

The most severe and most extensive pattern cracking was observed on bridge decks with the highest traffic loading. Pattern cracking could have initiated due to materials-related issues, but may have been exacerbated due to traffic loads. For many pairs of decks, both the lightweight deck and normalweight deck had similar pattern cracking present. However, for two bridge deck pairs, one bridge deck exhibited pattern cracking while the other bridge deck did not. Bridge deck 5N and 5L are on the same bridge, with the normalweight deck exhibiting pattern cracking while the lightweight deck did not. Bridge deck 8L exhibited pattern cracking, while bridge deck 8N did not; it is, however, noted that 8L and 8N are not the strongest pairing for comparison. Although these two bridge decks have similar traffic loadings and ages, they are two different roadways in two separate counties.

To summarize, based on cracks observed during the visual surveys of bridges selected for this study, it was not readily evident that one type of bridge deck consistently exhibited less cracking than another type of bridge deck. It is possible that over time, the differences in durability performance between the lightweight decks and normalweight decks will become more pronounced, and differences in the extent and severity of cracks between bridge deck pairs could be observed in future visual surveys.

The moisture content of concrete can influence a number of tests performed in this study. Specimens can be conditioned to minimize the effects of different moisture contents in interpretation of test results. In the field, however, tests must often be performed at the in-situ moisture content. In this work, all field tests except for surface resistivity were performed at the in-situ moisture content. Later, laboratory testing of selected cores and pieces of cores was performed to estimate the in-situ moisture content. For all pairs of bridge decks, the moisture content of cores removed from the lightweight bridge deck was higher than the moisture content of the cores removed from the normalweight bridge deck. The difference in moisture content was most pronounced in two of the coastal bridges with the greatest difference in moisture content was 3.4% between bridge decks 2N and 2L. As

part of this testing, the apparent density of selected concrete cores and pieces of cores was determined. The average apparent density of both normalweight and lightweight concrete specimens was slightly higher than the expected values.

Surface resistivity measurements can be used to indirectly measure concrete's susceptibility to chloride ingress. Higher resistivity readings indicate concrete that will exhibit lower permeability and therefore better durability performance. In recent years, surface resistivity tests using the Wenner probe apparatus have become increasingly attractive because they are quickly performed and are non-destructive. A number of recent studies have linked surface resistivity measurements to durability performance via the laboratory-performed RCPT procedure. Very few of these studies include data obtained in the field. As part of this study, a database of surface resistivity measurements of in-situ concrete of varying compositions, age, and exposure were obtained. As ongoing work continues in this area, the relationship between measured surface resistivity and durability performance will become better understood, and surface resistivity measurements obtained as part of this work could possibly be used to predict concrete performance with more certainty.

Overall, the mean temperature-corrected surface resistivity for the normalweight decks (81.9 kΩ-cm) was higher than that of the lightweight decks (65.5 kΩ-cm), indicating the potential for better durability performance. Looking at the results regionally, surface resistivity results were mixed. For the four pairs of coastal bridges, two decks had higher average temperature-corrected surface resistivity readings than their counterpart lightweight decks. For the other two pairs of coastal bridges, the lightweight concrete decks had higher average temperature-corrected surface resistivity readings. For both pairs of bridge decks in the mountains, the normalweight decks had higher average temperature-corrected surface resistivity values than the lightweight decks. However, some of the lowest temperature-corrected resistivity readings were obtained for these four bridge decks. These decks were also found to have some of the highest surface chloride contents, which may have also caused low resistivity readings. Additional work could be performed to link chloride content to surface resistivity measurements.

For this study, a field test to evaluate air permeability and water permeability was performed using commercially available test equipment. When compared to published values, air permeability ratings (AER) and water permeability ratings (WAR) for both normalweight and lightweight bridge decks typically correlated to mixtures with less than desirable durability characteristics. However, it is suspected that these readings are greatly influenced by the microcracking present in the vicinity of the test plugs. It is likely that if tested during early ages (prior to cracking due to environmental and traffic loads), the concrete comprising the bridge decks would show far better resistance to both air and permeability. Also, some field air and water permeability test results may have been influenced by the presence of highly porous aggregate(s) in the immediate vicinity of some drilled test holes, particularly for the lightweight bridge decks. Other researchers have cautioned about the effect of moisture content on permeability test results. For these reasons, it is suggested that other methods of assessing air and water permeability may offer better insights into these durability performance characteristics.

Although compressive strength is not generally viewed as a direct indicator of durability performance, several cores from each bridge deck were tested for compressive strength. Average adjusted compressive strengths for most bridges ranged from 3,200 psi to approximately 5,000 psi. These values are lower than what may be expected based on the typical design 28-day compressive strength for bridge decks. Several factors may have played a role in these relatively low compressive strength test results. Perhaps most importantly, the test specimens were comprised of concrete that had been in service for many years, and likely contained some internal damage. Additionally, most cores had a length to diameter ratio of less than the optimal L/D ratio specified in ASTM C42 of 2 to 1, and a correction factor was applied to the compressive strength test results. ASTM C42 emphasizes that "historically, it has been assumed that core strengths are general 85% of the corresponding standard-cured cylinder strengths."

Dynamic modulus testing of selected cores from each bridge deck was performed in accordance with ASTM C215. For each pair of bridge decks, the lightweight deck had a lower dynamic modulus than the normalweight deck. Both the static modulus and dynamic modulus are dependent on density; since lightweight aggregates have a lower density than normalweight aggregates, these test results are as expected. Although dynamic modulus can be used to assess damage, direct comparison between dynamic modulus test results for pairs of bridges is limited due to the

change in aggregate density. Using relationships between static and dynamic modulus as published by Neville (1995) and others, the dynamic modulus values can provide insight into the anticipated static modulus values.

Sorptivity tests performed as part of this work provide insight into the susceptibility of these concrete bridge decks to water permeability, and hence can be linked to durability performance. Results of the ponding sorptivity test provide insight into the gravity-aided absorption of water. Since the tests were performed on the actual wearing surface of the bridges (top end of cores), they include influences associated with microstructural damage and abrasion, and are representative of actual field sorptivity characteristics. The ASTM C1585 capillary suction test was performed on a surface 2 in deep from the wearing surface of the deck, where abrasion is not a factor, and microstructural damage is likely far less prevalent than nearer to the surface of the deck. Therefore, ASTM C1585 capillary suction test results may more closely represent the results that would have been obtained if these concrete mixtures had been tested prior to service. When comparing the sorptivity test results of pairs of bridge decks, the higher absorption of manufactured lightweight aggregates must be kept in mind. Results of these tests on the lightweight concrete specimens could be highly influenced by the exposed lightweight aggregate on the exposed surface (ponding test) or sawcut surface (suction test). Migration of water, and hence aggressive agents, through the paste, is typically of concern. Some research has indicated that lightweight concrete can show decreased permeability (compared similar normalweight mixtures) due to a formation of higher density paste in the near-aggregate interfacial transition zone and often a more compatible elastic modulus between the paste and lightweight aggregate.

For the bridge deck pairs included in this study, sorptivity test results did not clearly show that one type of concrete performed better than the other. However, some regional trends were evident. In the capillary suction sorptivity test, it is interesting to note that the coastal normalweight bridge decks typically had slightly higher initial absorption rates than the lightweight decks. Conversely the same decks had significantly lower secondary absorption rates than the lightweight bridge decks. In both sorptivity tests, both lightweight bridge decks and normalweight bridge decks in the piedmont and mountains often had higher initial absorption rates than coastal bridge decks. This should be of concern to NCDOT, as measured surface chloride contents were very high in mountain decks. High initial absorption rates coupled with heavy deicer application could result in accelerated chloride ingress, and ultimately more rapid deterioration of bridges.

FHWA recommends that concrete bridge decks be replaced when the chloride concentrations near reinforcing steel reach 2 pcy. Several mountain bridge decks were found to have areas where the chloride content exceeds the replacement level at a depth of 2 in below the surface. For one bridge deck pair, the lightweight bridge deck had more locations exceeding the replacement level at a depth of 2 in than the normalweight bridge deck. However, the number of locations where the corrosion threshold was exceeded at a depth of 2 in was similar. In the other pair of mountain bridge decks, the lightweight bridge deck showed similar performance to the normalweight bridge deck, with a similar number of locations where the replacement level and corrosion threshold were exceeded. No piedmont or coastal bridge decks included in this study had chloride contents that exceeded the replacement level at a depth of 2 in.

NCDOT utilizes a corrosion threshold chloride content of 1.4 pounds per cubic yard. Both the normalweight and lightweight deck in one pair of piedmont bridge decks had 2 of 8 of test locations where the corrosion threshold was exceeded at 2 in. For the other pair of piedmont decks, the corrosion threshold was exceeded at a 2 in depth at 4 of 8 test locations on the lightweight deck, but at no locations on the normalweight deck. The corrosion threshold was not exceeded at the 2 in depth for any of the coastal bridge decks included in this study.

Chloride contents at the 1 in depth also provided insight into the difference in performance between lightweight and normalweight bridge decks. For the four mountain bridge decks included in the study, the replacement level was exceeded at all test locations at the 1 in depth for one normalweight deck and one lightweight deck, and at 7 out of 8 test locations on the other normalweight deck. The other lightweight bridge deck showed better performance than the other bridge decks in the mountain region, with the replacement levels reached at only 2 of 8 of test locations at the 1 in depth. For the piedmont region bridge decks included in the study, the normalweight concrete bridge decks had fewer instances than lightweight bridge decks where the replacement level was exceeded at 1 in. For coastal bridges, a trend in the type of bridge deck showing greater chloride contents was not readily evident.

Chloride contents of non-coastal bridges were quite high in the piedmont and mountain region, providing findings similar to those of Gergely et al. (2004) in a study of North Carolina bridges. For the bridges in the coastal region, the normalweight concrete decks had higher diffusion coefficients. However, for the piedmont and mountain regions, the lightweight concrete bridge decks had higher diffusion coefficients. The mean apparent diffusion coefficient for normalweight bridge decks was significantly higher (0.190 in^2/year) than that of the lightweight bridge decks (0.119 in^2/yr). If the apparent diffusion coefficient for bridge deck 1N is removed from the dataset, this difference is reduced, and the mean apparent diffusion coefficient for the normalweight bridge decks is reduced to 0.109 in^2/year.

The RCPT test is used to evaluate the relative chloride permeability of concrete. Average coulomb values for all decks were relatively higher than those that would typically be expected from tests performed on specimen prepared from cast cylinders of bridge deck concrete mixtures. This is likely due to the damaged nature of the test specimens, and to some extent, the presence of ingressed chlorides in the test specimens. Most coastal bridges (both lightweight and normalweight) had the best performance in RCPT tests, tending to have coulomb values within the moderate range of chloride ion penetrability. Lightweight concrete coastal bridge decks tended to perform better, having average coulomb values lower than their counterpart normalweight bridge decks. Most average coulomb values for piedmont and mountain bridge decks were relatively higher than those on the coastal bridge decks. For piedmont bridge decks, normalweight concrete bridge decks had lower coulomb values than their counterpart lightweight concrete bridge decks, showing increased resistance to chloride penetration. For mountain bridge decks, results were mixed, with one of the normalweight bridge decks and one of the lightweight bridge decks having better resistance to chloride resistance than their counterpart decks.

Petrographic examinations provided some insight into the characteristics of concrete mixtures used in the bridge decks, and also provided insight into possible influences on some test results. Key findings of petrographic examinations included a relatively high air content in bridge decks 2N and 2L. Samples from these two bridge decks include areas of coalesced entrained air voids. This high air content may have been a key contributor to the relatively poor performance of these bridge decks in some tests. Samples from bridge deck 2L contained more microcracks than samples from bridge deck 2N, which may be due to the fact that localized areas of high air content appear to be more prevalent in samples from bridge deck 2L. Additionally, an ordinate number of water voids was observed in one sample from bridge deck 6L. This inordinate number of air voids may have contributed to relatively poor performance of specimens from bridge deck 6L in some tests. Samples from both 6N and 6L contained a number of microcracks, with samples from 6N appearing to contain more microcracks than samples from 6L. In bridge decks from both pairs 2N/2L and 6N/6L, however, more secondary deposits were observed in samples from the lightweight bridge deck than from the normalweight bridge deck. When comparing the extent of microcracks present in pairs of bridge decks, the extent of microcracks was often judged to be similar.

Based on NCDOT's history of specifying fly ash on bridge decks, several of the bridge decks included in this study should contain fly ash (in particular, 1L, 8N, and 9N). Petrographic observations using a stereomicroscope indicated that fly ash is likely present in some of these bridge decks, and good performance in some tests could be linked to the presence of fly ash. However, additional work would need to be performed to confirm the presence of fly ash in a several other bridge decks, as well as to provide a firm statement regarding the durability performance in bridge decks containing fly ash.

In conclusion, further laboratory-based study of lightweight concrete made with local materials may provide better insight into the durability performance of lightweight concrete. Findings of laboratory-based studies by a number of researchers indicate that lightweight concrete can provide enhanced durability performance, which would be an advantage beyond the reduced structural loads offered by use of lightweight aggregate. Recent studies on internal curing using saturated lightweight aggregate provide insight into the formation of a denser paste microstructure that can offer reduced permeability and better durability performance of lightweight concrete. Further laboratory-based study using local materials, and/or future visits to the bridge decks included in this study, may be useful in assisting NCDOT with decisions regarding possible changes to design and construction methods or specifications.

7. RECOMMENDATIONS

The results of this study have provided insight into the durability performance of lightweight and normalweight concrete bridge decks in a variety of service conditions. Although the Findings and Conclusions presented in Section 6 will be useful to NCDOT, additional work to supplement this study could be performed in the future, offering more insight into the relative performance of lightweight and normalweight concrete bridge decks. Also, some tests performed as part of this study are not currently utilized by NCDOT, and show promise for use in the future. Areas in which further research is recommended are discussed below.

- *Laboratory study on durability performance of lightweight concrete with materials used in North Carolina*

  Some differences in the performance of lightweight and normalweight concrete bridge decks were observed in field and laboratory tests. However, a distinct difference between the overall durability performance of lightweight bridge decks and normalweight bridge decks included in this study was not readily evident. Factors other than material characteristics, such as differences in structural characteristics and traffic loading between bridge deck pairs, may have played a significant role in the findings of this study. Much work to evaluate the durability of lightweight concrete has been performed in a laboratory setting, where the performance of materials can be evaluated without the influence of other factors such as structural characteristics, traffic loading, and environmental exposure. Findings of laboratory-based studies by a number of researchers indicate that lightweight concrete can provide enhanced durability performance. It is recommended that a laboratory study be performed, using materials typically utilized in North Carolina, where lightweight concrete mixtures will be compared to the performance of similar normalweight concrete mixtures. Findings of the laboratory study could be compared with the results of this field study to better understand the role of concrete material characteristics in field performance.

- *Additional fieldwork to supplement this research*

  It is possible that there has not been ample time for distinct differences in performance between lightweight and normalweight concrete decks included in this study to become evident during field observations, or measurable during field or laboratory tests. A number of bridge decks included in this study did not exhibit an appreciable amount of distress at the time of our visual survey. In other cases, the extent of distress observed on the normalweight bridge deck was very similar to the extent of the distress on the lightweight bridge deck. It is recommended that pairs of bridge decks (including both the lightweight and normalweight decks) that did not exhibit significant distress be revisited at future times to observe and document changes in condition, and if possible perform field and or/laboratory tests. If a full scope of field and laboratory testing cannot be performed on these pairs of bridge decks, observations of distress made during a visual survey could provide some insight into performance. Similarly, information collected as part of other research projects and/or periodic inspections could be used to supplement the findings of this study. Of particular interest would be the results of RCT tests to evaluate chloride ingress.

- *Laboratory study on internal curing using locally available lightweight aggregates*

  The increased absorptive capacity of lightweight aggregates has been shown to facilitate delivery of moisture to concrete for internal curing. Internal curing promotes formation of a denser paste microstructure, resulting in reduced permeability, higher strength, and better durability performance. A number of studies have shown that prewetted lightweight aggregate can be successfully used in concrete mixtures to provide additional water to facilitate internal curing (Delatte et al. 2007, Bentz 2009, and others). If it can be shown that the increased quality of concrete constructed using lightweight aggregates for internal curing provides long-term cost benefits, NCDOT may be able to justify changes in policy regarding when and where these mixtures should be specified. A laboratory study on internal curing using locally available lightweight aggregates is recommended.

- *Field and/or laboratory study on the durability performance of bridge decks constructed using fly ash.*

  As part of this work, test data was obtained that provides an indication on the durability performance of some North Carolina bridge decks that likely include fly ash. Currently, NCDOT specifies that fly ash must be used in bridge decks constructed in coastal locations, as well as in bridge decks constructed in certain other divisions. Additional field and laboratory studies could be performed to assist North Carolina in determining whether fly ash should be specified for bridge decks in other areas of the state.

- *Study to assess the use of surface resistivity to evaluate durability performance in field and laboratory*

  Work by a number of researchers (Sengul and Gjørv 2008, Presuel-Moreno et al. 2010, Spragg et al. 2011, and others) has shown that surface resistivity (and conductivity) test results can be used to predict the ease of fluid migration (and hence the migration of aggressive agents such as chlorides) in concrete. Surface resistivity and conductivity tests are rapid, fairly easy to perform, and can provide insight into the durability performance of bridge decks as well as other concrete structural components. Some state DOTs are considering specifying surface resistivity testing for use in construction projects (Rupnow and Icenogle 2012) in lieu of ASTM C1202 rapid chloride penetrability testing. This study has generated a database of surface resistivity measurements obtained in the field for in-situ concrete. Relatively few comprehensive studies of surface resistivity in field applications exist at this time. NCDOT could consider additional research to establish a correlation between laboratory measurements of surface resistivity and field measurements, in hopes of correlating durability performance to this relatively simple, non-destructive test procedure.

- *Study on incorporation of surface resistivity and/or conductivity into concrete materials testing program*

  NCDOT should consider identifying areas in which surface resistivity and/or conductivity testing could be used to supplement other materials testing. Cylinder specimens and core specimens used for other tests can quickly and easily be tested in accordance with AASHTO TP-95, and a database of measurements can be developed. Similar to work done by Rupnow and Icenogle (2012), rapid chloride permeability testing (ASTM C1202) could be performed on selected concrete specimens to correlate surface resistivity measurements to chloride penetrability. Once a correlation is established, surface resistivity measurements on concrete cylinders and cores could be utilized to predict the chloride penetrability, and hence predict the durability performance of a number of concrete mixtures used in North Carolina.

- *Identification of a preferred method for obtaining air and water permeability in field and laboratory settings*

  Air and water permeability test results are indicators of the ability of aggressive agents to be transported into concrete, and are therefore seen by many as good predictors of durability performance. In this study, commercially available test equipment was used to measure air and water permeability in the field. Although portable and relatively easy to use, the test procedure was found to be time consuming and required significant effort from the technician. Due to the duration of each test, work could only be completed at a few locations (typically one to three locations) during the allowable lane closure times. To have more confidence in the measurements, additional data would have been desirable. This test equipment may prove useful in testing other structural components in situations where adequate time is available. Also, although the WAR and AER can be correlated to standards established by the equipment manufacturer (and by extension, other published work), these standards have not been correlated to the performance of North Carolina materials. If NCDOT is interested in obtaining air and water permeability measurements of concrete for other purposes, it is recommended that other equipment or test methods be utilized and evaluated. Other tests that may prove to be more useful to NCDOT include sorptivity testing (in a laboratory setting) of test specimens prepared from cores. Sorptivity test results obtained from specimens included in this study were fairly reliable and consistent, and showed good correlation to the published results of others for similar applications (Bentz et al. 2002).

8. IMPLEMENTATION AND TECHNOLOGY TRANSFER PLAN

Research Product 1	Results of field evaluations and laboratory tests comparing lightweight and normalweight concrete bridge decks.
Suggested User	Bridge Management Unit and Materials and Tests Unit
Recommended Use	Recommendations of this study can be used to assist the Bridge Management Unit in deciding whether to use lightweight concrete bridge decks when designing new bridges or repairing existing bridges. The bridge decks included in this study are from a number of locations statewide, and represent a range of traffic loadings and ages. Insight into the durability performance of other bridge decks, both lightweight and normalweight concrete, could be gained from the results of this study. This information could be used to assist in design and in service life prediction. Some data could be used in selection of input values for service life prediction models. Decisions regarding maintenance and repair could also be aided by the results of this study. The visual survey drawings and chloride ingress information could be particularly helpful to those responsible for maintenance and repair decisions.
Recommended Training	None recommended at this time.

Research Product 2	Surface chloride contents, diffusion coefficients, and profiles of chloride content vs. depth for 18 normalweight and lightweight bridges in coastal, piedmont, and mountain regions.
Suggested User	Bridge Management Unit and all divisions
Recommended Use	Diffusion coefficients can be utilized in service life prediction models in design of future bridge decks. Information on chloride contents for non-coastal bridges can be used in evaluation of deicer applications, and can be used to supplement other ongoing research in this area. This information could also be useful in selection of mixture designs for use in future bridge deck construction.
Recommended Training	None recommended at this time.

Research Product 3	List of bridge decks where chloride contents exceed the corrosion threshold and replacement levels at 1 in and 2 in depths.
Suggested User	Bridge Management Unit and division personnel
Recommended Use	Bridges in which chloride contents exceed the corrosion threshold and replacement levels at 1 and 2 in depths could be considered when planning repair and rehabilitation. This information could also be relayed to other parties involved in periodic bridge evaluations to assist in future monitoring.
Recommended Training	None recommended at this time.

Research Product 4	**S**urface resistivity measurements of 18 normalweight and lightweight concrete bridge decks.
Suggested User	Materials and Tests Unit, Bridge Management Unit
Recommended Use	Surface resistivity tests results have been shown to correlate well with results of ASTM C1202 Rapid Chloride Ion Permeability Test results (Rupnow and Icenogle 2012). Other researchers are currently investigating the use of conductivity (inverse of resistivity) as a predictor of concrete durability. Ongoing research efforts by a number of researchers and agencies should result in additional guidance on use of surface resistivity in the near future. As findings and standards become available, surface resistivity data collected as part of this work could potentially be used to assess durability performance.
Recommended Training	If surface resistivity is integrated into procedures utilized by the Materials and Tests Unit, minimal training on the device would be required. AASHTO provisional standard TP 95-11 can be used as guidance for use of the surface resistivity meter in the laboratory setting. The field testing protocol utilized by UNC Charlotte researchers for this study could be used until other procedures are adopted by AASHTO or ASTM, or better procedures are identified by researcher and practitioners.

Research Product 5	Distress surveys of 18 normalweight and lightweight bridge decks in coastal, piedmont, and mountain regions.
Suggested User	Bridge Management Unit
Recommended Use	Cracking exhibited by bridge decks can be the result of design characteristics. Personnel involved in bridge design may be able to correlate some distresses observed on these bridge decks to design features or construction practices. Insight gained from these distress surveys could be used to assist in design of future bridges.
Recommended Training	None recommended at this time.

Research Product 6	Results of field evaluation and laboratory testing of two normalweight concrete bridge decks in Craven County, NC (240083 and 240231).
Suggested User	Bridge Management Unit, Materials and Tests Unit, and Division 2 personnel
Recommended Use	After field evaluations were performed, it became evident that bridge 240231 was incorrectly inventoried as a lightweight bridge deck. Therefore, this bridge deck along with its companion normalweight concrete deck 240083 could not be included in the performance comparisons or statistical analysis with the other 8 pairs of bridge decks. However, the same suite of field tests and laboratory tests performed for other bridge decks was performed on 240083 and 240231, and these results will be provided to NCDOT in a separate report. This information could be used to by Bridge Management Unit or Division 2 personnel to evaluate the performance of these two important bridges near Edenton, North Carolina.
Recommended Training	None recommended at this time.

Research Product 7	Results of field testing using air and water permeability test apparatus and surface resistivity meter.
Suggested User	Materials and Tests Unit
Recommended Use	UNC Charlotte gained insight into use of two pieces of test equipment not currently used by NCDOT. The Poroscope Plus apparatus is used to measure air and water permeability in the field, and the surface resistivity meter can be used to measure resistivity of concrete in both field and laboratory settings. Should the Materials and Tests Unit be interested in using these devices, this report outlines a field test procedure and presents a database of test results for North Carolina bridge deck concrete.
Recommended Training	Manufacturer's operating instructions are available for both pieces of test equipment. A number of publications regarding surface resistivity, as well as an AASHTO standard (AASHTO TP-95), are also available. UNC Charlotte personnel could meet with Materials and Tests Unit personnel to assist in training, if requested.

Research Product 8	Digital database of test results from field and laboratory testing
Suggested User	Materials and Tests Unit
Recommended Use	Information contained in this database could serve as reference data for evaluation of concrete mixtures and/or test methods in future work. Data could also be used to supplement additional databases on maintained by the Materials and Tests Unit.
Recommended Training	None recommended at this time.

Research Product 9	Information on role of fly ash in durability performance of 18 normalweight and lightweight concrete bridge decks.
Suggested User	Bridge Management Unit and Materials and Tests Unit
Recommended Use	As part of this work, preliminary observations were made regarding the performance of bridge decks containing fly ash. Some of these preliminary recommendations could be used to supplement other information used to assist in deciding whether to use fly ash in future bridge decks construction. This information could also be used to help NCDOT personnel in determining future changes to design and construction specifications regarding fly ash.
Recommended Training	None recommended at this time.

9. REFERENCES

American Association of State Highway and Transportation Officials (AASHTO) (2011). AASTHTO TP-95 "Surface Resistivity Indication of Concrete's Ability to Resist Chloride Ion Penetration."

American Concrete Institute (ACI) 116R, "Cement and Concrete Terminology. ACI Committee Report 116.

American Concrete Institute (ACI) 201.1R-08, "Guide for Conducting a Visual Inspection of Concrete in Service." ACI Committee Report 201.

American Concrete Institute (ACI) 228.2R-98, "Nondestructive Test Methods for Evaluation of Concrete in Structures," ACI Committee Report 228.

American Society for Testing and Materials (ASTM) (2005). ASTM C39-05, "Standard Test Method for Compressive Strength of Cylindrical Concrete Specimens."

American Society for Testing and Materials (ASTM) (2004). ASTM C42-04, "Standard Test Method for Obtaining and Testing Drilled Cores and Sawed Beams of Concrete."

American Society for Testing and Materials (ASTM) (2008). ASTM C215-08, "Standard Test Method for Fundamental Transverse, Longitudinal, and Torsional Frequencies of Concrete Specimens."

American Society for Testing and Materials (ASTM) (1998). ASTM C457-98, "Standard Test Method for Microscopical Determination of Parameters of the Air-Void System in Hardened Concrete."

American Society for Testing and Materials (ASTM) (2002). ASTM C469-02, "Standard Test Method for Static Modulus of Elasticity and Poisson's Ratio of Concrete in Compression."

American Society for Testing and Materials (ASTM) (2006). ASTM C642-06, "Standard Test Method of Density, Absorption, and Voids in Hardened Concrete."

American Society for Testing and Materials (ASTM) (2008). ASTM C805-08, "Standard Test Method for Rebound Number of Hardened Concrete."

American Society for Testing and Materials (ASTM) (2004). ASTM C856-04, "Standard Practice for Petrographic Examination of Hardened Concrete."

American Society for Testing and Materials (ASTM) (2009). ASTM C1202-09, "Standard Test Method for Electrical Indication of Concrete's Ability to Resist Chloride Ion Penetration."

American Society for Testing and Materials (ASTM) (2004). ASTM C1585-04, "Standard Test Method for Measurement of Rate of Absorption of Water by Hydraulic Cement Concretes."

Bairagi, N.K. and Dubal, N.S. (1996). "Effect of thermal cycles on the compressive strength, modulus of rupture and dynamic modulus of concrete." Indian Concrete Journal, 70(8), 423-426.

Bentz, D.P. (2009). "Influence of Internal Curing Using Lightweight Aggregates on Interfacial Transition Zone Percolation and Chloride Ingress in Mortars. Cement and Concrete Composites, 31(5), 285-289.

Bentz, D.P., Ehlen, M.A., Ferraris, C.F., and Winpigler, J.A. (2002). "Service Life Prediction Based on Sorptivity for Highway Concrete Exposed to Sulfate Attack and Freeze-Thaw Conditions." National Institute of Standards and Technology. FHWA Report FHWA-RD-01-162. Federal Highway Administration, Washington, D.C.

Brite EuRam III, (2000). "Chemical Stability, Wear Resistance and Freeze-Thaw Resistance of Lightweight Aggregate Concrete", *Document BE96-3942/R25, EuroLightCon, Economic Design and Construction with Light Weight Aggregate Concrete*, European Union.

Chariton, T. and Weiss, W.J. (2002). "Using Acoustic Emission to Monitor Damage Development in Mortars Restrained from Volumetric Changes," Concrete: Material Science to Application, A Tribute to Surendra P. Shah, SP-206, American Concrete Institute, Farmington Hills, MI, 205-219.

Chini, A.R., Muszynski, L.C. and Hicks, J. (2003). "Determination of Acceptance Permeability Characteristics for Performance-Related Specifications for Portland Cement Concrete." Report submitted to Florida Department of Transportation, July 11, 2003.

Cusson, D., Lounis, Z., Daigle, L. (2010) "Benefits of internal curing on service life and life-cycle cost of high-performance concrete bridge decks - A case study." Cement and Concrete Composites, 32(5), 339-350.

Darwin, D., Browning, J., and Lindquist, W.D. (2004). "Control of Cracking in Bridge Decks: Observations from the Field." Cement, Concrete, and Aggregates, 26(2), 148-154.

Delatte, N., Crowl, D., and Mack, E. (2007). "Reducing Cracking of High Performance Concrete Bridge Decks."Transportation Research Board 2007 Annual Meeting.

Delatte N., Mack, E., and Cleary, J. (2007). "Evaluation of High Absorptive Materials to Improve Internal Curing of Low Permeability Concrete."FHWA Report No.FHWA/OH-2007/06.Federal Highway Administration, Washington, D.C.

DeSousa, S.J., Hooton, R.D., and Bickley, J.A. (1997). "Evaluation of Laboratory Drying Procedures Relevant to Field Conditions for Concrete Sorptivity Measurements." Cement, Concrete, and Aggregates, 19(2), 59-63.

DeSousa, S.J., Hooton, R.D., and Bickley, J.A. (1998). "A field test for evaluating high performance concrete covercrete quality." Canadian Journal of Civil Engineering, 25(3), 551-556.

Dilek, U. (2008). "Assessment of damage gradients using dynamic modulus of thin concrete disks." ACI Materials Journal, 105(5), 429-437.

Ewertson, C., Petersson, P. (1993). "Influence of curing conditions on the permeability and durability of concrete. Results from a field exposure test." Cement and Concrete Research, 23(3), 683-692.

Federal Highway Administration (2003). "Distress Identification Manual for the Long-Term Pavement Performance Program." Publication FHWA-RD-03-031.

Figg, J. (1989). "Concrete Surface Permeability: Measurement and Meaning." Chemistry and Industry. November 6, 1989, 714-719.

Geiker, M., Grube, H., Luping, T., Nilsson, L., and Andrade, C. (1995). "Chapter 9: Laboratory Test Methods." In RILEM Report No. 12 Performance Criteria for Concrete Durability. Krupp, J., and Hilsdorf, H.K, editors.

Geiker, M.R., Nielsen, E., Herfort, D. (2004). "Phase equilibria of hydrated Portland cement" Cement and Concrete Research, 35(1), 109-115.

Gergely, J., Bledsoe, J.E., Tempest, B.Q., and Szabo, I. (2006). "Concrete Diffusion Coefficients and Existing Chloride Exposure in North Carolina." Report No. FHWA/NC/2006-26.

Ghosh, P. (2011). "Computation of Diffusion Coefficients and Prediction of Corrosion Initiation in Concrete Structures."Doctoral dissertation, The University of Utah.

Ghosh, P., Thomas, D., Hanson, S., Tepke, D., and Tikalsky, P.J. (2012). "Influence of HPC Mixtures on Diffusion Coefficients, Resistivity, and Chloride Concentrations." International Congress on Durability of Concrete (ICDC), 2012 Conference Proceedings, publication pending.

Gowers, K.R. and Millard, S.G. (1999). "Measurement of Concrete Resistivity for Assessment of Corrosion Severity of Steel Using Wenner Technique." ACI Materials Journal, 96(5), 536-541.

Guthrie, W.S., and Hema, J. (2005). "Concrete Bridge Deck Condition Assessment Guidelines." Utah Department of Transportation Research and Development Division. Report No. UT-05.01.

Hadidi, R., and Saadeghvaziri, M.A. (2005). "Transverse Cracking of Concrete Bridge Decks: State-of-the-Art." Journal of Bridge Engineering, 10(5), 503-510.

Hall, C. (1989). "Water sorptivity of mortars and concretes: a review." Magazine of Concrete Research, 1989, 41(147), 51-61.

Hammond, A.J. (2010). "Predicting Concrete Resistivity from Ohm's Law." Master's Thesis, The University of Utah.

Harmon, K.S., (2005). "Recent Research Projects to Investigate Mechanical Properties of High-Performance Lightweight Concrete." *Seventh International Symposium on the Utilization of High Strength / High-Performance Concrete*, American Concrete Institute, 991-1008.

Hooton, R.D., Mesic, T., and Beal, D.L. (1993). "Sorptivity Testing of Concrete as an Indicator of Concrete Durability and Curing Efficiency." Third Canadian Symposium on Cement and Concrete, Ottowa Ontario.

Issa, M. (1999). "Investigation of cracking in concrete bridge decks at early ages." Journal of Bridge Engineering, 4(2), 116-124.

Kessler, R.J., Powers, R.G., and Paredes, M.A. (2005). "Resistivity Measurements of Water Saturated Concrete as an Indicator of Permeability." NACE International Corrosion Conference 2005, Houston, Texas, Paper 5261.

Lee, K., Kim, D., Kim J. (1997). "Determination of dynamic Young's modulus of concrete at early ages by impact resonance test." KSCE Journal of Civil Engineering, 1(1), 11-18.

Leming, M., Nau, J., Fukuda, J. (1998). "Nondestructive determination of the dynamic modulus of concrete disks." ACI Materials Journal, 95(1), 50-57.

McKeel, W.T. (1985). "Evaluation of deck durability on continuous beam highway bridges." Report No. VHTRC 85-R32, Virginia Highway and Transportation Research Council, Charlottesville, VA.

Meletiou, C., Tia, M., Bloomquist, D. (1992) "Development of a field permeability test apparatus and method for concrete." ACI Materials Journal, 89(1), p 83-89.

Mindess, S., Young, J.F., and Darwin, D. (2003). Concrete, 2nd ed. Pearson Education. Upper Saddle River, New Jersey.

Mohammad, I.K. (2011). "Non-destructive testing for concrete: Dynamic modulus and ultrasonic velocity measurements." Advanced Materials Research, 243-249, 165-169.

Neville, A.M. (1995) Properties of Concrete, 4th ed. Pearson Education. Upper Saddle River, New Jersey.

NDT James Instruments, Inc. (2007). "P-6050 & P-6000 Poroscope Plus Operating Instructions." Chicago, Illinois.

Ozyildirim, C. (2008). "Durability of Structural Lightweight Concrete." *2008 Concrete Bridge Conference*, Federal Highway Administration, National Concrete Bridge Council, Missouri Department of Transportation, American Concrete Institute.

Perfetti, G.R., Johnson, D.W., and Bingham, W.L. (1985). "Incidence assessment of transverse cracking in concrete bridge decks: Structural considerations." FHWA Report No. FHWA/NC/85-002, Vol. 2. Federal Highway Administration, Washington D.C.

Polder, R.B. (2001). "Test Methods of on Site Measurement of Resistivity of Concrete – a RILEM TC-154 Technical Recommendation." Construction and Building Materials, 15, 125-131.

Presuel-Moreno, F. (2010). "Characterization of New and Old Concrete Structures Using Surface Resistivity Measurements." Final Report for Florida DOT, Contract Number BD546, RPWO #08, August 1, 2010.

Presuel-Moreno F.J., Suarez, A., Lasa, I., and Paredes, M. "Surface resistivity profiles on marine substructures to assess concrete permeability." Concrete Under Severe Conditions. Castro-Borgest et. al., eds. Taylor & Frances Group, London. 227-235.

Ramirez, J., Olek, J., Rolle, E., and Malone, B., (2000). "Performance of Bridge Decks and Girders with Lightweight Aggregate Concrete." Report FHWA/IN/JTRP-98/17, Joint Transportation Research Program, Purdue University, West Lafayette, IN.

Reinhardt, H. (2008). "Comparative performance tests and validation of NDT methods for concrete testing." Journal of Nondestructive Evaluation, 27 (1-3), 59-65.

Rupnow, T.D. and Icenogle, P. J. (2012). "Evaluation of Surface Resistivity Measurements as an Alternative to the Rapid Chloride Permeability Test for Quality Assurance and Acceptance." Baton Rouge. Presented at Transportation Research Board 91st Annual Meeting. Publication pending.

Russell, H.G., Miller, R.A., Ozyildirim, H.C., and Tadros, M.K., (2006). "Compilation and Evaluation of Results From High-Performance Concrete Projects, Volume I: Final Report." Federal Highway Administration. Report No. FHWA-HRT-05-056.

Saadeghvaziri, M.A. and Hadidi, R. (2005). "Transverse Cracking of Concrete Bridge Decks: Effects of Design Factors." Journal of Bridge Engineering, 10(5), 511-519.

Smith, K. (2002). "Evaluating Concrete Bridge Design Factors Using Concrete Resistivity," Master's Thesis, The Pennsylvania State University.

Spragg, R.P., Castro, J., Nantung, T.E., Paredes, M., Weiss, W.J. (2011). Variability Analysis of the Bulk Resistivity Measured Using Concrete Cylinders. Publication FHWA/IN/JTRP-2011/21. Joint Transportation Research Program, Indiana Department of Transportation and Purdue University, West Lafayette, Indiana.

Stanish, K.D., Hooton, R.D., and Thomas, M.D.A. (2000). Testing the Chloride Penetration Resistance of Concrete: A Literature Review." FHWA Contract DTFH61-9-R-00022.

Tempest, B.Q. (2004). "Measurement of Existing Chloride Exposure in North Carolina and Development of Chloride Diffusion Parameters for Bridge Design Modeling." Master's Thesis, University of North Carolina at Charlotte.

Thomas, M., Feng, X., Bremner, T., Balcom, B., Folliard, K. (2006). "Studies on lithium salts to mitigate ASR-induced expansion in new concrete: A critical review." Cement and Concrete Research, 35(9), 1789-1796.

Transportation Research Board (TRB), Basic Research and Emerging Technologies Related to Concrete Committee (2006). "Control of Cracking in Concrete: State of the Art." Transportation Research Circular E-C107.

Vaysburd, A. M., (1996). "Durability of Lightweight Concrete Bridges in Severe Environments." *Concrete International*, 18(7), 33-38.

Weiss, W.J., Yang, W., and Shah, S.P. (1999). "Factors Influencing Durability and Early-Age Cracking in High Strength Concrete Structures," SP-189-22, *High Performance Concrete: Research To Practice*, Farmington Hills, Michigan, 387-409.

Wolf, W. H., (2008). "Lightweight Concrete Bridge Deck Performance in Severe Climates." *2008 Concrete Bridge Conference*, Federal Highway Administration, National Concrete Bridge Council, Missouri Department of Transportation, American Concrete Institute.

APPENDIX A

Visual Survey Results

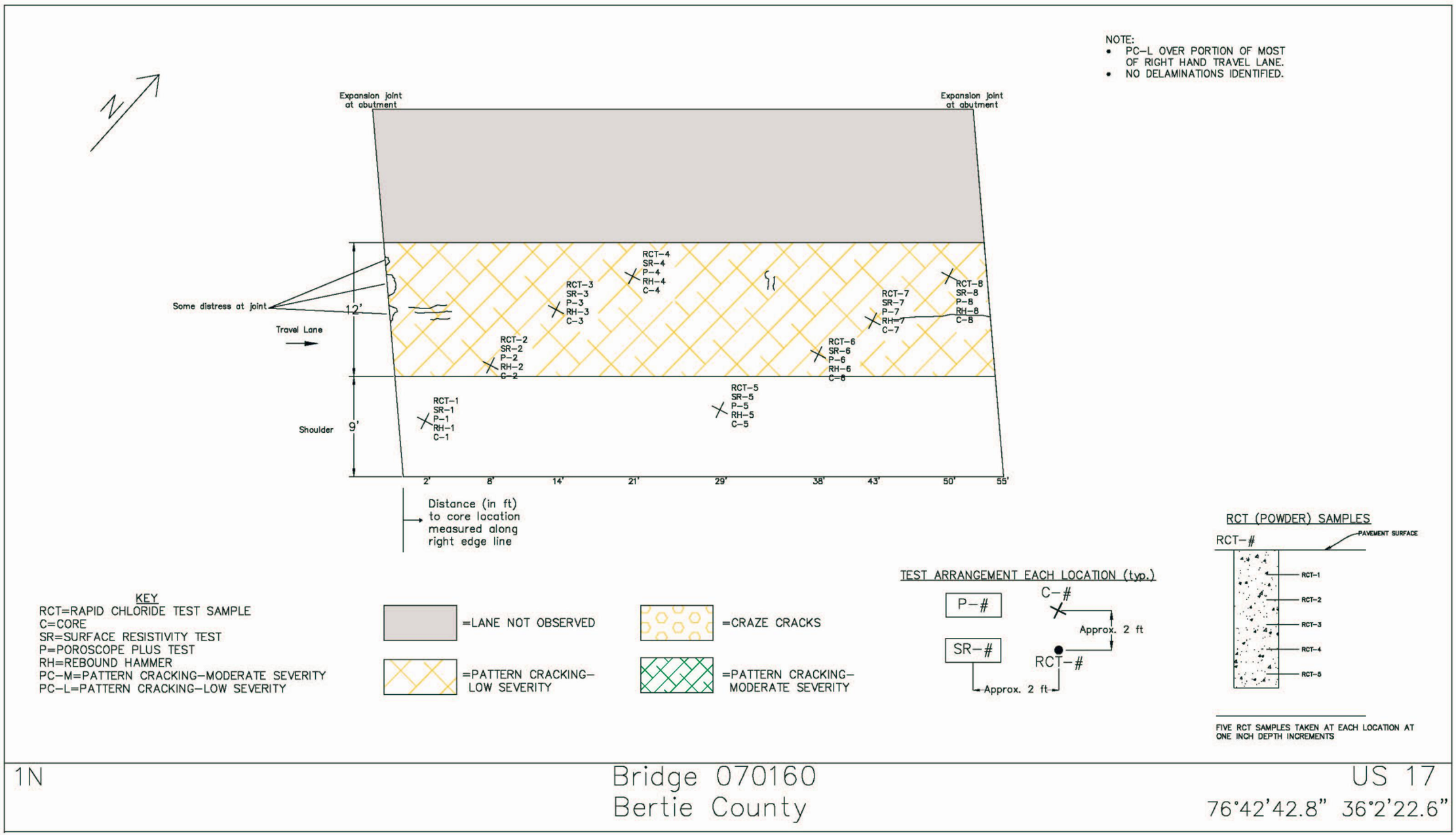

Figure A-1: Visual survey results for bridge deck IN.

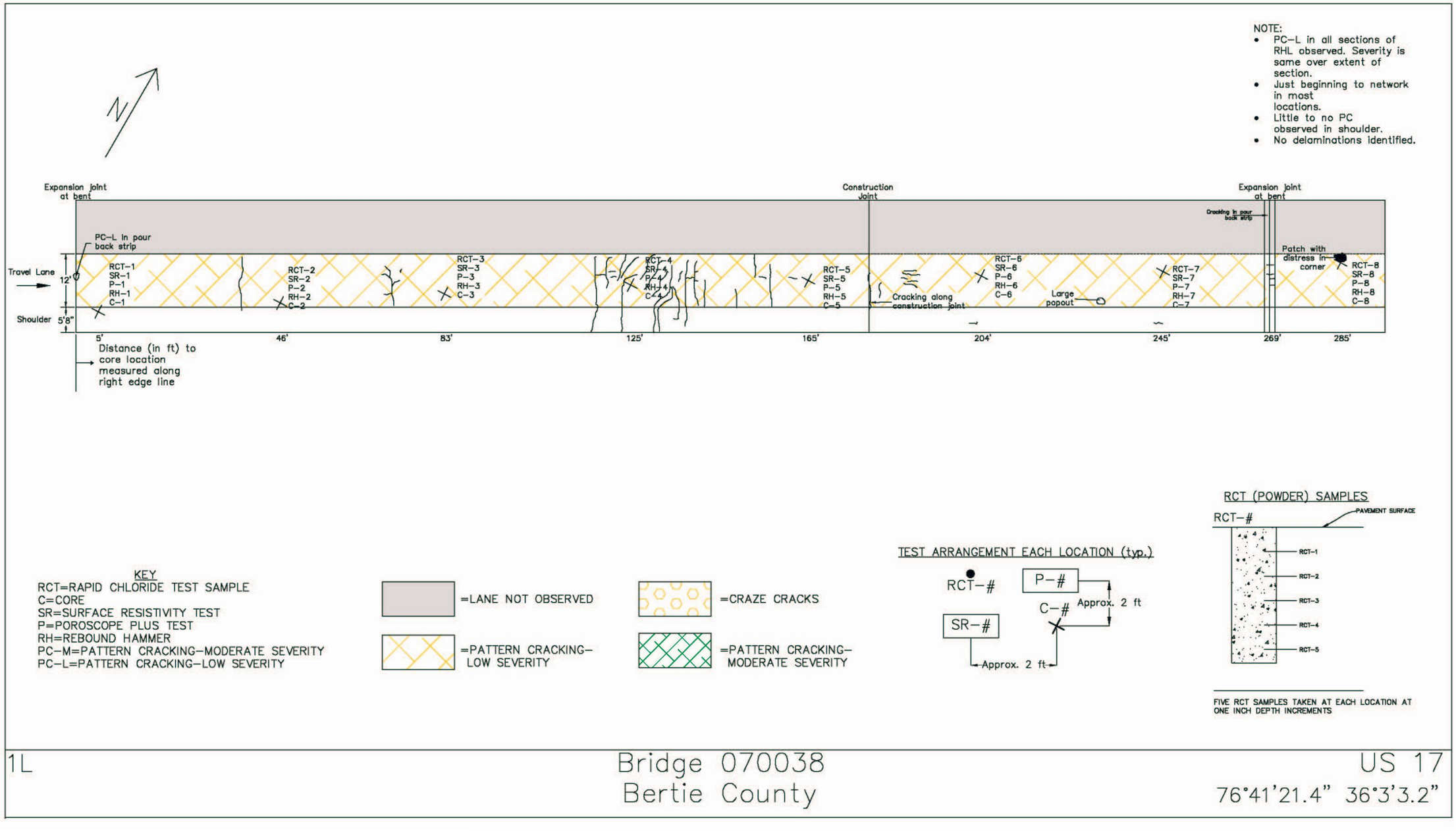

Figure A-2: Visual survey results for bridge deck 1L.

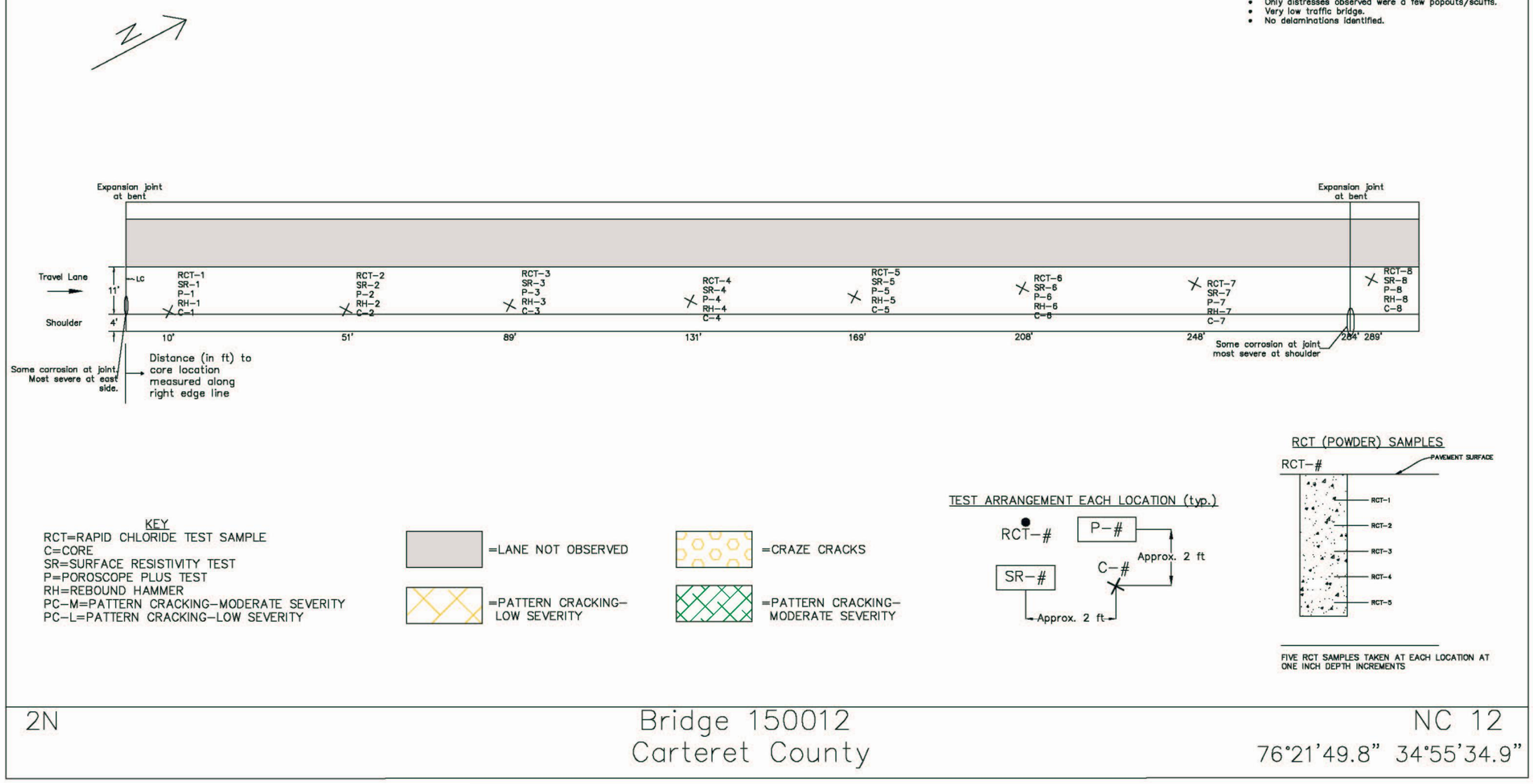

Figure A-3: Visual survey results for bridge deck 2N.

NOTE:
- No pattern cracks observed in travel lane.
- Only a few longitudinal cracks near Joint 1.
- No delaminations identified.

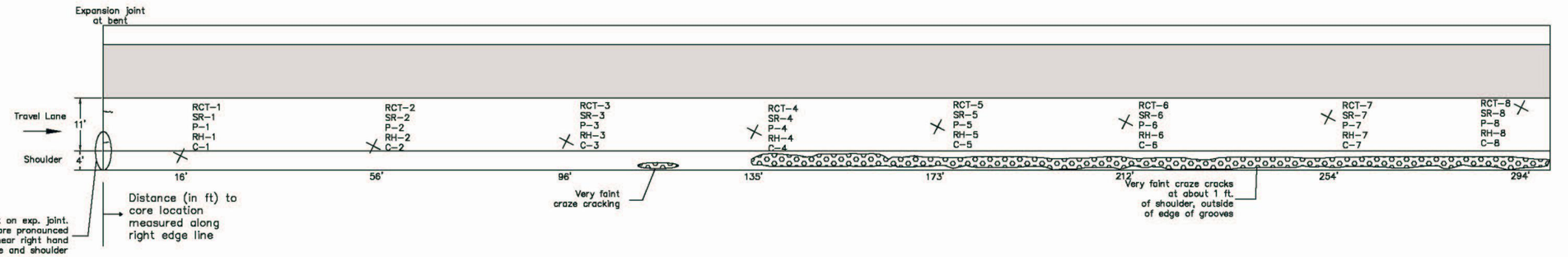

KEY
RCT=RAPID CHLORIDE TEST SAMPLE
C=CORE
SR=SURFACE RESISTIVITY TEST
P=POROSCOPE PLUS TEST
RH=REBOUND HAMMER
PC-M=PATTERN CRACKING-MODERATE SEVERITY
PC-L=PATTERN CRACKING-LOW SEVERITY

=LANE NOT OBSERVED
=CRAZE CRACKS
=PATTERN CRACKING-LOW SEVERITY
=PATTERN CRACKING-MODERATE SEVERITY

TEST ARRANGEMENT EACH LOCATION (typ.)

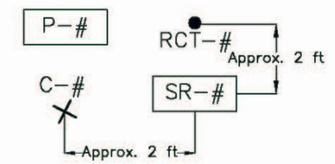

RCT (POWDER) SAMPLES

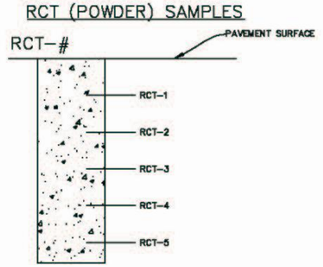

FIVE RCT SAMPLES TAKEN AT EACH LOCATION AT ONE INCH DEPTH INCREMENTS

2L

Bridge 150012
Carteret County

NC 12
76°21'49.8" 34°55'34.9"

Figure A-4: Visual survey results for bridge deck 2L.

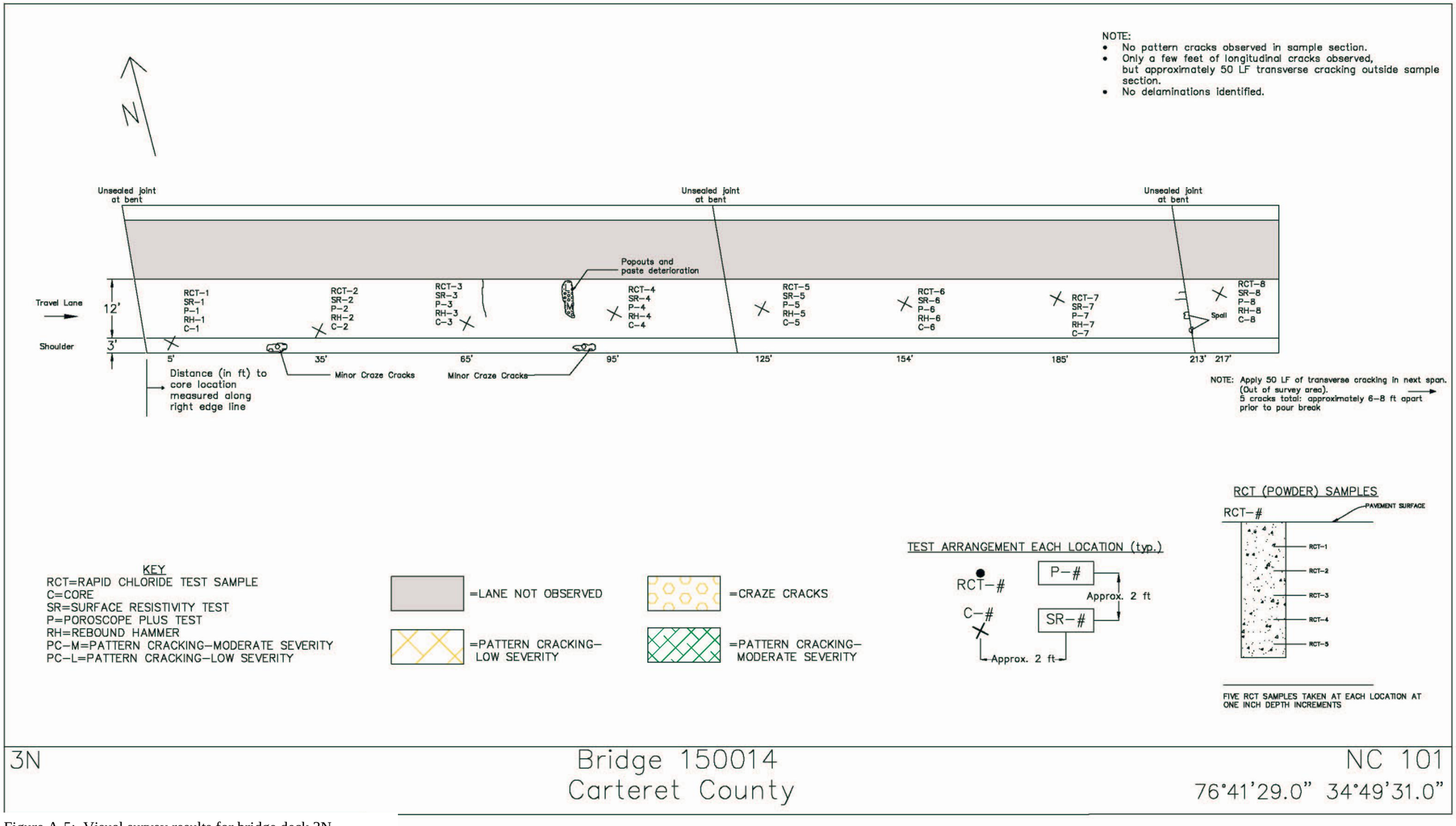

Figure A-5: Visual survey results for bridge deck 3N.

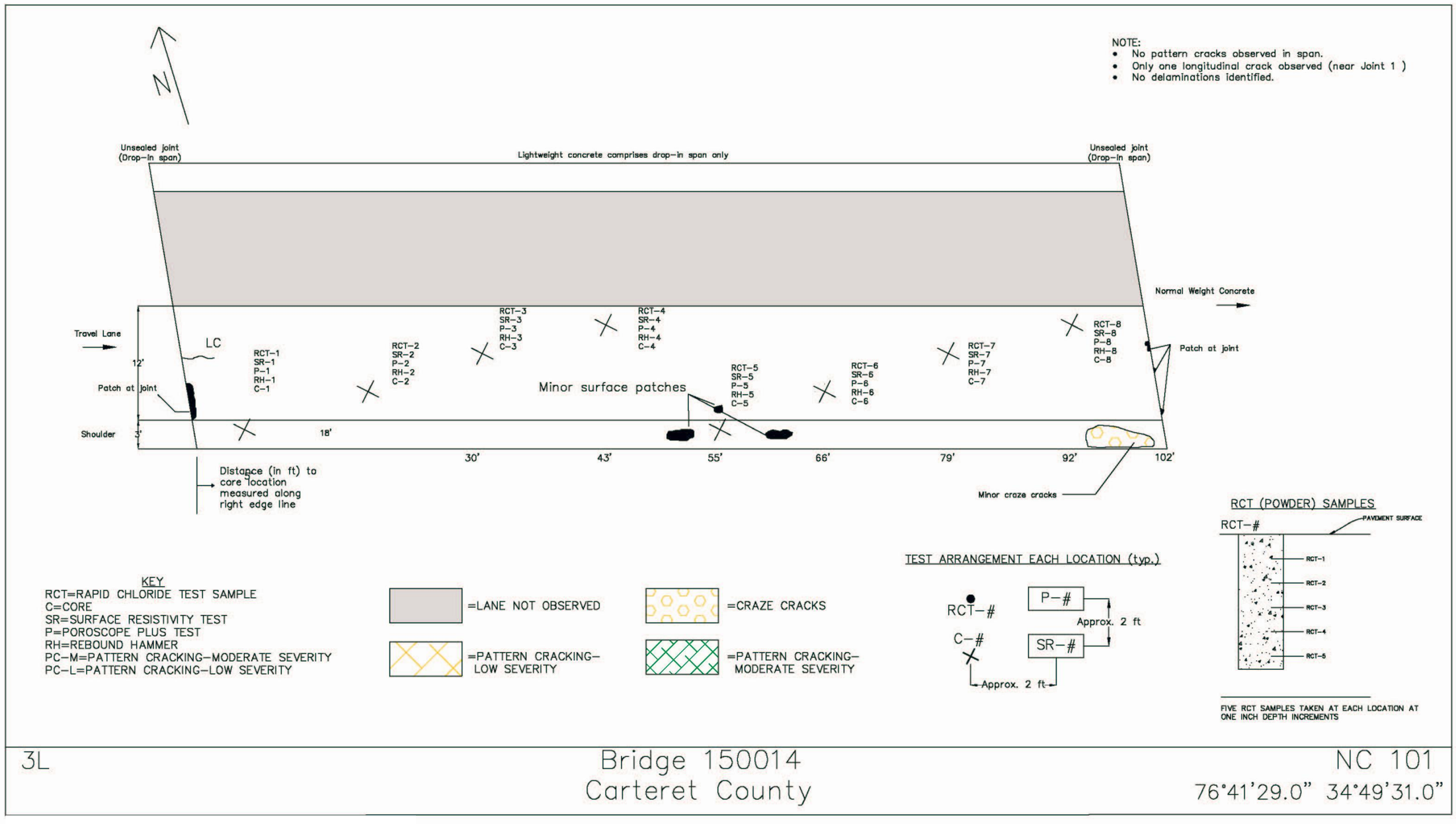

Figure A-6: Visual survey results for bridge deck 5N.

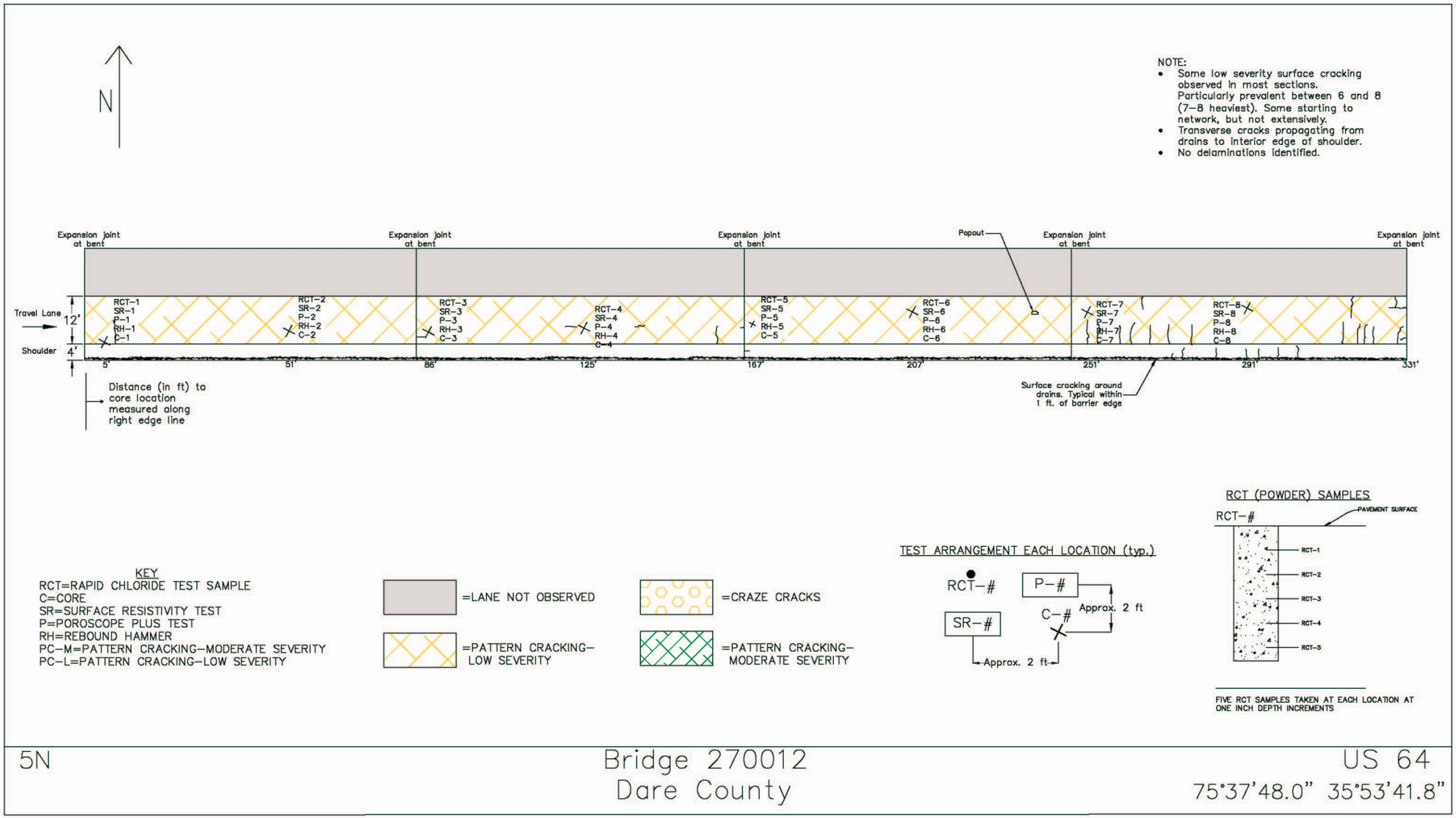

Figure A-7: Visual survey results for bridge deck 5N.

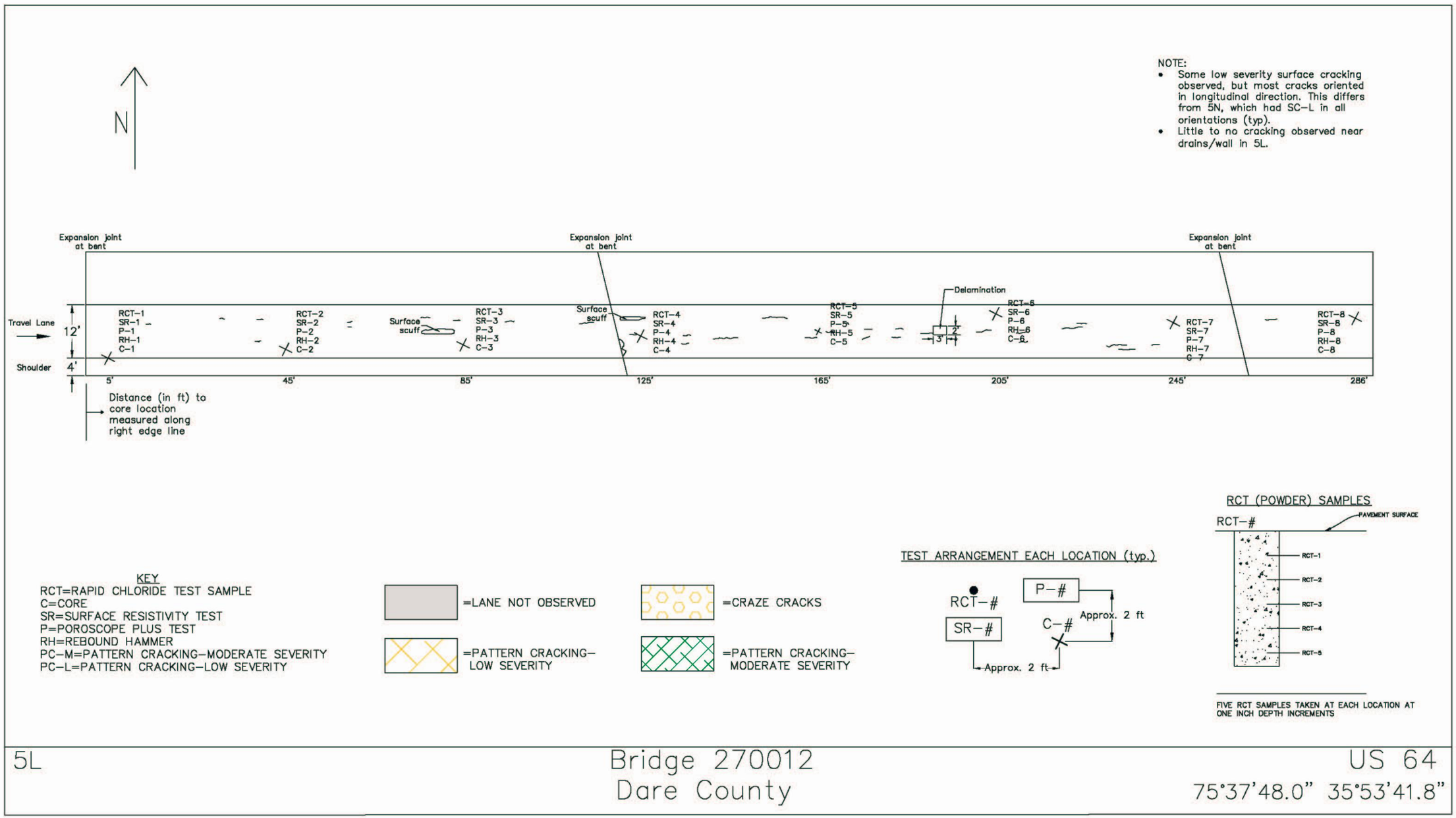

Figure A-8: Visual survey results for bridge deck 5L.

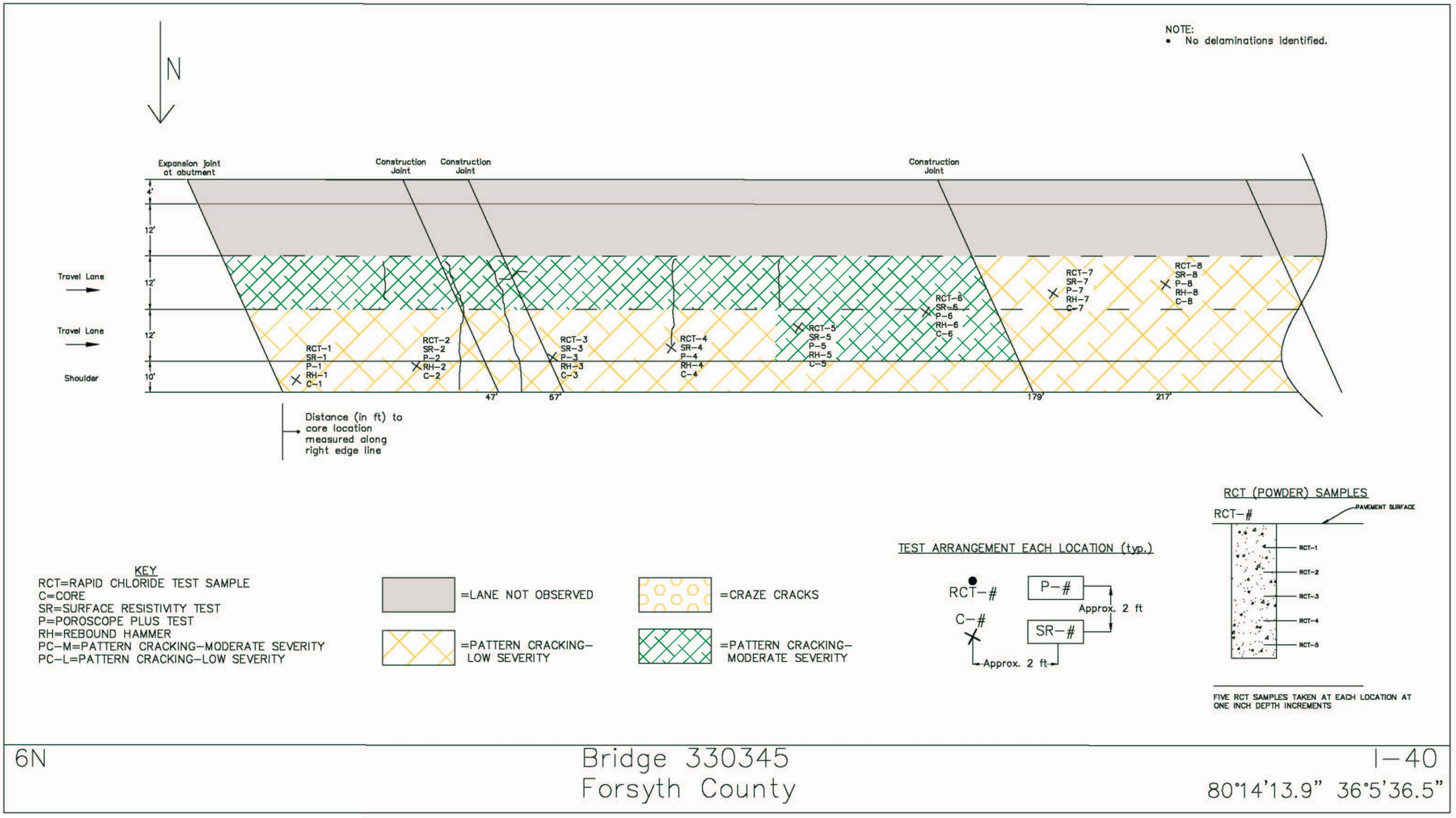

Figure A-9: Visual survey results for bridge deck 6N.

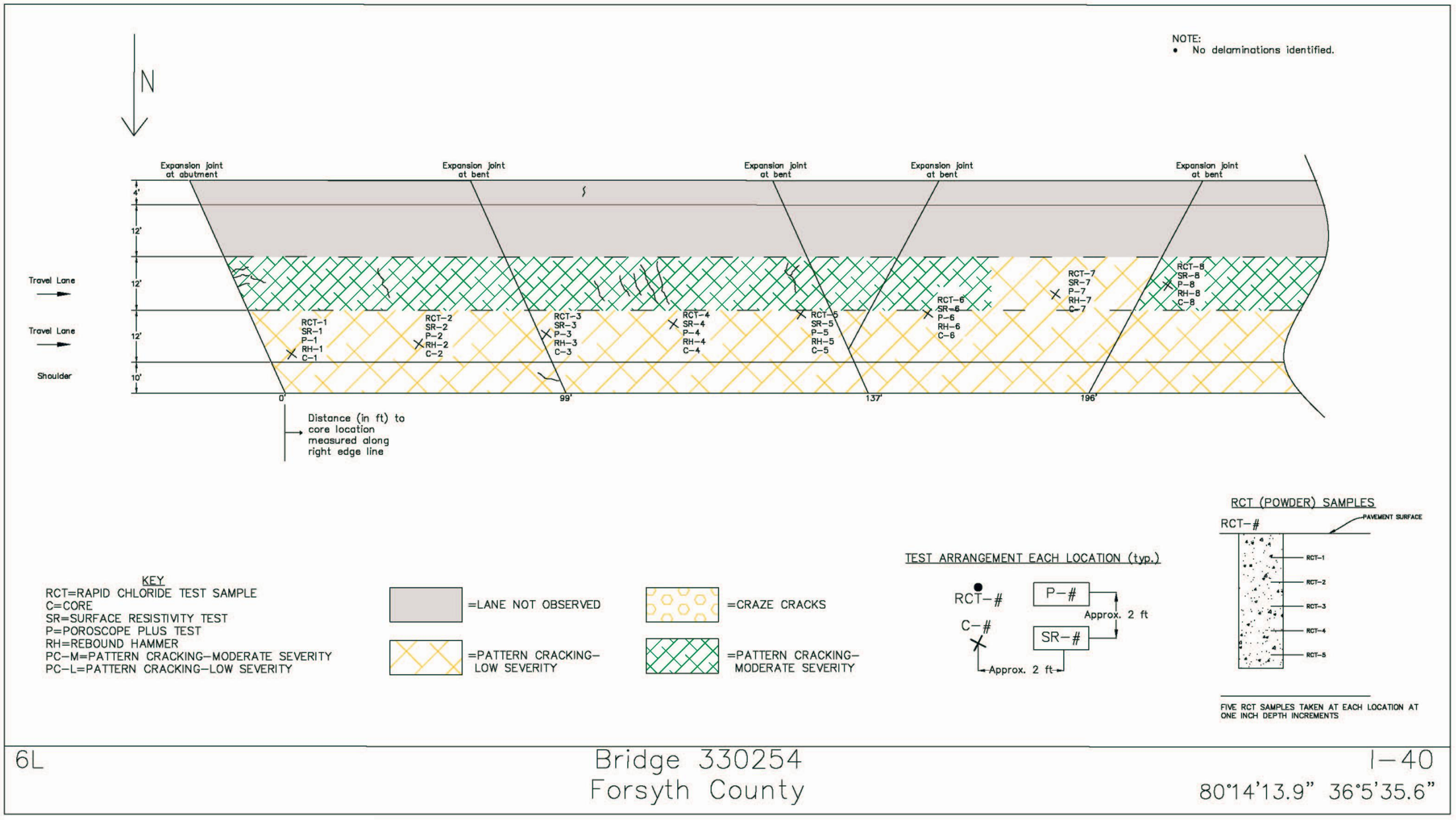

Figure A-10: Visual survey results for bridge deck 6L.

NOTE:
- No delaminations identified.

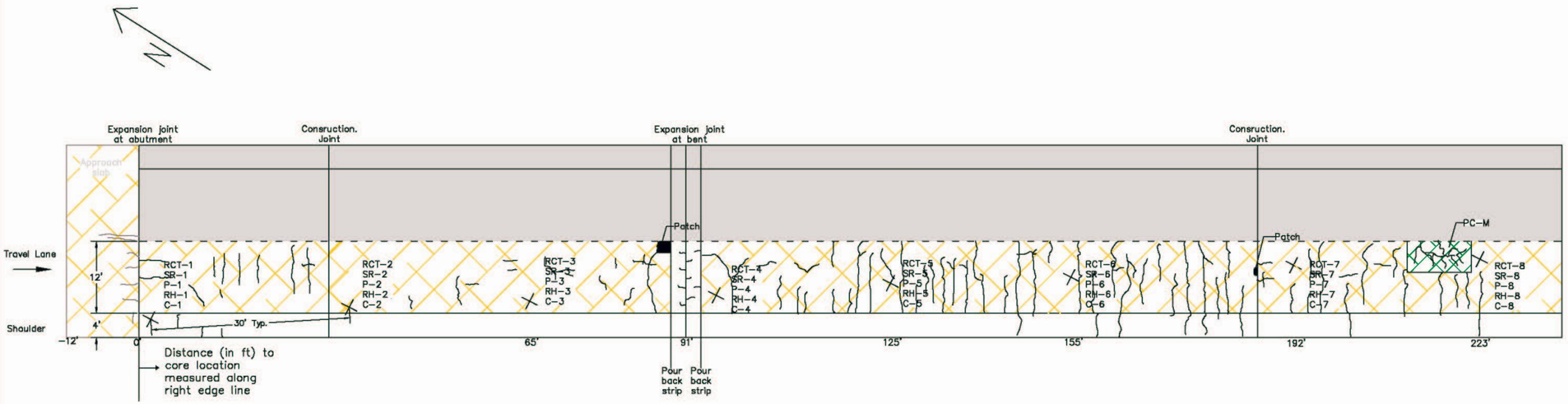

KEY
RCT=RAPID CHLORIDE TEST SAMPLE
C=CORE
SR=SURFACE RESISTIVITY TEST
P=POROSCOPE PLUS TEST
RH=REBOUND HAMMER
PC-M=PATTERN CRACKING-MODERATE SEVERITY
PC-L=PATTERN CRACKING-LOW SEVERITY

=LANE NOT OBSERVED

=CRAZE CRACKS

=PATTERN CRACKING-LOW SEVERITY

=PATTERN CRACKING-MODERATE SEVERITY

TEST ARRANGEMENT EACH LOCATION (typ.)

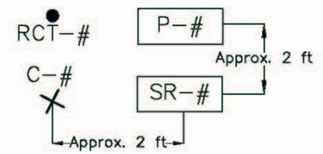

RCT (POWDER) SAMPLES

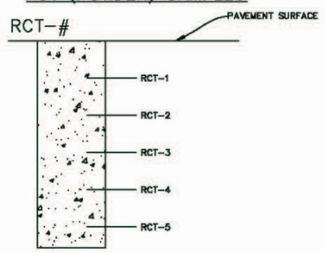

FIVE RCT SAMPLES TAKEN AT EACH LOCATION AT ONE INCH DEPTH INCREMENTS

7N

Bridge 590541
Mecklenburg County

NC 16
80°58'21.1" 35°21'48.4"

Figure A-11: Visual survey results for bridge deck 7N.

NOTE:
- Cracks propagating from transverse cracks appear to be just beginning to network in some locations.
- No delaminations identified.

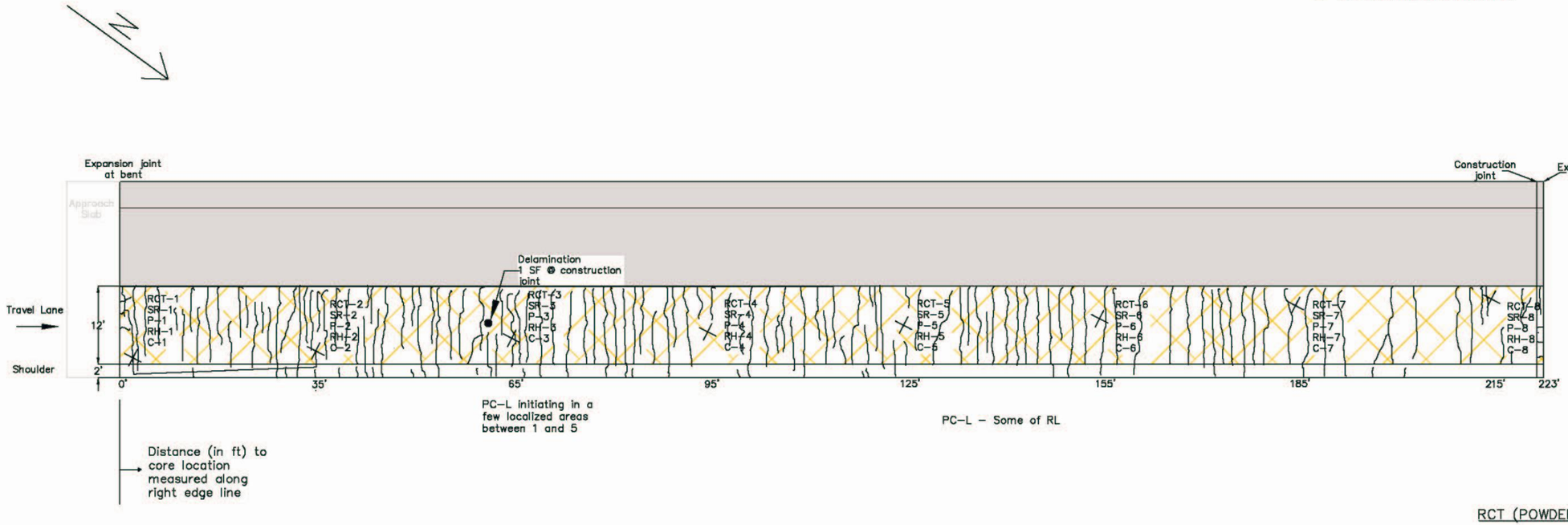

KEY
RCT=RAPID CHLORIDE TEST SAMPLE
C=CORE
SR=SURFACE RESISTIVITY TEST
P=POROSCOPE PLUS TEST
RH=REBOUND HAMMER
PC-M=PATTERN CRACKING-MODERATE SEVERITY
PC-L=PATTERN CRACKING-LOW SEVERITY

=LANE NOT OBSERVED
=CRAZE CRACKS
=PATTERN CRACKING-LOW SEVERITY
=PATTERN CRACKING-MODERATE SEVERITY

TEST ARRANGEMENT EACH LOCATION (typ.)

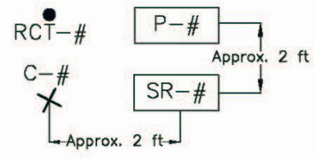

RCT (POWDER) SAMPLES

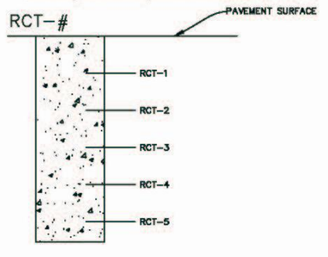

FIVE RCT SAMPLES TAKEN AT EACH LOCATION AT ONE INCH DEPTH INCREMENTS

7L
Bridge 590363
Mecklenburg County
US 17
80°58'21.1" 35°21'48.4"

Figure A-12: Visual survey results for bridge deck 7L.

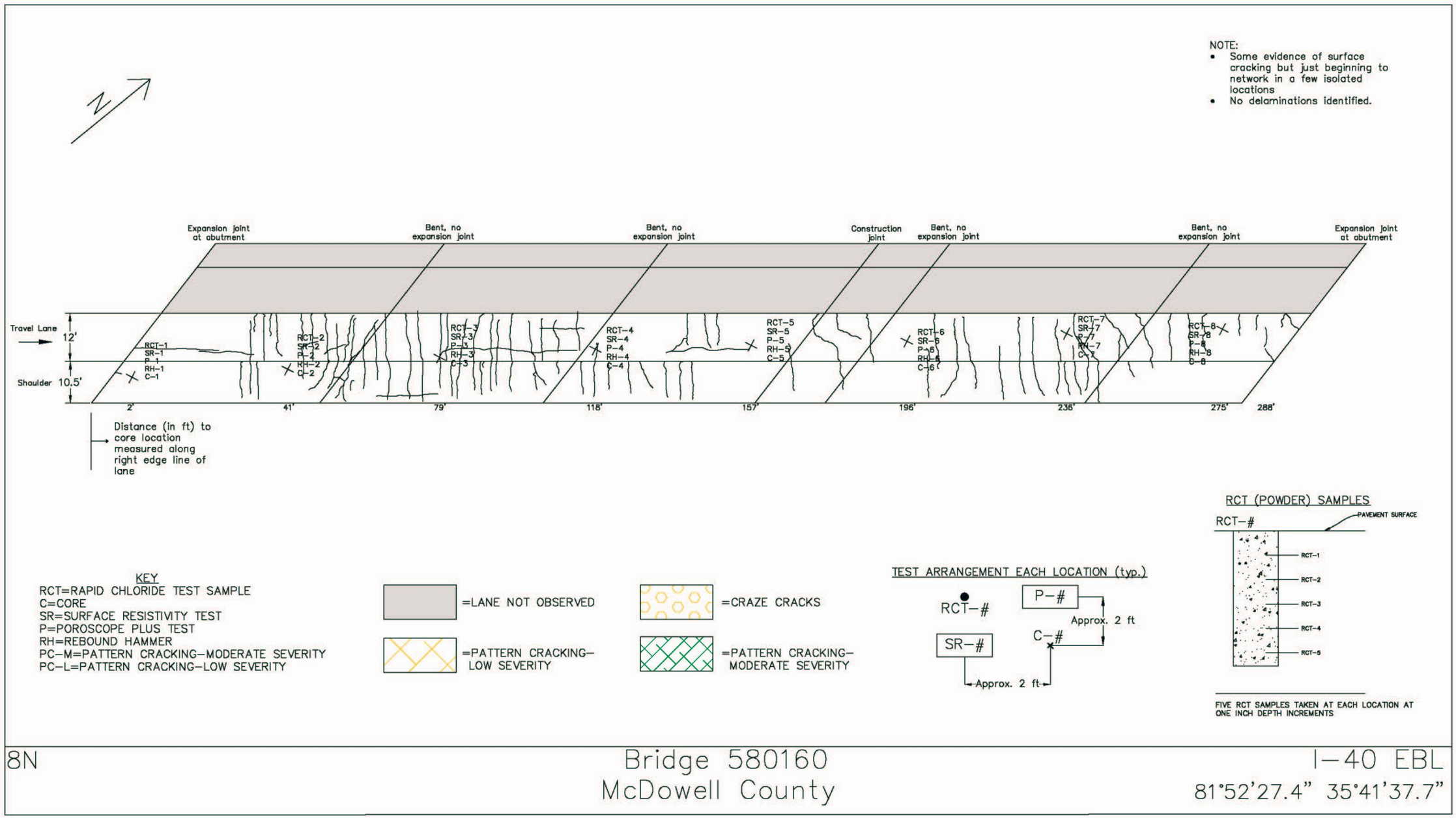

Figure A-13: Visual survey results for bridge deck 8N.

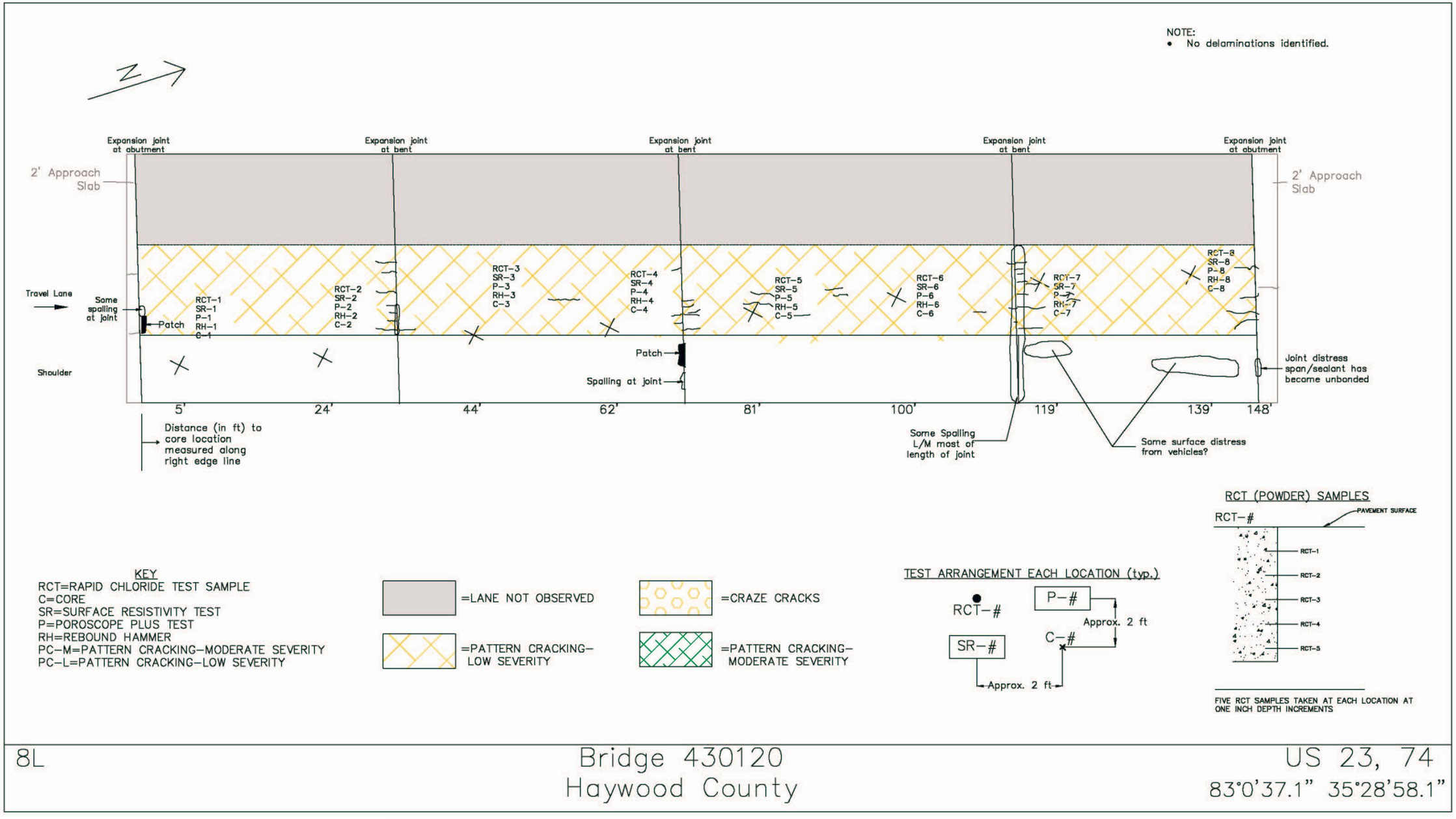

Figure A-14: Visual survey results for bridge deck 8L.

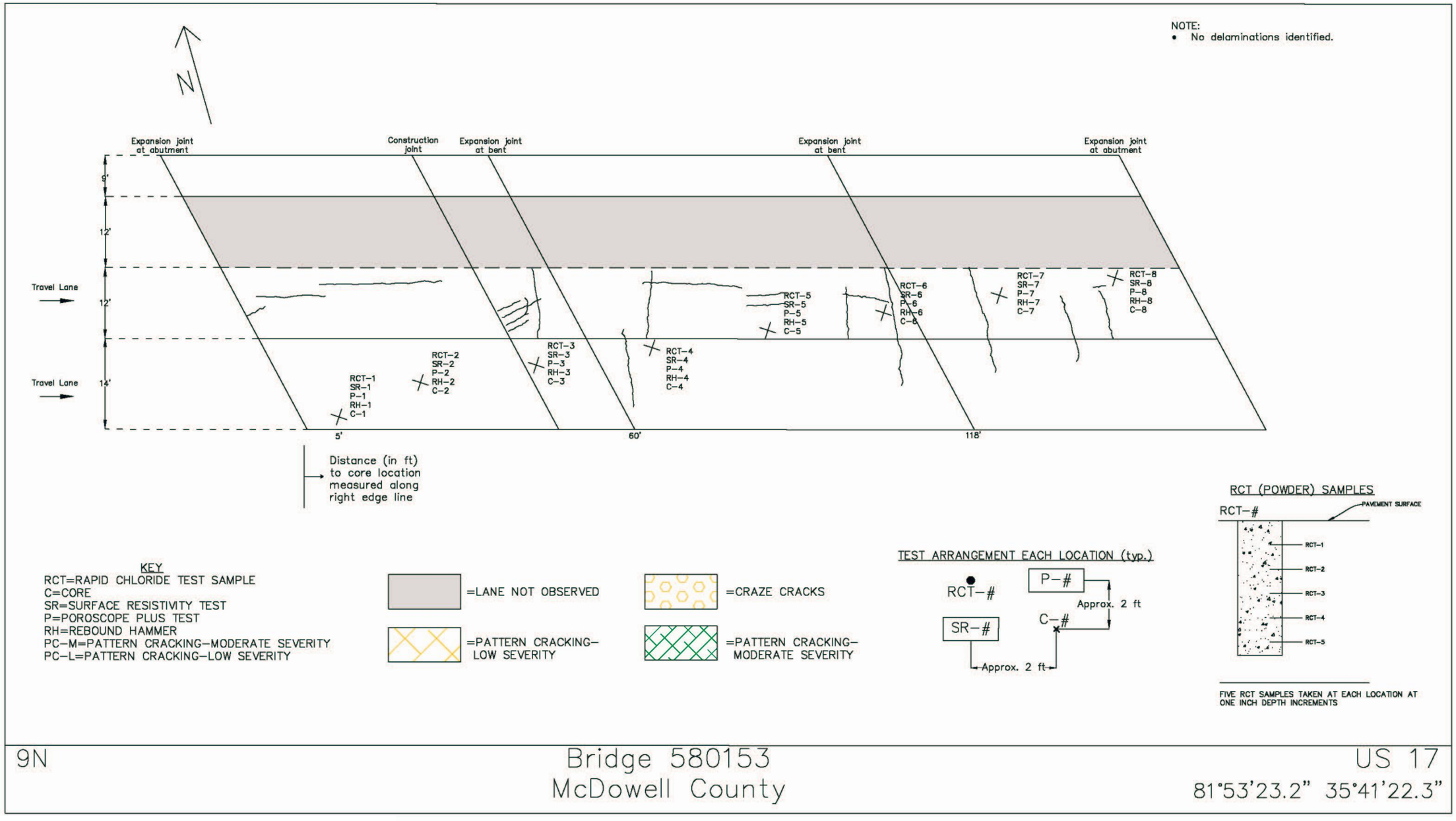

Figure A-15: Visual survey results for bridge deck 9N.

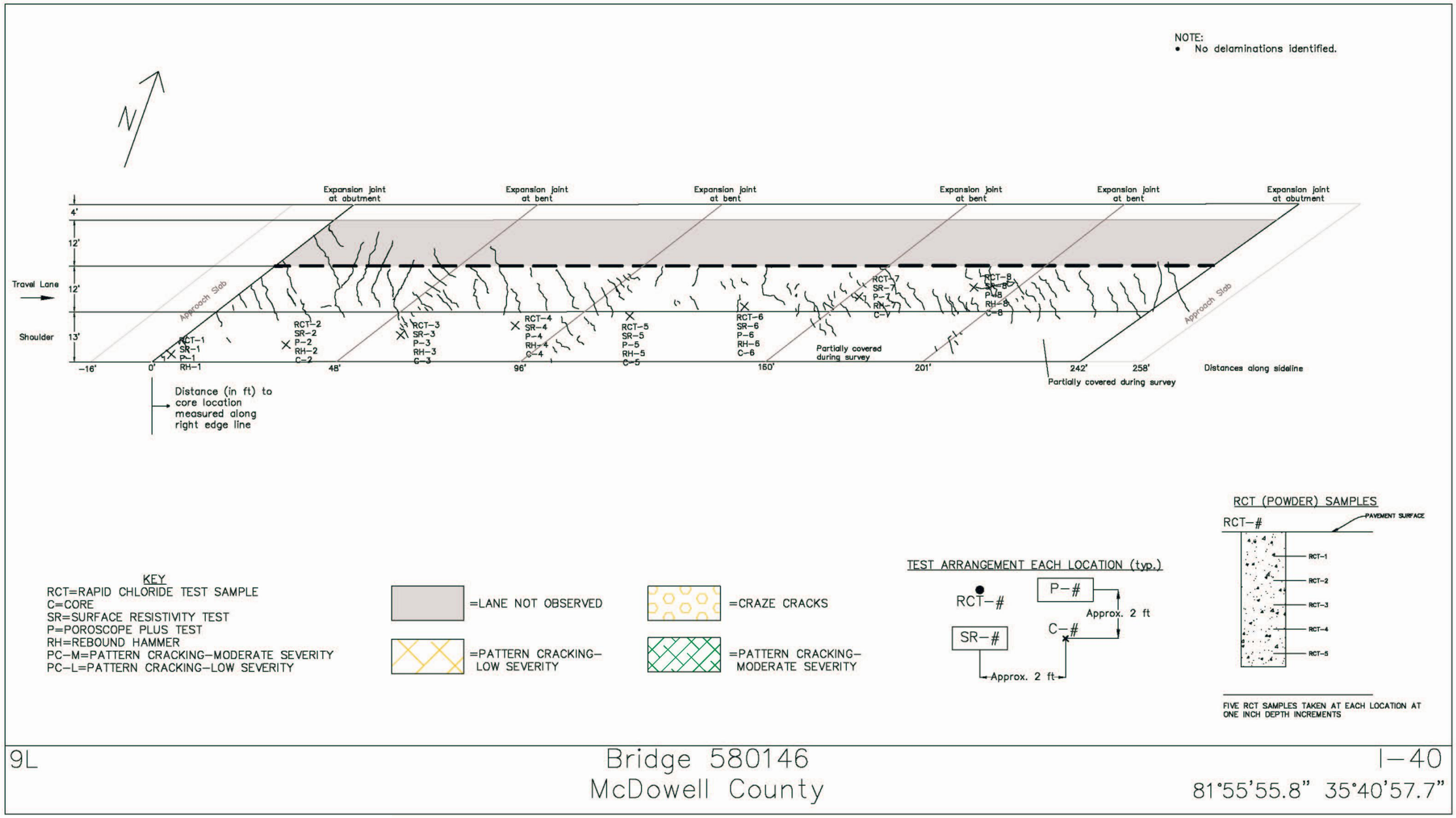

Figure A-16: Visual survey results for bridge deck 9L.

APPENDIX B

Air and Water Permeability Test Data and Results

Table B-1: Air permeability and water permeability test results for bridge deck 1N.

Air and Water Permeability	**Bridge**	070160	1N
	Date	5/17/2011	

Location 1 Air (sec)				
Test Plug	1	2	3	Average
A	40	40		40.0
B	18	17		17.5
C	7	7		7.0
D	13	13		13.0
Average for location				19.4

Location 1 Water (sec)				
Test Plug	1	2	3	Average
A	289			289.0
B	470			470.0
C	117			117.0
D	319			319.0
Average for location				298.8

Location 3 Air (sec)				
Test Plug	1	2	3	Average
A	261			261.0
B	200			200.0
C	247			247.0
D	161	170		165.5
Average for location				218.4

Location 3 Water (sec)				
Test Plug	1	2	3	Average
A	568			568.0
B	997			997.0
C				
D	212			212.0
Average for location				592.3

Bridge Deck Averages

Air (sec)	118.9
Water (sec)	445.5

Table B-2: Air permeability and water permeability test results for bridge deck 1L.

Air and Water Permeability	**Bridge**	070038	1L
	Date	5/16/2011	

Location 2 Air (sec)				
Test Plug	1	2	3	Average
A				
B	148			148.0
C	227			227.0
D	5	5		5.0
Average for location				126.7

Location 2 Water (sec)				
Test Plug	1	2	3	Average
A				
B	468			468.0
C	1001			1001.0
D	541			541.0
Average for location				670.0

Location 7 Air (sec)				
Test Plug	1	2	3	Average
A	10	11		10.5
B	8	9		8.5
C	9	10	10	9.7
D	7	8		7.5
Average for location				9.0

Location 7 Water (sec)				
Test Plug	1	2	3	Average
A	95			95.0
B	790			790.0
C	121			121.0
D	116			116.0
Average for location				280.5

Bridge Deck Averages

Air (sec)	67.9
Water (sec)	475.3

Table B-3: Air permeability and water permeability test results for bridge deck 2N.

Air and Water Permeability	**Bridge**	150012	2N
	Date	3/12/2011	

Location 3 Air (sec)				
Test Plug	1	2	3	Average
A	36	45		40.5
B	42	44		43.0
C	86	91		88.5
D	33	38		35.5
Average for location				51.9

Location 3 Water (sec)				
Test Plug	1	2	3	Average
A	32			32.0
B	63			63.0
C	67			67.0
D	26			26.0
Average for location				47.0

Location 7 Air (sec)				
Test Plug	1	2	3	Average
A	23	29	15	22.3
B	18	23		20.5
C	38	43		40.5
D	8	7	7	7.3
Average for location				22.7

Location 7 Water (sec)				
Test Plug	1	2	3	Average
A	28			28.0
B	53			53.0
C	27			27.0
D	49			49.0
Average for location				39.3

Bridge Deck Averages

Air (sec)	37.3
Water (sec)	43.1

Table B-4: Air permeability and water permeability test results for bridge deck 2L.

Air and Water Permeability	**Bridge**	150012	2L
	Date	3/11/2011	

Location 3 Air (s)				
Test Plug	1	2	3	Average
A				
B				
C	37	41		39.0
D	186	190		188.0
Average for location				113.5

Location 3 Water (s)				
Test Plug	1	2	3	Average
A	590			590.0
B				
C	657			657.0
D				
Average for location				623.5

Location 7 Air (s)				
Test Plug	1	2	3	Average
A	32	32		32.0
B	25	26		25.5
C	94	97		95.5
D	7	8		7.5
Average for location				40.1

Location 7 Water (s)				
Test Plug	1	2	3	Average
A	920			920.0
B	1033			1033.0
C	196	379		287.5
D				
Average for location				746.8

Bridge Deck Averages

Air (sec)	76.8
Water (sec)	685.2

Table B-5: Air permeability and water permeability test results for bridge deck 3N.

Air and Water Permeability	**Bridge**	150014	3N
	Date	3/9/2011	

Location 2 Air (s)				
Test Plug	1	2	3	Average
A	124	119		121.5
B	70	114		92.0
C	175	183		179.0
D	133	152		142.5
Average for location				133.8

Location 2 Water (s)				
Test Plug	1	2	3	Average
A				
B				
C				
D				
Average for location				

Location 3 Air (s)				
Test Plug	1	2	3	Average
A	29	30		29.5
B	170	176		173.0
C	15	15		15.0
D	50	54		52.0
Average for location				67.4

Location 3 Water (s)				
Test Plug	1	2	3	Average
A				
B				
C	179			179.0
D				
Average for location				179.0

Bridge Deck Averages

Air (sec)	100.6
Water (sec)	179.0

Table B-6: Air permeability and water permeability test results for bridge deck 3L.

Air and Water Permeability	**Bridge**	150014	3L
	Date	3/9/2011	

Location 3 Air (s)				
Test Plug	1	2	3	Average
A	29	30		29.5
B	9	9		9.0
C	2	3	2	2.3
D	47	49	50	48.7
Average for location				22.4

Location 3 Water (s)				
Test Plug	1	2	3	Average
A	738			738.0
B	544	863		703.5
C	257	369		313.0
D	253	783		518.0
Average for location				568.1

Location 6 Air (s)				
Test Plug	1	2	3	Average
A	56	59		57.5
B	77	80		78.5
C	32	30		31.0
D	12	11		11.5
Average for location				44.6

Location 6 Water (s)				
Test Plug	1	2	3	Average
A	1227			1227.0
B	254			254.0
C	1080			1080.0
D	1240			1240.0
Average for location				950.3

Bridge Deck Averages

Air (sec)	33.5
Water (sec)	759.2

Table B-7: Air permeability and water permeability test results for bridge deck 5N.

Air and Water Permeability	**Bridge**	270012	5N
	Date	5/19/2011	

Location 2 Air (s)				
Test Plug	1	2	3	Average
A	41	35		38.0
B	94	99		96.5
C	64	66		65.0
D	38	40		39.0
Average for location				59.6

Location 2 Water (s)				
Test Plug	1	2	3	Average
A				
B	56			56.0
C	57			57.0
D	36			36.0
Average for location				49.7

Location 6 Air (s)				
Test Plug	1	2	3	Average
A	21	23		22.0
B	13	18		15.5
C	12	14		13.0
D	15	18		16.5
Average for location				16.8

Location 6 Water (s)				
Test Plug	1	2	3	Average
A	21			21.0
B	22			22.0
C	12	16		14.0
D	11	14		12.5
Average for location				17.4

Bridge Deck Averages

Air (sec)	38.2
Water (sec)	33.5

Table B-8: Air permeability and water permeability test results for bridge deck 5L.

Air and Water Permeability	**Bridge**	270012	5L
	Date	5/18/2011	

Location 2 Air (s)					
Test Plug	1	2	3	4	Average
A	33	20	15	15	20.8
B	36	41			38.5
C	1	1			1.0
D	18	20			19.0
Average for location					19.8

Location 2 Water (s)				
Test Plug	1	2	3	Average
A	106			106.0
B	849			849.0
C	14			14.0
D	99	119		109.0
Average for location				269.5

Location 6 Air (s)				
Test Plug	1	2	3	Average
A	63	73		68.0
B	34	37		35.5
C	51	64		57.5
D	32	36		34.0
Average for location				48.8

Location 6 Water (s)				
Test Plug	1	2	3	Average
A	72			72.0
B	33			33.0
C	30	48		39.0
D	42			42.0
Average for location				46.5

Bridge Deck Averages

Air (sec)	34.3
Water (sec)	158.0

Table B-9: Air permeability and water permeability test results for bridge deck 6N.

Air and Water Permeability	**Bridge**	330254	6N
	Date	12/8/2010	

Location 1 Air (s)				
Test Plug	1	2	3	Average
A	11	11		11.0
B	52	52		52.0
C	13	13		13.0
D	29	27	25	27.0
Average for location				25.8

Location 1 Water (s)				
Test Plug	1	2	3	Average
A				
B				
C				
D				
Average for location				

Location 2 Air (s)				
Test Plug	1	2	3	Average
A	26	27		26.5
B	21	20		20.5
C	36	37		36.5
D	19	20		19.5
Average for location				25.8

Location 2 Water (s)				
Test Plug	1	2	3	Average
A				
B				
C				
D				
Average for location				

Bridge Deck Averages

Air (sec)	25.8
Water (sec)	

Table B-10: Air permeability and water permeability test results for bridge deck 6L.

Air and Water Permeability	**Bridge**	330254	6L
	Date	12/8/2010	

Location 1 Air (s)				
Test Plug	1	2	3	Average
A	77	81	83	80.3
B	50	53	54	52.3
C	29	29		29.0
D	28	31	30	29.7
Average for location				47.8

Location 1 Water (s)				
Test Plug	1	2	3	Average
A	9			9.0
B	219			219.0
C	6			6.0
D	65			65.0
Average for location				74.8

Location 2 Air (s)				
Test Plug	1	2	3	Average
A	32	31		31.5
B	78	41	42	53.7
C	12	12		12.0
D	17	21	21	19.7
Average for location				29.2

Location 2 Water (s)				
Test Plug	1	2	3	Average
A	7			7.0
B	6			6.0
C				
D	7			7.0
Average for location				6.7

Location 7 Air (s)				
Test Plug	1	2	3	Average
A	225	279	282	262.0
B	36	43	43	40.7
C	73	75		74.0
D	63	64		63.5
Average for location				110.0

Location 7 Water (s)				
Test Plug	1	2	3	Average
A				
B	484			484.0
C	86			86.0
D	98			98.0
Average for location				222.7

Location 8 Air (s)				
Test Plug	1	2	3	Average
A	49	48		48.5
B	61	55	47	54.3
C	43	43		43.0
D	12	12		12.0
Average for location				39.5

Location 8 Water (s)				
Test Plug	1	2	3	Average
A	69			69.0
B				
C	487			487.0
D	16			16.0
Average for location				190.7

Bridge Deck Averages

Air (sec)	56.6
Water (sec)	123.7

Table B-11: Air permeability and water permeability test results for bridge deck 7N.

Air and Water Permeability	**Bridge**	590541	7N
	Date	3/18/2011	

Location 2 Air (s)				
Test Plug	1	2	3	Average
A	3	3		3.0
B	5	5		5.0
C	0	1		0.5
D	1	2	2	1.7
Average for location				2.5

Location 2 Water (s)				
Test Plug	1	2	3	Average
A	14	33	30	25.7
B	21	5	15	13.7
C	40	46		43.0
D	36	57	37	43.3
Average for location				31.4

Location 4 Air (s)				
Test Plug	1	2	3	Average
A	21	21		21.0
B	64	71		67.5
C	36	40		38.0
D	33	35		34.0
Average for location				40.1

Location 4 Water (s)				
Test Plug	1	2	3	Average
A	8	11		9.5
B				
C				
D	53	69		61.0
Average for location				35.3

Location 6 Air (s)				
Test Plug	1	2	3	Average
A	3	3		3.0
B	11	12		11.5
C	8	8		8.0
D	20	21		20.5
Average for location				10.8

Location 6 Water (s)				
Test Plug	1	2	3	Average
A	51	87		69.0
B	160	88		124.0
C	85	62		73.5
D	121	48	74	81.0
Average for location				86.9

Bridge Deck Averages

Air (sec)	17.8
Water (sec)	51.2

Table B-12: Air permeability and water permeability test results for bridge deck 7L.

Air and Water Permeability	**Bridge**	590363	7L
	Date	3/17/2011	

Location 1 Air (s)				
Test Plug	1	2	3	Average
A	20	23	22	21.7
B	30	30		30.0
C	5	6	6	5.7
D	9	10	9	9.3
Average for location				16.7

Location 1 Water (s)				
Test Plug	1	2	3	Average
A	26	28		27.0
B	43	49		46.0
C	33			33.0
D	35	30		32.5
Average for location				34.6

Location 4 Air (s)				
Test Plug	1	2	3	Average
A	3	3		3.0
B	11	11		11.0
C	31	33		32.0
D	4	5	5	4.7
Average for location				12.7

Location 4 Water (s)				
Test Plug	1	2	3	Average
A	25	27		26.0
B	26	17	15	19.3
C	23	27		25.0
D	59	47		53.0
Average for location				30.8

Location 7 Air (s)				
Test Plug	1	2	3	Average
A	14	15		14.5
B	9	11	11	10.3
C	2	2	2	2.0
D	11	15	16	14.0
Average for location				10.2

Location 7 Water (s)				
Test Plug	1	2	3	Average
A	28	19	25	24.0
B	19	18		18.5
C	28	28		28.0
D	20	21		20.5
Average for location				22.8

Bridge Deck Averages

Air (sec)	13.2
Water (sec)	29.4

Table B-13: Air permeability and water permeability test results for bridge deck 8N.

Air and Water Permeability	**Bridge**	580160	8N
	Date	6/6/2011	

Location 2 Air (s)				
Test Plug	1	2	3	Average
A	150	157		153.5
B	254	265		259.5
C	199	211		205.0
D	204	220		212.0
Average for location				207.5

Location 7 Water (s)				
Test Plug	1	2	3	Average
A	98			98.0
B	53	65		59.0
C	68			68.0
D	73			73.0
Average for location				74.5

Location 7 Air (s)				
Test Plug	1	2	3	Average
A	131	142		136.5
B	164	190		177.0
C	168	178		173.0
D	275	290		282.5
Average for location				192.3

Location 2 Water (s)				
Test Plug	1	2	3	Average
A	1	1		1.0
B	137			137.0
C	47	63		55.0
D	128			128.0
Average for location				80.3

Bridge Deck Averages

Air (sec)	199.9
Water (sec)	77.4

Table B-14: Air permeability and water permeability test results for bridge deck 8L.

Air and Water Permeability	**Bridge**	430120	8L
	Date	4/4/2011	

Location 2 Air (s)				
Test Plug	1	2	3	Average
A	117	119		118.0
B	83	85		84.0
C	56	60		58.0
D	174	215		194.5
Average for location				113.6

Location 2 Water (s)				
Test Plug	1	2	3	Average
A	70			70.0
B	46			46.0
C	138			138.0
D	93			93.0
Average for location				86.8

Location 6 Air (s)				
Test Plug	1	2	3	Average
A	135	149		142.0
B	63	65		64.0
C	62	58		60.0
D	8	8		8.0
Average for location				68.5

Location 6 Water (s)				
Test Plug	1	2	3	Average
A	83			83.0
B	161			161.0
C	83			83.0
D	119			119.0
Average for location				111.5

Bridge Deck Averages

Air (sec)	91.1
Water (sec)	99.1

Table B-15: Air permeability and water permeability test results for bridge deck 9N.

Air and Water Permeability	**Bridge**	580153	9N
	Date	12/7/2010	

Location 1 Air (s)				
Test Plug	1	2	3	Average
A	27	27		27.0
B	200	211	198	203.0
C	20	20		20.0
D				
Average for location				83.3

Location 1 Water (s)				
Test Plug	1	2	3	Average
A	185			185.0
B	720			720.0
C				
D				
Average for location				452.5

Location 2 Air (s)				
Test Plug	1	2	3	Average
A	122	135		128.5
B	81	82		81.5
C	116	121		118.5
D	1	1		1.0
Average for location				82.4

Location 2 Water (s)				
Test Plug	1	2	3	Average
A				
B				
C				
D				
Average for location				

Location 8 Air (s)				
Test Plug	1	2	3	Average
A	104	107		105.5
B	100	100		100.0
C	92	92		92.0
D	110	115		112.5
Average for location				102.5

Location 8 Water (s)				
Test Plug	1	2	3	Average
A				
B				
C				
D				
Average for location				

Bridge Deck Averages

Air (sec)	89.4
Water (sec)	452.5

Table B-16: Air permeability and water permeability test results for bridge deck 9L.

Air and Water Permeability	**Bridge**	580146	9L
	Date	10/28/2010	

Location 2 Air (s)				
Test Plug	1	2	3	Average
A	8	8	7	7.7
B	11	11		11.0
C	174	184	193	183.7
D	94	114	115	107.7
Average for location				77.5

Location 2 Water (s)				
Test Plug	1	2	3	Average
A				
B				
C				
D				
Average for location				

Location 4 Air (s)				
Test Plug	1	2	3	Average
A	64	80	84	76.0
B				
C	76	92	97	88.3
D				
Average for location				82.2

Location 4 Water (s)				
Test Plug	1	2	3	Average
A				
B				
C				
D				
Average for location				

Location 6 Air (s)					
Test Plug	1	2	3	4	Average
A	32	33	38		34.3
B	106	115	111		110.7
C	133	148	158	152	147.8
D	139	155	158		150.7
Average for location					110.9

Location 6 Water (s)				
Test Plug	1	2	3	Average
A				
B				
C	71			71.0
D				
Average for location				71.0

Location 8 Air (s)				
Test Plug	1	2	3	Average
A	142	164	182	162.7
B	170	186	195	183.7
C	154	179		166.5
D	208	233		220.5
Average for location				183.3

Location 8 Water (s)				
Test Plug	1	2	3	Average
A				
B				
C				
D				
Average for location				

Bridge Deck Averages

Air (sec)	113.5
Water (sec)	71.0

APPENDIX C

Surface Resistivity Test Data and Results

Table C-1: Surface resistivity test results for bridge deck 1N.

Surface Resistivity	Bridge	70160	1N
	Date	5/17/2011	

Test Location 1

	Resistance	Temp
	KΩcm	°F
1	223	46
2	214	49
3	186	50
4	175	50
5	191	49
6	165	49
7	171	50
8	159	53
	186	Average Reading
	125	Corrected Average

Test Location 2

	Resistance	Temp
	KΩcm	°F
1	177	50
2	188	49
3	193	50
4	196	51
5	210	51
6	212	51
7	209	52
8	188	52
	197	Average Reading
	136	Corrected Average

Test Location 5

	Resistance	Temp
	KΩcm	°F
1	148	57
2	160	58
3	175	55
4	215	54
5	193	54
6	193	54
7	196	53
8	212	53
	187	Average Reading
	140	Corrected Average

Test Location 6

	Resistance	Temp
	KΩcm	°F
1	249	62
2	222	67
3	264	63
4	288	65
5	255	63
6	241	64
7	222	64
8	221	63
	245	Average Reading
	219	Corrected Average

Test Location 3

	Resistance	Temp
	KΩcm	°F
1	177	52
2	208	52
3	210	52
4	217	55
5	246	51
6	260	53
7	239	53
8	219	54
	222	Average Reading
	160	Corrected Average

Test Location 4

	Resistance	Temp
	KΩcm	°F
1	182	54
2	167	52
3	176	51
4	179	51
5	206	51
6	208	52
7	232	52
8	240	53
	199	Average Reading
	141	Corrected Average

Test Location 7

	Resistance	Temp
	KΩcm	°F
1	144	51
2	161	50
3	174	51
4	165	51
5	171	53
6	201	55
7	181	56
8	198	52
	174	Average Reading
	125	Corrected Average

Test Location 8

	Resistance	Temp
	KΩcm	°F
1	191	51
2	201	49
3	214	49
4	213	49
5	198	50
6	210	50
7	193	49
8	200	50
	203	Average Reading
	137	Corrected Average

Averages corrected to 69.8°F, as per equation developed by Elkey and Sellevold (1995) and presented in Presuel-Moreno (2010)

Table C-2: Surface resistivity test results for bridge deck 1L.

Surface Resistivity	Bridge	70038	1L
	Date	5/16/2011	

Test Location 1

	Resistance	Temp
	KΩcm	°F
1	119	63
2	137	59
3	126	58
4	119	57
5	117	57
6	116	57
7	115	59
8	117	59
	121	Average Reading
	98	Corrected Average

Test Location 2

	Resistance	Temp
	KΩcm	°F
1	139	56
2	163	58
3	182	56
4	189	56
5	170	56
6	153	57
7	170	57
8	179	57
	168	Average Reading
	131	Corrected Average

Test Location 5

	Resistance	Temp
	KΩcm	°F
1	83	56
2	134	56
3	133	55
4	103	54
5	107	53
6	97	53
7	93	54
8	91	53
	105	Average Reading
	78	Corrected Average

Test Location 6

	Resistance	Temp
	KΩcm	°F
1	38	86
2	53	57
3	75	58
4	75	58
5	86	57
6	84	57
7	84	58
8	75	56
9	64	57
	70	Average Reading
	59	Corrected Average

Test Location 3

	Resistance	Temp
	KΩcm	°F
1	125	46
2	139	46
3	129	46
4	1.9	45
5	135	45
6	165	44
7	136	45
8	100	48
	116	Average Reading
	73	Corrected Average

Test Location 4

	Resistance	Temp
	KΩcm	°F
1	112	49
2	173	47
3	131	48
4	104	49
5	125	57
6	127	50
7	147	50
8	139	49
	132	Average Reading
	90	Corrected Average

Test Location 7

	Resistance	Temp
	KΩcm	°F
1	36	62
2	43	60
3	51	60
4	57	58
5	59	58
6	59	58
7	62	58
8	55	57
	53	Average Reading
	43	Corrected Average

Test Location 8

	Resistance	Temp
	KΩcm	°F
1	96	59
2	90	60
3	84	60
4	103	60
5	96	60
6	83	61
7	100	61
8	95	64
	93	Average Reading
	79	Corrected Average

Averages corrected to 69.8°F, as per equation developed by Elkey and Sellevold (1995) and presented in Presuel-Moreno (2010)

Table C-3: Surface resistivity test results for bridge deck 2N.

Surface Resistivity	Bridge	150012	2N
	Date	3/12/2011	

Test Location 1

	Resistance KΩcm	Temp °F
1	46	38
2	42	39
3	40	39
4	38	38
5	39	41
6	39	43
7	37	44
8	36	46
	40	Average Reading
	23	Corrected Average

Test Location 2

	Resistance KΩcm	Temp °F
1	36	39
2	41	39
3	40	40
4	42	40
5	45	41
6	44	44
7	40	44
8	35	44
	40	Average Reading
	23	Corrected Average

Test Location 5

	Resistance KΩcm	Temp °F
1	68	36
2	26	337
3	90	38
4	82	39
5	89	39
6	81	40
7	82	41
8	75	41
	74	Average Reading
	84	Corrected Average

Test Location 6

	Resistance KΩcm	Temp °F
1	35	37
2	35	38
3	36	38
4	36	39
5	35	39
6	33	38
7	31	38
8	30	39
	34	Average Reading
	18	Corrected Average

Test Location 3

	Resistance KΩcm	Temp °F
1	26	39
2	30	39
3	27	39
4	28	41
5	26	42
6	24	43
7	23	44
8	26	41
	26	Average Reading
	15	Corrected Average

Test Location 4

	Resistance KΩcm	Temp °F
1	55	39
2	55	40
3	59	40
4	66	40
5	71	42
6	63	44
7	65	43
8	53	42
	61	Average Reading
	35	Corrected Average

Test Location 7

	Resistance KΩcm	Temp °F
1	41	38
2	44	39
3	46	41
4	46	40
5	49	40
6	51	39
7	44	38
8	39	38
	45	Average Reading
	25	Corrected Average

Test Location 8

	Resistance KΩcm	Temp °F
1	37	39
2	40	39
3	47	39
4	51	38
5	56	39
6	55	41
7	55	41
8	52	44
	49	Average Reading
	27	Corrected Average

Averages corrected to 69.8°F, as per equation developed by Elkey and Sellevold (1995) and presented in Presuel-Moreno (2010)

Table C-4: Surface resistivity test results for bridge deck 2L.

Surface Resistivity	Bridge	150012	2L
	Date	3/11/2011	

Test Location 1

	Resistance KΩcm	Temp °F
1	33	39
2	35	39
3	47	39
4	50	39
5	51	40
6	51	41
7	54	41
8	52	42
	47	Average Reading
	26	Corrected Average

Test Location 2

	Resistance KΩcm	Temp °F
1	51	41
2	43	40
3	45	40
4	44	41
5	39	42
6	36	42
7	39	42
8	46	41
	43	Average Reading
	24	Corrected Average

Test Location 5

	Resistance KΩcm	Temp °F
1	43	38
2	50	38
3	48	38
4	48	38
5	56	38
6	62	39
7	60	39
8	65	39
	54	Average Reading
	29	Corrected Average

Test Location 6

	Resistance KΩcm	Temp °F
1	87	36
2	98	36
3	102	37
4	116	37
5	113	37
6	105	38
7	93	40
8	91	42
	101	Average Reading
	54	Corrected Average

Test Location 3

	Resistance KΩcm	Temp °F
1	100	37
2	107	39
3	108	39
4	104	40
5	112	40
6	115	40
7	116	40
8	112	40
	109	Average Reading
	60	Corrected Average

Test Location 4

	Resistance KΩcm	Temp °F
1	101	39
2	124	38
3	129	38
4	129	38
5	138	38
6	140	38
7	122	39
8	124	39
	126	Average Reading
	68	Corrected Average

Test Location 7

	Resistance KΩcm	Temp °F
1	127	40
2	141	40
3	130	38
4	117	38
5	125	38
6	116	38
7	112	37
8	112	38
	123	Average Reading
	66	Corrected Average

Test Location 8

	Resistance KΩcm	Temp °F
1	96	37
2	94	37
3	110	36
4	110	36
5	121	37
6	113	37
7	105	37
8	104	38
	107	Average Reading
	56	Corrected Average

Averages corrected to 69.8°F, as per equation developed by Elkey and Sellevold (1995) and presented in Presuel-Moreno (2010)

Table C-5: Surface resistivity test results for bridge deck 3N.

Surface Resistivity	Bridge	150014	3N
	Date	3/9/2011	

Test Location 1

	Resistance KΩcm	Temp °F
1	317	46
2	311	44
3	296	44
4	307	44
5	300	43
6	285	43
7	285	43
8	296	43
	300	Average Reading
	180	Corrected Average

Test Location 2

	Resistance KΩcm	Temp °F
1	270	43
2	322	43
3	346	43
4	314	44
5	321	44
6	311	44
7	300	44
8	317	45
	313	Average Reading
	188	Corrected Average

Test Location 5

	Resistance KΩcm	Temp °F
1	377	43
2	384	44
3	401	46
4	412	46
5	409	46
6	399	46
7	395	47
8	404	46
	398	Average Reading
	248	Corrected Average

Test Location 6

	Resistance KΩcm	Temp °F
1	325	50
2	319	49
3	353	49
4	340	48
5	300	47
6	325	46
7	352	46
8	388	47
	338	Average Reading
	220	Corrected Average

Test Location 3

	Resistance KΩcm	Temp °F
1	358	40
2	348	40
3	335	41
4	321	40
5	334	40
6	334	40
7	366	41
8	348	41
	343	Average Reading
	192	Corrected Average

Test Location 4

	Resistance KΩcm	Temp °F
1	402	40
2	414	42
3	401	42
4	423	42
5	396	44
6	356	43
7	382	44
8	410	44
	398	Average Reading
	234	Corrected Average

Test Location 7

	Resistance KΩcm	Temp °F
1	253	44
2	300	44
3	286	44
4	295	44
5	297	44
6	274	45
7	282	45
8	262	45
	281	Average Reading
	171	Corrected Average

Test Location 8

	Resistance KΩcm	Temp °F
1	311	41
2	304	41
3	259	43
4	287	43
5	292	44
6	271	44
7	295	46
8	280	46
	287	Average Reading
	172	Corrected Average

Averages corrected to 69.8°F, as per equation developed by Elkey and Sellevold (1995) and presented in Presuel-Moreno (2010)

Table C-6: Surface resistivity test results for bridge deck 3L.

Surface Resistivity	Bridge	150014	3L
	Date	3/9/2011	

Test Location 1

	Resistance KΩcm	Temp °F
1	217	42
2	241	41
3	280	41
4	368	41
5	233	43
6	219	43
7	240	43
8	273	42
	259	Average Reading
	150	Corrected Average

Test Location 2

	Resistance KΩcm	Temp °F
1	300	41
2	300	41
3	334	43
4	329	43
5	342	43
6	327	43
7	389	44
8	300	44
	328	Average Reading
	193	Corrected Average

Test Location 4

	Resistance KΩcm	Temp °F
1	227	41
2	220	42
3	250	41
4	269	42
5	259	42
6	273	42
7	287	42
8	301	42
	261	Average Reading
	151	Corrected Average

Test Location 6

	Resistance KΩcm	Temp °F
1	257	37
2	275	38
3	253	39
4	244	40
5	283	41
6	267	41
7	267	41
8	237	41
	260	Average Reading
	144	Corrected Average

Test Location 3

	Resistance KΩcm	Temp °F
1	268	41
2	279	40
3	296	41
4	305	41
5	319	41
6	354	42
7	341	43
8	365	43
	316	Average Reading
	181	Corrected Average

Test Location 5

	Resistance KΩcm	Temp °F
1	288	40
2	268	41
3	314	41
4	307	42
5	295	41
6	299	43
7	261	43
8	276	42
	289	Average Reading
	166	Corrected Average

Test Location 7

	Resistance KΩcm	Temp °F
1	392	41
2	450	41
3	460	43
4	494	44
5	401	43
6	358	44
7	333	44
8	367	43
	407	Average Reading
	240	Corrected Average

Test Location 8

	Resistance KΩcm	Temp °F
1	166	42
2	194	43
3	240	43
4	253	44
5	273	44
6	276	44
7	279	45
8	246	45
	241	Average Reading
	145	Corrected Average

Averages corrected to 69.8°F, as per equation developed by Elkey and Sellevold (1995) and presented in Presuel-Moreno (2010)

Table C-7: Surface resistivity test results for bridge deck 5N.

Surface Resistivity	Bridge	270012	5N
	Date	5/18/2011	

Test Location 1

	Resistance KΩcm	Temp °F
1	20	45
2	27	48
3	35	47
4	35	47
5	41	47
6	42	47
7	43	47
8	41	47
	36	Average Reading
	23	Corrected Average

Test Location 2

	Resistance KΩcm	Temp °F
1	91	46
2	118	45
3	114	45
4	115	45
5	120	47
6	114	47
7	100	47
8	102	46
	109	Average Reading
	69	Corrected Average

Test Location 5

	Resistance KΩcm	Temp °F
1	24	48
2	36	48
3	38	48
4	43	48
5	50	48
6	54	48
7	50	48
8	57	48
	44	Average Reading
	29	Corrected Average

Test Location 6

	Resistance KΩcm	Temp °F
1	57	46
2	61	46
3	75	47
4	84	46
5	77	46
6	79	46
7	81	46
8	82	46
	75	Average Reading
	47	Corrected Average

Test Location 3

	Resistance KΩcm	Temp °F
1	43	46
2	51	46
3	60	46
4	68	46
5	71	46
6	65	46
7	61	46
8	58	46
	60	Average Reading
	38	Corrected Average

Test Location 4

	Resistance KΩcm	Temp °F
1	42	46
2	58	46
3	61	46
4	73	46
5	83	45
6	80	46
7	85	46
8	75	46
	70	Average Reading
	44	Corrected Average

Test Location 7

	Resistance KΩcm	Temp °F
1	26	55
2	33	50
3	42	51
4	51	51
5	51	50
6	51	50
7	53	50
8	50	51
	45	Average Reading
	31	Corrected Average

Test Location 8

	Resistance KΩcm	Temp °F
1	172	48
2	217	49
3	248	51
4	272	50
5	267	50
6	290	51
7	290	50
8	267	50
	253	Average Reading
	172	Corrected Average

Averages corrected to 69.8°F, as per equation developed by Elkey and Sellevold (1995) and presented in Presuel-Moreno (2010)

Table C-8: Surface resistivity test results for bridge deck 5L.

Surface Resistivity	Bridge	270012	5L
	Date	5/18/2011	

Test Location 1

	Resistance KΩcm	Temp °F
1	85	43
2	92	43
3	103	44
4	94	44
5	91	44
6	98	45
7	104	45
8	104	46
	96	Average Reading
	59	Corrected Average

Test Location 2

	Resistance KΩcm	Temp °F
1	181	45
2	177	48
3	175	48
4	176	48
5	186	49
6	169	49
7	155	49
8	173	49
	174	Average Reading
	114	Corrected Average

Test Location 5

	Resistance KΩcm	Temp °F
1	185	50
2	136	51
3	130	51
4	153	52
5	157	50
6	190	50
7	208	52
8	244	51
	175	Average Reading
	122	Corrected Average

Test Location 6

	Resistance KΩcm	Temp °F
1	129	47
2	132	48
3	127	48
4	120	48
5	102	49
6	97	49
7	109	49
8	100	49
	115	Average Reading
	76	Corrected Average

Test Location 3

	Resistance KΩcm	Temp °F
1	173	47
2	218	47
3	215	47
4	201	48
5	208	48
6	244	49
7	193	49
8	181	51
	204	Average Reading
	135	Corrected Average

Test Location 4

	Resistance KΩcm	Temp °F
1	119	47
2	107	48
3	114	49
4	110	49
5	116	49
6	96	49
7	93	50
8	89	49
	106	Average Reading
	70	Corrected Average

Test Location 7

	Resistance KΩcm	Temp °F
1	128	47
2	143	48
3	147	48
4	155	48
5	170	48
6	159	48
7	158	48
8	162	48
	153	Average Reading
	100	Corrected Average

Test Location 8

	Resistance KΩcm	Temp °F
1	100	48
2	116	48
3	124	48
4	111	49
5	104	49
6	95	49
7	106	49
8	88	50
	106	Average Reading
	70	Corrected Average

Averages corrected to 69.8°F, as per equation developed by Elkey and Sellevold (1995) and presented in Presuel-Moreno (2010)

Table C-9: Surface resistivity test results for bridge deck 6N.

Surface Resistivity	Bridge	330345	6N
	Date	12/9/2010	

Test Location 1

	Resistance KΩcm	Temp °F
1	304	40
2	249	41
3	279	40
4	253	41
5	257	41
6	254	40
7	280	41
8	272	41
	269	Average Reading
	151	Corrected Average

Test Location 2

	Resistance KΩcm	Temp °F
1	184	45
2	187	45
3	201	46
4	186	46
5	188	46
6	218	46
7	181	46
8	216	45
	195	Average Reading
	122	Corrected Average

Test Location 5

	Resistance KΩcm	Temp °F
1	153	48
2	163	48
3	155	48
4	166	48
5	177	48
6	181	48
7	161	47
8	203	47
	170	Average Reading
	111	Corrected Average

Test Location 6

	Resistance KΩcm	Temp °F
1	190	41
2	186	41
3	195	40
4	229	40
5	217	41
6	189	41
7	184	41
8	197	41
	198	Average Reading
	112	Corrected Average

Test Location 3

	Resistance KΩcm	Temp °F
1	191	46
2	202	47
3	211	46
4	208	46
5	211	46
6	223	46
7	209	46
8	206	46
	208	Average Reading
	131	Corrected Average

Test Location 4

	Resistance KΩcm	Temp °F
1	284	47
2	256	46
3	284	46
4	254	46
5	235	46
6	247	47
7	258	46
8	257	46
	259	Average Reading
	164	Corrected Average

Test Location 7

	Resistance KΩcm	Temp °F
1	227	45
2	231	45
3	221	44
4	238	44
5	247	44
6	245	44
7	236	44
8	232	45
	235	Average Reading
	143	Corrected Average

Test Location 8

	Resistance KΩcm	Temp °F
1	692	49
2	783	49
3	872	49
4	755	49
5	890	49
6	774	49
7	869	49
8	767	49
	800	Average Reading
	536	Corrected Average

Averages corrected to 69.8°F, as per equation developed by Elkey and Sellevold (1995) and presented in Presuel-Moreno (2010)

Table C-10: Surface resistivity test results for bridge deck 6L.

Surface Resistivity	Bridge	330254	6L
	Date	12/8/2010	

Test Location 1

	Resistance KΩcm	Temp °F
1	63	44
2	65	43
3	62	43
4	67	43
5	63	43
6	59	43
7	70	43
8	64	42
	64	Average Reading
	38	Corrected Average

Test Location 2

	Resistance KΩcm	Temp °F
1	48	37
2	48	36
3	50	36
4	46	36
5	48	36
6	48	36
7	46	35
8	47	35
	48	Average Reading
	24	Corrected Average

Test Location 5

	Resistance KΩcm	Temp °F
1	27	36
2	29	38
3	30	38
4	31	38
5	30	38
6	31	38
7	32	38
8	31	38
	30	Average Reading
	16	Corrected Average

Test Location 6

	Resistance KΩcm	Temp °F
1	50	38
2	51	38
3	49	38
4	51	38
5	51	38
6	49	38
7	50	38
8	49	37
	50	Average Reading
	27	Corrected Average

Test Location 3

	Resistance KΩcm	Temp °F
1	39	41
2	37	40
3	39	39
4	33	39
5	41	39
6	42	39
7	36	38
8	40	38
	38	Average Reading
	21	Corrected Average

Test Location 4

	Resistance KΩcm	Temp °F
1	38	30
2	43	30
3	41	30
4	41	30
5	29	30
6	25	30
7	35	30
8	33	30
	36	Average Reading
	16	Corrected Average

Test Location 7

	Resistance KΩcm	Temp °F
1	57	39
2	49	39
3	51	39
4	53	39
5	55	39
6	54	39
7	44	38
8	53	38
	52	Average Reading
	28	Corrected Average

Test Location 8

	Resistance KΩcm	Temp °F
1	32	41
2	32	41
3	33	42
4	33	42
5	29	42
6	31	42
7	32	43
8	33	43
	32	Average Reading
	18	Corrected Average

Averages corrected to 69.8°F, as per equation developed by Elkey and Sellevold (1995) and presented in Presuel-Moreno (2010)

Table C-11: Surface resistivity test results for bridge deck 7N.

Surface Resistivity	Bridge	590541	7N
	Date	3/18/2011	

Test Location 1

	Resistance KΩcm	Temp °F
1	82	47
2	86	47
3	82	48
4	83	49
5	74	49
6	68	48
7	65	49
8	66	50
	76	Average Reading
	50	Corrected Average

Test Location 2

	Resistance KΩcm	Temp °F
1	53	51
2	37	50
3	34	49
4	42	49
5	41	49
6	39	49
7	51	50
8	66	51
	45	Average Reading
	31	Corrected Average

Test Location 3

	Resistance KΩcm	Temp °F
1	51	53
2	53	54
3	57	50
4	51	54
5	48	52
6	50	51
7	54	52
8	49	52
	52	Average Reading
	37	Corrected Average

Test Location 4

	Resistance KΩcm	Temp °F
1	101	66
2	95	66
3	60	66
4	67	66
5	69	66
6	72	66
7	59	67
8	60	68
	73	Average Reading
	68	Corrected Average

Test Location 5

	Resistance KΩcm	Temp °F
1	78	64
2	77	64
3	76	63
4	82	63
5	87	64
6	62	64
7	64	63
8	60	63
9	61	64
	72	Average Reading
	64	Corrected Average

Test Location 6

	Resistance KΩcm	Temp °F
1	20	47
2	21	47
3	23	48
4	20	48
5	20	48
6	18	48
7	17	48
8	18	49
	20	Average Reading
	13	Corrected Average

Test Location 7

	Resistance KΩcm	Temp °F
1	48	53
2	38	51
3	40	50
4	38	51
5	32	51
6	32	50
7	31	52
8	29	51
	36	Average Reading
	25	Corrected Average

Test Location 8

	Resistance KΩcm	Temp °F
1	10	53
2	14	53
3	13	52
4	15	52
5	12	52
6	21	51
7	15	52
8	16	52
	15	Average Reading
	10	Corrected Average

Averages corrected to 69.8°F, as per equation developed by Elkey and Sellevold (1995) and presented in Presuel-Moreno (2010)

Table C-12: Surface resistivity test results for bridge deck 7L.

Surface Resistivity	Bridge	590363	7L
	Date	3/17/2011	

Test Location 1

	Resistance KΩcm	Temp °F
1	112	51
2	144	51
3	164	50
4	161	49
5	153	49
6	122	49
7	102	50
8	82	48
	130	Average Reading
	88	Corrected Average

Test Location 2

	Resistance KΩcm	Temp °F
1	127	50
2	134	50
3	117	51
4	119	52
5	122	50
6	123	50
7	122	50
8	126	50
	124	Average Reading
	85	Corrected Average

Test Location 5

	Resistance KΩcm	Temp °F
1	237	47
2	257	45
3	292	44
4	339	45
5	318	43
6	274	42
7	266	43
8	205	43
	274	Average Reading
	165	Corrected Average

Test Location 7

	Resistance KΩcm	Temp °F
1	60	55
2	73	56
3	77	54
4	84	52
5	76	57
6	67	57
7	60	50
8	75	50
	72	Average Reading
	53	Corrected Average

Test Location 3

	Resistance KΩcm	Temp °F
1	45	46
2	45	45
3	52	46
4	50	48
5	50	47
6	46	46
7	52	45
8	50	45
	49	Average Reading
	31	Corrected Average

Test Location 4

	Resistance KΩcm	Temp °F
1	44	49
2	56	47
3	61	47
4	73	47
5	78	47
6	71	46
7	71	45
8	69	45
	65	Average Reading
	42	Corrected Average

Test Location 6

	Resistance KΩcm	Temp °F
1	62	51
2	73	52
3	83	52
4	91	53
5	92	53
6	84	56
7	81	56
8	69	58
9	77	58
	79	Average Reading
	59	Corrected Average

Test Location 8

	Resistance KΩcm	Temp °F
1	126	43
2	114	42
3	121	41
4	136	41
5	100	40
6	94	40
7	87	40
8	80	40
	107	Average Reading
	61	Corrected Average

Averages corrected to 69.8°F, as per equation developed by Elkey and Sellevold (1995) and presented in Presuel-Moreno (2010)

Table C-13: Surface resistivity test results for bridge deck 8N.

Surface Resistivity	Bridge	580160	8N
	Date	6/6/2011	

Test Location 1

	Resistance	Temp
	KΩcm	°F
1	27	47.6
2	26	56
3	28	64
4	26	68.4
5	27	65
6	30	67.4
7	27	61
8	31	59
	28	Average Reading
	24	Corrected Average

Test Location 2

	Resistance	Temp
	KΩcm	°F
1	29	51
2	27	57
3	30	61
4	25	63
5	23	66
6	24	60
7	24	62
8	26	59
	26	Average Reading
	22	Corrected Average

Test Location 5

	Resistance	Temp
	KΩcm	°F
1	19	63
2	21	64
3	27	66
4	27	70
5	26	70
6	21	70
7	26	71
8	26	73
	24	Average Reading
	23	Corrected Average

Test Location 6

	Resistance	Temp
	KΩcm	°F
1	24	67
2	20	67
3	21	66
4	19	68
5	18	66
6	16	70
7	15	70
8	13	71
	18	Average Reading
	18	Corrected Average

Test Location 3

	Resistance	Temp
	KΩcm	°F
1	34	71
2	34	70
3	36	69
4	31	70
5	26	70
6	24	67
7	23	68
8	21	68
	29	Average Reading
	28	Corrected Average

Test Location 4

	Resistance	Temp
	KΩcm	°F
1	27	79
2	28	70
3	27	69
4	28	69
5	24	70
6	26	75
7	25	72
8	21	79
	26	Average Reading
	27	Corrected Average

Test Location 7

	Resistance	Temp
	KΩcm	°F
1	19	68
2	25	64
3	28	69
4	37	69
5	29	70
6	28	68
7	30	68
8	32	61
	29	Average Reading
	27	Corrected Average

Test Location 8

	Resistance	Temp
	KΩcm	°F
1	22	70
2	22	67
3	23	71
4	24	54
5	29	59
6	25	60
7	27	62
8	23	63
	24	Average Reading
	22	Corrected Average

Averages corrected to 69.8°F, as per equation developed by Elkey and Sellevold (1995) and presented in Presuel-Moreno (2010)

Table C-14: Surface resistivity test results for bridge deck 8L.

Surface Resistivity	Bridge	430120	8L
	Date	4/4/2011	

Test Location 1

	Resistance	Temp
	KΩcm	°F
1	30	39
2	31	40
3	28	39
4	26	39
5	29	40
6	28	39
7	36	39
8	24	39
	29	Average Reading
	16	Corrected Average

Test Location 2

	Resistance	Temp
	KΩcm	°F
1	20	40
2	22	39
3	15	39
4	13	39
5	14	40
6	19	41
7	21	42
8	21	42
	18	Average Reading
	10	Corrected Average

Test Location 5

	Resistance	Temp
	KΩcm	°F
1	16	45
2	15	46
3	18	46
4	15	48
5	16	47
6	14	47
7	14	47
8	17	46
	16	Average Reading
	10	Corrected Average

Test Location 6

	Resistance	Temp
	KΩcm	°F
1	19	46
2	13	49
3	15	47
4	16	47
5	17	49
6	18	47
7	16	50
8	15	50
	16	Average Reading
	11	Corrected Average

Test Location 3

	Resistance	Temp
	KΩcm	°F
1	16	40
2	17	39
3	16	39
4	17	41
5	15	41
6	15	41
7	16	41
8	16	42
	16	Average Reading
	9	Corrected Average

Test Location 4

	Resistance	Temp
	KΩcm	°F
1	13	44
2	13	44
3	14	44
4	12	45
5	13	45
6	14	45
7	13	46
8	12	46
	13	Average Reading
	8	Corrected Average

Test Location 7

	Resistance	Temp
	KΩcm	°F
1	21	47
2	21	48
3	26	48
4	29	47
5	25	48
6	15	48
7	13	47
8	12	48
	20	Average Reading
	13	Corrected Average

Test Location 8

	Resistance	Temp
	KΩcm	°F
1	12	47
2	14	50
3	14	49
4	14	49
5	17	49
6	20	50
7	24	50
8	22	50
	17	Average Reading
	12	Corrected Average

Averages corrected to 69.8°F, as per equation developed by Elkey and Sellevold (1995) and presented in Presuel-Moreno (2010)

Table C-15: Surface resistivity test results for bridge deck 9N.

Surface Resistivity	Bridge	580153	9N
	Date	12/7/2010	

Test Location 1

	Resistance KΩcm	Temp °F
1	44	35
2	47	35
3	47	35
4	49	35
5	48	35
6	52	35
7	47	30
8		
	48	Average Reading
	24	Corrected Average

Test Location 2

	Resistance KΩcm	Temp °F
1	43	41
2	42	38
3	45	38
4	48	37
5	45	37
6	45	37
7	49	37
8	45	36
	45	Average Reading
	24	Corrected Average

Test Location 5

	Resistance KΩcm	Temp °F
1	57	33
2	56	33
3	60	33
4	66	33
5	62	33
6	65	33
7	60	33
8	61	33
	61	Average Reading
	29	Corrected Average

Test Location 6

	Resistance KΩcm	Temp °F
1	70	33
2	72	33
3	78	33
4	80	34
5	74	34
6	71	34
7	73	35
8	74	35
	74	Average Reading
	36	Corrected Average

Test Location 3

	Resistance KΩcm	Temp °F
1	57	35
2	50	35
3	57	34
4	56	34
5	57	34
6	54	34
7	59	34
8		
	56	Average Reading
	27	Corrected Average

Test Location 4

	Resistance KΩcm	Temp °F
1	61	34
2	65	35
3	38	36
4	62	35
5	69	35
6	72	34
7	63	34
8	64	34
	62	Average Reading
	31	Corrected Average

Test Location 7

	Resistance KΩcm	Temp °F
1	56	40
2	54	40
3	57	40
4	53	41
5	58	41
6	51	41
7	58	42
8	60	42
	56	Average Reading
	32	Corrected Average

Test Location 8

	Resistance KΩcm	Temp °F
1	82	33
2	89	33
3	93	33
4	102	33
5	88	32
6	86	32
7	91	32
8		
	90	Average Reading
	43	Corrected Average

Averages corrected to 69.8°F, as per equation developed by Elkey and Sellevold (1995) and presented in Presuel-Moreno (2010)

Table C-16: Surface resistivity test results for bridge deck 9L.

Surface Resistivity	Bridge	580146	9L
	Date	10/28/2010	

Test Location 1

	Resistance KΩcm	Temp °F
1	25	46
2	25	46
3	21	47
4	24	47
5	23	49
6	24	49
	24	Average Reading
	15	Corrected Average

Test Location 2

	Resistance KΩcm	Temp °F
1	19	46
2	20	47
3	17	50
4	29	50
5	17	51
6	21	52
	21	Average Reading
	14	Corrected Average

Test Location 5

	Resistance KΩcm	Temp °F
1	29	49
2	35	49
3	29	50
4	29	51
5	31	52
6	27	52
	30	Average Reading
	21	Corrected Average

Test Location 6

	Resistance KΩcm	Temp °F
1	18	45
2	16	45
3	20	46
4	20	47
5	19	47
6	17	49
	18	Average Reading
	12	Corrected Average

Test Location 3

	Resistance KΩcm	Temp °F
1	24	46
2	25	48
3	23	48
4	25	49
5	26	51
6	28	51
	25	Average Reading
	17	Corrected Average

Test Location 4

	Resistance KΩcm	Temp °F
1	43	49
2	48	51
3	35	51
4	40	52
5	42	52
6	36	52
	41	Average Reading
	28	Corrected Average

Test Location 7

	Resistance KΩcm	Temp °F
1	23	48
2	21	48
3	29	49
4	27	49
5	27	50
6	29	50
	26	Average Reading
	17	Corrected Average

Test Location 8

	Resistance KΩcm	Temp °F
1	36	50
2	39	51
3	35	52
4	36	53
5	36	53
6	31	54
	36	Average Reading
	25	Corrected Average

Averages corrected to 69.8°F, as per equation developed by Elkey and Sellevold (1995) and presented in Presuel-Moreno (2010)

APPENDIX D

Macroscopic Observations of Concrete Core Samples

Table D-1: Macroscopic observations of concrete core samples from bridge deck 1N.

Bridge No.	Bridge ID	Sample ID	Sample Length (inches)	Depth of Reinforcement (inches)	Type of Reinforcement	Typical Depth of Grooves (inches)	Other Notes
70160	1N	C-1	6	-	-	1/16	1. Minor damage to top edge due to removal from deck 2. Some exposed aggregate 3. Square groove edges 4. No visible surface cracking
70160	1N	C-2	5.25	3.5-5.25 5.25	Chair WWM	1/16	1. Some exposed aggregate 2. Square groove edges 3. No visible surface cracking
70160	1N	C-3	3	-	-	1/16	1. Considerable damage to top edge due to removal from deck 2. Some exposed aggregate 3. Few surface cracks visible
70160	1N	C-4	6.25	5	WWM	1/8	1. Some exposed aggregate 2. Square groove edges 3. Few surface cracks visible
70160	1N	C-5	5.5	3	No. 4	1/8	1. No exposed aggregate 2. Square groove edges 3. No visible surface cracking
70160	1N	C-6	6	-	-	1/8	1. No exposed aggregate 2. Square groove edges 3. Few surface cracks visible
70160	1N	C-7	5.25	-	-	1/16	1. Minor damage to top edge due to removal from deck 2. Some exposed aggregate 3. Square groove edges 4. Several large surface cracks visible
70160	1N	C-8	7	5.125	WWM	1/16	1. Minor damage to top edge due to removal from deck 2. Some exposed aggregate 3. Square groove edges 4. Few surface cracks visible

Table D-2: Macroscopic observations of concrete core samples from bridge deck 1L.

Bridge No.	Bridge ID	Sample ID	Sample Length (inches)	Depth of Reinforcement (inches)	Type of Reinforcement	Typical Depth of Grooves (inches)	Other Notes
70038	1L	C-1	3.5	3	No. 5	1/8	1. Considerable damage to top edge due to removal from deck 2. Large amount of exposed aggregate 3. Square groove edges 4. No visible surface cracking
70038	1L	C-2	6	-	-	1/16	1. Large amount of exposed aggregate 2. Worn groove edges 3. No visible surface cracking
70038	1L	C-3A	3.75	-	-	1/16	1. Considerable damage to top edge due to removal from deck 2. Square groove edges 3. Few surface cracks visible
70038	1L	C-3B	6.125	2.25	No. 5	1/8	1. Large amount of exposed aggregate 2. Square groove edges 3. Several large surface cracks visible
70038	1L	C-4	7	3	No. 5	1/8	1. Large amount of exposed aggregate 2. Worn groove edges 3. Several large surface cracks visible
70038	1L	C-6	6.75	-	-	1/16	1. Large amount of exposed aggregate 2. Square groove edges 3. Few surface cracks visible
70038	1L	C-7A	7	-	-	1/8	1. Some exposed aggregate 2. Square groove edges 3. Few surface cracks visible
70038	1L	C-7B	4.25	-	-	1/16	1. Large amount of exposed aggregate 2. Worn groove edges 3. Few surface cracks visible
70038	1L	C-8	6.75	-	-	1/8	1. Some exposed aggregate 2. Square groove edges 3. Few surface cracks visible

Table D-3: Macroscopic observations of concrete core samples from bridge deck 2N.

Bridge No.	Bridge ID	Sample ID	Sample Length (inches)	Depth of Reinforcement (inches)	Type of Reinforcement	Typical Depth of Grooves (inches)	Other Notes
150012	2N	C-1	4	3	No. 5	1/8	1. Square groove edges 2. No visible surface cracking 3. Half of surface covered in white line marking
150012	2N	C-2	6	3.5 5.5	WWM WWM	1/8	1. Minor damage to top edge due to removal from deck 2. Some exposed aggregate 3. Square groove edges 4. No visible surface cracking
150012	2N	C-3	6.5	5.5	WWM	1/8	1. Large amount of exposed aggregate 2. Square groove edges 3. No visible surface cracking
150012	2N	C-4	3	-	-	1/8	1. Minor damage to top edge due to removal from deck 2. Square groove edges 3. Few surface cracks visible
150012	2N	C-5	3.25	-	-	1/8	1. Square groove edges 2. No visible surface cracking
150012	2N	C-6	3	-	-	3/16	1. Considerable damage to top edge due to removal from deck 2. Square groove edges 3. No visible surface cracking
150012	2N	C-7	3.25	-	-	1/8	1. Minor damage to top edge due to removal from deck 2. Square groove edges 3. Few surface cracks visible
150012	2N	C-8A	3.75	-	-	1/8	1. Minor damage to top edge due to removal from deck 2. Square groove edges 3. Few surface cracks visible
150012	2N	C-8B	4	-	-	1/8	1. Minor damage to top edge due to removal from deck 2. Square groove edges 3. Few surface cracks visible

Table D-4: Macroscopic observations of concrete core samples from bridge deck 2L.

Bridge No.	Bridge ID	Sample ID	Sample Length (inches)	Depth of Reinforcement (inches)	Type of Reinforcement	Typical Depth of Grooves (inches)	Other Notes
150012	2L	C-1	8.75	-	-	1/8	1. Some exposed aggregate 2. Square groove edges 3. No visible surface cracking
150012	2L	C-2	8	6	No. 5	1/8	1. Some exposed aggregate 2. Square groove edges 3. No visible surface cracking
150012	2L	C-3	4	-	-	1/8	1. Considerable damage to top edge due to removal from deck 2. Some exposed aggregate 3. Square groove edges
150012	2L	C-4	4.5	-	-	1/16	1. Large amount of exposed aggregate 2. Square groove edges 3. No visible surface cracking
150012	2L	C-5	4.5	3.75	No. 8	1/8	1. Some exposed aggregate 2. Square groove edges 3. Few surface cracks visible
150012	2L	C-6	8.5	3.75	No. 5	1/8	1. Some exposed aggregate 2. Square groove edges 3. No visible surface cracking
150012	2L	C-7	6.5	4	No. 7	1/8	1. Some exposed aggregate 2. Square groove edges 3. Few surface cracks visible
150012	2L	C-8	8	3.5	No. 7	1/8	1. Minor damage to top edge due to removal from deck 2. Some exposed aggregate 3. Square groove edges 4. Few surface cracks visible

Table D-5: Macroscopic observations of concrete core samples from bridge deck 3N.

Bridge No.	Bridge ID	Sample ID	Sample Length (inches)	Depth of Reinforcement (inches)	Type of Reinforcement	Typical Depth of Grooves (inches)	Other Notes
150014	3N	C-1	6	-	-	1/16	1. Large amount of exposed aggregate 2. Worn groove edges 3. No visible surface cracking
150014	3N	C-2	6	4	No. 4	1/16	1. Some exposed aggregate 2. Square groove edges 3. Few surface cracks visible
150014	3N	C-3	4	-	-	1/16	1. Considerable damage to top edge due to removal from deck 2. Large amount of exposed aggregate 3. Worn groove edges 4. Few surface cracks visible
150014	3N	C-4	6	-	-	1/32	1. Minor damage to top edge due to removal from deck 2. Some exposed aggregate 3. Worn groove edges 4. Few surface cracks visible
150014	3N	C-5	5.75	-	-	1/16	1. Some exposed aggregate 2. Square groove edges 3. Few surface cracks visible
150014	3N	C-6	5.5	4 5.25	WWM WWM	1/16	1. Some exposed aggregate 2. Square groove edges 3. Few surface cracks visible
150014	3N	C-7	5.5	-	-	1/16	1. Large amount of exposed aggregate 2. Worn groove edges 3. Few surface cracks visible
150014	3N	C-8	5	2.25	No. 6	1/16	1. Minor damage to top edge due to removal from deck 2. Square groove edges 3. Several large surface cracks visible

Table D-6: Macroscopic observations of concrete core samples from bridge deck 3L.

Bridge No.	Bridge ID	Sample ID	Sample Length (inches)	Depth of Reinforcement (inches)	Type of Reinforcement	Typical Depth of Grooves (inches)	Other Notes
150014	3L	C-1	5.75	2.5	No. 6	1/8	1. Minor damage to top edge due to removal from deck 2. Square groove edges 3. No visible surface cracking
150014	3L	C-2	5.75	3	No. 6	1/8	1. Minor damage to top edge due to removal from deck 2. Large amount of exposed aggregate 3. Square groove edges 4. Few surface cracks visible
150014	3L	C-3	5.75	3.75 2.75 5.5	No. 4 No. 6 WWM	1/8	1. Some exposed aggregate 2. Square groove edges 3. No visible surface cracking
150014	3L	C-4	6.5	3.5	No. 6	1/16	1. Minor damage to top edge due to removal from deck 2. Worn groove edges 3. Large amount of exposed aggregate 4. Few surface cracks visible
150014	3L	C-5	3.5	3.25	No. 6	3/16	1. Minor damage to top edge due to removal from deck 2. Some exposed aggregate 3. Square groove edges 4. No visible surface cracking
150014	3L	C-6	3.25	-	-	1/8	1. Minor damage to top edge due to removal from deck 2. Some exposed aggregate 3. Square groove edges 4. Few surface cracks visible
150014	3L	C-7	7.5	3.25	No. 4	1/8	1. Large amount of exposed aggregate 2. No visible surface cracking
150014	3L	C-8	7.5	2	No. 6	1/8	1. Large amount of exposed aggregate 2. Square groove edges 3. No visible surface cracking

Table D-7: Macroscopic observations of concrete core samples from bridge deck 5N.

Bridge No.	Bridge ID	Sample ID	Sample Length (inches)	Depth of Reinforcement (inches)	Type of Reinforcement	Typical Depth of Grooves (inches)	Other Notes
270012	5N	C-1	5.25	-	-	1/8	1. Considerable damage to top edge due to removal from deck 2. Some exposed aggregate 3. Square groove edges 4. No visible surface cracking
270012	5N	C-2	5	-	-	1/8	1. Square groove edges 2. Several large surface cracks visible 3. Cover paste worn off
270012	5N	C-3	4.5	3.5	No. 4	1/8	1. Minor damage to top edge due to removal from deck 2. Square groove edges 3. Several large surface cracks visible 4. Crack extending 1.75 inches down the side
270012	5N	C-4	5.25	-	-	1/8	1. Some exposed aggregate 2. Square groove edges 3. Few surface cracks visible
270012	5N	C-5	4.75	-	-	1/8	1. Minor damage to top edge due to removal from deck 2. Square groove edges 3. Few surface cracks visible
270012	5N	C-6	4.25	-	-	1/8	1. Considerable damage to top edge due to removal from deck 2. Some exposed aggregate 3. Square groove edges 4. Few surface cracks visible
270012	5N	C-7	5.25	-	-	1/8	1. Some exposed aggregate 2. Square groove edges 3. Few surface cracks visible
270012	5N	C-8	4	-	-	1/8	1. Minor damage to top edge due to removal from deck 2. Some exposed aggregate 3. Square groove edges 4. Several large surface cracks visible

Table D-8: Macroscopic observations of concrete core samples from bridge deck 5L.

Bridge No.	Bridge ID	Sample ID	Sample Length (inches)	Depth of Reinforcement (inches)	Type of Reinforcement	Typical Depth of Grooves (inches)	Other Notes
270012	5L	C-1	3.25	-	-	1/8	1. Minor damage to top edge due to removal from deck 2. Several large surface cracks visible 3. Cover paste worn off
270012	5L	C-2	5.75	3.75 4.5	WWM Part of chair	1/8	1. Minor damage to top edge due to removal from deck 2. Few surface cracks visible 3. Cover paste worn off
270012	5L	C-3	5.75	2.5 3.5 5	No. 5 WWM WWM	1/8	1. Square groove edges 2. Surface is badly worn and pitted 3. Cover paste worn off
270012	5L	C-4	5.75	-	-	1/8	1. Considerable damage to top edge due to removal from deck 2. Large amount of exposed aggregate 3. Several large surface cracks visible
270012	5L	C-5	6	-	-	1/8	1. Considerable damage to top edge due to removal from deck 2. Large amount of exposed aggregate 3. Square groove edges 4. Several large surface cracks visible
270012	5L	C-6	6	3.25	No. 4	1/8	1. Minor damage to top edge due to removal from deck 2. Several large surface cracks visible 3. Cover paste worn off
270012	5L	C-7	5.25	-	-	1/8	1. Some exposed aggregate 2. Worn groove edges 3. Several large surface cracks visible
270012	5L	C-8	5.5	2.5	No. 5	1/8	1. Considerable damage to top edge due to removal from deck 2. Several large surface cracks visible 3. Cover paste worn off

Table D-9: Macroscopic observations of concrete core samples from bridge deck 6N.

Bridge No.	Bridge ID	Sample ID	Sample Length (inches)	Depth of Reinforcement (inches)	Type of Reinforcement	Typical Depth of Grooves (inches)	Other Notes
330345	6N	C-1	7.25	5.5 7	WWM WWM	1/8	1. Minor damage to top edge due to removal from deck 2. Some exposed aggregate 3. Square groove edges 4. Few surface cracks visible
330345	6N	C-2	5.75	-	-	1/8	1. Minor damage to top edge due to removal from deck 2. Some exposed aggregate 3. Square groove edges 4. Several large surface cracks visible
330345	6N	C-3	5	2.5	WWM	3/16	1. Considerable damage to top edge due to removal from deck 2. Some exposed aggregate 3. Square groove edges 4. Few surface cracks visible
330345	6N	C-4A	4.25	-	-	1/16	1. Large amount of exposed aggregate 2. Worn groove edges 3. Few surface cracks visible
330345	6N	C-5	7	3.75	No. 6	1/16	1. Considerable damage to top edge due to removal from deck 2. Some exposed aggregate 3. Worn groove edges 4. No visible surface cracking
330345	6N	C-6A	4	-	-	1/8	1. Large amount of exposed aggregate 2. Square groove edges 3. Few surface cracks visible
330345	6N	C-6B	3.75	3.5	No. 6	1/8	1. Some exposed aggregate 2. Square groove edges 3. Few surface cracks visible 4. Large void on side
330345	6N	C-7	7	-	-	1/8	1. Some exposed aggregate 2. Worn groove edges 3. Several large surface cracks visible 4. Heavy cracking through center 5. Rust stains on side
330345	6N	C-8	7	-	-	1/16	1. Considerable damage to top edge due to removal from deck 2. Some exposed aggregate 3. Worn groove edges 4. Several large surface cracks visible

Table D-10: Macroscopic observations of concrete core samples from bridge deck 6L.

Bridge No.	Bridge ID	Sample ID	Sample Length (inches)	Depth of Reinforcement (inches)	Type of Reinforcement	Typical Depth of Grooves (inches)	Other Notes
330254	6L	C-1	8	4	No. 4	1/8	1. Minor damage to top edge due to removal from deck 2. Square groove edges 3. Few surface cracks visible
330254	6L	C-2	6.25	-	-	1/4	1. Considerable damage to top edge due to removal from deck 2. Some exposed aggregate 3. Few surface cracks visible 4. 1/3 of the top surface painted with white lane paint
330254	6L	C-3	6.75	-	-	1/8	1. Some exposed aggregate 2. Square groove edges 3. Few surface cracks visible 4. Rebar indentation 3" from top
330254	6L	C-4	5.75	-	-	1/8	1. Large amount of exposed aggregate 2. Square groove edges 3. Few surface cracks visible
330254	6L	C-5	6.25	5.75 4.5	WWM Part of chair	1/8	1. Large amount of exposed aggregate 2. Square groove edges 3. Several large surface cracks visible
330254	6L	C-6A	3.25	-	-	1/8	1. Some exposed aggregate 2. Worn groove edges 3. Few surface cracks visible 4. Small yellow inclusion approximately 2.5" from the top
330254	6L	C-6B	7	-	-	1/8	1. Minor damage to top edge due to removal from deck 2. Some exposed aggregate 3. Several large surface cracks visible
330254	6L	C-7	5.75	-	-	1/8	1. Large amount of exposed aggregate 2. Several large surface cracks visible
330254	6L	C-8	5.75	5.5 3.5 4.5	WWM WWM Part of chair	1/8	1. Considerable damage to top edge due to removal from deck 2. Large amount of exposed aggregate 3. Few surface cracks visible 4. 1 large crack across top

Table D-11: Macroscopic observations of concrete core samples from bridge deck 7N.

Bridge No.	Bridge ID	Sample ID	Sample Length (inches)	Depth of Reinforcement (inches)	Type of Reinforcement	Typical Depth of Grooves (inches)	Other Notes
590541	7N	C-1	6.25	-	-	1/16	1. Some exposed aggregate 2. Worn groove edges 3. Few surface cracks visible
590541	7N	C-2	3.5	-	-	0	1. Minor damage to top edge due to removal from deck 2. Some exposed aggregate 3. Few surface cracks visible
590541	7N	C-3	6.5	-	-	1/32	1. Large amount of exposed aggregate 2. Worn groove edges 3. Few surface cracks visible
590541	7N	C-4	5.75	-	-	1/16	1. Large amount of exposed aggregate 2. Worn groove edges 3. Few surface cracks visible
590541	7N	C-5	6	-	-	1/32	1. Minor damage to top edge due to removal from deck 2. Some exposed aggregate 3. Worn groove edges 4. Few surface cracks visible
590541	7N	C-6	5	-	-	1/8	1. Considerable damage to top edge due to removal from deck 2. Some exposed aggregate 3. Worn groove edges 4. Few surface cracks visible
590541	7N	C-7	4	-	-	0	1. Minor damage to top edge due to removal from deck 2. Some exposed aggregate 3. Worn groove edges 4. Few surface cracks visible
590541	7N	C-8	5.75	-	-	0	1. Some exposed aggregate 2. Worn groove edges 3. Several large surface cracks visible

Table D-12: Macroscopic observations of concrete core samples from bridge deck 7L.

Bridge No.	Bridge ID	Sample ID	Sample Length (inches)	Depth of Reinforcement (inches)	Type of Reinforcement	Typical Depth of Grooves (inches)	Other Notes
590363	7L	C-1	6.25	5.5	No. 6	1/16	1. Large amount of exposed aggregate 2. Few surface cracks visible
590363	7L	C-2	5	-	-	1/16	1. Large amount of exposed aggregate 2. Square groove edges 3. Large Crack crossing the diameter of the sample, entending approx. 2" down the core
590363	7L	C-3	5.5	-	-	1/8	1. Large amount of exposed aggregate 2. Square groove edges 3. Many faint cracks visible
590363	7L	C-4	7.75	3.5 4.25 5.75 6	No. 6 WWM WWM No. 6	1/8	1. Large amount of exposed aggregate 2. Square groove edges 3. Few surface cracks visible
590363	7L	C-5A	3.25	-	-	1/8	1. Large amount of exposed aggregate 2. Square groove edges 3. Few surface cracks visible
590363	7L	C-5B	3	2.5	Tie Wire	1/8	1. Considerable damage to top edge due to removal from deck 2. Large amount of exposed aggregate 3. Worn groove edges
590363	7L	C-6	8	4.75 4.5	No. 6 WWM	1/8	1. Large amount of exposed aggregate 2. Square groove edges 3. Several large surface cracks visible 4. Crack extending from the bottom of the core up approx. 3"
590363	7L	C-7	3.5	-	-	1/8	1. Minor damage to top edge due to removal from deck 2. Large amount of exposed aggregate 3. Square groove edges 4. Few surface cracks visible
590363	7L	C-8	6	-	-	1/8	1. Some exposed aggregate 2. Square groove edges 3. Few surface cracks visible

Table D-13: Macroscopic observations of concrete core samples from bridge deck 8N.

Bridge No.	Bridge ID	Sample ID	Sample Length (inches)	Depth of Reinforcement (inches)	Type of Reinforcement	Typical Depth of Grooves (inches)	Other Notes
580160	8N	C-1	6.75	3.25 5.25	WWM WWM	1/8	1. Some exposed aggregate 2. Square groove edges 3. Few surface cracks visible
580160	8N	C-2	6	3.25 4.5 5.5	WWM WWM WWM	1/8	1. Considerable damage to top edge due to removal from deck 2. Square groove edges 3. Few surface cracks visible
580160	8N	C-3	6	-	-	1/8	1. Minor damage to top edge due to removal from deck 2. Large amount of exposed aggregate 3. Worn groove edges 4. Several large surface cracks visible
580160	8N	C-4	4	-	-	3/16	1. Considerable damage to top edge due to removal from deck 2. Some exposed aggregate 3. Square groove edges 4. Several large surface cracks visible
580160	8N	C-5	5.5	-	-	1/8	1. Large amount of exposed aggregate 2. Worn groove edges 3. Large grack extending down approx. 1" from top
580160	8N	C-6	5.5	-	-	1/8	1. Some exposed aggregate 2. Square groove edges 3. Several large surface cracks visible
580160	8N	C-7	4	-	-	3/16	1. Minor damage to top edge due to removal from deck 2. Some exposed aggregate 3. Several large surface cracks visible
580160	8N	C-8	5.5	-	-	1/8	1. Large amount of exposed aggregate 2. Worn groove edges 3. Several large surface cracks visible

Table D-14: Macroscopic observations of concrete core samples from bridge deck 8L.

Bridge No.	Bridge ID	Sample ID	Sample Length (inches)	Depth of Reinforcement (inches)	Type of Reinforcement	Typical Depth of Grooves (inches)	Other Notes
430120	8L	C-1	7	-	-	1/16	1. Considerable damage to top edge due to removal from deck 2. Some exposed aggregate 3. Square groove edges 4. Few surface cracks visible
430120	8L	C-2	6.75	-	-	1/16	1. Some exposed aggregate 2. Worn groove edges 3. No visible surface cracking
430120	8L	C-3	6.5	6	No. 6	1/8	1. Considerable damage to top edge due to removal from deck 2. Some exposed aggregate 3. Square groove edges 4. No visible surface cracking
430120	8L	C-4	3	-	-	1/8	1. Minor damage to top edge due to removal from deck 2. Some exposed aggregate 3. Worn groove edges 4. Few surface cracks visible
430120	8L	C-5	7	-	-	1/8	1. Some exposed aggregate 2. Worn groove edges 3. Several large surface cracks visible
430120	8L	C-6	6.5	-	-	1/8	1. Some exposed aggregate 2. Few surface cracks visible
430120	8L	C-7	6.75	3.5 4.5 6.25	No. 6 WWM WWM	1/8	1. Minor damage to top edge due to removal from deck 2. Some exposed aggregate 3. Square groove edges 4. Few surface cracks visible
430120	8L	C-8	6.25	3.5 4.25 6	WWM WWM WWM	0	1. Some exposed aggregate 2. Worn groove edges 3. Few surface cracks visible

Table D-15: Macroscopic observations of concrete core samples from bridge deck 9N.

Bridge No.	Bridge ID	Sample ID	Sample Length (inches)	Depth of Reinforcement (inches)	Type of Reinforcement	Typical Depth of Grooves (inches)	Other Notes
580153	9N	C-1	7.25	3.5 5.5	No. 4 WWM	1/4	1. No exposed aggregate 2. Square groove edges 3. No visible surface cracking
580153	9N	C-2	6.75	4.5 5	WWM WWM	3/16	1. Minor damage to top edge due to removal from deck 2. Some exposed aggregate 3. Square groove edges 4. Few surface cracks visible
580153	9N	C-3	6.75	3.75 6.5	No. 8 WWM	1/8	1. Some exposed aggregate 2. Square groove edges 3. Several large surface cracks visible 4. Major surface damage
580153	9N	C-4	6.5	-	-	1/8	1. Some exposed aggregate 2. Square groove edges 3. Few surface cracks visible 4. Large voids 5.5" down
580153	9N	C-5	7.25	4.5 6	WWM WWM	1/8	1. Minor damage to top edge due to removal from deck 2. Some exposed aggregate 3. Square groove edges 4. Few surface cracks visible
580153	9N	C-6	6.5	-	-	1/8	1. Minor damage to top edge due to removal from deck 2. Large amount of exposed aggregate 3. Square groove edges 4. Large crack running across the diameter of the sample
580153	9N	C-7	8	-	-	1/8	1. Considerable damage to top edge due to removal from deck 2. Some exposed aggregate 3. Square groove edges 4. Few surface cracks visible
580153	9N	C-8	7.5	-	-	1/8	1. Minor damage to top edge due to removal from deck 2. Square groove edges 3. Few surface cracks visible

Table D-16: Macroscopic observations of concrete core samples from bridge deck 9L.

Bridge No.	Bridge ID	Sample ID	Sample Length (inches)	Depth of Reinforcement (inches)	Type of Reinforcement	Typical Depth of Grooves (inches)	Other Notes
580146	9L	C-1	8	-	-	1/8	1. Large amount of exposed aggregate 2. Worn groove edges 3. No visible surface cracking
580146	9L	C-2	8	5.25	No. 5	1/32	1. Some exposed aggregate 2. Worn groove edges 3. Several large surface cracks visible
580146	9L	C-3	7.75	-	-	0	1. Considerable damage to top edge due to removal from deck 2. Some exposed aggregate 3. Worn groove edges 4. Few surface cracks visible
580146	9L	C-4	7.5	3.25	No. 4	1/32	1. Some exposed aggregate 2. Square groove edges 3. Few surface cracks visible
580146	9L	C-5	7.5	-	-	1/32	1. Large amount of exposed aggregate 2. Worn groove edges 3. Few surface cracks visible
580146	9L	C-6	7.75	-	-	0	1. Large amount of exposed aggregate 2. Worn groove edges 3. Few surface cracks visible
580146	9L	C-7A	7.5	-	-	1/32	1. Considerable damage to top edge due to removal from deck 2. Large amount of exposed aggregate 3. Worn groove edges 4. Few surface cracks visible
580146	9L	C-7B	4	-	-	1/32	1. Minor damage to top edge due to removal from deck 2. Large amount of exposed aggregate 3. Square groove edges 4. Few surface cracks visible
580146	9L	C-8	7	-	-	1/32	1. Minor damage to top edge due to removal from deck 2. Some exposed aggregate 3. Worn groove edges 4. One large crack extending aoorix 3.5" down from the top of sample

APPENDIX E

Compressive Strength Test Data and Results

Table E-1: Compressive strength test data and results

Bridge Deck	Specimen ID	Length, including cap (in.)	Diameter (in.)	L/D Ratio	Compressive Strength (psi)	Strength Correction Factor	Adjusted Compressive Strength (psi)	Average Adjusted Compressive Strength for Deck (psi)
1N	1N C1	5.0625	4.0	1.27	4,897	0.93	4,560	4,370
	1N C6	5.3125	4.0	1.33	4,446	0.94	4,180	
1L	1L C6	6.25	4.0	1.56	2,657	0.96	2,560	3,950
	1L C7A	6.375	4.0	1.59	5,535	0.97	5,340	
2N	2N C3	5.0	4.0	1.25	6,197	0.93	5,755	3,940
	2N C8B	3.75	4.0	0.94	2,511	0.85	2,125	
2L	2L C1	6.8125	4.0	1.70	4,222	0.97	4,110	4,555
	2L C2	5.875	4.0	1.47	5,235	0.96	5,000	
3N	3N C1	5.5	4.0	1.38	4,669	0.95	4,415	4,415
3L	3L C7	3.875	4.0	0.97	3,992	0.86	3,425	3,013
	3L C8	4.438	4.0	1.11	2,892	0.90	2,600	
5N	5N C2	4.625	4.0	1.16	3,609	0.91	3,290	3,290
5L	5L C4	5.25	4.0	1.31	5,810	0.94	5,450	4,850
	5L C7	4.25	4.0	1.06	4,785	0.89	4,250	
6N	6N C1	5.125	4.0	1.28	5,030	0.93	4,695	4,075
	6N C7	4.625	4.0	1.16	4,587	0.91	4,175	
	6N C8	5.75	4.0	1.44	3,524	0.95	3,355	
6L	6L C2	5.75	4.0	1.44	4,103	0.95	3,910	4,328
	6L C3	6.375	4.0	1.59	4,917	0.97	4,745	
7N	7N C1	5.5	4.0	1.38	4,438	0.95	4,200	3,953
	7N C3	5.875	4.0	1.47	3,877	0.96	3,705	
7L	7L C1	5.375	4.0	1.34	3,400	0.94	3,200	3,130
	7L C8	5.375	4.0	1.34	3,248	0.94	3,060	
8N	8N C3	5.625	4.0	1.41	3,606	0.95	3,425	4,248
	8N C8	4.938	4.0	1.23	5,475	0.93	5,070	
8L	8L C1	6.125	4.0	1.53	3,949	0.96	3,790	3,893
	8L C5	6.3125	4.0	1.58	4,144	0.96	3,995	
9N	9N C6	5.3125	4.0	1.33	5,699	0.94	5,360	4,688
	9N C8	6.625	4.0	1.66	4,138	0.97	4,015	
9L	9L C3	7.625	4.0	1.91	6,014	1.00	6,015	6,015

APPENDIX F

Dynamic Modulus Test Data and Results

Table F-1: Dynamic modulus test data and results

Bridge Deck	Specimen ID	Length (in) After Saw Cut - Before Capping	Diameter (in)	L/D Ratio	Dynamic Modulus (ksi)	Average Dynamic Modulus (ksi)
1N	1N C1	5.0625	4	1.265625	4,600	4,640
	1N C6	5.3125	4	1.328125	4,680	
1L	1L C6	6.25	4	1.5625	3,110	3,120
	1L C7A	6.375	4	1.59375	3,130	
2N	2N C3	5	4	1.25	4,700	4,590
	2N C8B	3.25	4	0.8125	4,480	
2L	2L C1	6.8125	4	1.703125	3,390	3,290
	2L C2	5.625	4	1.40625	3,190	
3N	3N C1	5.1875	4	1.296875	4,640	4,720
	3N C4	5.625	4	1.40625	4,760	
3L	3L C7	3.25	4	0.8125	2,320	2,440
	3L C8	4.438	4	1.1095	2,560	
5N	5N C2	4.625	4	1.15625	4,055	4,050
	5N C4	4.875	4	1.21875	4,045	
5L	5L C4	4.875	4	1.21875	3,355	3,330
	5L C7	4.25	4	1.0625	3,305	
6N	6N C1	5.125	4	1.28125	4,560	4,630
	6N C7	4.625	4	1.15625	4,600	
	6N C8	5.75	4	1.4375	4,730	
6L	6L C2	5.25	4	1.3125	3,365	3,400
	6L C3	6.125	4	1.53125	3,425	
	6L C6B	6.25	4	1.5625	3,410	
7N	7N C1	5.5	4	1.375	4,560	4,610
	7N C3	5.875	4	1.46875	4,660	
7L	7L C1	4.75	4	1.1875	2,610	2,690
	7L C8	5.375	4	1.34375	2,770	
8N	8N C3	5.375	4	1.34375	4,635	4,670
	8N C8	4.938	4	1.2345	4,705	
8L	8L C1	6.125	4	1.53125	3,080	3,050
	8L C5	6.3125	4	1.578125	3,020	
9N	9N C6	5.3125	4	1.328125	4,680	4,710
	9N C8	6.4375	4	1.609375	4,740	
9L	9L C3	7.25	4	1.8125	3,700	3,710
	9L C6	7.3125	4	1.828125	3,720	

APPENDIX G

Sorptivity Test Data and Results

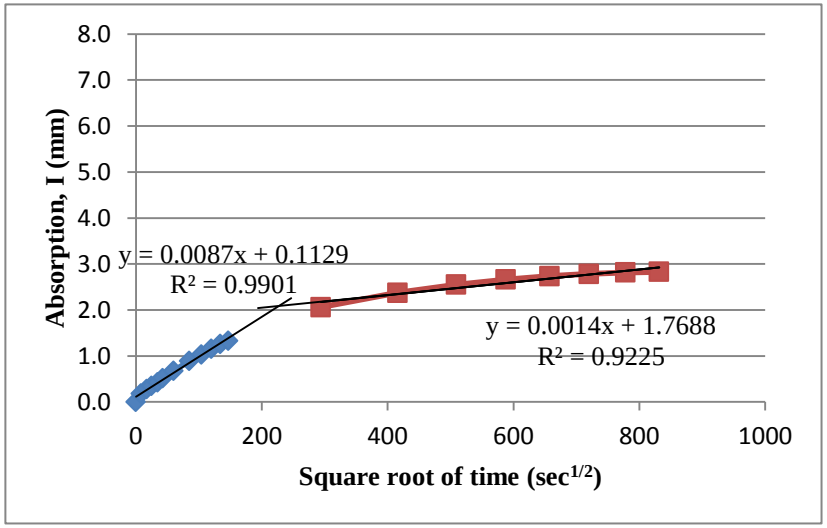

Figure G-1: Results of ASTM C1585 capillary suction test for specimen prepared from bridge deck 1N, core C-7.

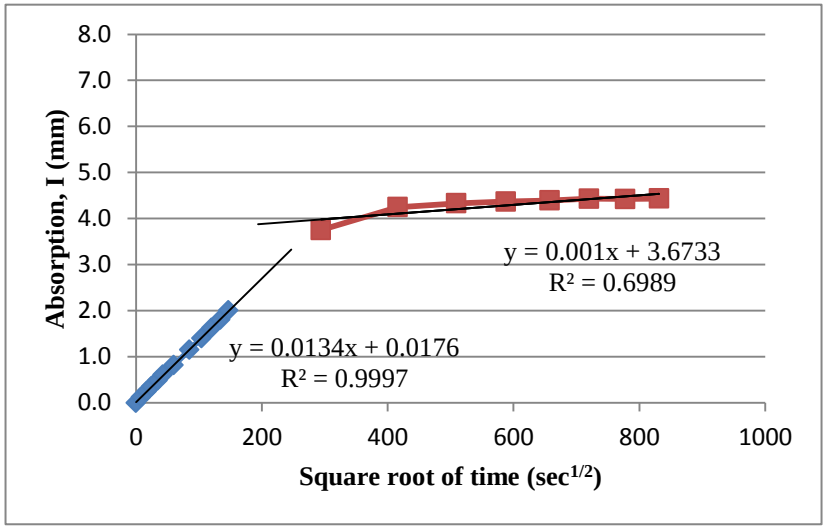

Figure G-2: Results of ASTM C1585 capillary suction test for specimen prepared from bridge deck 1N, core C-8.

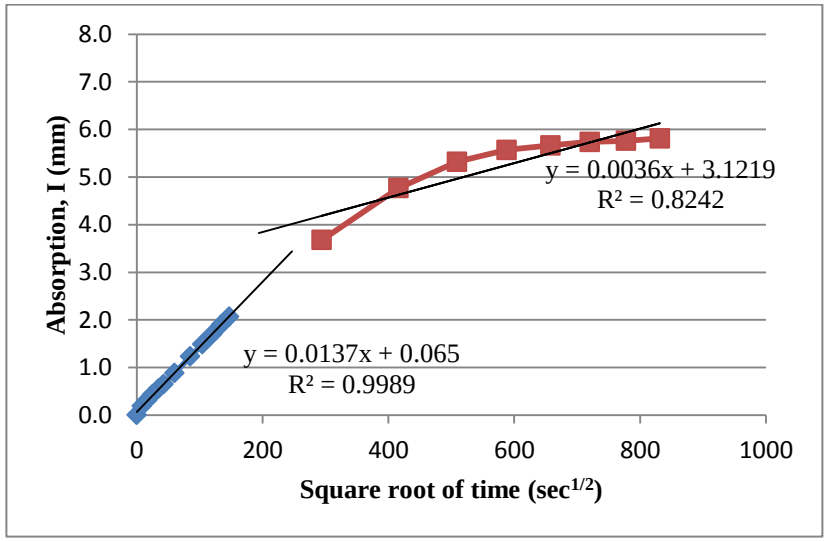

Figure G-3: Results of ASTM C1585 capillary suction test for specimen prepared from bridge deck 1L, core C-3B.

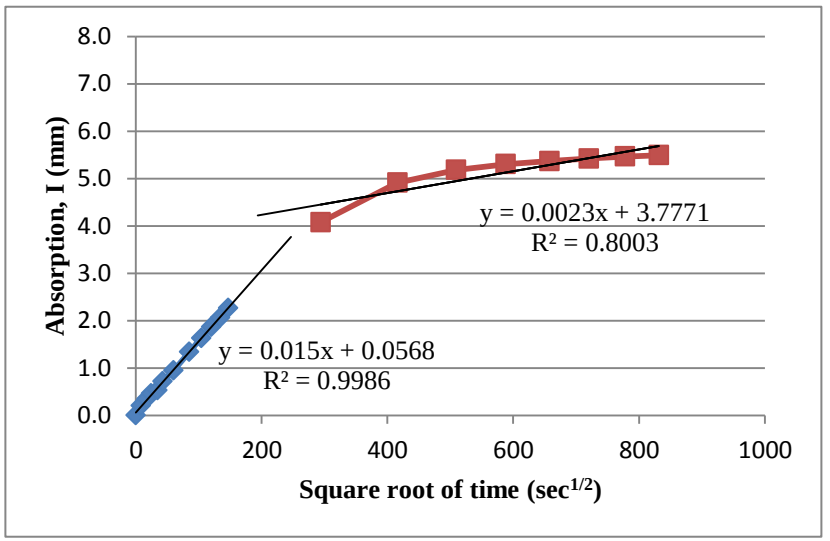

Figure G-4: Results of ASTM C1585 capillary suction test for specimen prepared from bridge deck 1L, core C-4.

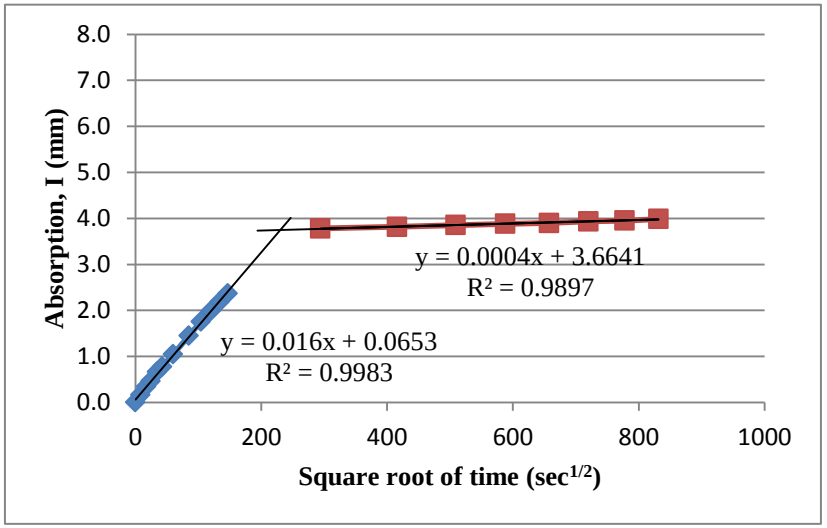

Figure G-5: Results of ASTM C1585 capillary suction test for specimen prepared from bridge deck 2N, core C-4

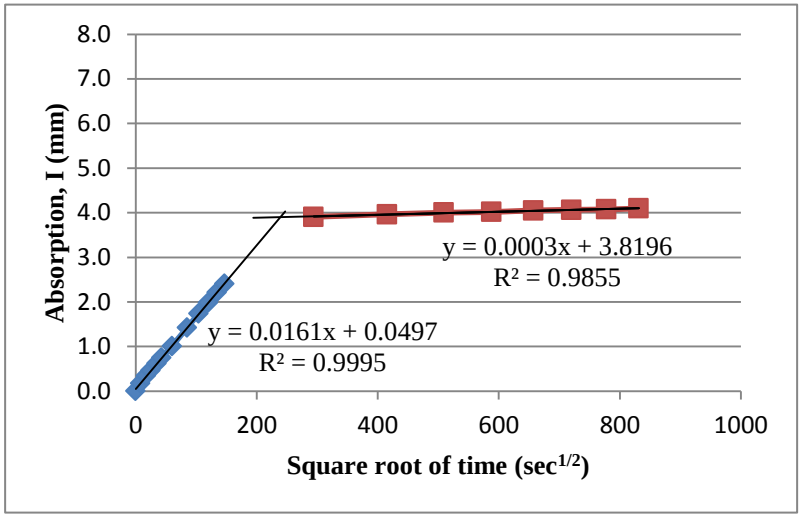

Figure G-6: Results of ASTM C1585 capillary suction test for specimen prepared from bridge deck 2N, core C-5.

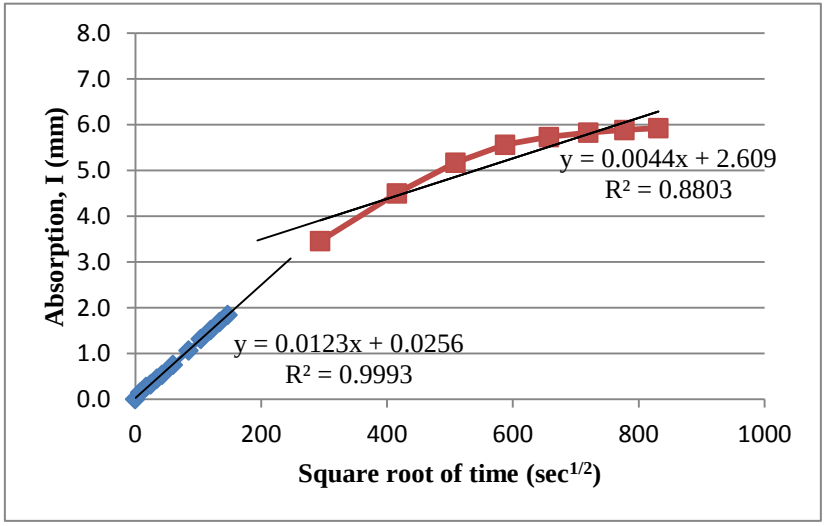

Figure G-7: Results of ASTM C1585 capillary suction test for specimen prepared from bridge deck 2L, core C-5.

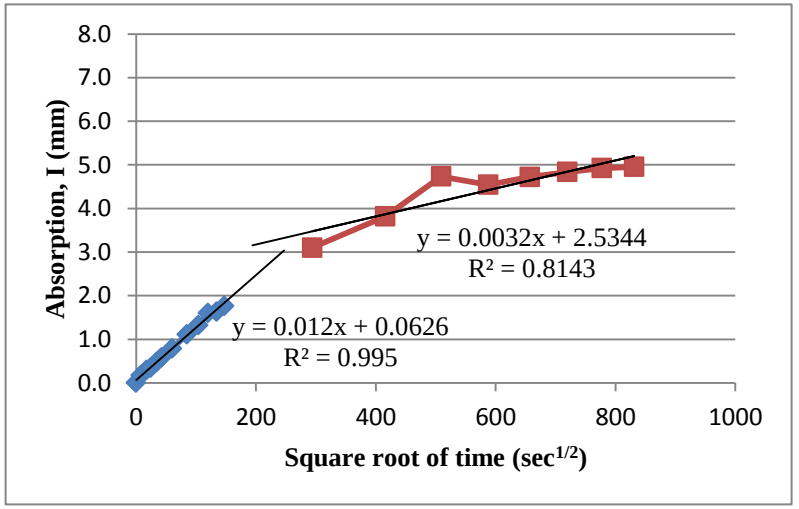

Figure G-8: Results of ASTM C1585 capillary suction test for specimen prepared from bridge deck 2L, core C-7.

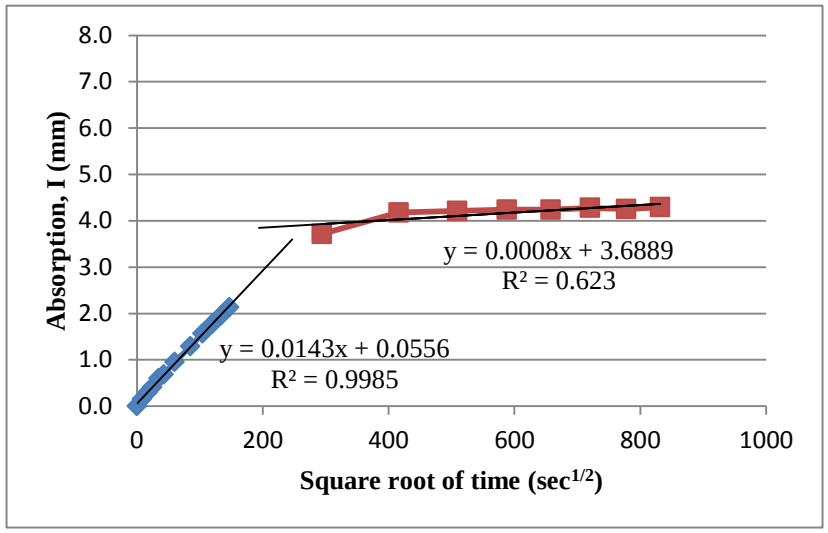

Figure G-9: Results of ASTM C1585 capillary suction test for specimen prepared from bridge deck 3N, core C-5.

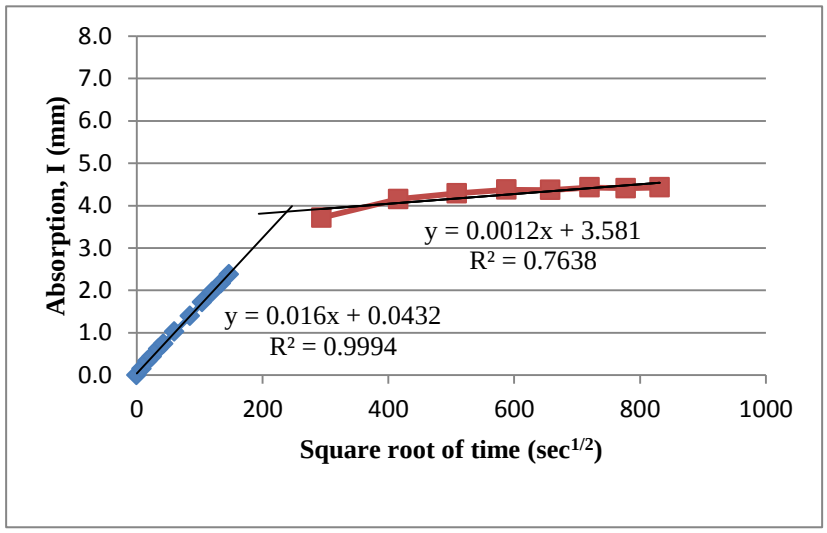

Figure G-10: Results of ASTM C1585 capillary suction test for specimen prepared from bridge deck 3N, core C-8.

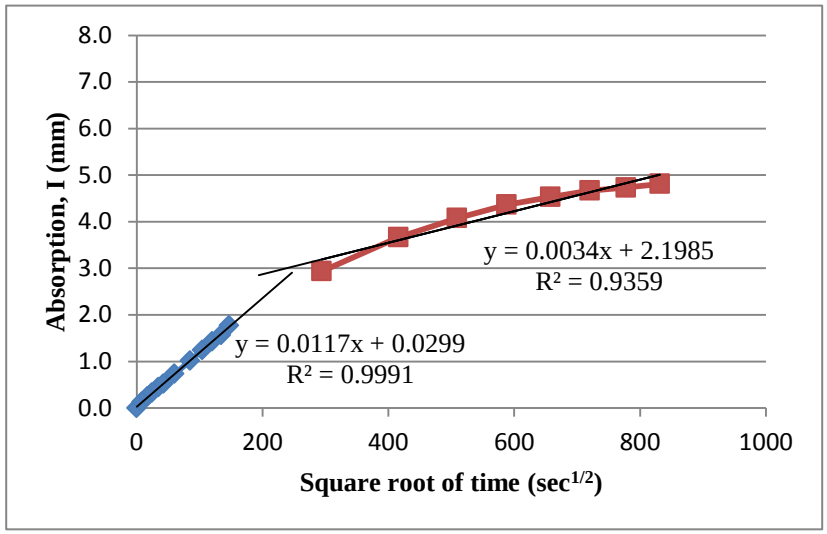

Figure G-11: Results of ASTM C1585 capillary suction test for specimen prepared from bridge deck 3L, core C-1.

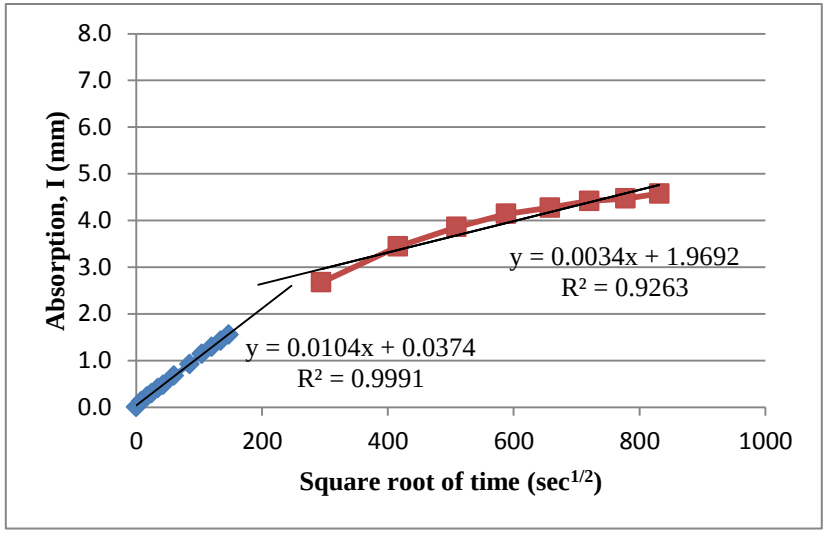

Figure G-12: Results of ASTM C1585 capillary suction test for specimen prepared from bridge deck 3L, core C-3.

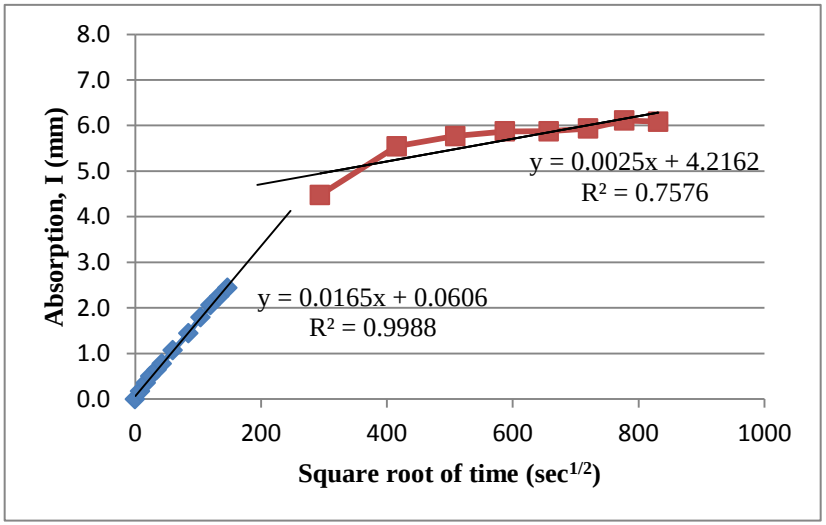

Figure G-13: Results of ASTM C1585 capillary suction test for specimen prepared from bridge deck 5N, core C-5.

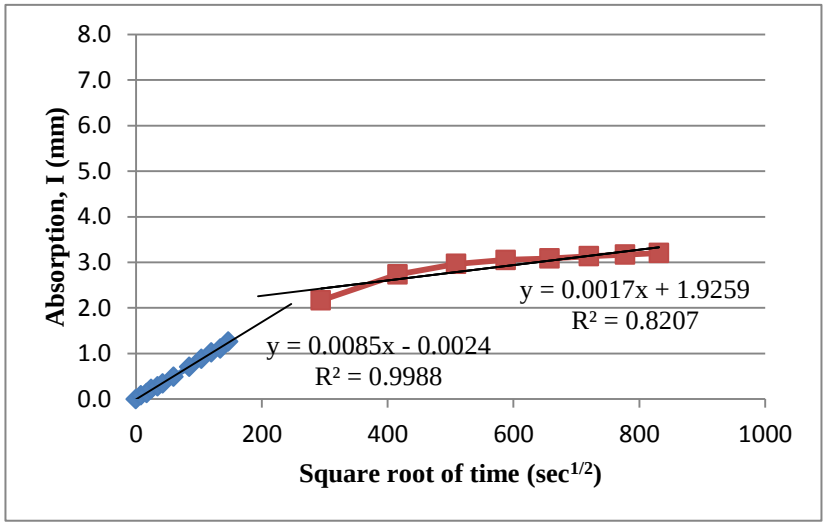

Figure G-14: Results of ASTM C1585 capillary suction test for specimen prepared from bridge deck 5N, core C-7.

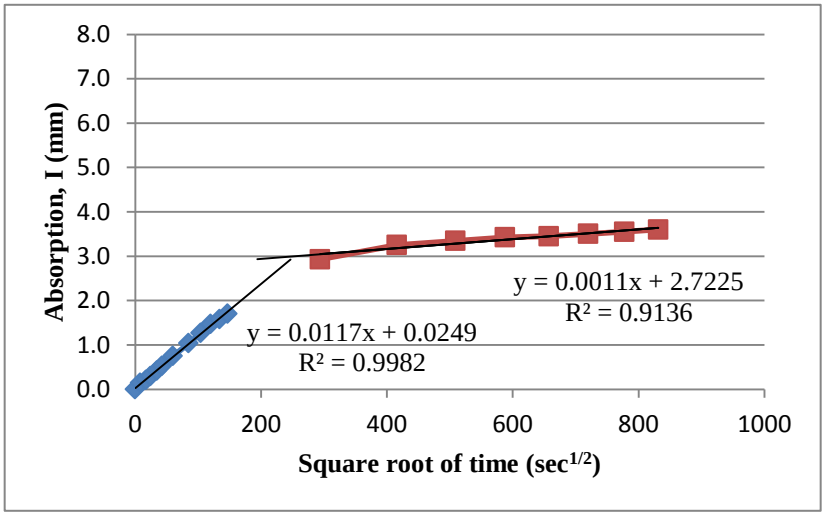

Figure G-15: Results of ASTM C1585 capillary suction test for specimen prepared from bridge deck 5L, core C-3.

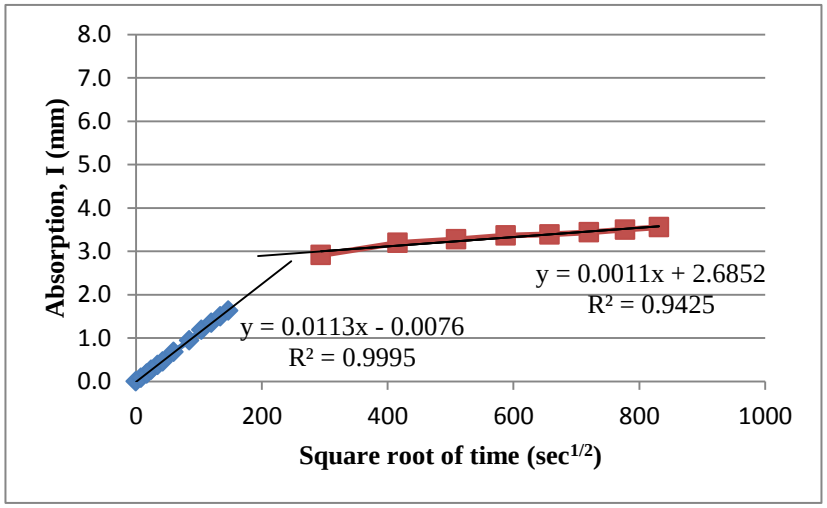

Figure G-16: Results of ASTM C1585 capillary suction test for specimen prepared from bridge deck 5L, core C-6.

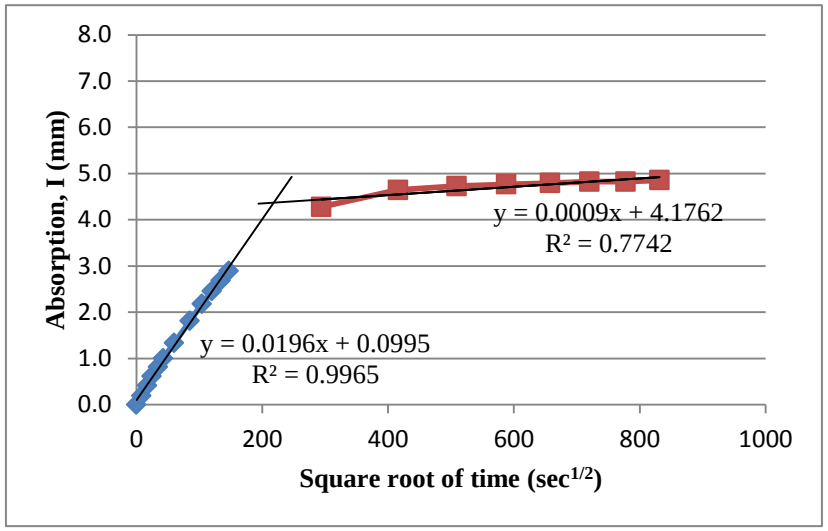

Figure G-17: Results of ASTM C1585 capillary suction test for specimen prepared from bridge deck 6N, core C-4A.

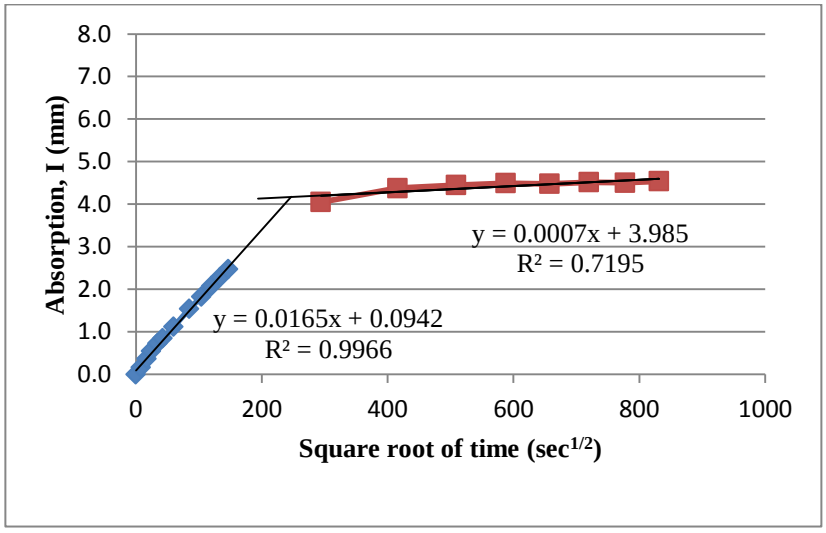

Figure G-18: Results of ASTM C1585 capillary suction test for specimen prepared from bridge deck 6N, core C-6A.

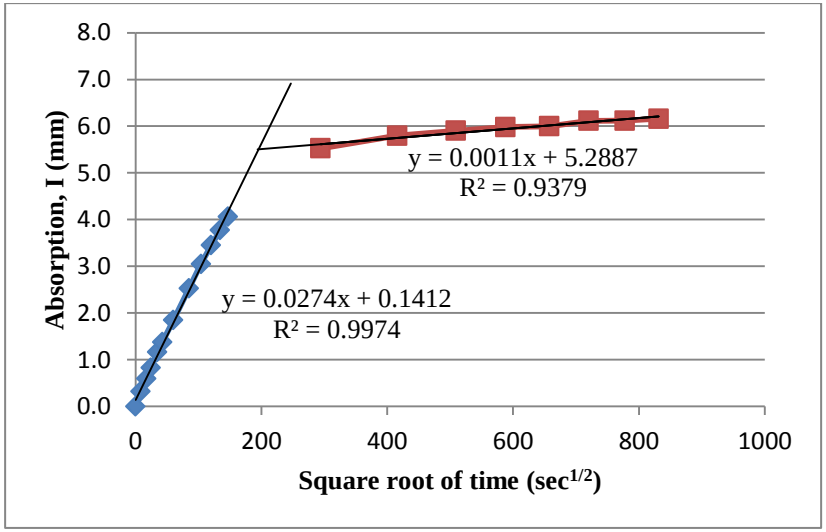

Figure G-19: Results of ASTM C1585 capillary suction test for specimen prepared from bridge deck 6L, core C-5.

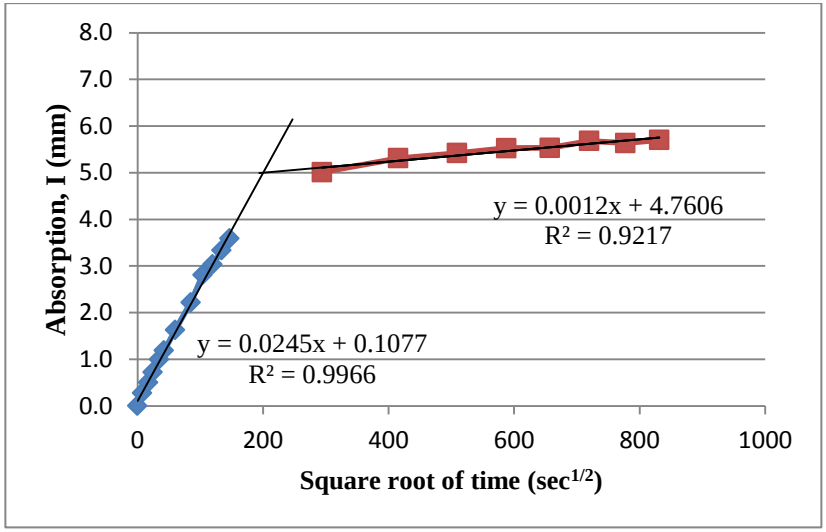

Figure G-20: Results of ASTM C1585 capillary suction test for specimen prepared from bridge deck 6L, core C-8.

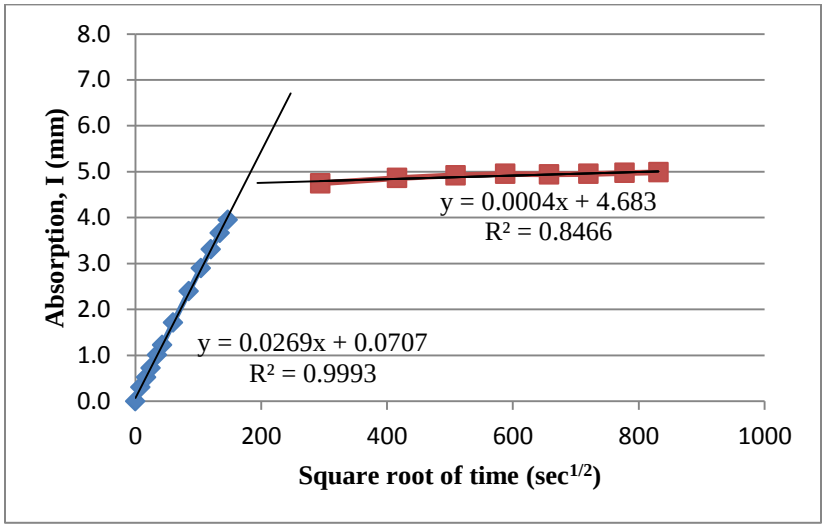

Figure G-21: Results of ASTM C1585 capillary suction test for specimen prepared from bridge deck 7N, core C-2.

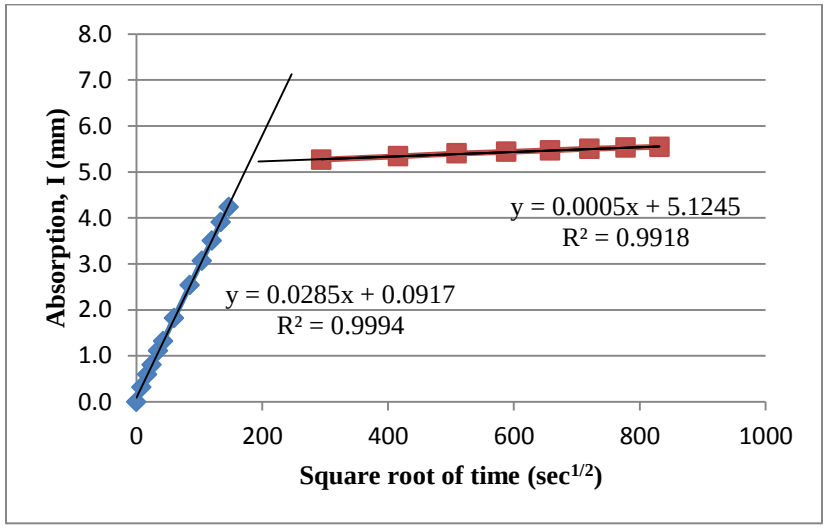

Figure G-22: Results of ASTM C1585 capillary suction test for specimen prepared from bridge deck 7N, core C-7.

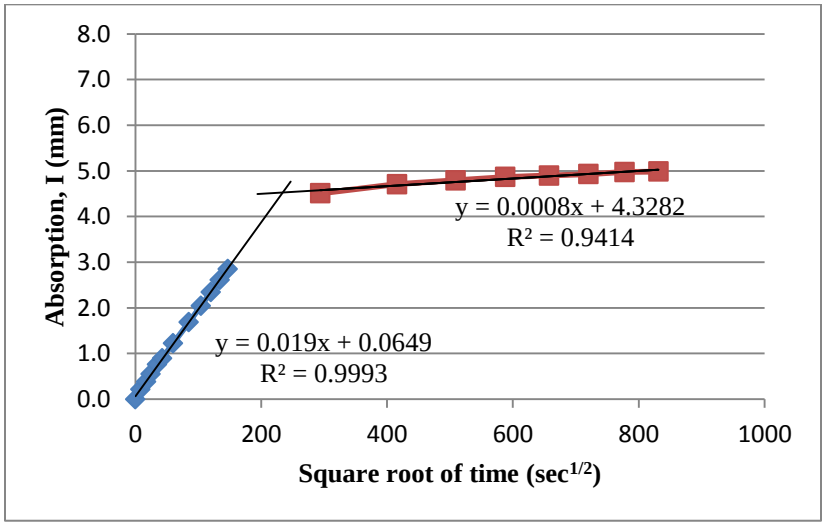

Figure G-23: Results of ASTM C1585 capillary suction test for specimen prepared from bridge deck 7L, core C-3.

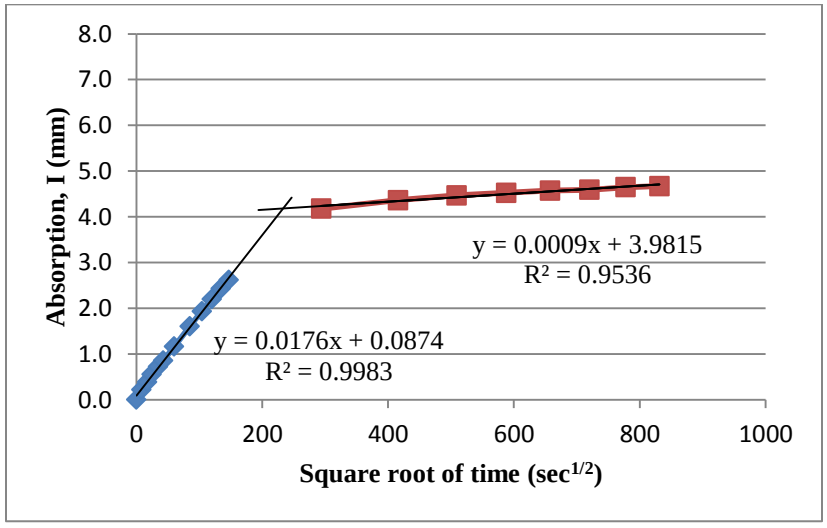

Figure G-24: Results of ASTM C1585 capillary suction test for specimen prepared from bridge deck 7L, core C-6.

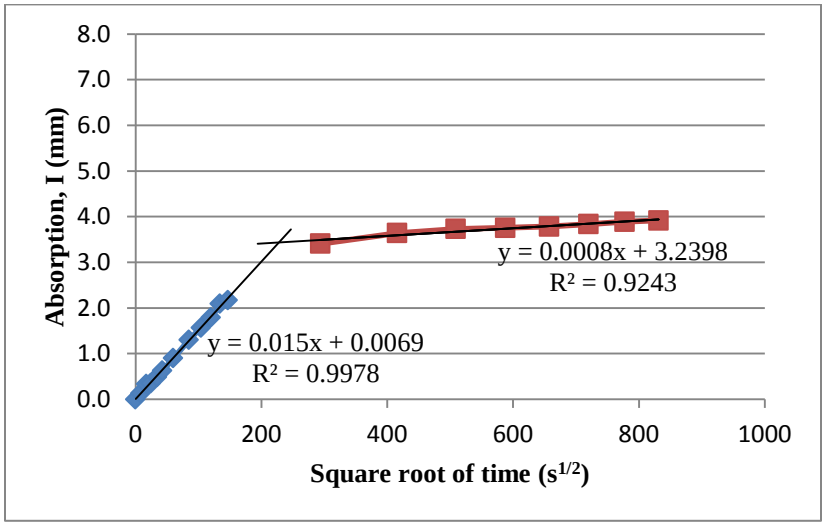

Figure G-25: Results of ASTM C1585 capillary suction test for specimen prepared from bridge deck 8N, core C-4.

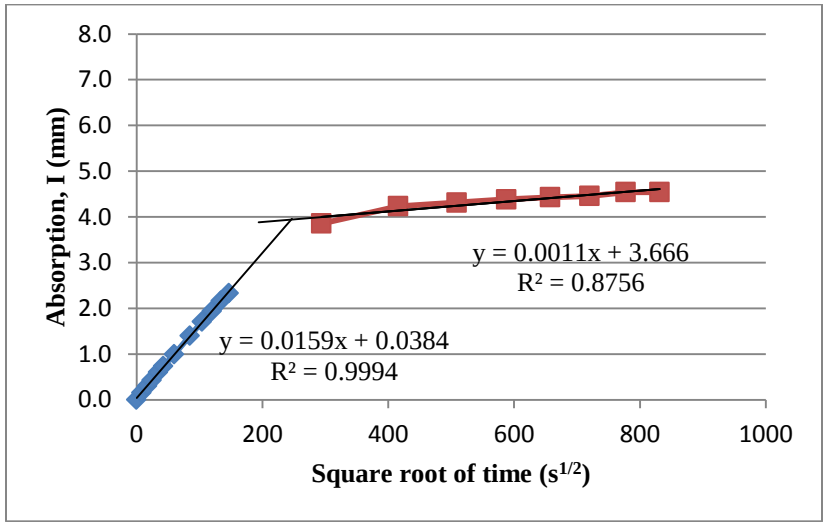

Figure G-26: Results of ASTM C1585 capillary suction test for specimen prepared from bridge deck 8N, core C-6.

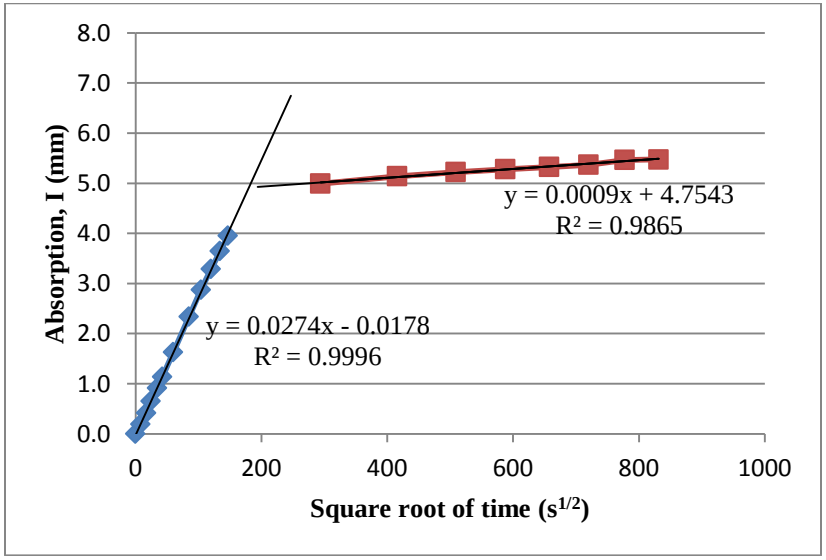

Figure G-27: Results of ASTM C1585 capillary suction test for specimen prepared from bridge deck 8L, core C-3.

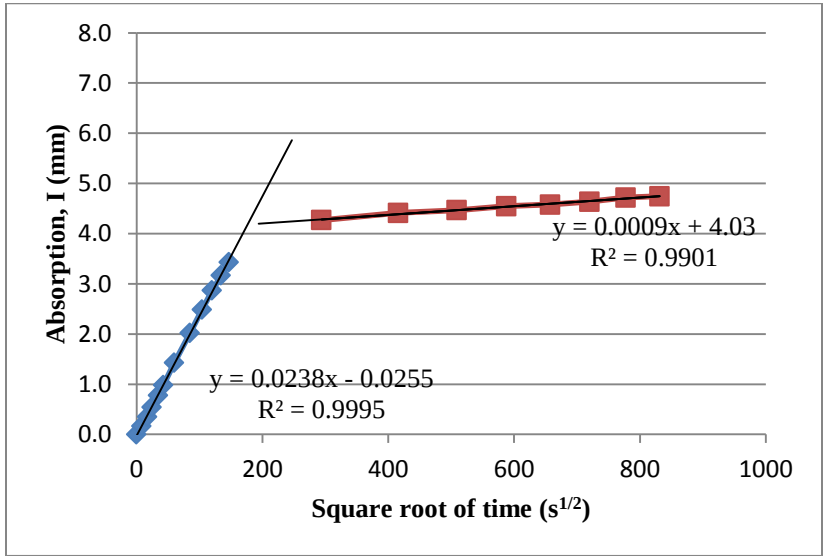

Figure G-28: Results of ASTM C1585 capillary suction test for specimen prepared from bridge deck 8L, core C-7.

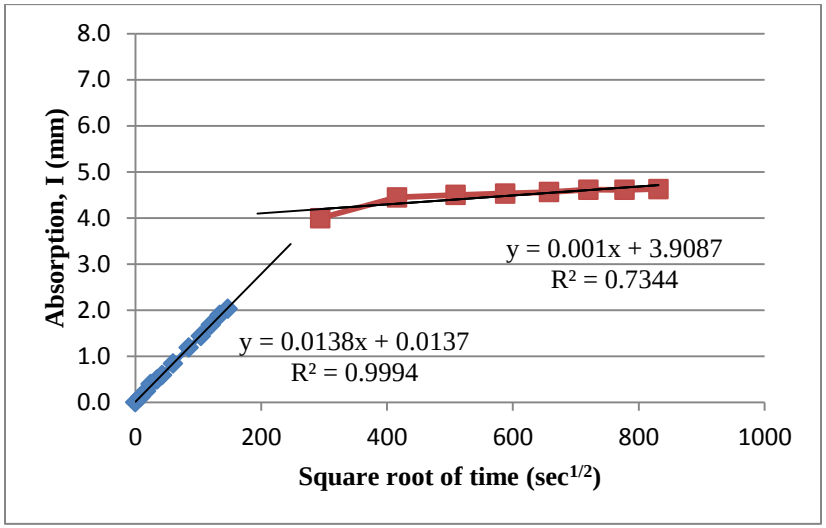

Figure G-29: Results of ASTM C1585 capillary suction test for specimen prepared from bridge deck 9N, core C-1.

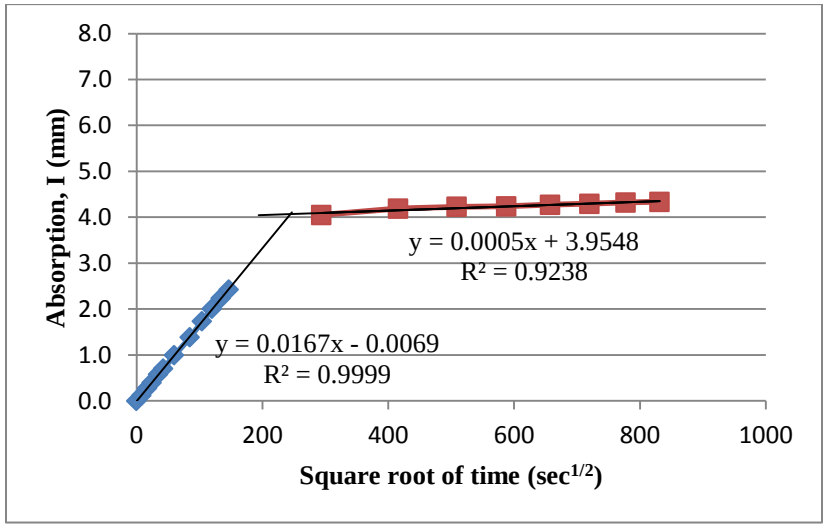

Figure G-30: Results of ASTM C1585 capillary suction test for specimen prepared from bridge deck 9N, core C-2.

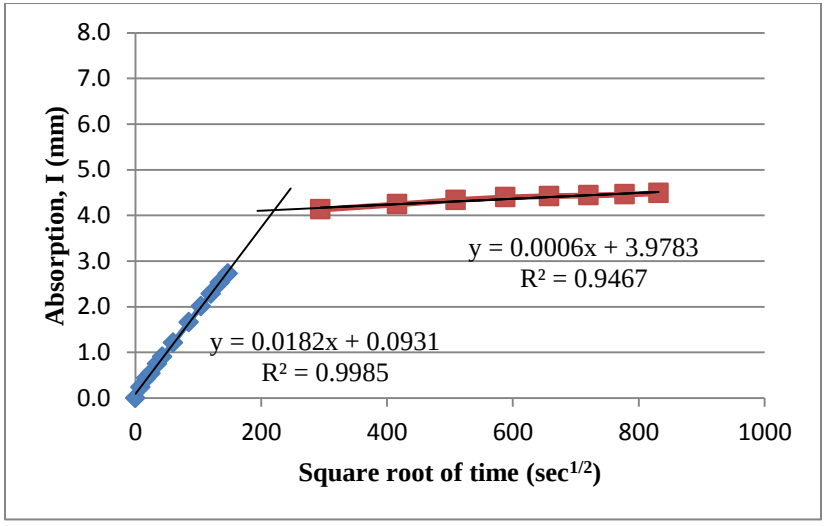

Figure G-31: Results of ASTM C1585 capillary suction test for specimen prepared from bridge deck 9L, core C-1.

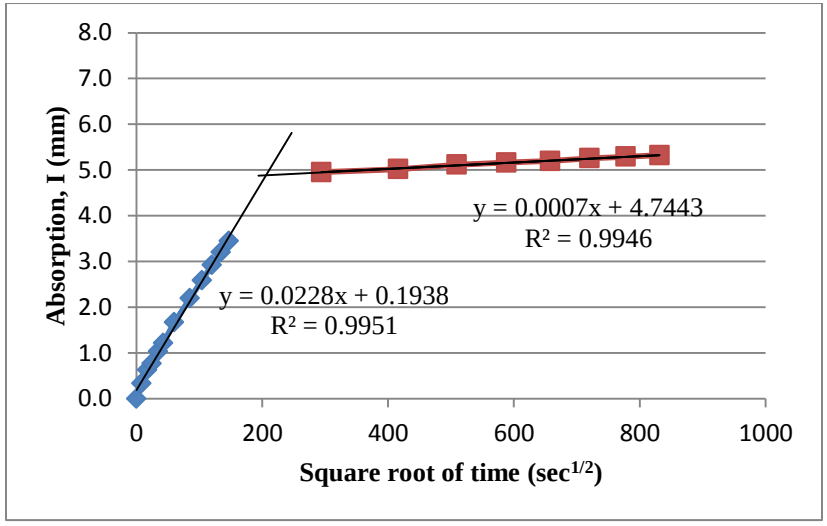

Figure G-32: Results of ASTM C1585 capillary suction test for specimen prepared from bridge deck 9L, core C-2.

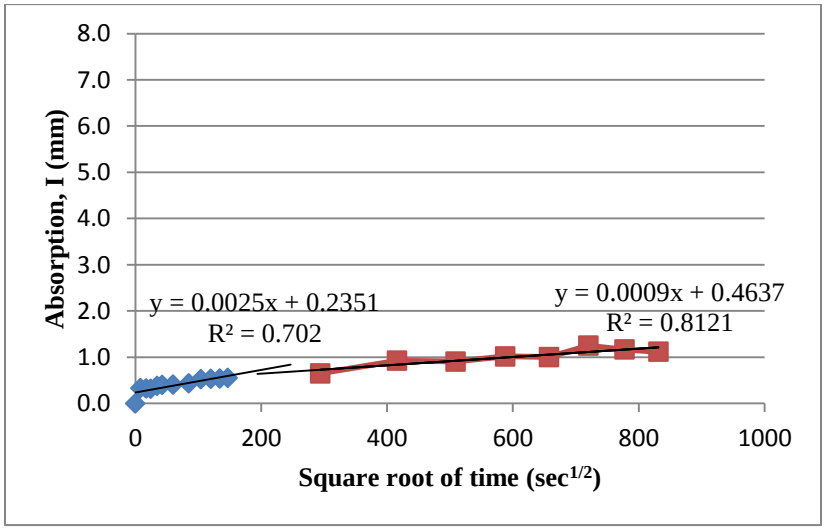

Figure G-33: Results of ponding test (per Bentz et al. 2002) for specimen prepared from bridge deck 1N, core C-7.

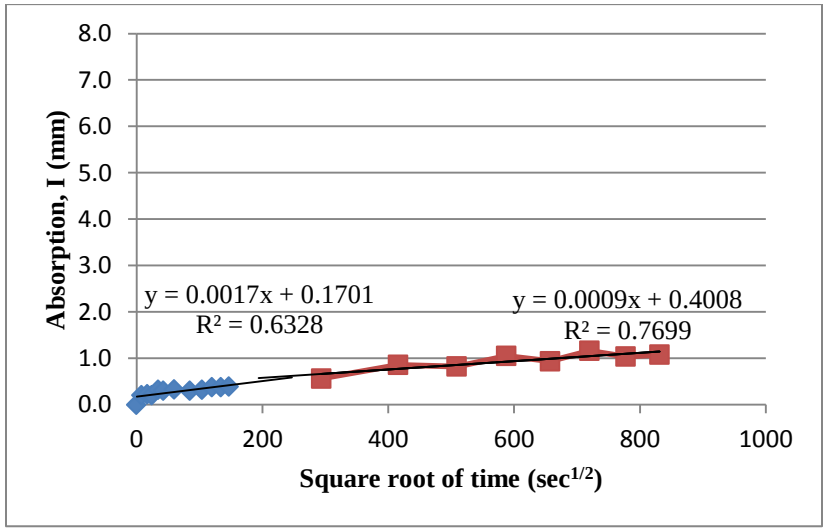

Figure G-34: Results of ponding test (per Bentz et al. 2002) for specimen prepared from bridge deck 1N, core C-8.

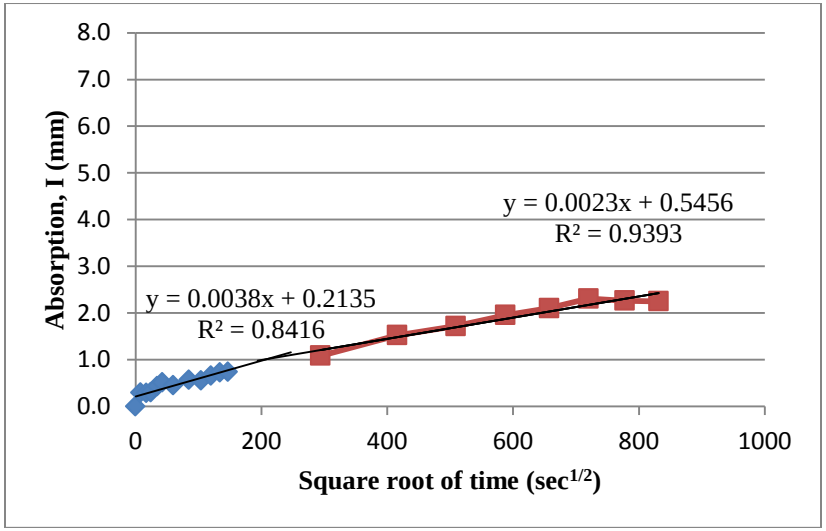

Figure G-35: Results of ponding test (per Bentz et al. 2002) for specimen prepared from bridge deck 1L, core C-3B.

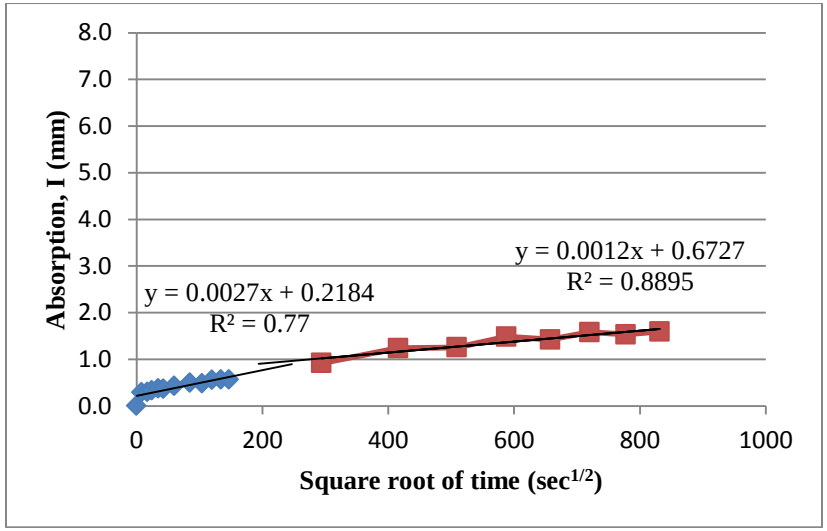

Figure G-36: Results of ponding test (per Bentz et al. 2002) for specimen prepared from bridge deck 1L, core C-4.

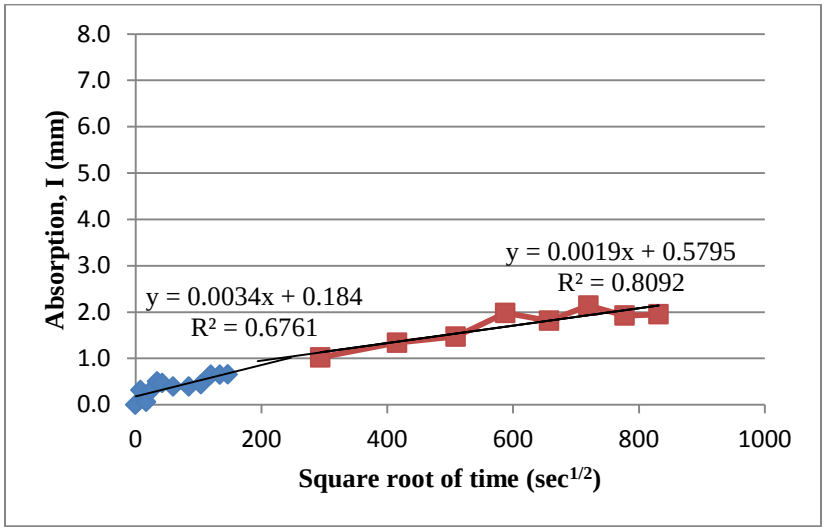

Figure G-37: Results of ponding test (per Bentz et al. 2002) for specimen prepared from bridge deck 2N, core C-4.

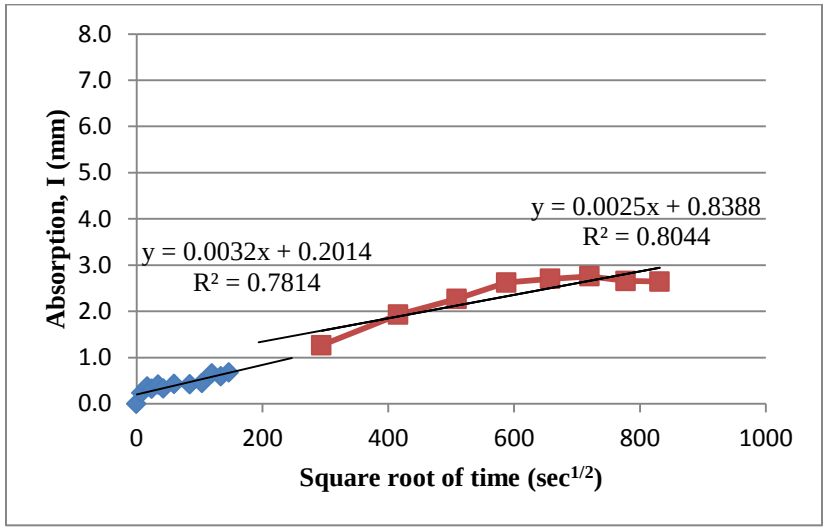

Figure G-38: Results of ponding test (per Bentz et al. 2002) for specimen prepared from bridge deck 2N, core C-5.

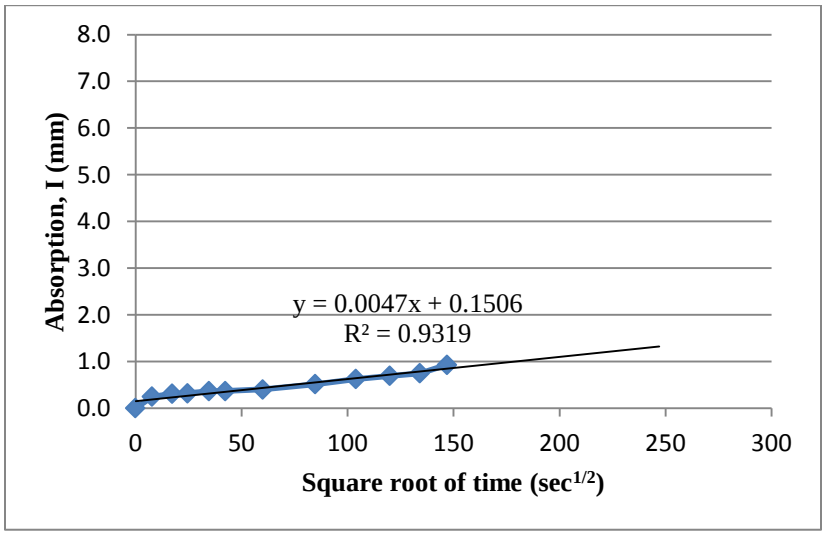

Figure G-39: Results of ponding test (per Bentz et al. 2002) for specimen prepared from bridge deck 2L, core C-5.

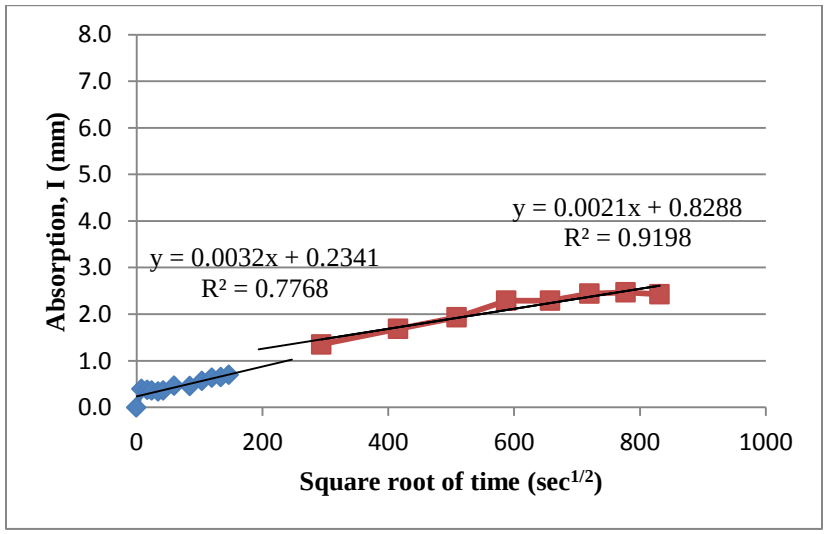

Figure G-40: Results of ponding test (per Bentz et al. 2002) for specimen prepared from bridge deck 2L, core C-7.

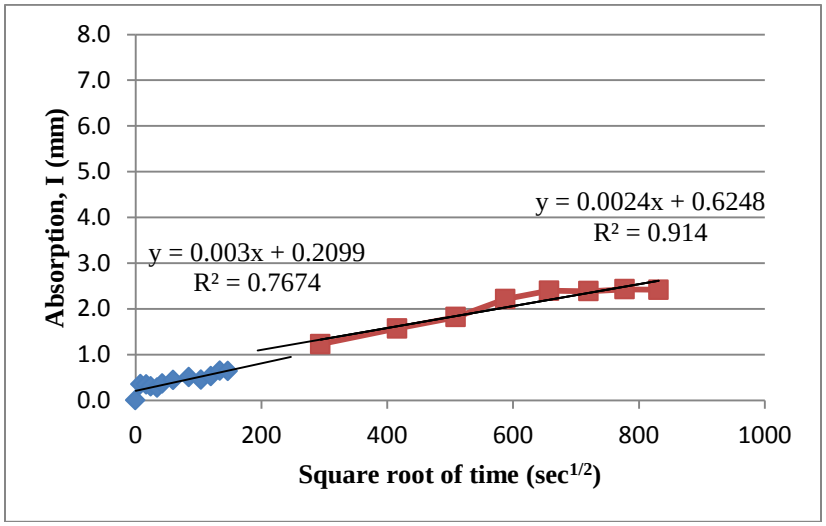

Figure G-41: Results of ponding test (per Bentz et al. 2002) for specimen prepared from bridge deck 3N, core C-6.

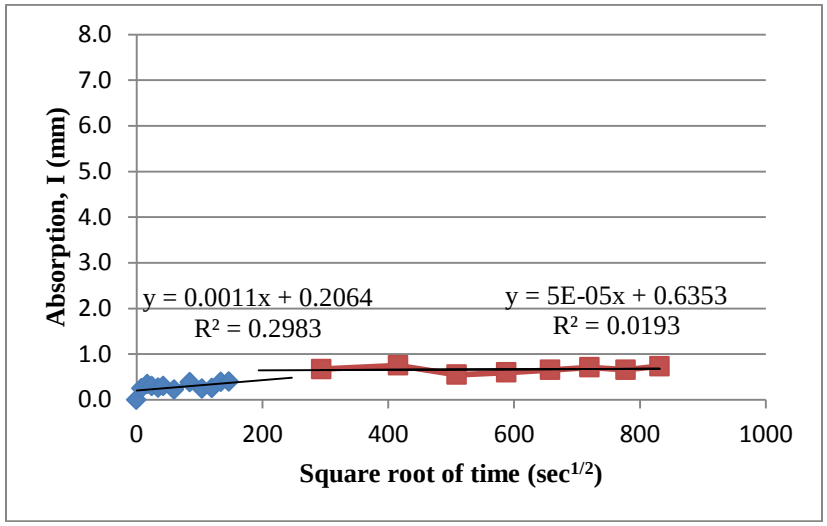

Figure G-42: Results of ponding test (per Bentz et al. 2002) for specimen prepared from bridge deck 3N, core C-8.

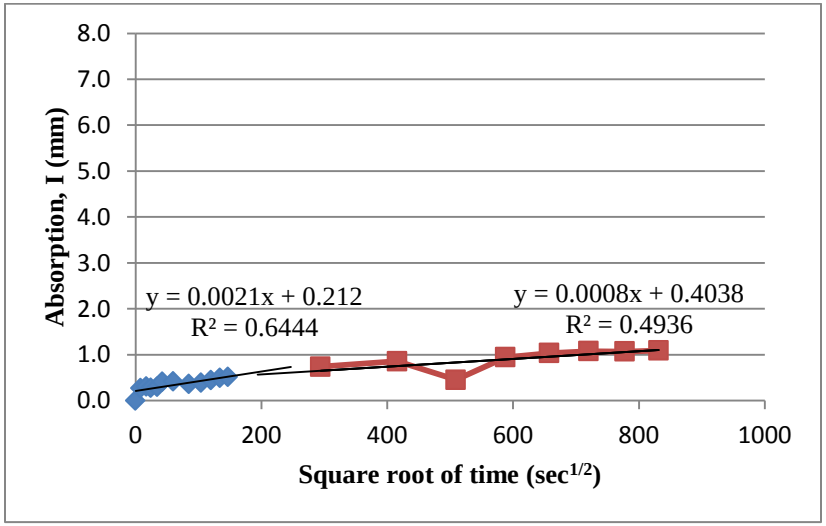

Figure G-43: Results of ponding test (per Bentz et al. 2002) for specimen prepared from bridge deck 3L, core C-1.

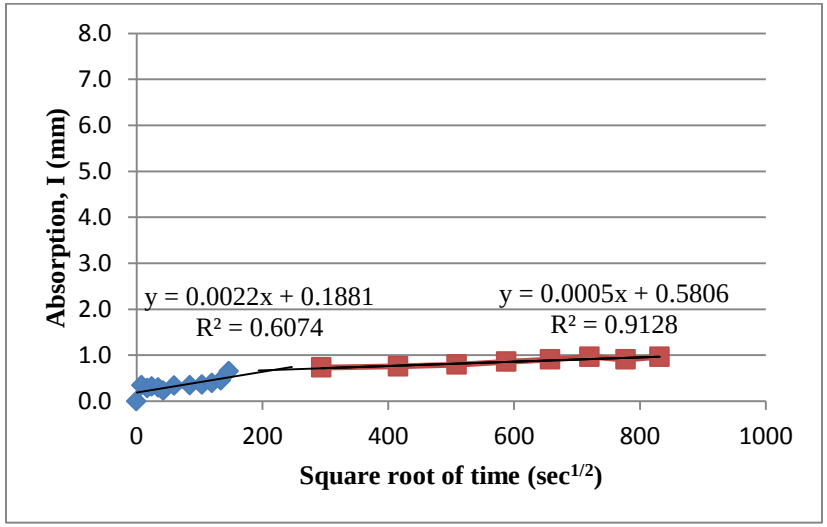

Figure G-44: Results of ponding test (per Bentz et al. 2002) for specimen prepared from bridge deck 3L, core C-3.

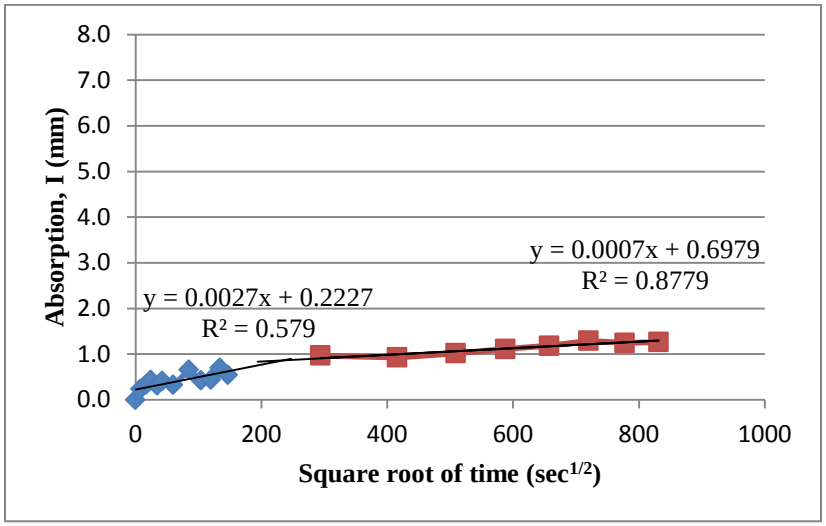

Figure G-45: Results of ponding test (per Bentz et al. 2002) for specimen prepared from bridge deck 5N, core C-5.

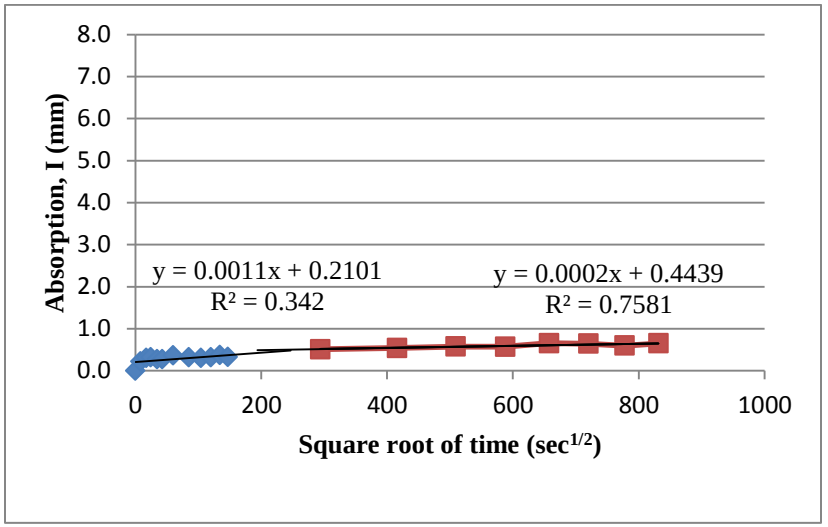

Figure G-46: Results of ponding test (per Bentz et al. 2002) for specimen prepared from bridge deck 5N, core C-7.

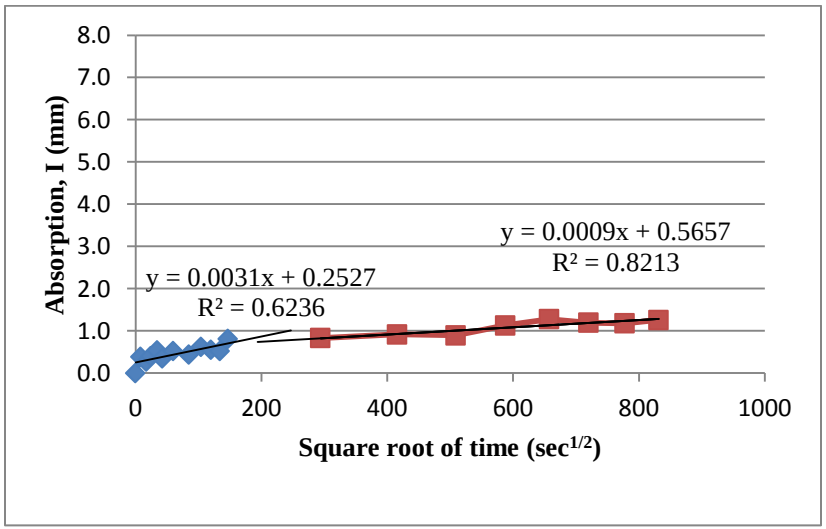

Figure G-47: Results of ponding test (per Bentz et al. 2002) for specimen prepared from bridge deck 5L, core C-3.

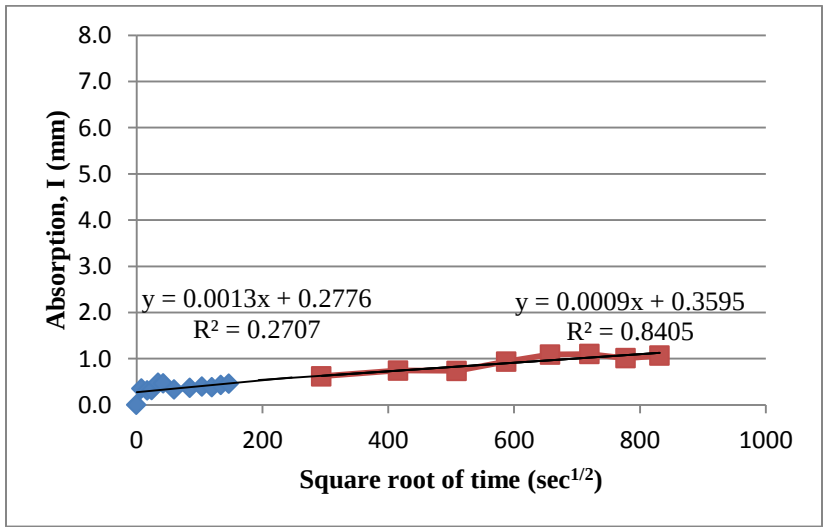

Figure G-48: Results of ponding test (per Bentz et al. 2002) for specimen prepared from bridge deck 5L, core C-6.

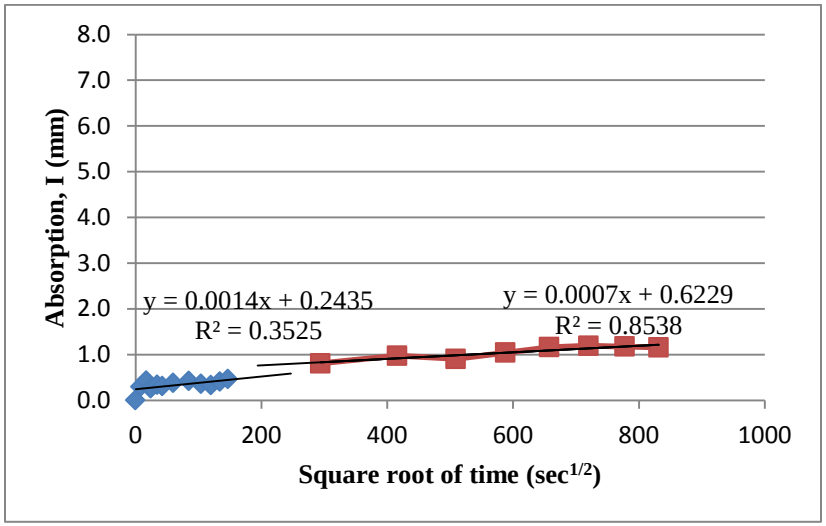

Figure G-49: Results of ponding test (per Bentz et al. 2002) for specimen prepared from bridge deck 6N, core C-4A.

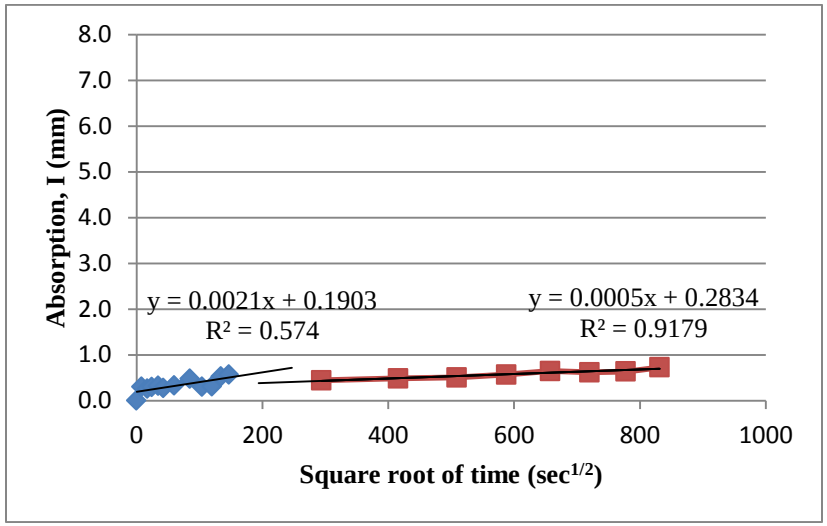

Figure G-50: Results of ponding test (per Bentz et al. 2002) for specimen prepared from bridge deck 6N, core C-6A.

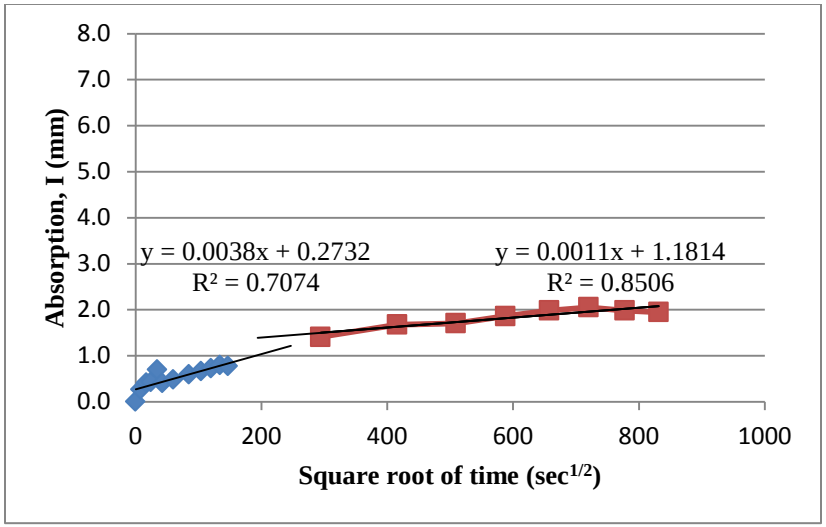

Figure G-51: Results of ponding test (per Bentz et al. 2002) for specimen prepared from bridge deck 6L, core C-5.

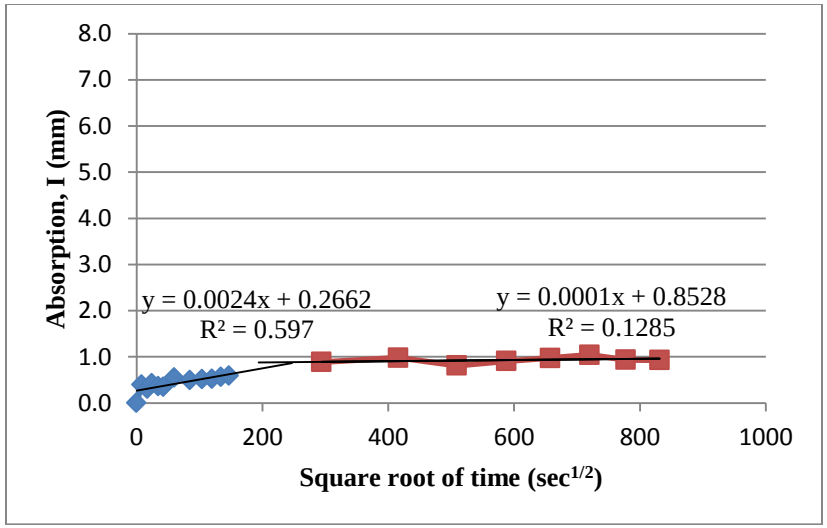

Figure G-52: Results of ponding test (per Bentz et al. 2002) for specimen prepared from bridge deck 6L, core C-8.

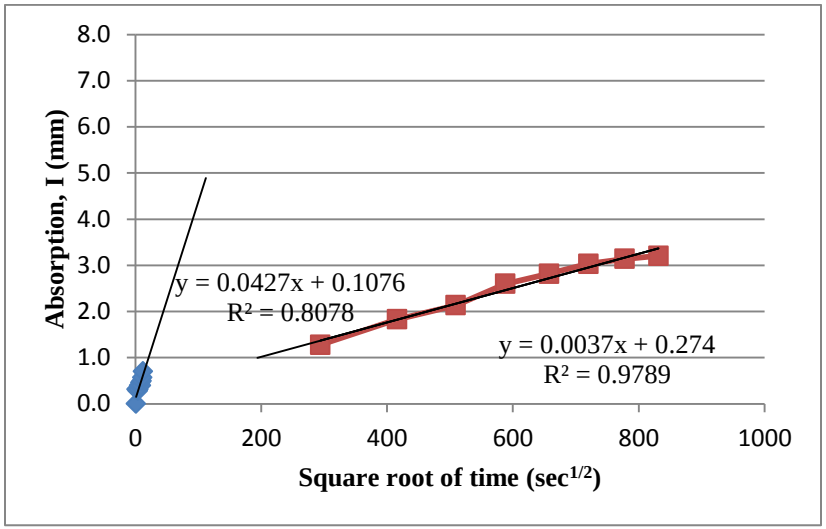

Figure G-53: Results of ponding test (per Bentz et al. 2002) for specimen prepared from bridge deck 7N, core C-2.

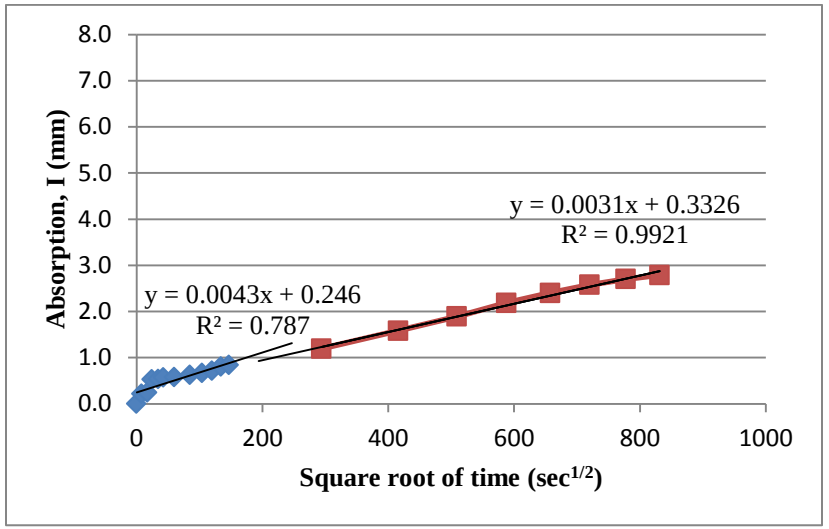

Figure G-54: Results of ponding test (per Bentz et al. 2002) for specimen prepared from bridge deck 7N, core C-7.

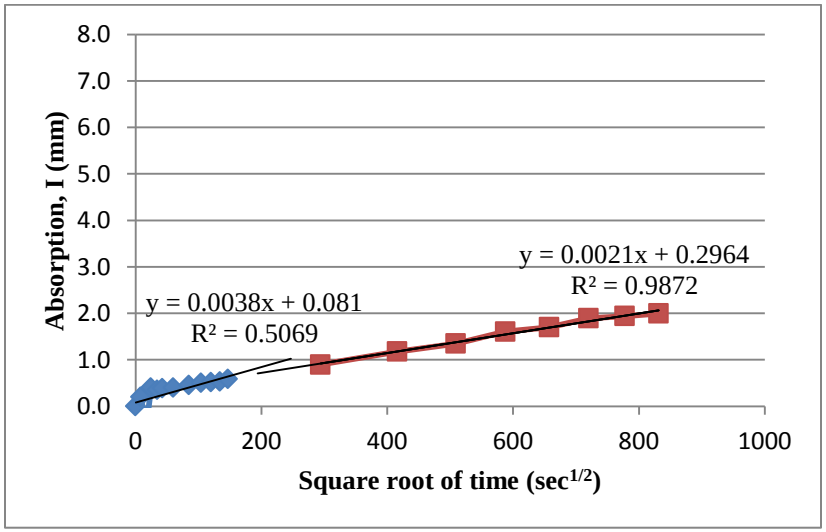

Figure G-55: Results of ponding test (per Bentz et al. 2002) for specimen prepared from bridge deck 7L, core C-3.

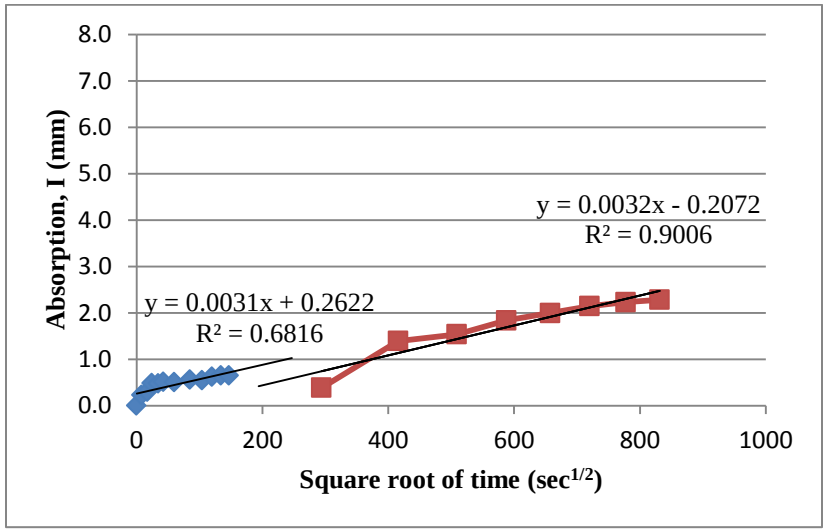

Figure G-56: Results of ponding test (per Bentz et al. 2002) for specimen prepared from bridge deck 7L, core C-6.

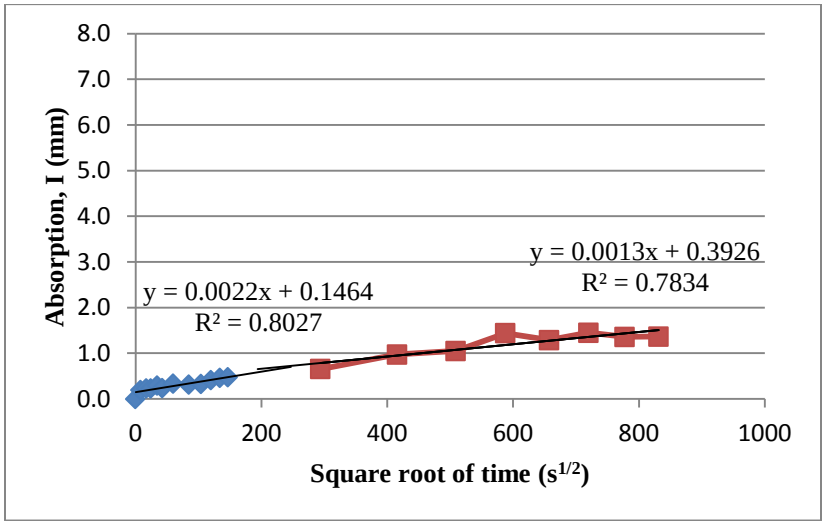

Figure G-57: Results of ponding test (per Bentz et al. 2002) for specimen prepared from bridge deck 8N, core C-4.

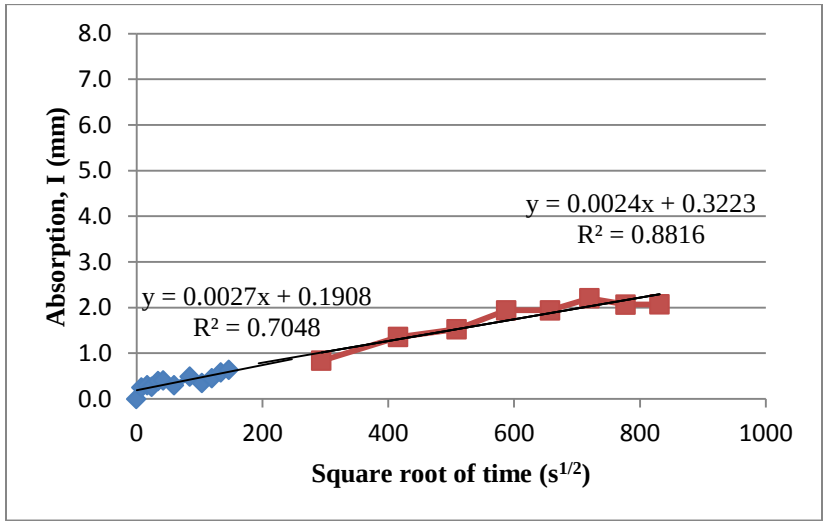

Figure G-58: Results of ponding test (per Bentz et al. 2002) for specimen prepared from bridge deck 8N, core C-6.

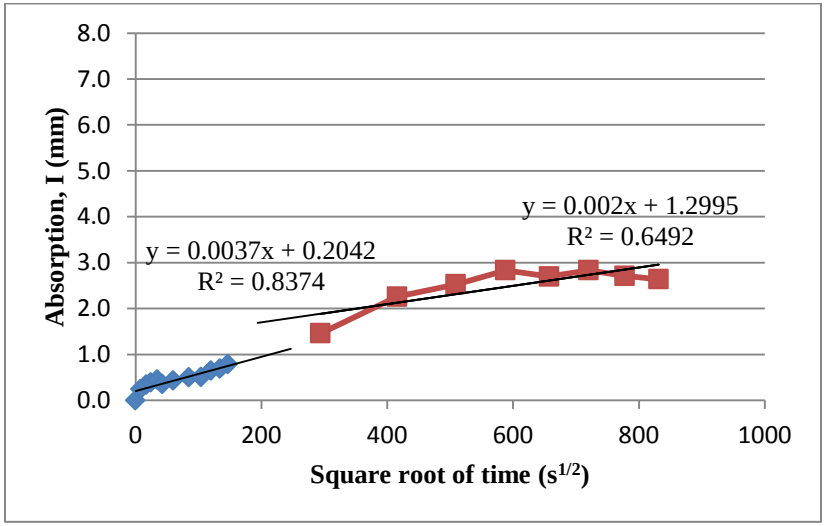

Figure G-59: Results of ponding test (per Bentz et al. 2002) for specimen prepared from bridge deck 8L, core C-3.

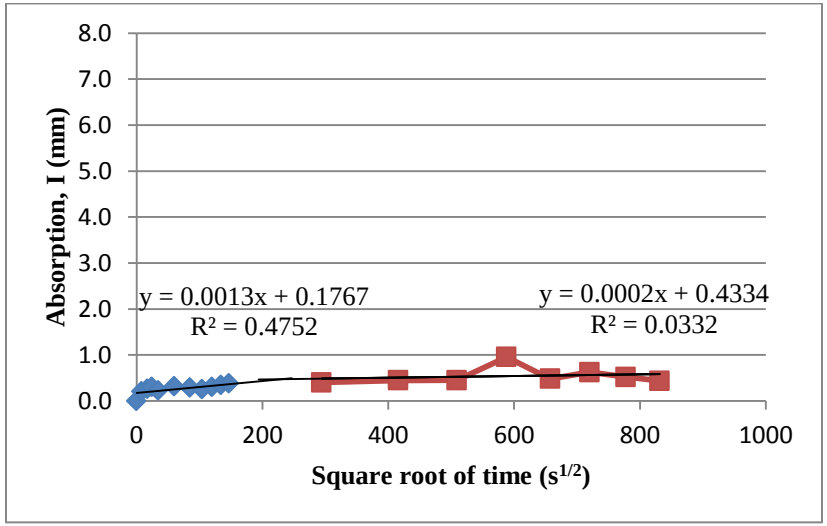

Figure G-60: Results of ponding test (per Bentz et al. 2002) for specimen prepared from bridge deck 8L, core C-7.

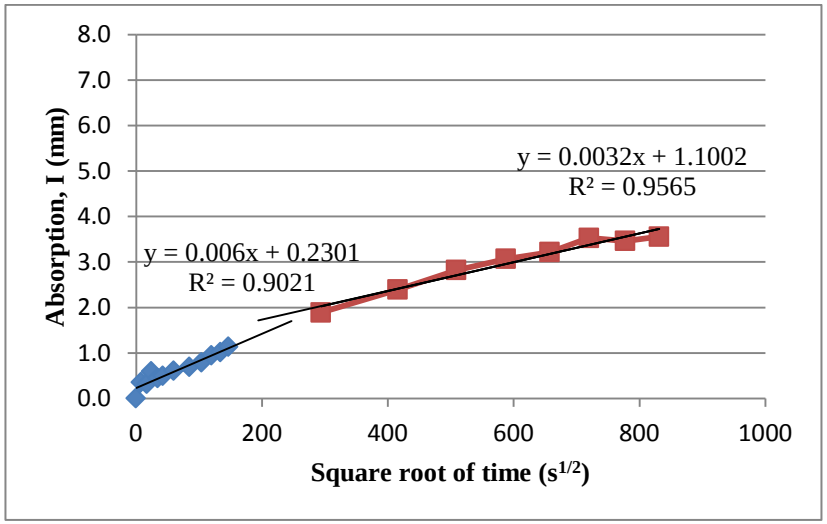

Figure G-61: Results of ponding test (per Bentz et al. 2002) for specimen prepared from bridge deck 9N, core C-1.

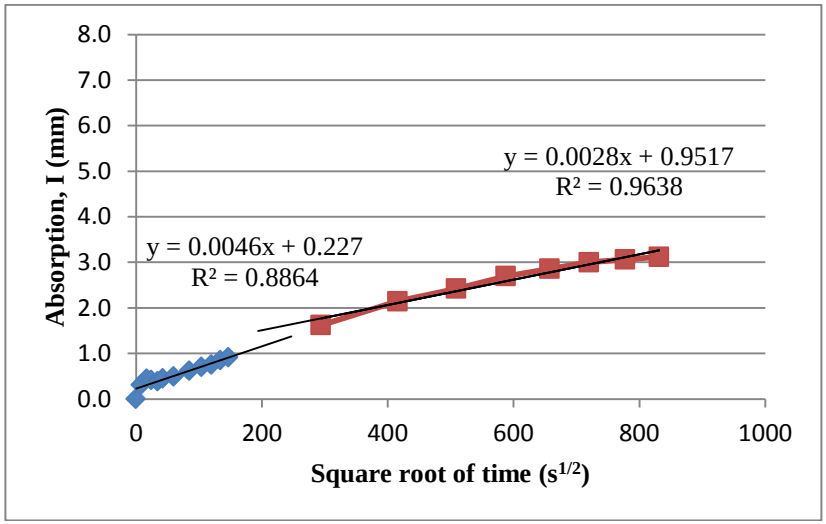

Figure G-62: Results of ponding test (per Bentz et al. 2002) for specimen prepared from bridge deck 9N, core C-2.

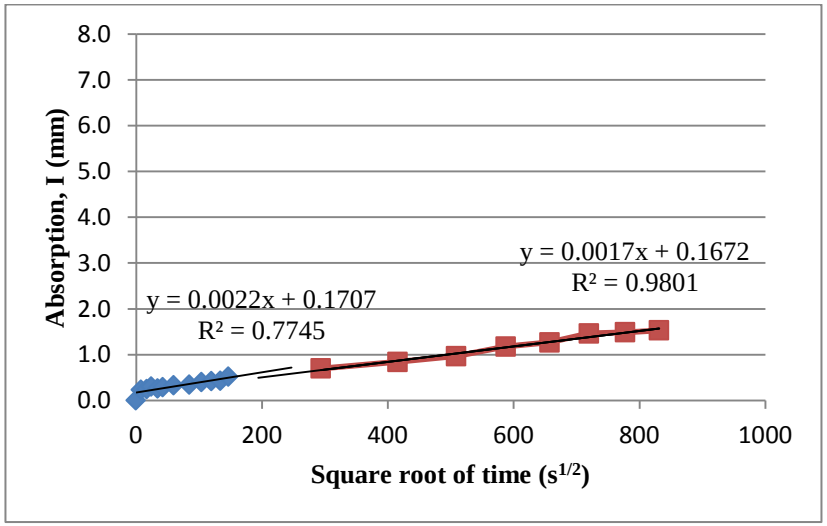

Figure G-63: Results of ponding test (per Bentz et al. 2002) for specimen prepared from bridge deck 9L, core C-1.

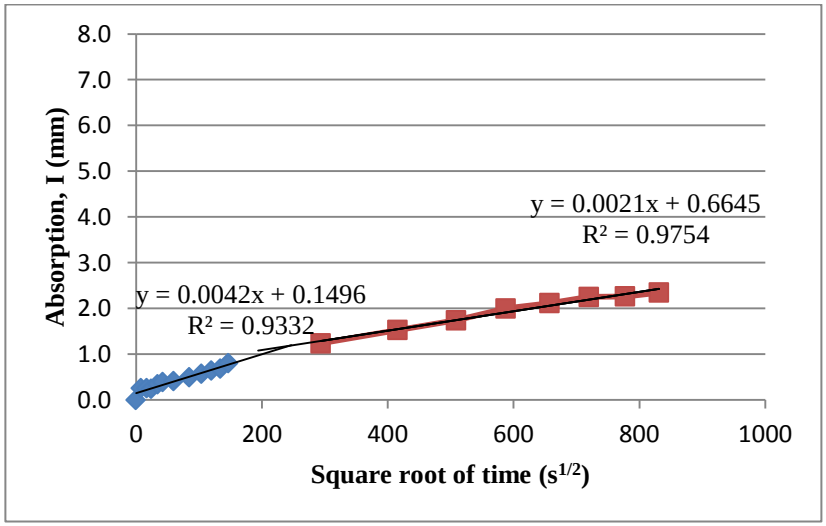

Figure G-64: Results of ponding test (per Bentz et al. 2002) for specimen prepared from bridge deck 9L, core C-2

APPENDIX H

Rapid Chloride Test (RCT) Data and Results

Table H-1: Summary RCT test results for bridge deck 1N.

Bridge ID: **070160 1N**
Test Date: **6/28/2011**

Test ID	Depth (in)	Reading (mV)	Cl %	Cl Content (pcy)
C-1-1	1	114.2	0.53%	0.2015
C-2-1	1	99.6	0.96%	0.3657
C-3-1	1	125.6	0.34%	0.1292
C-4-1	1	113.0	0.56%	0.2139
C-5-1	1	99.1	0.98%	0.3730
C-6-1	1	97.0	1.06%	0.4057
C-7-1	1	103.0	0.84%	0.3192
C-8-1	1	117.2	0.47%	0.1809
C-1-2	2	130.4	0.28%	0.1067
C-2-2	2	123.8	0.36%	0.1389
C-3-2	2	130.0	0.28%	0.1084
C-4-2	2	123.9	0.36%	0.1383
C-5-2	2	128.6	0.30%	0.1146
C-6-2	2	85.9	1.66%	0.6325
C-7-2	2	132.2	0.26%	0.0993
C-8-2	2	128.9	0.30%	0.1133
C-1-3	3	132.6	0.26%	0.0977
C-2-3	3	131.0	0.27%	0.1041
C-3-3	3	129.8	0.29%	0.1093
C-4-3	3	128.8	0.30%	0.1137
C-5-3	3	129.8	0.29%	0.1093
C-6-3	3	123.4	0.37%	0.1411
C-7-3	3	132.6	0.26%	0.0977
C-8-3	3	115.0	0.52%	0.1975
C-1-4	4	131.2	0.27%	0.1033
C-2-4	4	118.1	0.46%	0.1745
C-3-4	4	124.8	0.35%	0.1334
C-4-4	4	132.8	0.25%	0.0969
C-5-4	4	130.0	0.28%	0.1084
C-6-4	4	130.0	0.28%	0.1084
C-7-4	4	130.0	0.28%	0.1084
C-8-4	4	133.5	0.25%	0.0942
C-1-5	5	132.2	0.26%	0.0993
C-2-5	5	132.5	0.26%	0.0981
C-3-5	5	128.9	0.30%	0.1133
C-4-5	5	130.9	0.27%	0.1046
C-5-5	5	130.1	0.28%	0.1080
C-6-5	5	130.1	0.28%	0.1080
C-7-5	5	132.0	0.26%	0.1001
C-8-5	5	125.0	0.35%	0.1324

Table H-2: RCT test results by location for bridge deck 1N.

Bridge ID: 070160 1N

Location C-1	
Test ID	**Cl Content (lb/cy)**
C-1-1	0.2015
C-1-2	0.1067
C-1-3	0.0977
C-1-4	0.1033
C-1-5	0.0993

Location C-2	
Test ID	**Cl Content (lb/cy)**
C-2-1	0.3657
C-2-2	0.1389
C-2-3	0.1041
C-2-4	0.1745
C-2-5	0.0981

Location C-3	
Test ID	**Cl Content (lb/cy)**
C-3-1	0.1292
C-3-2	0.1084
C-3-3	0.1093
C-3-4	0.1334
C-3-5	0.1133

Location C-4	
Test ID	**Cl Content (lb/cy)**
C-4-1	0.2139
C-4-2	0.1383
C-4-3	0.1137
C-4-4	0.0969
C-4-5	0.1046

Location C-5	
Test ID	**Cl Content (lb/cy)**
C-5-1	0.3730
C-5-2	0.1146
C-5-3	0.1093
C-5-4	0.1084
C-5-5	0.1080

Location C-6	
Test ID	**Cl Content (lb/cy)**
C-6-1	0.4057
C-6-2	0.6325
C-6-3	0.1411
C-6-4	0.1084
C-6-5	0.1080

Location C-7	
Test ID	**Cl Content (lb/cy)**
C-7-1	0.3192
C-7-2	0.0993
C-7-3	0.0977
C-7-4	0.1084
C-7-5	0.1001

Location C-8	
Test ID	**Cl Content (lb/cy)**
C-8-1	0.1809
C-8-2	0.1133
C-8-3	0.1975
C-8-4	0.0942
C-8-5	0.1324

Table H-3: Summary RCT test results for bridge deck 1L.

Bridge ID: **070038 1L**

Test Date: **6/22/2011**

Test ID	Depth (in)	Reading (mV)	Cl %	Cl Content (pcy)
C-1-1	1	124.6	0.35%	0.1345
C-2-1	1	93.4	1.23%	0.4686
C-3-1	1	96.4	1.09%	0.4156
C-4-1	1	115.7	0.50%	0.1920
C-5-1	1	104.4	0.79%	0.3018
C-6-1	1	67.1	3.52%	1.3417
C-7-1	1	86.0	1.65%	0.6300
C-8-1	1	90.6	1.37%	0.5241
C-1-2	2	126.8	0.32%	0.1232
C-2-2	2	127.3	0.32%	0.1207
C-3-2	2	121.9	0.39%	0.1499
C-4-2	2	124.8	0.35%	0.1334
C-5-2	2	127.0	0.32%	0.1222
C-6-2	2	112.0	0.58%	0.2227
C-7-2	2	121.4	0.40%	0.1529
C-8-2	2	123.1	0.37%	0.1428
C-1-3	3	127.0	0.32%	0.1222
C-2-3	3	127.8	0.31%	0.1184
C-3-3	3	127.1	0.32%	0.1217
C-4-3	3	123.0	0.38%	0.1434
C-5-3	3	127.6	0.31%	0.1193
C-6-3	3	122.8	0.38%	0.1446
C-7-3	3	122.4	0.39%	0.1469
C-8-3	3	119.6	0.43%	0.1643
C-1-4	4	125.3	0.34%	0.1308
C-2-4	4	124.2	0.36%	0.1367
C-3-4	4	127.1	0.32%	0.1217
C-4-4	4	125.8	0.34%	0.1282
C-5-4	4	127.2	0.32%	0.1212
C-6-4	4	122.2	0.39%	0.1481
C-7-4	4	123.0	0.38%	0.1434
C-8-4	4	122.1	0.39%	0.1487
C-1-5	5	123.7	0.37%	0.1394
C-2-5	5	122.2	0.39%	0.1481
C-3-5	5	125.3	0.34%	0.1308
C-4-5	5	123.5	0.37%	0.1406
C-5-5	5	122.7	0.38%	0.1451
C-6-5	5	121.3	0.40%	0.1535
C-7-5	5	124.0	0.36%	0.1378
C-8-5	5	120.2	0.42%	0.1604

Table H-4: RCT test results by location for bridge deck 1L.

Bridge ID: 070038 1L

Location C-1	
Test ID	**Cl Content (lb/cy)**
C-1-1	0.1345
C-1-2	0.1232
C-1-3	0.1222
C-1-4	0.1308
C-1-5	0.1394

Location C-2	
Test ID	**Cl Content (lb/cy)**
C-2-1	0.4686
C-2-2	0.1207
C-2-3	0.1184
C-2-4	0.1367
C-2-5	0.1481

Location C-3	
Test ID	**Cl Content (lb/cy)**
C-3-1	0.4156
C-3-2	0.1499
C-3-3	0.1217
C-3-4	0.1217
C-3-5	0.1308

Location C-4	
Test ID	**Cl Content (lb/cy)**
C-4-1	0.1920
C-4-2	0.1334
C-4-3	0.1434
C-4-4	0.1282
C-4-5	0.1406

Location C-5	
Test ID	**Cl Content (lb/cy)**
C-5-1	0.3018
C-5-2	0.1222
C-5-3	0.1193
C-5-4	0.1212
C-5-5	0.1451

Location C-6	
Test ID	**Cl Content (lb/cy)**
C-6-1	1.3417
C-6-2	0.2227
C-6-3	0.1446
C-6-4	0.1481
C-6-5	0.1535

Location C-7	
Test ID	**Cl Content (lb/cy)**
C-7-1	0.6300
C-7-2	0.1529
C-7-3	0.1469
C-7-4	0.1434
C-7-5	0.1378

Location C-8	
Test ID	**Cl Content (lb/cy)**
C-8-1	0.5241
C-8-2	0.1428
C-8-3	0.1643
C-8-4	0.1487
C-8-5	0.1604

Table H-5: Summary RCT test results for bridge deck 2N.

Bridge ID: **150012 2N**

Test Date: **6/30/2011**

Test ID	Depth (in)	Reading (mV)	Cl %	Cl Content (pcy)
C-1-1	1	57.6	5.33%	2.0343
C-2-1	1	55.7	5.75%	2.1950
C-3-1	1	60.1	4.83%	1.8407
C-4-1	1	64.7	4.01%	1.5314
C-5-1	1	61.7	4.53%	1.7266
C-6-1	1	51.2	6.89%	2.6279
C-7-1	1	60.7	4.71%	1.7971
C-8-1	1	64.4	4.06%	1.5499
C-1-2	2	79.5	2.22%	0.8472
C-2-2	2	83.8	1.87%	0.7133
C-3-2	2	79.7	2.20%	0.8404
C-4-2	2	87.0	1.65%	0.6276
C-5-2	2	97.0	1.10%	0.4207
C-6-2	2	78.1	2.35%	0.8960
C-7-2	2	84.3	1.83%	0.6992
C-8-2	2	89.4	1.49%	0.5702
C-1-3	3	116.1	0.51%	0.1960
C-2-3	3	121.4	0.42%	0.1585
C-3-3	3	129.5	0.30%	0.1147
C-4-3	3	125.7	0.35%	0.1335
C-5-3	3	137.8	0.22%	0.0823
C-6-3	3	110.4	0.65%	0.2461
C-7-3	3	116.6	0.50%	0.1921
C-8-3	3	129.4	0.30%	0.1151
C-1-4	4	131.8	0.27%	0.1046
C-2-4	4	135.2	0.24%	0.0913
C-3-4	4	135.1	0.24%	0.0916
C-4-4	4	134.4	0.25%	0.0942
C-5-4	4	135.3	0.24%	0.0909
C-6-4	4	131.0	0.28%	0.1080
C-7-4	4	131.5	0.28%	0.1058
C-8-4	4	130.4	0.29%	0.1106
C-1-5	5	135.6	0.24%	0.0898
C-2-5	5	138.0	0.21%	0.0816
C-3-5	5	133.9	0.25%	0.0962
C-4-5	5	126.1	0.34%	0.1314
C-5-5	5	139.7	0.20%	0.0762
C-6-5	5	134.5	0.25%	0.0939
C-7-5	5	127.4	0.33%	0.1247
C-8-5	5	128.6	0.31%	0.1189

Table H-6: RCT test results by location for bridge deck 2N.

Bridge ID: 150012 2N

Location C-1	
Test ID	**Cl Content (lb/cy)**
C-1-1	2.0343
C-1-2	0.8472
C-1-3	0.1960
C-1-4	0.1046
C-1-5	0.0898

Location C-2	
Test ID	**Cl Content (lb/cy)**
C-2-1	2.1950
C-2-2	0.7133
C-2-3	0.1585
C-2-4	0.0913
C-2-5	0.0816

Location C-3	
Test ID	**Cl Content (lb/cy)**
C-3-1	1.8407
C-3-2	0.8404
C-3-3	0.1147
C-3-4	0.0916
C-3-5	0.0962

Location C-4	
Test ID	**Cl Content (lb/cy)**
C-4-1	1.5314
C-4-2	0.6276
C-4-3	0.1335
C-4-4	0.0942
C-4-5	0.1314

Location C-5	
Test ID	**Cl Content (lb/cy)**
C-5-1	1.7266
C-5-2	0.4207
C-5-3	0.0823
C-5-4	0.0909
C-5-5	0.0762

Location C-6	
Test ID	**Cl Content (lb/cy)**
C-6-1	2.6279
C-6-2	0.8960
C-6-3	0.2461
C-6-4	0.1080
C-6-5	0.0939

Location C-7	
Test ID	**Cl Content (lb/cy)**
C-7-1	1.7971
C-7-2	0.6992
C-7-3	0.1921
C-7-4	0.1058
C-7-5	0.1247

Location C-8	
Test ID	**Cl Content (lb/cy)**
C-8-1	1.5499
C-8-2	0.5702
C-8-3	0.1151
C-8-4	0.1106
C-8-5	0.1189

Table H-7: Summary RCT test results for bridge deck 2L.

Bridge ID: **150012 2L**

Test Date: **6/29/2011**

Test ID	Depth (in)	Reading (mV)	Cl %	Cl Content (pcy)
C-1-1	1	66.4	3.60%	1.2416
C-2-1	1	69.5	3.18%	1.0968
C-3-1	1	81.6	1.96%	0.6760
C-4-1	1	76.9	2.37%	0.8158
C-5-1	1	69.4	3.20%	1.1012
C-6-1	1	59.3	4.79%	1.6493
C-7-1	1	69.1	3.23%	1.1145
C-8-1	1	70.8	3.02%	1.0412
C-1-2	2	129.9	0.28%	0.0979
C-2-2	2	113.2	0.55%	0.1910
C-3-2	2	142.2	0.17%	0.0599
C-4-2	2	114.0	0.54%	0.1850
C-5-2	2	135.1	0.23%	0.0795
C-6-2	2	118.5	0.45%	0.1545
C-7-2	2	142.8	0.17%	0.0584
C-8-2	2	135.0	0.23%	0.0798
C-1-3	3	137.4	0.21%	0.0725
C-2-3	3	142.6	0.17%	0.0589
C-3-3	3	138.8	0.20%	0.0686
C-4-3	3	136.0	0.22%	0.0767
C-5-3	3	140.2	0.19%	0.0649
C-6-3	3	141.7	0.18%	0.0611
C-7-3	3	147.6	0.14%	0.0482
C-8-3	3	145.2	0.15%	0.0531
C-1-4	4	143.6	0.16%	0.0566
C-2-4	4	140.1	0.19%	0.0651
C-3-4	4	133.4	0.25%	0.0851
C-4-4	4	140.3	0.19%	0.0646
C-5-4	4	123.9	0.36%	0.1245
C-6-4	4	139.4	0.19%	0.0670
C-7-4	4	147.5	0.14%	0.0484
C-8-4	4	143.4	0.17%	0.0571
C-1-5	5	135.5	0.23%	0.0783
C-2-5	5	141.9	0.18%	0.0606
C-3-5	5	143.5	0.16%	0.0568
C-4-5	5	143.2	0.17%	0.0575
C-5-5	5	136.7	0.22%	0.0746
C-6-5	5	142.1	0.17%	0.0601
C-7-5	5	123.7	0.36%	0.1255
C-8-5	5	142.7	0.17%	0.0587

Table H-8: RCT test results by location for bridge deck 2L.

Bridge ID: 150012 2L

Location C-1	
Test ID	**Cl Content (lb/cy)**
C-1-1	1.2416
C-1-2	0.0979
C-1-3	0.0725
C-1-4	0.0566
C-1-5	0.0783

Location C-2	
Test ID	**Cl Content (lb/cy)**
C-2-1	1.0968
C-2-2	0.1910
C-2-3	0.0589
C-2-4	0.0651
C-2-5	0.0606

Location C-3	
Test ID	**Cl Content (lb/cy)**
C-3-1	0.6760
C-3-2	0.0599
C-3-3	0.0686
C-3-4	0.0851
C-3-5	0.0568

Location C-4	
Test ID	**Cl Content (lb/cy)**
C-4-1	0.8158
C-4-2	0.1850
C-4-3	0.0767
C-4-4	0.0646
C-4-5	0.0575

Location C-5	
Test ID	**Cl Content (lb/cy)**
C-5-1	1.1012
C-5-2	0.0795
C-5-3	0.0649
C-5-4	0.1245
C-5-5	0.0746

Location C-6	
Test ID	**Cl Content (lb/cy)**
C-6-1	1.6493
C-6-2	0.1545
C-6-3	0.0611
C-6-4	0.0670
C-6-5	0.0601

Location C-7	
Test ID	**Cl Content (lb/cy)**
C-7-1	1.1145
C-7-2	0.0584
C-7-3	0.0482
C-7-4	0.0484
C-7-5	0.1255

Location C-8	
Test ID	**Cl Content (lb/cy)**
C-8-1	1.0412
C-8-2	0.0798
C-8-3	0.0531
C-8-4	0.0571
C-8-5	0.0587

Table H-9: Summary RCT test results for bridge deck 3N.

Bridge ID: **150014 3N**

Test Date: **6/31/2011**

Test ID	Depth (in)	Reading (mV)	Cl %	Cl Content (pcy)
C-1-1	1	110.5	0.65%	0.2498
C-2-1	1	109.0	0.70%	0.2652
C-3-1	1	119.9	0.45%	0.1715
C-4-1	1	108.8	0.70%	0.2673
C-5-1	1	106.4	0.77%	0.2943
C-6-1	1	132.0	0.28%	0.1057
C-7-1	1	114.2	0.56%	0.2154
C-8-1	1	102.6	0.90%	0.3426
C-1-2	2	141.6	0.19%	0.0720
C-2-2	2	140.1	0.20%	0.0764
C-3-2	2	133.9	0.26%	0.0980
C-4-2	2	146.1	0.16%	0.0601
C-5-2	2	144.5	0.17%	0.0641
C-6-2	2	147.0	0.15%	0.0580
C-7-2	2	141.2	0.19%	0.0731
C-8-2	2	145.0	0.16%	0.0628
C-1-3	3	144.6	0.17%	0.0638
C-2-3	3	146.1	0.16%	0.0601
C-3-3	3	142.6	0.18%	0.0692
C-4-3	3	143.5	0.17%	0.0667
C-5-3	3	144.6	0.17%	0.0638
C-6-3	3	137.2	0.23%	0.0858
C-7-3	3	140.8	0.19%	0.0743
C-8-3	3	145.2	0.16%	0.0623
C-1-4	4	127.2	0.34%	0.1281
C-2-4	4	145.7	0.16%	0.0611
C-3-4	4	142.7	0.18%	0.0689
C-4-4	4	144.2	0.17%	0.0649
C-5-4	4	144.6	0.17%	0.0638
C-6-4	4	141.6	0.19%	0.0720
C-7-4	4	143.4	0.18%	0.0670
C-8-4	4	142.2	0.18%	0.0703
C-1-5	5	146.6	0.15%	0.0589
C-2-5	5	146.9	0.15%	0.0582
C-3-5	5	143.7	0.17%	0.0662
C-4-5	5	147.4	0.15%	0.0571
C-5-5	5	144.6	0.17%	0.0638
C-6-5	5	145.6	0.16%	0.0613
C-7-5	5	144.8	0.17%	0.0633
C-8-5	5	142.0	0.19%	0.0708

Table H-10: RCT test results by location for bridge deck 3N.

Bridge ID: 150014 3N

Location C-1	
Test ID	**Cl Content (lb/cy)**
C-1-1	0.2498
C-1-2	0.0720
C-1-3	0.0638
C-1-4	0.1281
C-1-5	0.0589

Location C-2	
Test ID	**Cl Content (lb/cy)**
C-2-1	0.2652
C-2-2	0.0764
C-2-3	0.0601
C-2-4	0.0611
C-2-5	0.0582

Location C-3	
Test ID	**Cl Content (lb/cy)**
C-3-1	0.1715
C-3-2	0.0980
C-3-3	0.0692
C-3-4	0.0689
C-3-5	0.0662

Location C-4	
Test ID	**Cl Content (lb/cy)**
C-4-1	0.2673
C-4-2	0.0601
C-4-3	0.0667
C-4-4	0.0649
C-4-5	0.0571

Location C-5	
Test ID	**Cl Content (lb/cy)**
C-5-1	0.2943
C-5-2	0.0641
C-5-3	0.0638
C-5-4	0.0638
C-5-5	0.0638

Location C-6	
Test ID	**Cl Content (lb/cy)**
C-6-1	0.1057
C-6-2	0.0580
C-6-3	0.0858
C-6-4	0.0720
C-6-5	0.0613

Location C-7	
Test ID	**Cl Content (lb/cy)**
C-7-1	0.2154
C-7-2	0.0731
C-7-3	0.0743
C-7-4	0.0670
C-7-5	0.0633

Location C-8	
Test ID	**Cl Content (lb/cy)**
C-8-1	0.3426
C-8-2	0.0628
C-8-3	0.0623
C-8-4	0.0703
C-8-5	0.0708

Table H-11: Summary RCT test results for bridge deck 3L.

Bridge ID: **150014 3L**

Test Date: **7/6/2011**

Test ID	Depth (in)	Reading (mV)	Cl %	Cl Content (pcy)
C-1-1	1	105.6	0.76%	0.2629
C-2-1	1	117.0	0.48%	0.1666
C-3-1	1	129.6	0.29%	0.1006
C-4-1	1	117.8	0.47%	0.1614
C-5-1	1	124.4	0.36%	0.1239
C-6-1	1	90.0	1.42%	0.4906
C-7-1	1	125.0	0.35%	0.1210
C-8-1	1	135.2	0.23%	0.0804
C-1-2	2	150.1	0.13%	0.0443
C-2-2	2	14807.0	0.00%	0.0000
C-3-2	2	149.3	0.13%	0.0458
C-4-2	2	143.2	0.17%	0.0584
C-5-2	2	144.8	0.16%	0.0548
C-6-2	2	150.4	0.13%	0.0438
C-7-2	2	148.6	0.14%	0.0471
C-8-2	2	148.4	0.14%	0.0474
C-1-3	3	153.2	0.11%	0.0392
C-2-3	3	150.1	0.13%	0.0443
C-3-3	3	149.2	0.13%	0.0460
C-4-3	3	143.6	0.17%	0.0575
C-5-3	3	146.8	0.15%	0.0506
C-6-3	3	149.4	0.13%	0.0456
C-7-3	3	150.2	0.13%	0.0442
C-8-3	3	148.4	0.14%	0.0474
C-1-4	4	154.5	0.11%	0.0372
C-2-4	4	150.5	0.13%	0.0436
C-3-4	4	151.6	0.12%	0.0417
C-4-4	4	146.8	0.15%	0.0506
C-5-4	4	148.4	0.14%	0.0474
C-6-4	4	133.8	0.25%	0.0851
C-7-4	4	147.0	0.15%	0.0502
C-8-4	4	151.8	0.12%	0.0414
C-1-5	5	152.9	0.11%	0.0396
C-2-5	5	150.6	0.13%	0.0434
C-3-5	5	150.0	0.13%	0.0445
C-4-5	5	147.3	0.14%	0.0496
C-5-5	5	150.2	0.13%	0.0442
C-6-5	5	140.8	0.19%	0.0643
C-7-5	5	150.6	0.13%	0.0434
C-8-5	5	147.8	0.14%	0.0486

Table H-12: RCT test results by location for bridge deck 3L.

Bridge ID: 150014 3L

Location C-1	
Test ID	**Cl Content (lb/cy)**
C-1-1	0.2629
C-1-2	0.0443
C-1-3	0.0392
C-1-4	0.0372
C-1-5	0.0396

Location C-2	
Test ID	**Cl Content (lb/cy)**
C-2-1	0.1666
C-2-2	0.0000
C-2-3	0.0443
C-2-4	0.0436
C-2-5	0.0434

Location C-3	
Test ID	**Cl Content (lb/cy)**
C-3-1	0.1006
C-3-2	0.0458
C-3-3	0.0460
C-3-4	0.0417
C-3-5	0.0445

Location C-4	
Test ID	**Cl Content (lb/cy)**
C-4-1	0.1614
C-4-2	0.0584
C-4-3	0.0575
C-4-4	0.0506
C-4-5	0.0496

Location C-5	
Test ID	**Cl Content (lb/cy)**
C-5-1	0.1239
C-5-2	0.0548
C-5-3	0.0506
C-5-4	0.0474
C-5-5	0.0442

Location C-6	
Test ID	**Cl Content (lb/cy)**
C-6-1	0.4906
C-6-2	0.0438
C-6-3	0.0456
C-6-4	0.0851
C-6-5	0.0643

Location C-7	
Test ID	**Cl Content (lb/cy)**
C-7-1	0.1210
C-7-2	0.0471
C-7-3	0.0442
C-7-4	0.0502
C-7-5	0.0434

Location C-8	
Test ID	**Cl Content (lb/cy)**
C-8-1	0.0804
C-8-2	0.0474
C-8-3	0.0474
C-8-4	0.0414
C-8-5	0.0486

Table H-13: Summary RCT test results for bridge deck 5N.

Bridge ID: **270012 5N**

Test Date: **7/12/2011**

Test ID	Depth (in)	Reading (mV)	Cl %	Cl Content (pcy)
C-1-1	1	127.2	0.33%	0.1255
C-2-1	1	66.8	3.68%	1.4054
C-3-1	1	103.0	0.87%	0.3303
C-4-1	1	99.2	1.01%	0.3845
C-5-1	1	96.0	1.15%	0.4370
C-6-1	1	90.2	1.44%	0.5512
C-7-1	1	88.4	1.55%	0.5923
C-8-1	1	100.2	0.97%	0.3695
C-1-2	2	140.6	0.19%	0.0734
C-2-2	2	131.2	0.28%	0.1069
C-3-2	2	139.2	0.20%	0.0776
C-4-2	2	121.6	0.41%	0.1570
C-5-2	2	140.4	0.19%	0.0740
C-6-2	2	136.8	0.22%	0.0855
C-7-2	2	134.8	0.24%	0.0926
C-8-2	2	134.8	0.24%	0.0926
C-1-3	3	138.4	0.21%	0.0802
C-2-3	3	138.8	0.21%	0.0789
C-3-3	3	137.8	0.22%	0.0821
C-4-3	3	132.4	0.27%	0.1019
C-5-3	3	133.8	0.25%	0.0964
C-6-3	3	138.2	0.21%	0.0808
C-7-3	3	138.6	0.21%	0.0795
C-8-3	3	139.0	0.21%	0.0783
C-1-4	4	140.2	0.20%	0.0746
C-2-4	4	137.0	0.22%	0.0848
C-3-4	4	140.8	0.19%	0.0728
C-4-4	4	138.2	0.21%	0.0808
C-5-4	4	135.6	0.24%	0.0897
C-6-4	4	139.4	0.20%	0.0770
C-7-4	4	140.4	0.19%	0.0740
C-8-4	4	139.2	0.20%	0.0776
C-1-5	5	138.8	0.21%	0.0789
C-2-5	5	116.8	0.50%	0.1902
C-3-5	5	138.2	0.21%	0.0808
C-4-5	5	133.2	0.26%	0.0987
C-5-5	5	129.8	0.30%	0.1131
C-6-5	5	128.6	0.31%	0.1186
C-7-5	5	129.6	0.30%	0.1140
C-8-5	5	137.8	0.22%	0.0821

Table H-14: RCT test results by location for bridge deck 5N.

Bridge ID: 270012 5N

Location C-1	
Test ID	**Cl Content (lb/cy)**
C-1-1	0.1255
C-1-2	0.0734
C-1-3	0.0802
C-1-4	0.0746
C-1-5	0.0789

Location C-2	
Test ID	**Cl Content (lb/cy)**
C-2-1	1.4054
C-2-2	0.1069
C-2-3	0.0789
C-2-4	0.0848
C-2-5	0.1902

Location C-3	
Test ID	**Cl Content (lb/cy)**
C-3-1	0.3303
C-3-2	0.0776
C-3-3	0.0821
C-3-4	0.0728
C-3-5	0.0808

Location C-4	
Test ID	**Cl Content (lb/cy)**
C-4-1	0.3845
C-4-2	0.1570
C-4-3	0.1019
C-4-4	0.0808
C-4-5	0.0987

Location C-5	
Test ID	**Cl Content (lb/cy)**
C-5-1	0.4370
C-5-2	0.0740
C-5-3	0.0964
C-5-4	0.0897
C-5-5	0.1131

Location C-6	
Test ID	**Cl Content (lb/cy)**
C-6-1	0.5512
C-6-2	0.0855
C-6-3	0.0808
C-6-4	0.0770
C-6-5	0.1186

Location C-7	
Test ID	**Cl Content (lb/cy)**
C-7-1	0.5923
C-7-2	0.0926
C-7-3	0.0795
C-7-4	0.0740
C-7-5	0.1140

Location C-8	
Test ID	**Cl Content (lb/cy)**
C-8-1	0.3695
C-8-2	0.0926
C-8-3	0.0783
C-8-4	0.0776
C-8-5	0.0821

Table H-15: Summary RCT test results for bridge deck 5L.

Bridge ID: **270012 5L**

Test Date: **7/12/2011**

Test ID	Depth (in)	Reading (mV)	Cl %	Cl Content (pcy)
C-1-1	1	56.4	5.58%	1.9244
C-2-1	1	91.2	1.39%	0.4784
C-3-1	1	99.4	1.00%	0.3446
C-4-1	1	111.6	0.61%	0.2115
C-5-1	1	104.2	0.83%	0.2844
C-6-1	1	57.2	5.41%	1.8638
C-7-1	1	102.0	0.90%	0.3106
C-8-1	1	89.2	1.50%	0.5182
C-1-2	2	139.0	0.21%	0.0707
C-2-2	2	139.4	0.20%	0.0696
C-3-2	2	138.0	0.21%	0.0736
C-4-2	2	143.8	0.17%	0.0583
C-5-2	2	143.2	0.17%	0.0598
C-6-2	2	108.4	0.70%	0.2404
C-7-2	2	142.2	0.18%	0.0622
C-8-2	2	140.2	0.20%	0.0674
C-1-3	3	142.4	0.18%	0.0617
C-2-3	3	139.6	0.20%	0.0690
C-3-3	3	142.0	0.18%	0.0627
C-4-3	3	145.8	0.16%	0.0539
C-5-3	3	139.4	0.20%	0.0696
C-6-3	3	139.2	0.20%	0.0701
C-7-3	3	143.6	0.17%	0.0588
C-8-3	3	142.4	0.18%	0.0617
C-1-4	4	142.6	0.18%	0.0612
C-2-4	4	143.6	0.17%	0.0588
C-3-4	4	143.8	0.17%	0.0583
C-4-4	4	142.0	0.18%	0.0627
C-5-4	4	146.4	0.15%	0.0526
C-6-4	4	140.8	0.19%	0.0658
C-7-4	4	145.8	0.16%	0.0539
C-8-4	4	143.0	0.17%	0.0602
C-1-5	5	142.8	0.18%	0.0607
C-2-5	5	142.0	0.18%	0.0627
C-3-5	5	144.6	0.16%	0.0565
C-4-5	5	143.0	0.17%	0.0602
C-5-5	5	144.2	0.17%	0.0574
C-6-5	5	144.8	0.16%	0.0561
C-7-5	5	144.6	0.16%	0.0565
C-8-5	5	145.2	0.16%	0.0552

Table H-16: RCT test results by location for bridge deck 5L.

Bridge ID: 270012 5L

Location C-1	
Test ID	**Cl Content (lb/cy)**
C-1-1	1.9244
C-1-2	0.0707
C-1-3	0.0617
C-1-4	0.0612
C-1-5	0.0607

Location C-2	
Test ID	**Cl Content (lb/cy)**
C-2-1	0.4784
C-2-2	0.0696
C-2-3	0.0690
C-2-4	0.0588
C-2-5	0.0627

Location C-3	
Test ID	**Cl Content (lb/cy)**
C-3-1	0.3446
C-3-2	0.0736
C-3-3	0.0627
C-3-4	0.0583
C-3-5	0.0565

Location C-4	
Test ID	**Cl Content (lb/cy)**
C-4-1	0.2115
C-4-2	0.0583
C-4-3	0.0539
C-4-4	0.0627
C-4-5	0.0602

Location C-5	
Test ID	**Cl Content (lb/cy)**
C-5-1	0.2844
C-5-2	0.0598
C-5-3	0.0696
C-5-4	0.0526
C-5-5	0.0574

Location C-6	
Test ID	**Cl Content (lb/cy)**
C-6-1	1.8638
C-6-2	0.2404
C-6-3	0.0701
C-6-4	0.0658
C-6-5	0.0561

Location C-7	
Test ID	**Cl Content (lb/cy)**
C-7-1	0.3106
C-7-2	0.0622
C-7-3	0.0588
C-7-4	0.0539
C-7-5	0.0565

Location C-8	
Test ID	**Cl Content (lb/cy)**
C-8-1	0.5182
C-8-2	0.0674
C-8-3	0.0617
C-8-4	0.0602
C-8-5	0.0552

Table H-17: Summary RCT test results for bridge deck 6N.

Bridge ID: **330345 6N**

Test Date: **7/13/2011**

Test ID	Depth (in)	Reading (mV)	Cl %	Cl Content (pcy)
C-1-1	1	129.8	0.30%	0.1135
C-2-1	1	58.6	5.13%	1.9582
C-3-1	1	84.4	1.83%	0.6977
C-4-1	1	68.6	3.44%	1.3126
C-5-1	1	95.0	1.20%	0.4566
C-6-1	1	67.2	3.64%	1.3882
C-7-1	1	49.0	7.54%	2.8750
C-8-1	1	89.4	1.50%	0.5712
C-1-2	2	86.0	1.72%	0.6544
C-2-2	2	85.0	1.79%	0.6812
C-3-2	2	131.8	0.27%	0.1048
C-4-2	2	109.2	0.68%	0.2587
C-5-2	2	129.0	0.31%	0.1172
C-6-2	2	119.2	0.45%	0.1734
C-7-2	2	117.8	0.48%	0.1834
C-8-2	2	101.6	0.92%	0.3507
C-1-3	3	137.2	0.22%	0.0844
C-2-3	3	127.2	0.33%	0.1259
C-3-3	3	125.6	0.35%	0.1343
C-4-3	3	126.8	0.34%	0.1280
C-5-3	3	130.6	0.29%	0.1099
C-6-3	3	124.8	0.36%	0.1386
C-7-3	3	133.6	0.26%	0.0975
C-8-3	3	134.2	0.25%	0.0952
C-1-4	4	137.0	0.22%	0.0851
C-2-4	4	132.6	0.27%	0.1015
C-3-4	4	132.2	0.27%	0.1031
C-4-4	4	119.4	0.45%	0.1721
C-5-4	4	133.2	0.26%	0.0991
C-6-4	4	131.8	0.27%	0.1048
C-7-4	4	131.8	0.27%	0.1048
C-8-4	4	140.2	0.20%	0.0749
C-1-5	5	133.0	0.26%	0.0999
C-2-5	5	123.8	0.38%	0.1443
C-3-5	5	131.8	0.27%	0.1048
C-4-5	5	129.8	0.30%	0.1135
C-5-5	5	135.6	0.24%	0.0900
C-6-5	5	133.0	0.26%	0.0999
C-7-5	5	132.6	0.27%	0.1015
C-8-5	5	127.8	0.32%	0.1230

Table H-18: RCT test results by location for bridge deck 6N.

Bridge ID: 330345 6N

Location C-1	
Test ID	**Cl Content (lb/cy)**
C-1-1	0.1135
C-1-2	0.6544
C-1-3	0.0844
C-1-4	0.0851
C-1-5	0.0999

Location C-2	
Test ID	**Cl Content (lb/cy)**
C-2-1	1.9582
C-2-2	0.6812
C-2-3	0.1259
C-2-4	0.1015
C-2-5	0.1443

Location C-3	
Test ID	**Cl Content (lb/cy)**
C-3-1	0.6977
C-3-2	0.1048
C-3-3	0.1343
C-3-4	0.1031
C-3-5	0.1048

Location C-4	
Test ID	**Cl Content (lb/cy)**
C-4-1	1.3126
C-4-2	0.2587
C-4-3	0.1280
C-4-4	0.1721
C-4-5	0.1135

Location C-5	
Test ID	**Cl Content (lb/cy)**
C-5-1	0.4566
C-5-2	0.1172
C-5-3	0.1099
C-5-4	0.0991
C-5-5	0.0900

Location C-6	
Test ID	**Cl Content (lb/cy)**
C-6-1	1.3882
C-6-2	0.1734
C-6-3	0.1386
C-6-4	0.1048
C-6-5	0.0999

Location C-7	
Test ID	**Cl Content (lb/cy)**
C-7-1	2.8750
C-7-2	0.1834
C-7-3	0.0975
C-7-4	0.1048
C-7-5	0.1015

Location C-8	
Test ID	**Cl Content (lb/cy)**
C-8-1	0.5712
C-8-2	0.3507
C-8-3	0.0952
C-8-4	0.0749
C-8-5	0.1230

Table H-19: Summary RCT test results for bridge deck 6L.

Bridge ID: **330254 6L**

Test Date: **7/14/2011**

Test ID	Depth (in)	Reading (mV)	Cl %	Cl Content (pcy)
C-1-1	1	59.6	4.97%	1.7123
C-2-1	1	39.2	11.24%	3.8722
C-3-1	1	38.0	11.79%	4.0626
C-4-1	1	42.6	9.81%	3.3798
C-5-1	1	36.0	12.77%	4.4009
C-6-1	1	43.2	9.57%	3.2997
C-7-1	1	29.4	16.63%	5.7306
C-8-1	1	39.6	11.06%	3.8107
C-1-2	2	93.2	1.30%	0.4466
C-2-2	2	62.0	4.51%	1.5555
C-3-2	2	61.8	4.55%	1.5680
C-4-2	2	84.4	1.84%	0.6350
C-5-2	2	61.6	4.59%	1.5806
C-6-2	2	87.2	1.65%	0.5677
C-7-2	2	61.4	4.62%	1.5933
C-8-2	2	69.0	3.41%	1.1756
C-1-3	3	116.0	0.52%	0.1794
C-2-3	3	105.2	0.80%	0.2763
C-3-3	3	97.0	1.11%	0.3836
C-4-3	3	119.6	0.45%	0.1553
C-5-3	3	97.4	1.10%	0.3775
C-6-3	3	120.2	0.44%	0.1516
C-7-3	3	101.6	0.93%	0.3191
C-8-3	3	104.2	0.83%	0.2876
C-1-4	4	119.6	0.45%	0.1553
C-2-4	4	117.6	0.49%	0.1683
C-3-4	4	120.6	0.43%	0.1492
C-4-4	4	119.8	0.45%	0.1541
C-5-4	4	121.6	0.42%	0.1434
C-6-4	4	119.4	0.45%	0.1566
C-7-4	4	121.8	0.41%	0.1422
C-8-4	4	120.8	0.43%	0.1481
C-1-5	5	120.2	0.44%	0.1516
C-2-5	5	120.4	0.44%	0.1504
C-3-5	5	116.8	0.50%	0.1737
C-4-5	5	120.4	0.44%	0.1504
C-5-5	5	124.8	0.37%	0.1262
C-6-5	5	118.2	0.48%	0.1643
C-7-5	5	118.0	0.48%	0.1656
C-8-5	5	116.6	0.51%	0.1751

Table H-20: RCT test results by location for bridge deck 6L.

Bridge ID: 330254 6L

Location C-1	
Test ID	**Cl Content (lb/cy)**
C-1-1	1.7123
C-1-2	0.4466
C-1-3	0.1794
C-1-4	0.1553
C-1-5	0.1516

Location C-2	
Test ID	**Cl Content (lb/cy)**
C-2-1	3.8722
C-2-2	1.5555
C-2-3	0.2763
C-2-4	0.1683
C-2-5	0.1504

Location C-3	
Test ID	**Cl Content (lb/cy)**
C-3-1	4.0626
C-3-2	1.5680
C-3-3	0.3836
C-3-4	0.1492
C-3-5	0.1737

Location C-4	
Test ID	**Cl Content (lb/cy)**
C-4-1	3.3798
C-4-2	0.6350
C-4-3	0.1553
C-4-4	0.1541
C-4-5	0.1504

Location C-5	
Test ID	**Cl Content (lb/cy)**
C-5-1	4.4009
C-5-2	1.5806
C-5-3	0.3775
C-5-4	0.1434
C-5-5	0.1262

Location C-6	
Test ID	**Cl Content (lb/cy)**
C-6-1	3.2997
C-6-2	0.5677
C-6-3	0.1516
C-6-4	0.1566
C-6-5	0.1643

Location C-7	
Test ID	**Cl Content (lb/cy)**
C-7-1	5.7306
C-7-2	1.5933
C-7-3	0.3191
C-7-4	0.1422
C-7-5	0.1656

Location C-8	
Test ID	**Cl Content (lb/cy)**
C-8-1	3.8107
C-8-2	1.1756
C-8-3	0.2876
C-8-4	0.1481
C-8-5	0.1751

Table H-21: Summary RCT test results for bridge deck 7N.

Bridge ID: **590541 7N**

Test Date: **7/15/2011**

Test ID	Depth (in)	Reading (mV)	Cl %	Cl Content (pcy)
C-1-1	1	61.4	4.49%	1.7147
C-2-1	1	58.0	5.15%	1.9645
C-3-1	1	59.2	4.91%	1.8725
C-4-1	1	61.4	4.49%	1.7147
C-5-1	1	65.0	3.89%	1.4848
C-6-1	1	53.6	6.14%	2.3426
C-7-1	1	52.4	6.44%	2.4578
C-8-1	1	51.2	6.76%	2.5786
C-1-2	2	76.2	2.49%	0.9486
C-2-2	2	73.2	2.80%	1.0696
C-3-2	2	70.2	3.16%	1.2059
C-4-2	2	80.8	2.07%	0.7892
C-5-2	2	76.2	2.49%	0.9486
C-6-2	2	63.8	4.08%	1.5578
C-7-2	2	69.2	3.29%	1.2552
C-8-2	2	61.2	4.53%	1.7285
C-1-3	3	96.2	1.12%	0.4262
C-2-3	3	87.2	1.60%	0.6110
C-3-3	3	80.9	2.06%	0.7860
C-4-3	3	100.6	0.94%	0.3575
C-5-3	3	87.2	1.60%	0.6110
C-6-3	3	73.8	2.74%	1.0442
C-7-3	3	85.0	1.75%	0.6672
C-8-3	3	72.4	2.89%	1.1044
C-1-4	4	119.6	0.44%	0.1672
C-2-4	4	108.4	0.69%	0.2617
C-3-4	4	100.4	0.94%	0.3603
C-4-4	4	107.6	0.71%	0.2702
C-5-4	4	99.4	0.98%	0.3750
C-6-4	4	84.4	1.79%	0.6834
C-7-4	4	108.0	0.70%	0.2659
C-8-4	4	86.0	1.68%	0.6410
C-1-5	5	121.8	0.40%	0.1531
C-2-5	5	113.2	0.57%	0.2159
C-3-5	5	116.6	0.49%	0.1885
C-4-5	5	118.4	0.46%	0.1754
C-5-5	5	115.8	0.51%	0.1946
C-6-5	5	94.4	1.20%	0.4581
C-7-5	5	108.4	0.69%	0.2617
C-8-5	5	108.4	0.69%	0.2617

Table H-22: RCT test results by location for bridge deck 7N.

Bridge ID: 590541 7N

Location C-1	
Test ID	**Cl Content (lb/cy)**
C-1-1	1.7147
C-1-2	0.9486
C-1-3	0.4262
C-1-4	0.1672
C-1-5	0.1531

Location C-2	
Test ID	**Cl Content (lb/cy)**
C-2-1	1.9645
C-2-2	1.0696
C-2-3	0.6110
C-2-4	0.2617
C-2-5	0.2159

Location C-3	
Test ID	**Cl Content (lb/cy)**
C-3-1	1.8725
C-3-2	1.2059
C-3-3	0.7860
C-3-4	0.3603
C-3-5	0.1885

Location C-4	
Test ID	**Cl Content (lb/cy)**
C-4-1	1.7147
C-4-2	0.7892
C-4-3	0.3575
C-4-4	0.2702
C-4-5	0.1754

Location C-5	
Test ID	**Cl Content (lb/cy)**
C-5-1	1.4848
C-5-2	0.9486
C-5-3	0.6110
C-5-4	0.3750
C-5-5	0.1946

Location C-6	
Test ID	**Cl Content (lb/cy)**
C-6-1	2.3426
C-6-2	1.5578
C-6-3	1.0442
C-6-4	0.6834
C-6-5	0.4581

Location C-7	
Test ID	**Cl Content (lb/cy)**
C-7-1	2.4578
C-7-2	1.2552
C-7-3	0.6672
C-7-4	0.2659
C-7-5	0.2617

Location C-8	
Test ID	**Cl Content (lb/cy)**
C-8-1	2.5786
C-8-2	1.7285
C-8-3	1.1044
C-8-4	0.6410
C-8-5	0.2617

Table H-23: Summary RCT test results for bridge deck 7L.

Bridge ID: **590363 7L**

Test Date: **7/19/2011**

Test ID	Depth (in)	Reading (mV)	Cl %	Cl Content (pcy)
C-1-1	1	50.4	7.19%	2.4785
C-2-1	1	59.6	4.98%	1.7154
C-3-1	1	51.2	6.97%	2.4005
C-4-1	1	48.0	7.92%	2.7283
C-5-1	1	96.6	1.13%	0.3905
C-6-1	1	51.0	7.02%	2.4198
C-7-1	1	49.4	7.49%	2.5797
C-8-1	1	55.8	5.79%	1.9971
C-1-2	2	56.4	5.66%	1.9497
C-2-2	2	106.4	0.77%	0.2639
C-3-2	2	61.6	4.60%	1.5836
C-4-2	2	75.8	2.60%	0.8973
C-5-2	2	130.0	0.30%	0.1027
C-6-2	2	71.8	3.06%	1.0530
C-7-2	2	66.2	3.82%	1.3174
C-8-2	2	68.6	3.47%	1.1968
C-1-3	3	58.2	5.26%	1.8142
C-2-3	3	97.8	1.08%	0.3722
C-3-3	3	82.6	1.98%	0.6836
C-4-3	3	114.2	0.56%	0.1931
C-5-3	3	130.2	0.30%	0.1018
C-6-3	3	99.4	1.01%	0.3491
C-7-3	3	59.4	5.02%	1.7292
C-8-3	3	107.8	0.72%	0.2495
C-1-4	4	100.8	0.96%	0.3301
C-2-4	4	124.6	0.37%	0.1274
C-3-4	4	71.8	3.06%	1.0530
C-4-4	4	125.2	0.36%	0.1244
C-5-4	4	132.2	0.27%	0.0940
C-6-4	4	78.6	2.33%	0.8023
C-7-4	4	92.2	1.35%	0.4656
C-8-4	4	119.2	0.46%	0.1581
C-1-5	5	97.4	1.10%	0.3782
C-2-5	5	110.2	0.66%	0.2267
C-3-5	5	115.2	0.54%	0.1856
C-4-5	5	126.8	0.34%	0.1167
C-5-5	5	122.6	0.40%	0.1380
C-6-5	5	111.6	0.62%	0.2143
C-7-5	5	97.2	1.11%	0.3812
C-8-5	5	116.8	0.51%	0.1741

Table H-24: RCT test results by location for bridge deck 7L.

Bridge ID: 590363 7L

Location C-1	
Test ID	**Cl Content (lb/cy)**
C-1-1	2.4785
C-1-2	1.9497
C-1-3	1.8142
C-1-4	0.3301
C-1-5	0.3782

Location C-2	
Test ID	**Cl Content (lb/cy)**
C-2-1	1.7154
C-2-2	0.2639
C-2-3	0.3722
C-2-4	0.1274
C-2-5	0.2267

Location C-3	
Test ID	**Cl Content (lb/cy)**
C-3-1	2.4005
C-3-2	1.5836
C-3-3	0.6836
C-3-4	1.0530
C-3-5	0.1856

Location C-4	
Test ID	**Cl Content (lb/cy)**
C-4-1	2.7283
C-4-2	0.8973
C-4-3	0.1931
C-4-4	0.1244
C-4-5	0.1167

Location C-5	
Test ID	**Cl Content (lb/cy)**
C-5-1	0.3905
C-5-2	0.1027
C-5-3	0.1018
C-5-4	0.0940
C-5-5	0.1380

Location C-6	
Test ID	**Cl Content (lb/cy)**
C-6-1	2.4198
C-6-2	1.0530
C-6-3	0.3491
C-6-4	0.8023
C-6-5	0.2143

Location C-7	
Test ID	**Cl Content (lb/cy)**
C-7-1	2.5797
C-7-2	1.3174
C-7-3	1.7292
C-7-4	0.4656
C-7-5	0.3812

Location C-8	
Test ID	**Cl Content (lb/cy)**
C-8-1	1.9971
C-8-2	1.1968
C-8-3	0.2495
C-8-4	0.1581
C-8-5	0.1741

Table H-25: Summary RCT test results for bridge deck 8N.

Bridge ID: **580160 8N**

Test Date: **7/21/2011**

Test ID	Depth (in)	Reading (mV)	Cl %	Cl Content (pcy)
C-1-1	1	30.0	16.32%	6.2279
C-2-1	1	31.4	15.44%	5.8887
C-3-1	1	32.4	14.83%	5.6578
C-4-1	1	37.0	12.34%	4.7069
C-5-1	1	31.8	15.19%	5.7952
C-6-1	1	21.0	23.40%	8.9266
C-7-1	1	35.2	13.26%	5.0583
C-8-1	1	31.8	15.19%	5.7952
C-1-2	2	53.4	6.40%	2.4425
C-2-2	2	63.4	4.29%	1.6373
C-3-2	2	65.8	3.90%	1.4874
C-4-2	2	63.4	4.29%	1.6373
C-5-2	2	71.0	3.17%	1.2081
C-6-2	2	44.4	9.18%	3.5010
C-7-2	2	73.0	2.92%	1.1152
C-8-2	2	65.2	3.99%	1.5235
C-1-3	3	85.6	1.77%	0.6737
C-2-3	3	91.2	1.41%	0.5385
C-3-3	3	109.4	0.68%	0.2600
C-4-3	3	89.4	1.52%	0.5787
C-5-3	3	115.4	0.54%	0.2045
C-6-3	3	69.4	3.38%	1.2879
C-7-3	3	110.2	0.66%	0.2518
C-8-3	3	97.2	1.11%	0.4236
C-1-4	4	115.2	0.54%	0.2062
C-2-4	4	117.8	0.49%	0.1858
C-3-4	4	115.0	0.54%	0.2078
C-4-4	4	116.8	0.51%	0.1934
C-5-4	4	115.2	0.54%	0.2062
C-6-4	4	89.8	1.49%	0.5695
C-7-4	4	119.6	0.45%	0.1729
C-8-4	4	110.8	0.64%	0.2459
C-1-5	5	112.2	0.61%	0.2325
C-2-5	5	115.4	0.54%	0.2045
C-3-5	5	120.6	0.44%	0.1661
C-4-5	5	121.2	0.43%	0.1622
C-5-5	5	123.0	0.40%	0.1509
C-6-5	5	108.8	0.70%	0.2663
C-7-5	5	120.6	0.44%	0.1661
C-8-5	5	110.4	0.65%	0.2498

Table H-26: RCT test results by location for bridge deck 8N.

Bridge ID: 580160 8N

Location C-1	
Test ID	**Cl Content (lb/cy)**
C-1-1	6.2279
C-1-2	2.4425
C-1-3	0.6737
C-1-4	0.2062
C-1-5	0.2325

Location C-2	
Test ID	**Cl Content (lb/cy)**
C-2-1	5.8887
C-2-2	1.6373
C-2-3	0.5385
C-2-4	0.1858
C-2-5	0.2045

Location C-3	
Test ID	**Cl Content (lb/cy)**
C-3-1	5.6578
C-3-2	1.4874
C-3-3	0.2600
C-3-4	0.2078
C-3-5	0.1661

Location C-4	
Test ID	**Cl Content (lb/cy)**
C-4-1	4.7069
C-4-2	1.6373
C-4-3	0.5787
C-4-4	0.1934
C-4-5	0.1622

Location C-5	
Test ID	**Cl Content (lb/cy)**
C-5-1	5.7952
C-5-2	1.2081
C-5-3	0.2045
C-5-4	0.2062
C-5-5	0.1509

Location C-6	
Test ID	**Cl Content (lb/cy)**
C-6-1	8.9266
C-6-2	3.5010
C-6-3	1.2879
C-6-4	0.5695
C-6-5	0.2663

Location C-7	
Test ID	**Cl Content (lb/cy)**
C-7-1	5.0583
C-7-2	1.1152
C-7-3	0.2518
C-7-4	0.1729
C-7-5	0.1661

Location C-8	
Test ID	**Cl Content (lb/cy)**
C-8-1	5.7952
C-8-2	1.5235
C-8-3	0.4236
C-8-4	0.2459
C-8-5	0.2498

Table H-27: Summary RCT test results for bridge deck 8L.

Bridge ID: **430120 8L**

Test Date: **7/20/2011**

Test ID	Depth (in)	Reading (mV)	Cl %	Cl Content (pcy)
C-1-1	1	28.4	17.21%	5.9313
C-2-1	1	27.8	17.63%	6.0753
C-3-1	1	26.2	18.79%	6.4769
C-4-1	1	27.0	18.20%	6.2729
C-5-1	1	33.8	13.87%	4.7790
C-6-1	1	39.8	10.91%	3.7593
C-7-1	1	86.8	1.66%	0.5736
C-8-1	1	39.4	11.08%	3.8199
C-1-2	2	49.2	7.49%	2.5812
C-2-2	2	58.2	5.23%	1.8008
C-3-2	2	53.8	6.23%	2.1474
C-4-2	2	65.2	3.95%	1.3610
C-5-2	2	61.4	4.60%	1.5844
C-6-2	2	62.6	4.38%	1.5102
C-7-2	2	66.4	3.76%	1.2972
C-8-2	2	67.8	3.56%	1.2266
C-1-3	3	88.4	1.56%	0.5381
C-2-3	3	98.2	1.06%	0.3636
C-3-3	3	85.2	1.77%	0.6115
C-4-3	3	77.2	2.44%	0.8422
C-5-3	3	92.0	1.35%	0.4659
C-6-3	3	89.2	1.51%	0.5211
C-7-3	3	46.2	8.44%	2.9102
C-8-3	3	86.2	1.70%	0.5876
C-1-4	4	118.0	0.48%	0.1647
C-2-4	4	113.8	0.57%	0.1948
C-3-4	4	109.4	0.67%	0.2323
C-4-4	4	89.2	1.51%	0.5211
C-5-4	4	120.2	0.44%	0.1508
C-6-4	4	117.0	0.50%	0.1714
C-7-4	4	112.0	0.61%	0.2093
C-8-4	4	110.2	0.65%	0.2250
C-1-5	5	116.8	0.50%	0.1728
C-2-5	5	107.6	0.72%	0.2496
C-3-5	5	110.4	0.65%	0.2232
C-4-5	5	90.0	1.46%	0.5047
C-5-5	5	115.4	0.53%	0.1827
C-6-5	5	121.6	0.41%	0.1426
C-7-5	5	122.2	0.40%	0.1392
C-8-5	5	115.8	0.52%	0.1798

Table H-28: RCT test results by location for bridge deck 8L.

Bridge ID: 430120 8L

Location C-1	
Test ID	**Cl Content (lb/cy)**
C-1-1	5.9313
C-1-2	2.5812
C-1-3	0.5381
C-1-4	0.1647
C-1-5	0.1728

Location C-2	
Test ID	**Cl Content (lb/cy)**
C-2-1	6.0753
C-2-2	1.8008
C-2-3	0.3636
C-2-4	0.1948
C-2-5	0.2496

Location C-3	
Test ID	**Cl Content (lb/cy)**
C-3-1	6.4769
C-3-2	2.1474
C-3-3	0.6115
C-3-4	0.2323
C-3-5	0.2232

Location C-4	
Test ID	**Cl Content (lb/cy)**
C-4-1	6.2729
C-4-2	1.3610
C-4-3	0.8422
C-4-4	0.5211
C-4-5	0.5047

Location C-5	
Test ID	**Cl Content (lb/cy)**
C-5-1	4.7790
C-5-2	1.5844
C-5-3	0.4659
C-5-4	0.1508
C-5-5	0.1827

Location C-6	
Test ID	**Cl Content (lb/cy)**
C-6-1	3.7593
C-6-2	1.5102
C-6-3	0.5211
C-6-4	0.1714
C-6-5	0.1426

Location C-7	
Test ID	**Cl Content (lb/cy)**
C-7-1	0.5736
C-7-2	1.2972
C-7-3	2.9102
C-7-4	0.2093
C-7-5	0.1392

Location C-8	
Test ID	**Cl Content (lb/cy)**
C-8-1	3.8199
C-8-2	1.2266
C-8-3	0.5876
C-8-4	0.2250
C-8-5	0.1798

Table H-29: Summary RCT test results for bridge deck 9N.

Bridge ID: **580153 9N**

Test Date: **7/26/2011**

Test ID	Depth (in)	Reading (mV)	Cl %	Cl Content (pcy)
C-1-1	1	44.6	8.65%	3.3000
C-2-1	1	58.0	5.06%	1.9308
C-3-1	1	35.8	12.30%	4.6924
C-4-1	1	35.0	12.70%	4.8450
C-5-1	1	33.4	13.54%	5.1652
C-6-1	1	26.6	17.77%	6.7797
C-7-1	1	31.6	14.55%	5.5508
C-8-1	1	34.4	13.01%	4.9626
C-1-2	2	69.6	3.18%	1.2140
C-2-2	2	99.4	0.97%	0.3686
C-3-2	2	58.0	5.06%	1.9308
C-4-2	2	61.4	4.42%	1.6853
C-5-2	2	67.2	3.50%	1.3363
C-6-2	2	48.4	7.43%	2.8347
C-7-2	2	80.0	2.10%	0.8009
C-8-2	2	61.0	4.49%	1.7125
C-1-3	3	102.0	0.87%	0.3322
C-2-3	3	121.2	0.40%	0.1541
C-3-3	3	76.2	2.44%	0.9323
C-4-3	3	85.8	1.66%	0.6350
C-5-3	3	88.4	1.50%	0.5723
C-6-3	3	78.4	2.24%	0.8538
C-7-3	3	89.6	1.43%	0.5455
C-8-3	3	81.8	1.95%	0.7452
C-1-4	4	124.0	0.36%	0.1378
C-2-4	4	121.4	0.40%	0.1529
C-3-4	4	96.6	1.08%	0.4123
C-4-4	4	98.2	1.01%	0.3867
C-5-4	4	96.2	1.10%	0.4189
C-6-4	4	100.2	0.94%	0.3570
C-7-4	4	98.6	1.00%	0.3806
C-8-4	4	112.2	0.58%	0.2209
C-1-5	5	127.4	0.32%	0.1203
C-2-5	5	123.6	0.37%	0.1400
C-3-5	5	104.2	0.80%	0.3042
C-4-5	5	102.0	0.87%	0.3322
C-5-5	5	96.0	1.11%	0.4223
C-6-5	5	105.2	0.77%	0.2923
C-7-5	5	106.2	0.74%	0.2808
C-8-5	5	107.6	0.70%	0.2655

Table H-30: RCT test results by location for bridge deck 9N.

Bridge ID: 580153 9N

Location C-1	
Test ID	**Cl Content (lb/cy)**
C-1-1	3.3000
C-1-2	1.2140
C-1-3	0.3322
C-1-4	0.1378
C-1-5	0.1203

Location C-2	
Test ID	**Cl Content (lb/cy)**
C-2-1	1.9308
C-2-2	0.3686
C-2-3	0.1541
C-2-4	0.1529
C-2-5	0.1400

Location C-3	
Test ID	**Cl Content (lb/cy)**
C-3-1	4.6924
C-3-2	1.9308
C-3-3	0.9323
C-3-4	0.4123
C-3-5	0.3042

Location C-4	
Test ID	**Cl Content (lb/cy)**
C-4-1	4.8450
C-4-2	1.6853
C-4-3	0.6350
C-4-4	0.3867
C-4-5	0.3322

Location C-5	
Test ID	**Cl Content (lb/cy)**
C-5-1	5.1652
C-5-2	1.3363
C-5-3	0.5723
C-5-4	0.4189
C-5-5	0.4223

Location C-6	
Test ID	**Cl Content (lb/cy)**
C-6-1	6.7797
C-6-2	2.8347
C-6-3	0.8538
C-6-4	0.3570
C-6-5	0.2923

Location C-7	
Test ID	**Cl Content (lb/cy)**
C-7-1	5.5508
C-7-2	0.8009
C-7-3	0.5455
C-7-4	0.3806
C-7-5	0.2808

Location C-8	
Test ID	**Cl Content (lb/cy)**
C-8-1	4.9626
C-8-2	1.7125
C-8-3	0.7452
C-8-4	0.2209
C-8-5	0.2655

Table H-31: Summary RCT test results for bridge deck 9L.

Bridge ID: **580146 9L**

Test Date: **7/22/2011**

Test ID	Depth (in)	Reading (mV)	Cl %	Cl Content (pcy)
C-1-1	1	27.6	17.87%	6.1584
C-2-1	1	39.0	11.33%	3.9033
C-3-1	1	51.4	6.90%	2.3769
C-4-1	1	36.2	12.67%	4.3659
C-5-1	1	37.2	12.17%	4.1947
C-6-1	1	31.6	15.23%	5.2478
C-7-1	1	47.8	7.97%	2.7451
C-8-1	1	38.0	11.79%	4.0626
C-1-2	2	43.4	9.50%	3.2734
C-2-2	2	52.4	6.63%	2.2837
C-3-2	2	68.2	3.52%	1.2139
C-4-2	2	62.4	4.44%	1.5308
C-5-2	2	67.2	3.67%	1.2634
C-6-2	2	54.2	6.17%	2.1251
C-7-2	2	66.0	3.85%	1.3255
C-8-2	2	55.2	5.92%	2.0418
C-1-3	3	64.4	4.10%	1.4131
C-2-3	3	71.2	3.12%	1.0766
C-3-3	3	90.0	1.47%	0.5075
C-4-3	3	99.4	1.01%	0.3485
C-5-3	3	100.0	0.99%	0.3402
C-6-3	3	80.4	2.16%	0.7451
C-7-3	3	85.8	1.74%	0.6004
C-8-3	3	73.2	2.88%	0.9938
C-1-4	4	92.6	1.33%	0.4574
C-2-4	4	91.6	1.38%	0.4761
C-3-4	4	135.2	0.24%	0.0832
C-4-4	4	137.2	0.22%	0.0768
C-5-4	4	137.0	0.22%	0.0774
C-6-4	4	113.0	0.59%	0.2023
C-7-4	4	118.4	0.47%	0.1630
C-8-4	4	91.8	1.37%	0.4723
C-1-5	5	130.2	0.29%	0.1017
C-2-5	5	122.6	0.40%	0.1378
C-3-5	5	140.6	0.19%	0.0671
C-4-5	5	130.4	0.29%	0.1008
C-5-5	5	130.8	0.29%	0.0992
C-6-5	5	125.2	0.36%	0.1242
C-7-5	5	139.4	0.20%	0.0704
C-8-5	5	128.8	0.31%	0.1075

Table H-32: RCT test results by location for bridge deck 9L.

Bridge ID: 580146 9L

Location C-1	
Test ID	**Cl Content (lb/cy)**
C-1-1	6.1584
C-1-2	3.2734
C-1-3	1.4131
C-1-4	0.4574
C-1-5	0.1017

Location C-2	
Test ID	**Cl Content (lb/cy)**
C-2-1	3.9033
C-2-2	2.2837
C-2-3	1.0766
C-2-4	0.4761
C-2-5	0.1378

Location C-3	
Test ID	**Cl Content (lb/cy)**
C-3-1	2.3769
C-3-2	1.2139
C-3-3	0.5075
C-3-4	0.0832
C-3-5	0.0671

Location C-4	
Test ID	**Cl Content (lb/cy)**
C-4-1	4.3659
C-4-2	1.5308
C-4-3	0.3485
C-4-4	0.0768
C-4-5	0.1008

Location C-5	
Test ID	**Cl Content (lb/cy)**
C-5-1	4.1947
C-5-2	1.2634
C-5-3	0.3402
C-5-4	0.0774
C-5-5	0.0992

Location C-6	
Test ID	**Cl Content (lb/cy)**
C-6-1	5.2478
C-6-2	2.1251
C-6-3	0.7451
C-6-4	0.2023
C-6-5	0.1242

Location C-7	
Test ID	**Cl Content (lb/cy)**
C-7-1	2.7451
C-7-2	1.3255
C-7-3	0.6004
C-7-4	0.1630
C-7-5	0.0704

Location C-8	
Test ID	**Cl Content (lb/cy)**
C-8-1	4.0626
C-8-2	2.0418
C-8-3	0.9938
C-8-4	0.4723
C-8-5	0.1075

APPENDIX I

Petrographic Examination Results

Figure I-1: Scanned image of polished surface prepared from bridge deck 1N, core C-5. Bridge deck surface is at top.

Figure I-2: Scanned image of polished surface prepared from bridge deck 1L, core C-7B. Bridge deck surface is at top.

Figure I-3: Scanned image of polished surface prepared from bridge deck 2N, core C-6. Bridge deck surface is at top.

Figure I-4: Scanned image of polished surface prepared from bridge deck 2N, core C-7. Bridge deck surface is at top.

Figure I-5: Scanned image of polished surface prepared from bridge deck 2L, core C-3. Bridge deck surface is at top.

Figure I-6: Scanned image of polished surface prepared from bridge deck 2L, core C-4. Bridge deck surface is at top.

Figure I-7: Scanned image of polished surface prepared from bridge deck 3N, core C-2. Bridge deck surface is at top.

Figure I-8: Scanned image of polished surface prepared from bridge deck 3N, core C-3. Bridge deck surface is at top.

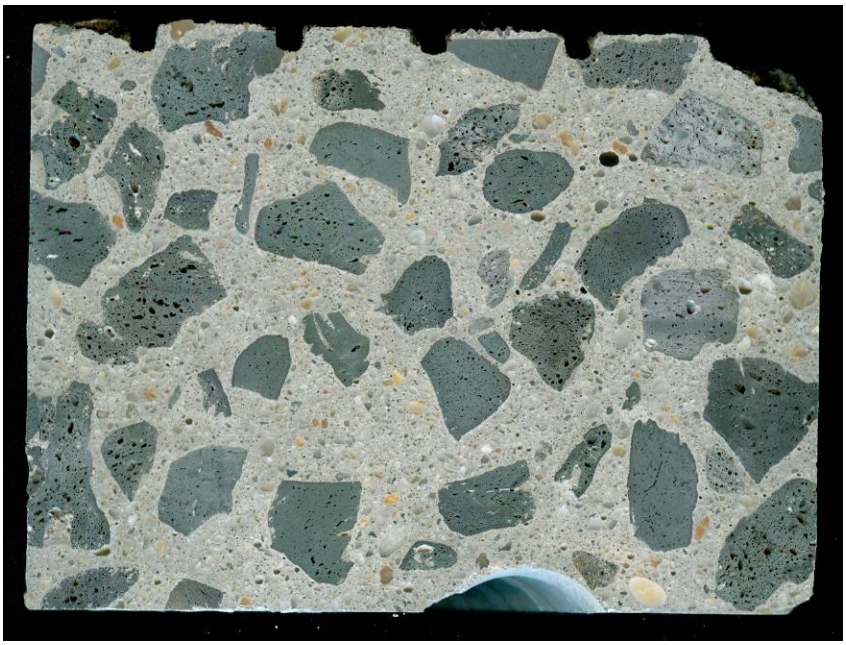

Figure I-9: Scanned image of polished surface prepared from bridge deck 3L, core C-6. Bridge deck surface is at top.

Figure I-10: Scanned image of polished surface prepared from bridge deck 5N, core C-3. Bridge deck surface is at top.

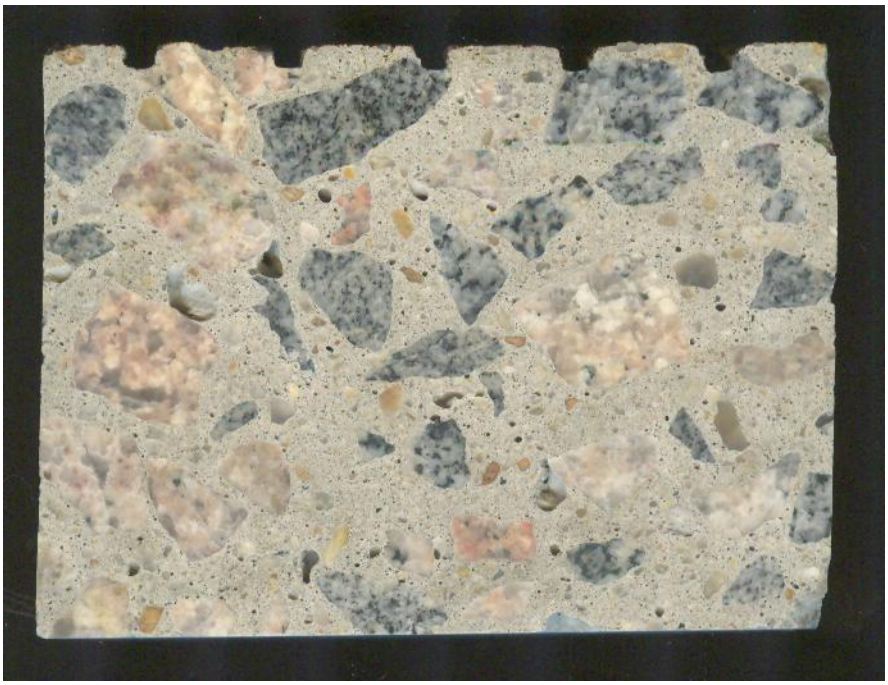

Figure I-11: Scanned image of polished surface prepared from bridge deck 5N, core C-8. Bridge deck surface is at top.

Figure I-12: Scanned image of polished surface prepared from bridge deck 5L, core C-8. Bridge deck surface is at top.

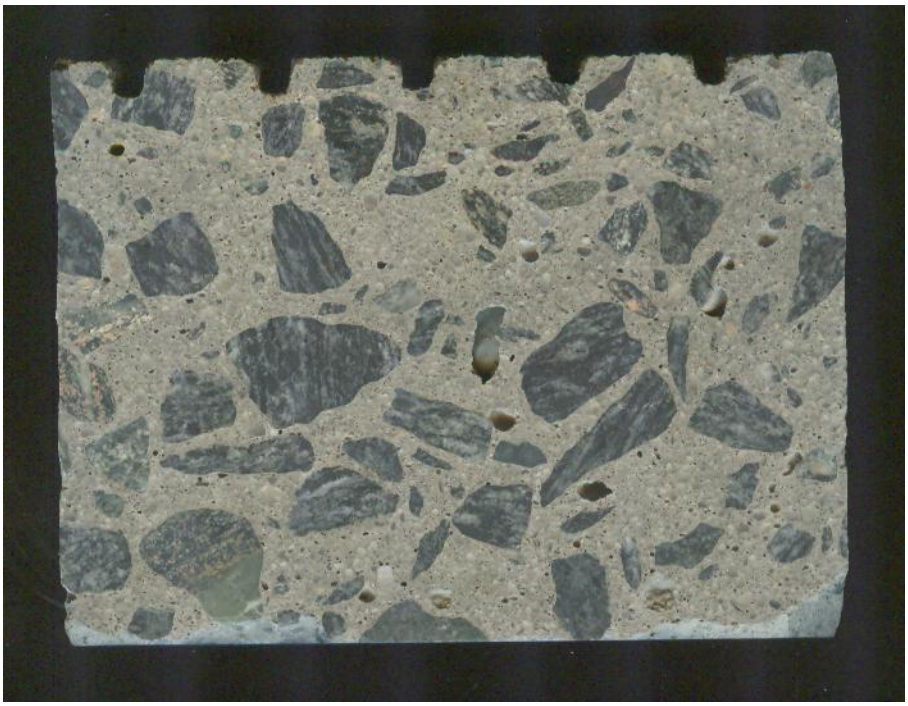

Figure I-13: Scanned image of polished surface prepared from bridge deck 6N, core C-3. Bridge deck surface is at top.

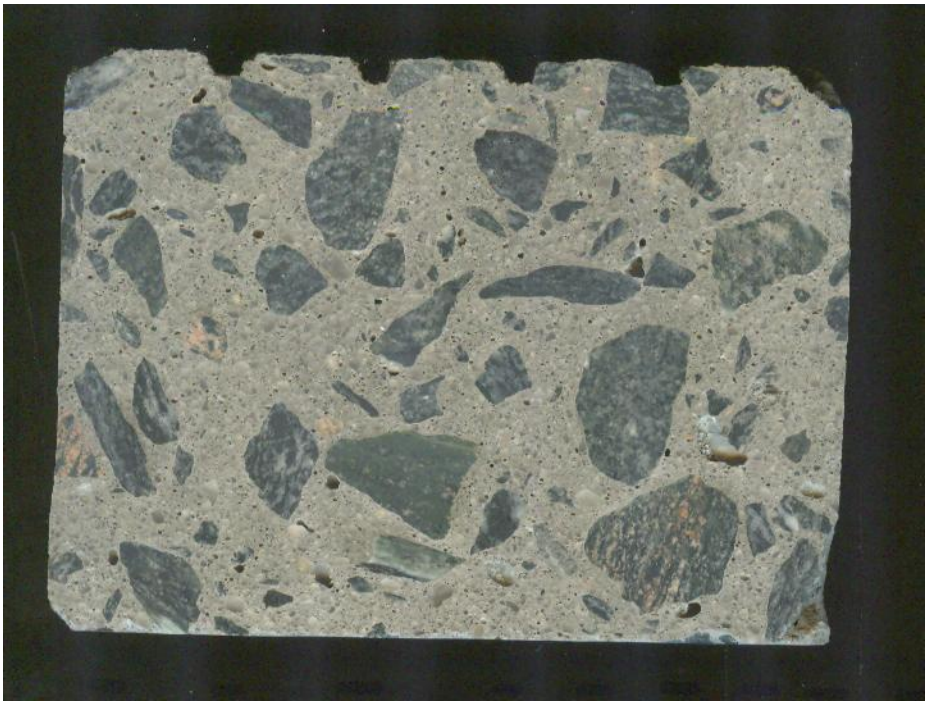

Figure I-14: Scanned image of polished surface prepared from bridge deck 6N, core C-6B. Bridge deck surface is at top.

Figure I-15: Scanned image of polished surface prepared from bridge deck 6L, core C-1. Bridge deck surface is at top.

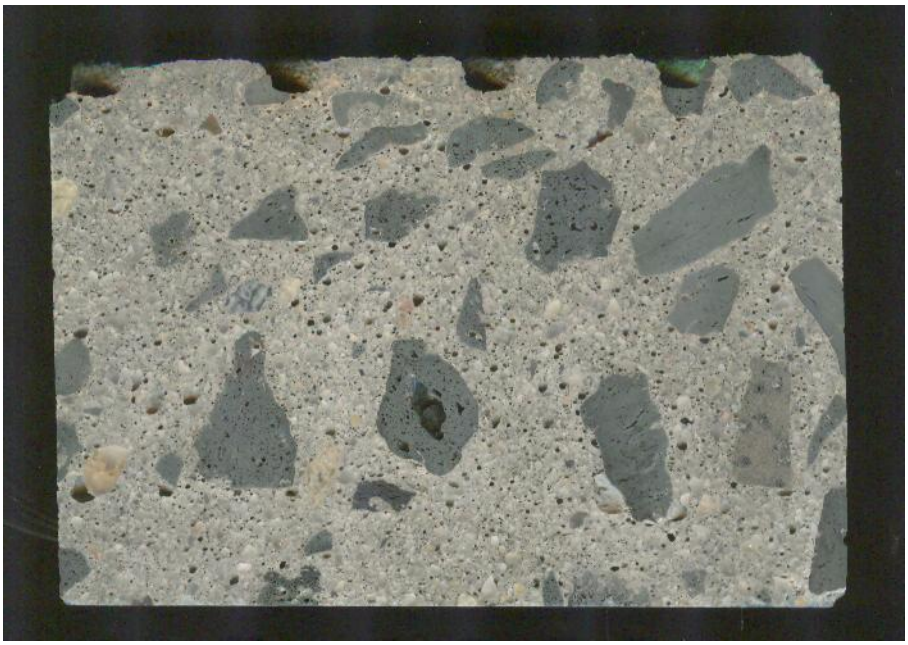

Figure I-16: Scanned image of polished surface prepared from bridge deck 6L, core C-3. Bridge deck surface is at top.

Figure I-17: Scanned image of polished surface prepared from bridge deck 7N, core C-6. Bridge deck surface is at top.

Figure I-18: Scanned image of polished surface prepared from bridge deck 7N, core C-8. Bridge deck surface is at top.

Figure I-19: Scanned image of polished surface prepared from bridge deck 7L, core C-5A. Bridge deck surface is at top.

Figure I-20: Scanned image of polished surface prepared from bridge deck 7L, core C-7A. Bridge deck surface is at top.

Figure I-21: Scanned image of polished surface prepared from bridge deck 8N, core C-2. Bridge deck surface is at top.

Figure I-22: Scanned image of polished surface prepared from bridge deck 8N, core C-7. Bridge deck surface is at top.

Figure I-23: Scanned image of polished surface prepared from bridge deck 8L, core C-4. Bridge deck surface is at top.

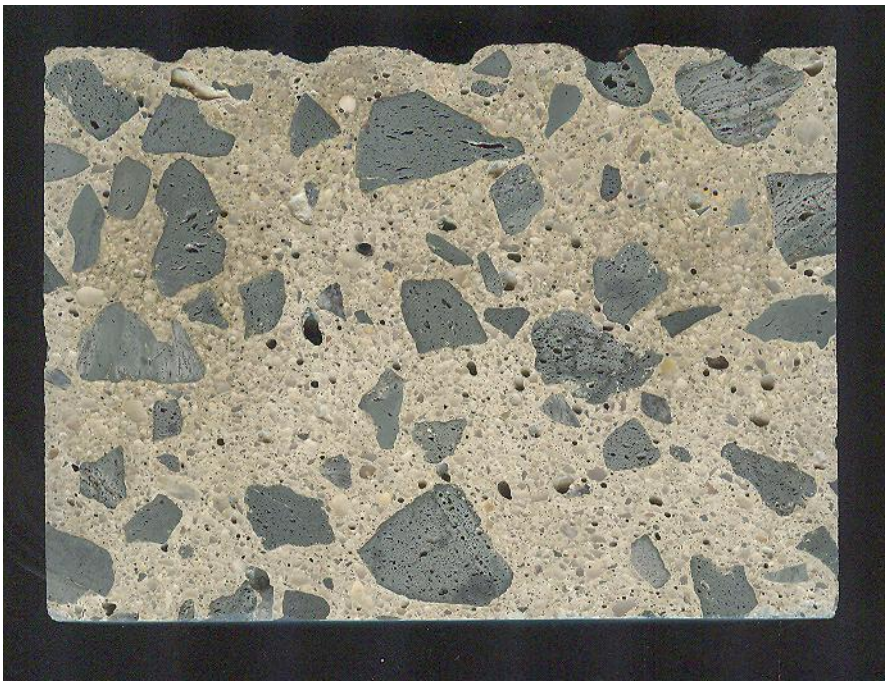

Figure I-24: Scanned image of polished surface prepared from bridge deck 8L, core C-8. Bridge deck surface is at top.

Figure I-25: Scanned image of polished surface prepared from bridge deck 9N, core C-3. Bridge deck surface is at top.

Figure I-26: Scanned image of polished surface prepared from bridge deck 9N, core C-5. Bridge deck surface is at top.

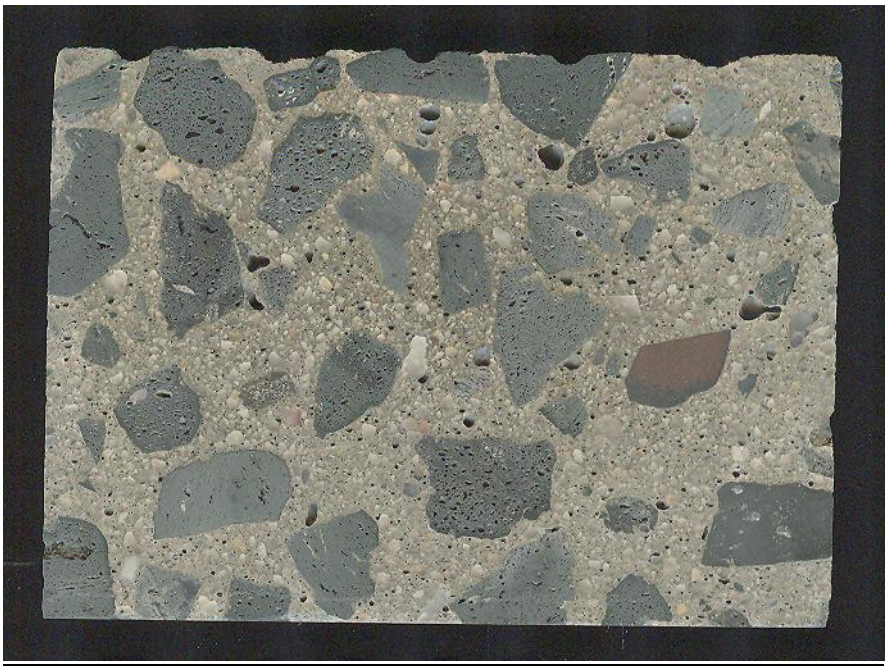

Figure I-27: Scanned image of polished surface prepared from bridge deck 9L, core C-5. Bridge deck surface is at top.

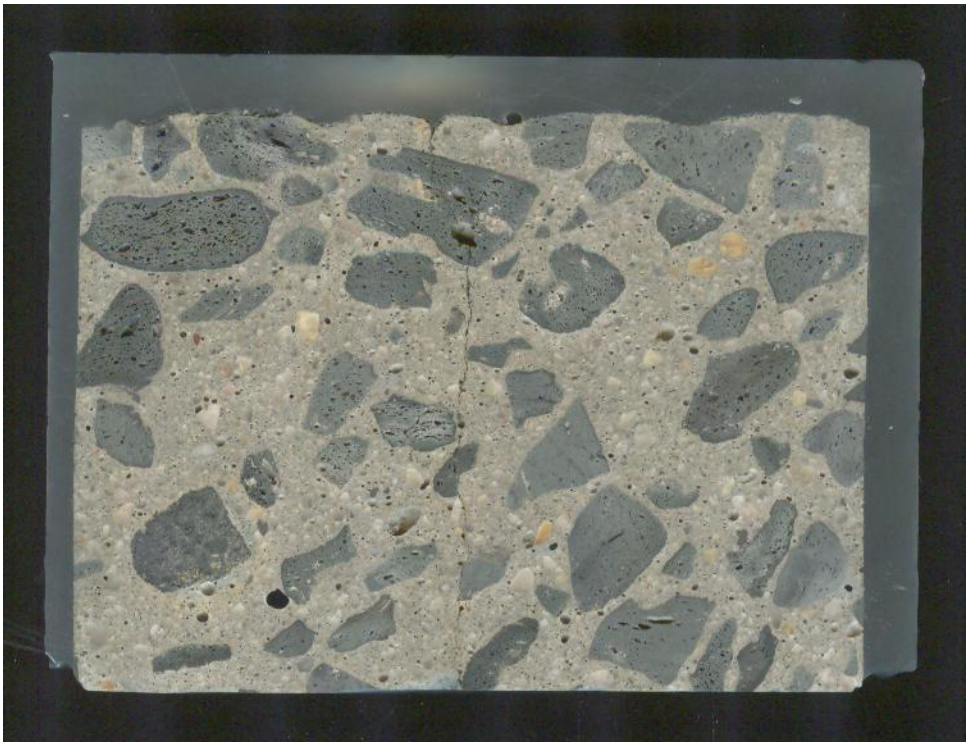

Figure I-28: Scanned image of polished surface prepared from bridge deck 9L, core C-8. Bridge deck surface is at top. Note that core has been encapsulated in resin prior to sawcutting due to crack.

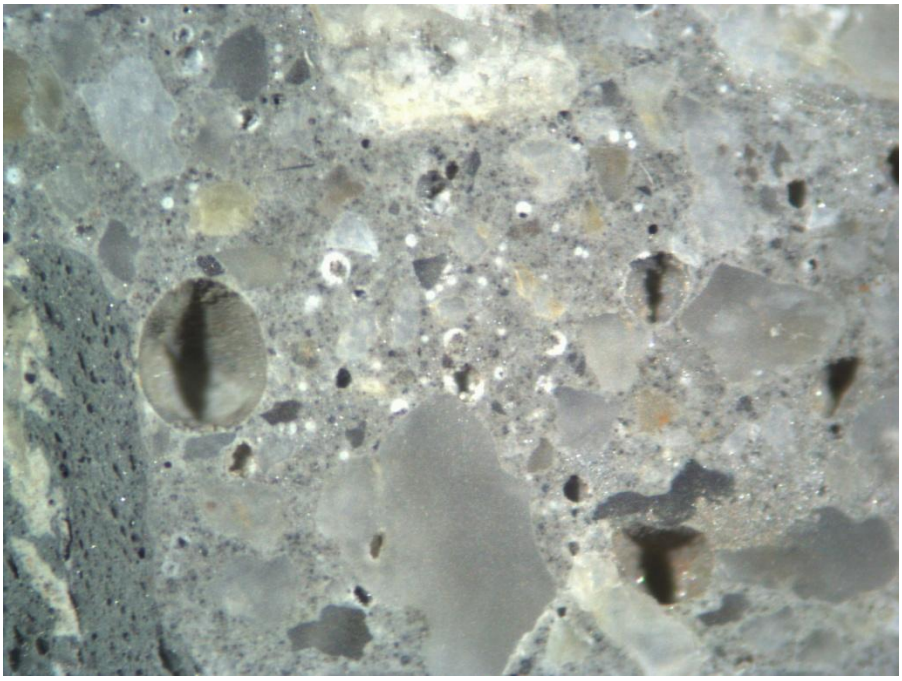

Figure I-29: Photomicrograph of polished surface prepared from bridge deck 1L, core C-7B, taken at a magnification of 25x. White secondary deposits are present in some entrained air voids.

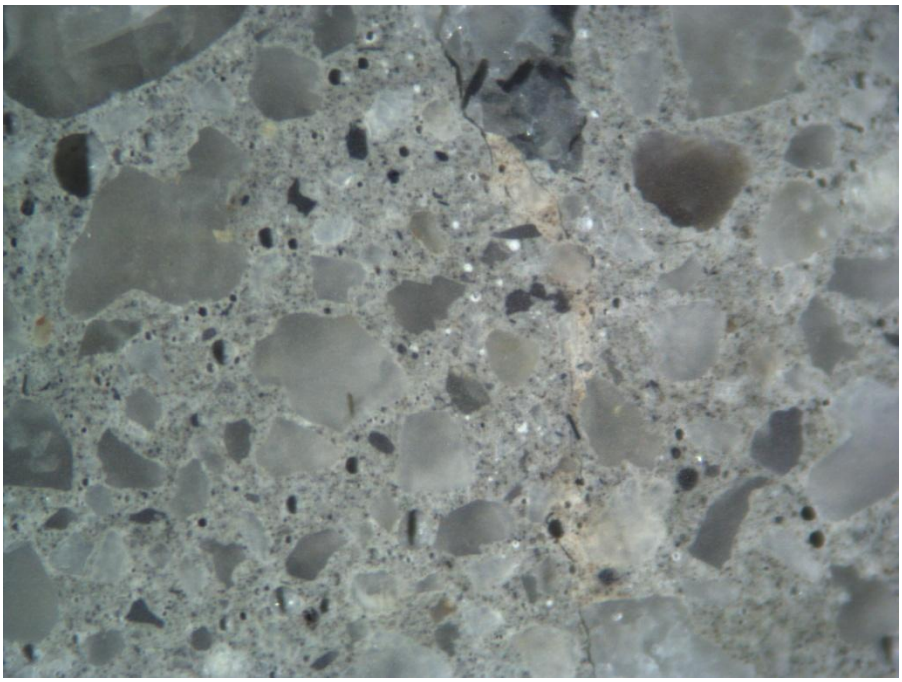

Figure I-30: Photomicrograph of polished surface prepared from bridge deck 1N, core C-5, taken at a magnification of 20x. White secondary deposits are present in some entrained air voids near microcrack.

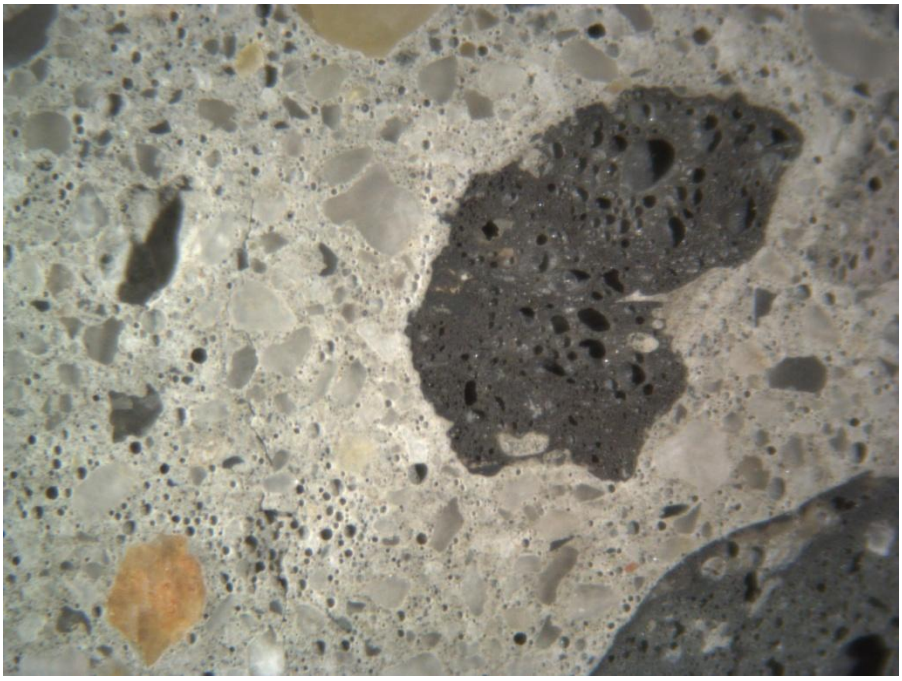

Figure I-31: Photomicrograph of polished surface prepared from bridge deck 2L, core C-4, taken at a magnification of 10x. Localized areas of very high entrained air content can be seen at lower left of image.

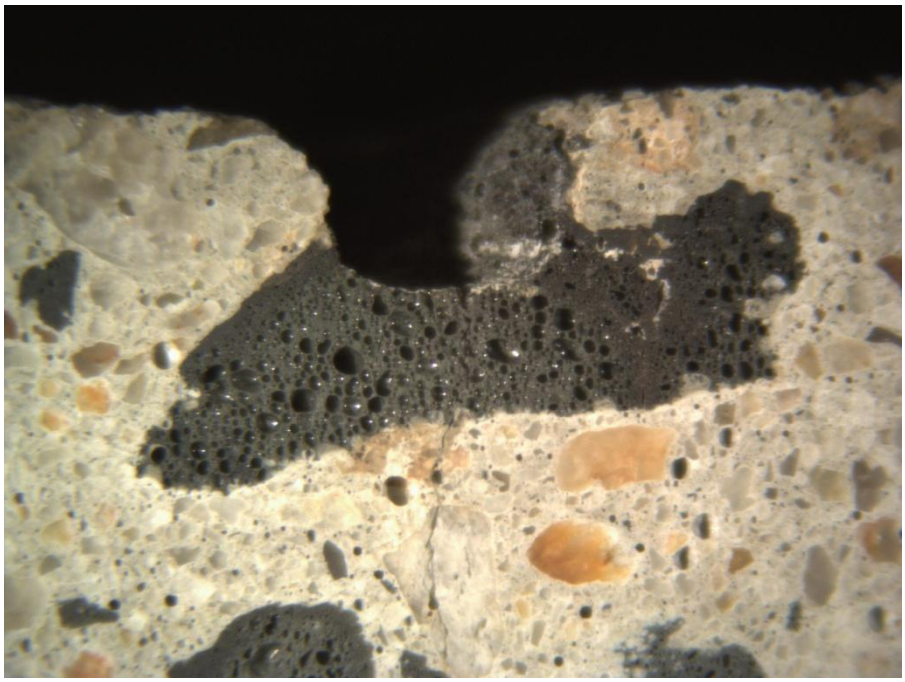

Figure I-32: Photomicrograph of polished surface prepared from bridge deck 5L, core C-8, taken at a magnification of 7x. Microcrack extends from groove, through lightweight aggregate, into mortar.

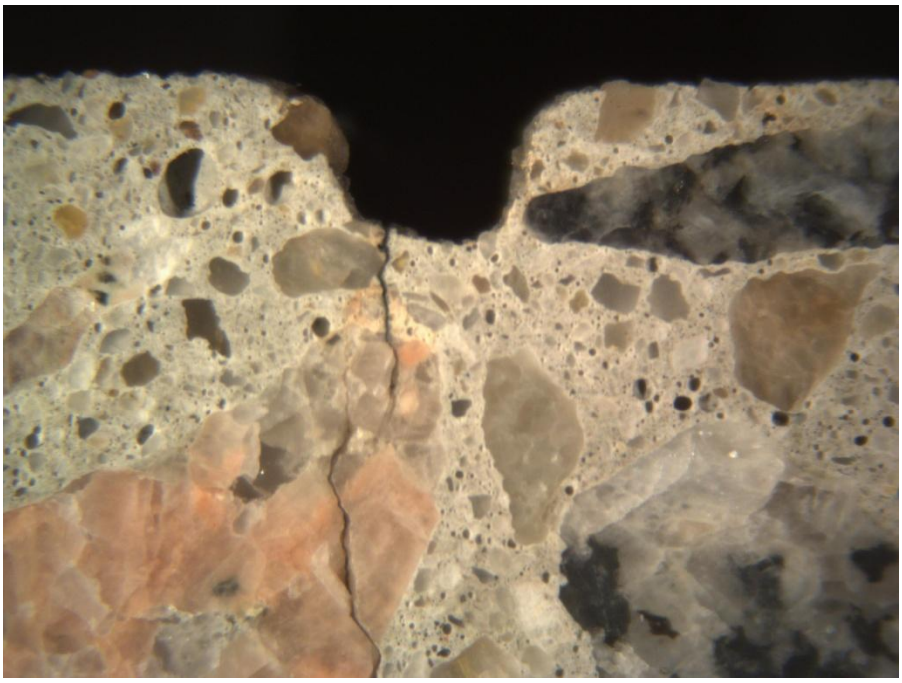

Figure I-33: Photomicrograph of polished surface prepared from bridge deck 5N, core C-7, taken at a magnification of 7x. Microcrack extends from groove, through normalweight aggregate, into mortar.

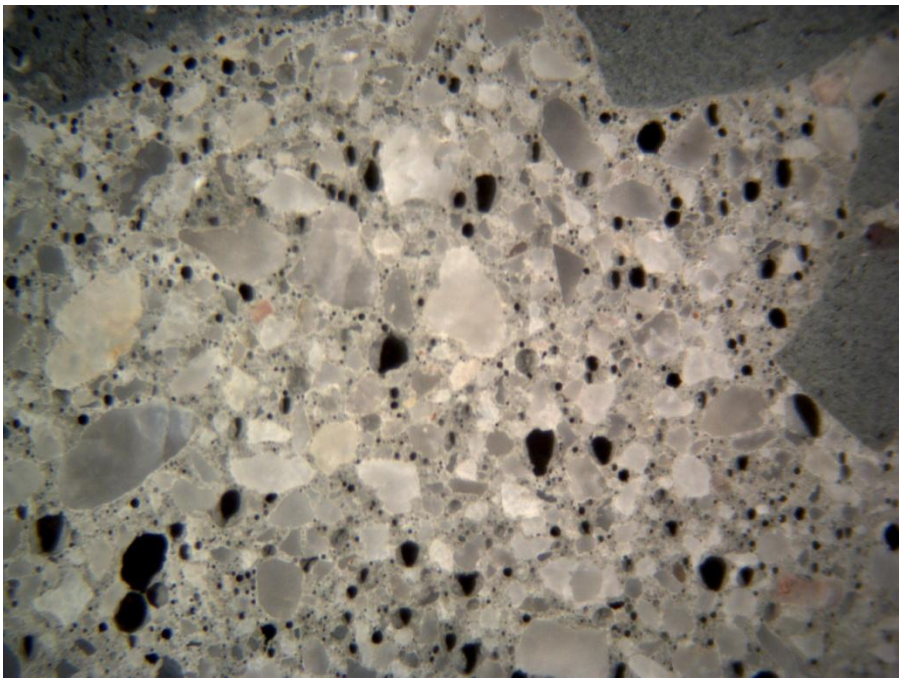

Figure I-34: Photomicrograph of polished surface prepared from bridge deck 6L, core C-6A, taken at a magnification of 7x. A number of irregularly shaped water voids are present.

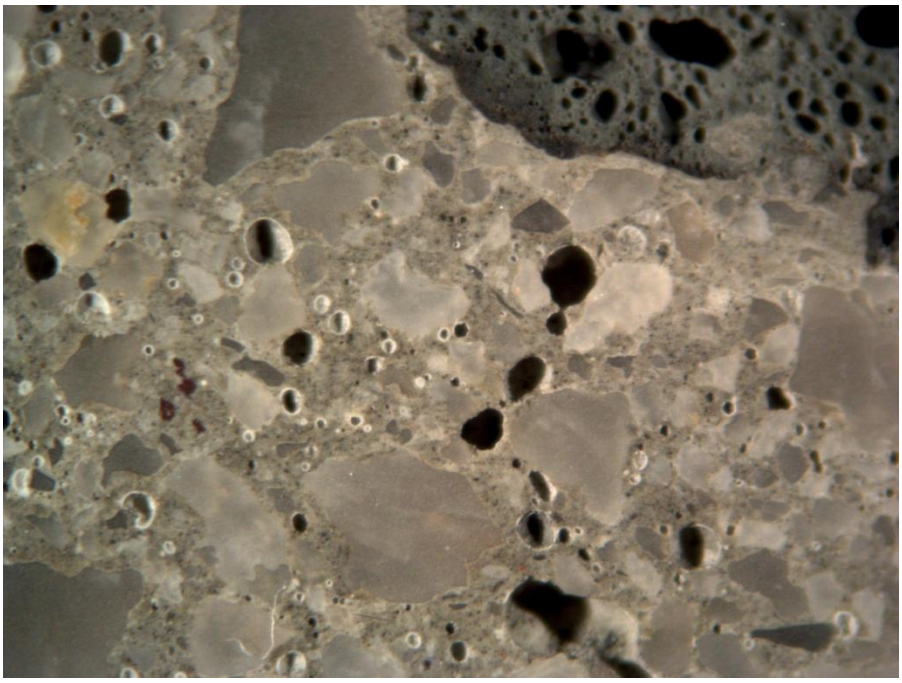

Figure I-35: Photomicrograph of polished surface prepared from bridge deck 6L, core C-1, taken at a magnification of 15x. White secondary deposits are present, lining some entrained air voids.

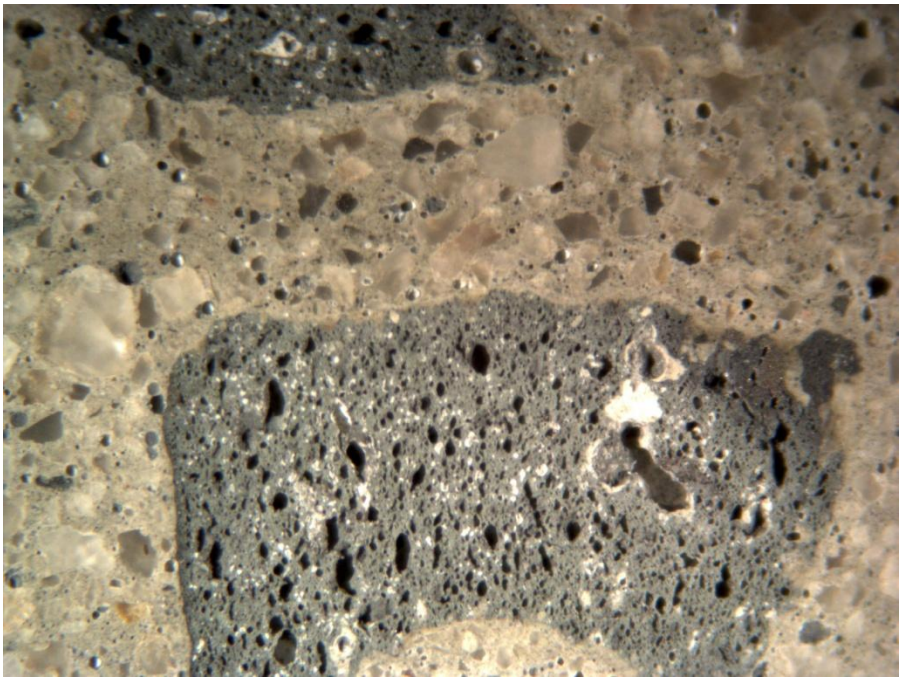

Figure I-36: Photomicrograph of polished surface prepared from bridge deck 7L, core C-5A, taken at a magnification of 10x. White secondary deposits are present, lining some entrained air voids and in some voids in lightweight aggregate.

Figure I-37: Photomicrograph of polished surface prepared from bridge deck 8N, core C-7, taken at a magnification of 15x. Macrocrack extending from top surface through coarse aggregate.

Figure I-38: Photomicrograph of polished surface prepared from bridge deck 9N, core C-5, taken at a magnification of 10x. Microcrack from top surface propagates around coarse aggregate perimeter and through coarse aggregate.

MACROSCOPIC AND MICROSCOPIC OBSERVATION OF HARDENED CONCRETE – POLISHED SAMPLE

Project Name:	NCDOT 2011-06		
Client:	NCDOT	**Project No.:**	520180
Observations by:	Tara Cavalline	**Date:**	Spring / Summer 2012

Type of Structure: Concrete bridge deck 070160 (1N)
Location: Bertie County, North Carolina
Purpose: Observe general characteristics

Sample ID: 1N C-5

Sample Description

Dimensions: 4-1/16 inches wide, 2¾ inch long
Top surface finish: Grooves evident
Bottom surface finish: Sawcut from full core sample
Reinforcement: None in polished section
Cracks, Joints, Voids: A few small voids where not fully consolidated, typically in lower portion of sample

Aggregates

Coarse aggregate:

- Type: Multi-colored foliated granite with some mafic minerals. Typically dark gray, white, and light gray, some beige.
- Gradation and top size: Well-graded, ¾ inch max nominal size.
- Shape and distribution: Subangular to subrounded, relatively evenly distributed.

Fine aggregate:

- Type: Multi-colored natural silica, mainly white, clear, and light gray. Some tan.
- Gradation and top size: Well-graded, 3/8 inch max nominal size.
- Shape and distribution: Subrounded to subangular

Paste

Color: Medium gray
Luster: Subvitreous
Hardness: Moderately hard to hard
Supplementary cementitious matls: Appears to contain fly ash (some particles suspected to be cenospheres visible via acid etch), dark particles evident. No mixture design submittal available.
Depth of carbonation: Approx. ¼ inch

Other observations

Paste-aggregate bond: Good
Secondary deposits: A few secondary deposits lining or partially filling a few entrained air voids. A few small voids in vicinity of a microcrack are filled with secondary deposits.
Air content: Air entrained, approximately 5-7 percent.
Microcracking: Several microcracks extending downward from top surface. Some propagate around aggregates perimeters, some propagate through aggregates. Typically located within top 1 inch.
Estimated water-cement ratio: 0.35 to 0.40 (with water-reducing admixture, assumed)

Notes

1. More microcracks observed in 1N C-5 than observed in 1L C-7B. Microcracks in 1N C-5 extend significantly deeper.
2. Appears to contain fly ash (some particles suspected to be cenospheres visible via acid etch), dark particles evident. No mixture design submittal was available with information regarding SCMs.

Figure I-39: Datasheet for petrographic examination of sample 1N C-5.

MACROSCOPIC AND MICROSCOPIC OBSERVATION OF HARDENED CONCRETE – POLISHED SAMPLE

Project Name:	NCDOT 2011-06		
Client:	NCDOT	**Project No.:**	520180
Observations by:	Tara Cavalline	**Date:**	Spring / Summer 2012

Type of Structure: Concrete bridge deck 070038 (1L)
Location: Bertie County, North Carolina
Purpose: Observe general characteristics

Sample ID: 1L C-7B

Sample Description

Dimensions: 4-1/16 inches wide, 3 inches long
Top surface finish: Grooves evident
Bottom surface finish: Sawcut from full core sample
Reinforcement: None in polished section
Cracks, Joints, Voids: Several moderate sized voids where not fully consolidated.

Aggregates

Coarse aggregate:
- Type: Manufactured lightweight aggregate, typically medium gray to gray green.
- Gradation and top size: Well-graded, ¾ inch max nominal size.
- Shape and distribution: Subequant, subrounded to subangular edges. Not well distributed in lower half of sample.

Fine aggregate:
- Type: Multi-colored natural silica, mainly white, clear, and light gray. Some tan and brown.
- Gradation and top size: Well-graded, 3/8 inch max nominal size.
- Shape and distribution: Subrounded to subangular

Paste

Color:	Medium gray
Luster:	Subvitreous
Hardness:	Moderately hard to hard
Supplementary cementitious matls:	Appears to contain fly ash (some particles suspected to be cenospheres visible via acid etch), dark particles evident. Fly ash also included in approved submittal for mixture design.
Depth of carbonation:	Approx. ¾ inch

Other observations

Paste-aggregate bond:	Good
Secondary deposits:	In upper portion of sample, secondary deposits lining many voids. Some small voids filled with secondary deposit, particularly near top surface.
Air content:	Air entrained, approximately 5-7 percent.
Microcracking:	A few small microcracks extending downward from top surface, typically to aggregate perimeters. Typically located within the top 1/8 inch of sample.
Estimated water-cement ratio:	0.35 per approved submittal for mixture design (includes water-reducing admixture)

Notes

1. Significant number of entrapped air voids (visible on macro photo of sample)
2. Mixture submittals provided indicate Type I/II cement (341 kg/m^3), fly ash (100 kg/m^3).
3. Fewer microcracks observed in 1L C-7B than observed in 1N C-5. Microcracks in 1L C-7B do not extend as deep as microcracks in 1N C-5.
4. Appears to contain fly ash (some particles suspected to be cenospheres visible via acid etch), dark particles evident. Fly ash also included in approved submittal for mixture design.

Figure I-40: Datasheet for petrographic examination of sample 1L C-7B.

MACROSCOPIC AND MICROSCOPIC OBSERVATION OF HARDENED CONCRETE – POLISHED SAMPLE

Project Name:	NCDOT 2011-06		
Client:	NCDOT	**Project No.:**	520180
Observations by:	Tara Cavalline	**Date:**	Spring / Summer 2012

Type of Structure: Concrete bridge deck 150012 (2N)
Location: Carteret County, North Carolina
Purpose: Observe general characteristics

Sample ID: 2N C-6

Sample Description

Dimensions:	4-1/16 inches wide, 2½ inches long
Top surface finish:	Grooves evident
Bottom surface finish:	Sawcut from full core sample
Reinforcement:	None in polished section
Cracks, Joints, Voids:	A few very small voids where not fully consolidated.

Aggregates

Coarse aggregate:

Type:	Multi-colored foliated granite, with some mafic minerals. Typically dark gray, light gray, white, pink and green.
Gradation and top size:	¾ inch max nominal size. Relatively few or larger sized particles in sample.
Shape and distribution:	Subangular to angular, not evenly distributed in some areas of sample (particularly near top). Some particles elongated.

Fine aggregate:

Type:	Multi-colored natural silica, mainly white, clear, and light gray. Some tan and light brown.
Gradation and top size:	Well-graded, 3/8 inch max nominal size
Shape and distribution:	Subrounded to subangular

Paste

Color:	Medium gray
Luster:	Subvitreous
Hardness:	Moderately hard to hard. A few areas of deteriorated paste along some near-surface microcracks.
Supplementary cementitious matls:	Possibly contains fly ash, but not confirmed. Dark particles evident, which may be fly ash, but cenospheres not observed after acid etch. Mixture submittals not available.
Depth of carbonation:	Approx. ¼ inch

Other observations

Paste-aggregate bond:	Good, except along perimeters where entrained air voids have coalesced
Secondary deposits:	Trace deposits observed in a few voids.
Air content:	Air-entrained, approx. 6-8%
Microcracking:	Several microcracks extending from top surface, typically within top ½ inch.
Estimated water-cement ratio:	0.35-0.40 (with water-reducing admixture, assumed)

Notes

1. In a number of areas, entrained air voids have coalesced, resulting in a localized high air content.
2. Some areas of the sample have relatively higher air contents than other areas.
3. Samples 2L C-3 and 2L C-4 contain more microcracks than samples 2N C-6 and 2N C-7. Localized areas of high air content are more prevalent in samples 2L C-6 and 2L C-7.

Figure I-41: Datasheet for petrographic examination of sample 2N C-6.

MACROSCOPIC AND MICROSCOPIC OBSERVATION OF HARDENED CONCRETE – POLISHED SAMPLE

Project Name:	NCDOT 2011-06		
Client:	NCDOT	**Project No.:**	520180
Observations by:	Tara Cavalline	**Date:**	Spring / Summer 2012

Type of Structure: Concrete bridge deck 150012 (2N)
Location: Carteret County, North Carolina
Purpose: Observe general characteristics

Sample ID: 2N C-7

Sample Description

Dimensions:	4-1/16 inches wide, 2 9/16 inches long
Top surface finish:	Grooves evident
Bottom surface finish:	Sawcut from full core sample
Reinforcement:	None in polished section
Cracks, Joints, Voids:	Several moderate and small voids where not fully consolidated. Two located within top ½ inch.

Aggregates

Coarse aggregate:

Type:	Multi-colored foliated granite, with some mafic minerals. Typically dark gray, light gray, white, pink and green.
Gradation and top size:	Well-graded, ¾ inch or 1 inch max nominal size
Shape and distribution:	Subangular to angular, evenly distributed. Some particles elongated.

Fine aggregate:

Type:	Multi-colored natural silica, mainly white, clear, and light gray. Some tan and brown.
Gradation and top size:	Well-graded, 3/8 inch max nominal size
Shape and distribution:	Subangular to subrounded

Paste

Color:	Medium gray
Luster:	Subvitreous
Hardness:	Moderately hard to hard.
Supplementary cementitious matls:	Possibly contains fly ash, but not confirmed. Dark particles evident, which may be fly ash, but cenospheres not observed after acid etch. Mixture submittals not available.
Depth of carbonation:	Approx. 1/8 inch

Other observations

Paste-aggregate bond:	Good, except along aggregate perimeters where entrained air voids have coalesced.
Secondary deposits:	Trace deposits observed in a few voids.
Air content:	Air-entrained, approx 6-8%
Microcracking:	Several microcracks extending from top surface, typically within top ½ inch.
Estimated water-cement ratio:	0.35-0.40 (with water-reducing admixture, assumed)

Notes

1. In a number of areas, entrained air voids have coalesced, resulting in a localized high air content.
2. Some areas of sample have relatively higher air content than other areas.
3. Samples 2L C-3 and 2L C-4 contain more microcracks than samples 2N C-6 and 2N C-7. Localized areas of high air content are more prevalent in samples 2L C-6 and 2L C-7.

Figure I-42: Datasheet for petrographic examination of sample 2N C-7.

MACROSCOPIC AND MICROSCOPIC OBSERVATION OF HARDENED CONCRETE – POLISHED SAMPLE

Project Name:	NCDOT 2011-06		
Client:	NCDOT	**Project No.:**	520180
Observations by:	Tara Cavalline	**Date:**	Spring / Summer 2012

Type of Structure: Concrete bridge deck 150012 (2L)
Location: Carteret County, North Carolina
Purpose: Observe general characteristics

Sample ID: 2L C-3

Sample Description

Dimensions: 4-1/16 inches wide, 3 1/16 inches long
Top surface finish: Grooves evident
Bottom surface finish: Sawcut from full core sample
Reinforcement: None in polished section
Cracks, Joints, Voids: Only air-entrained voids within coarse aggregates are visible

Aggregates

Coarse aggregate:
- Type: Manufactured lightweight aggregate typically medium gray to dark gray.
- Gradation and top size: Well-graded, ¾ inch max nominal size
- Shape and distribution: Subangular, relatively evenly distributed.

Fine aggregate:
- Type: Multi-colored natural silica, mainly white, clear, and light gray. Some tan and brown.
- Gradation and top size: Well-graded, 3/8 inch max nominal size.
- Shape and distribution: Subangular to subrounded.

Paste

Color: Medium gray
Luster: Subvitreous
Hardness: Moderately hard to hard. Areas of deteriorated paste along some near-surface microcracks.
Supplementary cementitious matls: Possibly contains fly ash, but not confirmed. Dark particles evident, which may be fly ash, but cenospheres not observed after acid etch. Mixture submittals not available.
Depth of carbonation: Approx. ½ inch

Other observations

Paste-aggregate bond: Good, except along aggregate perimeters where entrained air voids have coalesced.
Secondary deposits: Secondary deposits observed lining or filling a number of entrained air voids in the vicinity of microcracks. Secondary deposits typically limited to voids near microcracks.
Air content: Air-entrained, approx. 6-8%
Microcracking: Several microcracks extending from top surface, mainly through coarse aggregate, some around aggregate perimeters, typically within top 1 inch. A few microcracks in interior of sample.
Estimated water-cement ratio: 0.35-0.40 (with water reducing admixture, assumed)

Notes

1. In a number of areas, entrained air voids have coalesced, resulting in a localized high air content.
2. Microcracks tend to propogate through localized areas of high air content.
3. Samples 2L C-3 and 2N C-4 contain more microcracks than samples 2N C-6 and 2N C-7. Localized areas of high air content are more prevalent in samples 2L C-6 and 2L C-7.

Figure I-43: Datasheet for petrographic examination of sample 2L C-3.

MACROSCOPIC AND MICROSCOPIC OBSERVATION OF HARDENED CONCRETE – POLISHED SAMPLE

Project Name:	NCDOT 2011-06		
Client:	NCDOT	**Project No.:**	520180
Observations by:	Tara Cavalline	**Date:**	Spring / Summer 2012

Type of Structure: Concrete bridge deck 150012 (2L)
Location: Carteret County, North Carolina
Purpose: Observe general characteristics

Sample ID: 2L C-4

Sample Description

Dimensions: 4-1/16 inches wide, 3 inches long
Top surface finish: Grooves evident
Bottom surface finish: Sawcut from full core sample
Reinforcement: None in polished section
Cracks, Joints, Voids: A few small voids where not fully consolidated, typically in lower portion of sample.

Aggregates

Coarse aggregate:

Type:	Manufactured lightweight aggregate, typically medium gray to dark gray.
Gradation and top size:	Well-graded, ¾ inch to 1 inch max nominal size.
Shape and distribution:	Subangular, relatively evenly distributed.

Fine aggregate:

Type:	Multi-colored natural silica, mainly white, clear, and light gray. Some tan and brown.
Gradation and top size:	Well-graded, 3/8 inch max nominal size.
Shape and distribution:	Subangular to subrounded.

Paste

Color:	Medium Gray
Luster:	Subvitreous
Hardness:	Moderately hard to hard. Areas of deteriorated paste along some near-surface microcracks.
Supplementary cementitious matls:	Possibly contains fly ash, but not confirmed. Dark particles evident, which may be fly ash, but cenospheres not observed after acid etch. Mixture submittals not available.
Depth of carbonation:	Approx. ¼ inch

Other observations

Paste-aggregate bond:	Good, except along aggregate perimeters where entrained air voids have coalesced.
Secondary deposits:	Secondary deposits observed lining or filling a number of entrained air voids in the vicinity of microcracks. Secondary deposits typically limited to voids near microcracks.
Air content:	Air-entrained, approx. 6-8%
Microcracking:	Several microcracks extending from topsurface, some through coarse aggregate, most around aggregate perimeters typically within top 1 inch. A few microcracks in interior of sample.
Estimated water-cement ratio:	0.35-0.40 (with water-reducing admixture, assumed)

Notes

1. In a number of areas, entrained air voids have coalesced, resulting in a localized high air content.
2. Microcracks tend to propagate through localized areas of high air content.
3. Samples 2L C-3 and 2L C-4 contain more microcracks than samples 2N C-6 and 2N C-7. Localized areas of high air content are more prevalent in samples 2L C-3 and 2L C-4.

Figure I-44: Datasheet for petrographic examination of sample 2L C-4.

MACROSCOPIC AND MICROSCOPIC OBSERVATION OF HARDENED CONCRETE – POLISHED SAMPLE

Project Name:	NCDOT 2011-06		
Client:	NCDOT	**Project No.:**	520180
Observations by:	Tara Cavalline	**Date:**	Spring / Summer 2012

Type of Structure: Concrete bridge deck 150014 (3N)
Location: Carteret County, North Carolina
Purpose: Observe general charactistics

Sample ID: 3N C-2

Sample Description

Dimensions:	4-1/16 inches wide, 2-5/16 inches long
Top surface finish:	Grooves evident, but shallower (surface more worn) than grooves in sample 3L C-6.
Bottom surface finish:	Sawcut from full core sample
Reinforcement:	None in polished section
Cracks, Joints, Voids:	A few small voids and one moderate sized void where not fully consolidated.

Aggregates

Coarse aggregate:

Type:	Multicolored foliated granite, with some mafic minerals. Typically light gray, dark gray, and white, with some pink and green.
Gradation and top size:	Well-graded, ¾ inch max nominal size.
Shape and distribution:	Larger particles subangular to subrounded. Smaller particles tend to be flatter and more elongated. Tends to be a little sparse in some areas of sample.

Fine aggregate:

Type:	Multi-colored natural silica, mainly white, clear, and light gray. Some tan and brown.
Gradation and top size:	Well-graded, 3/8 inch max nominal size.
Shape and distribution:	Subangular to subrounded

Paste

Color:	Medium gray
Luster:	Subvitreous
Hardness:	Moderately hard to hard
Supplementary cementitious matls:	Possibly contains fly ash, but not confirmed. Dark particles evident, which may be fly ash, but cenospheres not observed after acid etch. Mixture submittals not available.
Depth of carbonation:	Approx. 1/8 inch

Other observations

Paste-aggregate bond:	Good
Secondary deposits:	Trace amounts observed in a few small voids.
Air content:	Air-entrained, approx. 5-7%
Microcracking:	One microcrack extending from top surface. Initiates at near-surface void where concrete not consolidated. Another microcrack extending from top surface to depth of ½ inch. Several shorter microcracks extending from top surface to depth less than ¼ inch.
Estimated water-cement ratio:	0.35-0.40 (with water reducing admixture, assumed)

Notes

1. Extent of microcracking observed in this sample is similar to the extent observed in sample 3L C-6.

Figure I-45: Datasheet for petrographic examination of sample 3N C-2.

MACROSCOPIC AND MICROSCOPIC OBSERVATION OF HARDENED CONCRETE – POLISHED SAMPLE

Project Name:	NCDOT 2011-06		
Client:	NCDOT	**Project No.:**	520180
Observations by:	Tara Cavalline	**Date:**	Spring / Summer 2012

Type of Structure: Concrete bridge deck 150014 (3N)
Location: Carteret County, North Carolina
Purpose: Observe general characteristics

Sample ID: 3N C-3

Sample Description

Dimensions:	4-1/16 inches wide, 3 inches long
Top surface finish:	Grooves evident, but shallower than grooves in sample 3L C-6 (surface more worn)
Bottom surface finish:	Sawcut from full core sample
Reinforcement:	None in polished section
Cracks, Joints, Voids:	A few small voids where not fully consolidated

Aggregates

Coarse aggregate:

Type:	Multicolored foliated granite, with some mafic minerals. Typically light gray, dark gray, and white, with some pink and green.
Gradation and top size:	Well-graded, ¾ inch max nominal size
Shape and distribution:	Larger particles subequant to subrounded. Smaller particles tend to be flatter and more elongated. Well-distributed

Fine aggregate:

Type:	Multi-colored natural silica, mainly white, clear, and light gray. Some tan and brown
Gradation and top size:	Well-graded, 3/8 inch nominal size
Shape and distribution:	Subangular to subrounded

Paste

Color:	Medium gray
Luster:	Subvitreous
Hardness:	Moderately hard to hard
Supplementary cementitious matls:	Possibly contains fly ash, but not confirmed. Dark particles evident, which may be fly ash, but cenospheres not observed after acid etch. Mixture submittals not available.
Depth of carbonation:	Approx. ¼ inch

Other observations

Paste-aggregate bond:	Good
Secondary deposits:	Trace deposits observed in a few voids.
Air content:	Air-entrained, approx. 4-6%
Microcracking:	Several microcracks extending from top surface, typically within top ½ inch. A few small microcracks in interior, typical propagating from air voids or coarse aggregate perimeters. One larger microcrack propagates through a flat coarse aggregate.
Estimated water-cement ratio:	0.35-0.40 (with water-reducing admixture, assumed)

Notes

1. Extent of microcracking observed in this sample is similar to the extent observed in sample 3L C-6.

Figure I-46: Datasheet for petrographic examination of sample 3N C-3.

MACROSCOPIC AND MICROSCOPIC OBSERVATION OF HARDENED CONCRETE – POLISHED SAMPLE

Project Name:	NCDOT 2011-06		
Client:	NCDOT	**Project No.:**	520180
Observations by:	Tara Cavalline	**Date:**	Spring / Summer 2012

Type of Structure: Concrete bridge deck 150014 (3L)
Location: Carteret County, North Carolina
Purpose: Observe general characteristics

Sample ID: 3L C-6

Sample Description

Dimensions: 4-1/16 inches wide, 3 inches long
Top surface finish: Grooves evident
Bottom surface finish: Sawcut from full core sample
Reinforcement: None in polished section
Cracks, Joints, Voids:

Aggregates

Coarse aggregate:

Type:	Manufactured lightweight aggregate, typically dark gray to medium gray
Gradation and top size:	Well-graded, 3/4 inch max nominal size
Shape and distribution:	Subequant to subangular, well distributed

Fine aggregate:

Type:	Multi-colored natural silica, mainly white, clear, and light gray. Some tan and brown
Gradation and top size:	Well-graded, 3/8 inch max nominal size
Shape and distribution:	Subangular to subrounded

Paste

Color:	Medium gray
Luster:	Subvitreous
Hardness:	Moderately hard to hard
Supplementary cementitious matls:	Possibly contains fly ash, but not confirmed. Dark particles evident, which may be fly ash, but cenospheres not observed after acid etch. Mixture submittals not available.
Depth of carbonation:	Approx. ½ inch

Other observations

Paste-aggregate bond:	Good
Secondary deposits:	Trace amounts observed in a few voids
Air content:	Air-entrained, approx. 4-6%
Microcracking:	Several small microcracks extending from top surface, typically within top ½ inch. A few small microcracks in the interior, typical propagating from air voids or coarse aggregate perimeters.
Estimated water-cement ratio:	0.35-0.40 (with water-reducing admixture, assumed)

Notes

1. Extent of microcracking observed in this sample is similar to that observed in samples 3N C-2 and 3N C-3.

Figure I-47: Datasheet for petrographic examination of sample 3L C-6.

MACROSCOPIC AND MICROSCOPIC OBSERVATION OF HARDENED CONCRETE – POLISHED SAMPLE

Project Name:	NCDOT 2011-06		
Client:	NCDOT	**Project No.:**	520180
Observations by:	Tara Cavalline	**Date:**	Spring / Summer 2012

Type of Structure: Concrete bridge deck 270012 (5N)
Location: Dare County, North Carolina
Purpose: Observe general characteristics

Sample ID: 5N C-3

Sample Description

Dimensions: 4-1/16 inches wide, 3 inches long
Top surface finish: Grooves evident
Bottom surface finish: Sawcut from full core sample
Reinforcement: None in polished section
Cracks, Joints, Voids: Macrocrack propagating vertically from top surface to approx. ¾ inch depth. Some small to moderate voids where not fully consolidated, mostly near top of sample.

Aggregates

Coarse aggregate:

Type:	Multicolored granite, mainly potassium feldspar, with some quartz, some plagioclase feldspar, and some mafic material. Typically pink, beige, white, dark gray, and light gray.
Gradation and top size:	Well-graded, ¾ inch max nominal size
Shape and distribution:	Subequant to subrounded. Well-distributed

Fine aggregate:

Type:	Multi-colored natural silica, mainly white, clear and light gray, some tan and brown.
Gradation and top size:	Well-graded, 3/8 inch max nominal size
Shape and distribution:	Subrounded to subangular

Paste

Color:	Medium gray
Luster:	Subvitreous
Hardness:	Moderately hard to hard
Supplementary cementitious matls:	Possibly contains fly ash, but not confirmed. Dark particles evident, which may be fly ash, but cenospheres not observed after acid etch. Mixture submittals not available.
Depth of carbonation:	None

Other observations

Paste-aggregate bond:	Good
Secondary deposits:	A few secondary deposits lining a few voids.
Air content:	Air-entrained, approx. 5-7%
Microcracking:	Microcrack extending from macrocrack, extends to depth approx. 2 ½ inches from top surface. Macrocrack propagates through coarse aggregate, then microcrack propagates around aggregate boundaries. No others microcracks observed.
Estimated water-cement ratio:	0.35-0.40 (with water-reducing admixture, assumed)

Notes

1. Although one large micro/macrocrack present in this sample, more microcracks observed in 5N C-8.

Figure I-48: Datasheet for petrographic examination of sample 5N C-3.

MACROSCOPIC AND MICROSCOPIC OBSERVATION OF HARDENED CONCRETE – POLISHED SAMPLE

Project Name:	NCDOT 2011-06		
Client:	NCDOT	**Project No.:**	520180
Observations by:	Tara Cavalline	**Date:**	Spring / Summer 2012

Type of Structure: Concrete bridge deck 270012 (5N)
Location: Dare County, North Carolina
Purpose: Observe general characteristics

Sample ID: 5N C-8

Sample Description

Dimensions:	4-1/16 inches wide, 3-1/16 inches long
Top surface finish:	Grooves evident
Bottom surface finish:	Sawcut from full core sample
Reinforcement:	None in polished section
Cracks, Joints, Voids:	A few small voids where not fully consolidated.

Aggregates

Coarse aggregate:

Type:	Multicolored granite, mainly potassium feldspar, with some quartz, some plagioclase feldspar, and some mafic material. Typically pink, beige, white, dark gray, and light gray.
Gradation and top size:	Well-graded, ¾ inch max nominal size
Shape and distribution:	Subequant to subrounded. Well-distributed

Fine aggregate:

Type:	Multi-colored natural silica, mainly white, clear, and light gray. Some tan and brown.
Gradation and top size:	Well-graded, 3/8 inch max nominal size
Shape and distribution:	Subrounded to subangular

Paste

Color:	Medium gray
Luster:	Subvitreous
Hardness:	Moderately hard to hard
Supplementary cementitious matls:	Possibly contains fly ash, but not confirmed. Dark particles evident, which may be fly ash, but cenospheres not observed after acid etch. Mixture submittals not available.
Depth of carbonation:	Approx. 1/8 inch

Other observations

Paste-aggregate bond:	Good
Secondary deposits:	A few trace deposits in some voids. A few very small voids near surface filled with white secondary deposit.
Air content:	Air-entrained, approx. 5-7%
Microcracking:	Several microcracks extending vertically from top surface of sample. Typically propagate through paste, microcrack propagates through a coarse aggregate. Most microcracks located within top ½ inch.
Estimated water-cement ratio:	0.35-0.40 (with water-reducing admixture, assumed)

Notes

1. Relatively more microcracks observed in 5N C-8 then observed in 5N C-3.
2. Extent of microcracking observed is similar to microcracking observed in 5L C-8.

Figure I-49: Datasheet for petrographic examination of sample 5N C-8.

MACROSCOPIC AND MICROSCOPIC OBSERVATION OF HARDENED CONCRETE – POLISHED SAMPLE

Project Name:	NCDOT 2011-06		
Client:	NCDOT	**Project No.:**	520180
Observations by:	Tara Cavalline	**Date:**	Spring / Summer 2012

Type of Structure: Concrete bridge deck 270012 (5L)
Location: Dare County, North Carolina
Purpose: Observe general characteristics

Sample ID: 5L C-5

Sample Description

Dimensions:	4-1/16 inches wide, 2-7/16 inches long
Top surface finish:	Grooves evident
Bottom surface finish:	Sawcut from full core sample
Reinforcement:	None in polished section
Cracks, Joints, Voids:	A few small voids where not fully consolidated.

Aggregates

Coarse aggregate:

Type:	Manufactured lightweight aggregate, typically dark gray to medium gray
Gradation and top size:	Well-graded, ¾ inch max nominal size
Shape and distribution:	Subequant to subangular, well-distributed

Fine aggregate:

Type:	Multi-colored natural silica, mainly white, clear, light gray, tan and brown
Gradation and top size:	Well-graded, 3/8 inch max nominal size
Shape and distribution:	Subrounded to subangular

Paste

Color:	Medium gray
Luster:	Subvitreous
Hardness:	Moderately hard to hard
Supplementary cementitious matls:	Possibly contains fly ash, but not confirmed. Dark particles evident, which may be fly ash, but cenospheres not observed after acid etch. Mixture submittals not available.
Depth of carbonation:	None

Other observations

Paste-aggregate bond:	Good
Secondary deposits:	A few white secondary deposits present in a few voids in paste and in coarse aggregates.
Air content:	Air-entrained, approx. 3-5%
Microcracking:	A few microcracks extending downward from top surface, some diagonally. Typical propagate through paste, some through coarse aggregate particles.
Estimated water-cement ratio:	0.35-0.40 (with water-reducing admixture, assumed)

Notes

1. Relatively lower entrained air content compared to samples 5N C-3 and 5N C-8.
2. Extent of microcracking observed is similar to microcracking observed in 5N C-8.

Figure I-50: Datasheet for petrographic examination of sample 5L C-5.

MACROSCOPIC AND MICROSCOPIC OBSERVATION OF HARDENED CONCRETE – POLISHED SAMPLE

Project Name:	NCDOT 2011-06		
Client:	NCDOT	**Project No.:**	520180
Observations by:	Tara Cavalline	**Date:**	Spring / Summer 2012

Type of Structure: Concrete bridge deck 270012 (5L)
Location: Dare County, North Carolina
Purpose: Observe general characteristics

Sample ID: 5L C-8

Sample Description

Dimensions:	4-1/16 inches wide, 2-7/16 inches long
Top surface finish:	Grooves evident
Bottom surface finish:	Sawcut from full core sample
Reinforcement:	None in polished section
Cracks, Joints, Voids:	A few small voids where not fully consolidated.

Aggregates

Coarse aggregate:

Type:	Manufactured lightweight aggregate, typically dark gray to medium gray
Gradation and top size:	Well-graded, ¾ inch max nominal size
Shape and distribution:	Subrounded to subangular

Fine aggregate:

Type:	Multi-colored natural silica, mainly white, clear, light gray, tan and brown
Gradation and top size:	Well-graded, 3/8 inch max nominal size
Shape and distribution:	Subrounded to subangular

Paste

Color:	Medium gray
Luster:	Subvitreous
Hardness:	Moderately hard to hard
Supplementary cementitious matls:	Possibly contains fly ash, but not confirmed. Dark particles evident, which may be fly ash, but cenospheres not observed after acid etch. Mixture submittals not available.
Depth of carbonation:	Approx. ½ inch

Other observations

Paste-aggregate bond:	Good
Secondary deposits:	A few white secondary deposits present in a few voids in paste and in coarse aggregates.
Air content:	Air-entrained, approx. 3-5%
Microcracking:	A few microcracks extending downward from top surface, some diagonally. Typically propagate through paste, some through coarse aggregate particles
Estimated water-cement ratio:	0.35-0.40 (with water-reducing admixture, assumed)

Notes

1. Relatively lower entrained air content compared to samples 5N C-3 and 5N C-8.
2. Extent of microcracking observed is similar to microcracking observed in 5N C-8.

Figure I-51: Datasheet for petrographic examination of sample 5L C-8.

MACROSCOPIC AND MICROSCOPIC OBSERVATION OF HARDENED CONCRETE – POLISHED SAMPLE

Project Name:	NCDOT 2011-06		
Client:	NCDOT	**Project No.:**	520180
Observations by:	Tara Cavalline	**Date:**	Spring / Summer 2012

Type of Structure: Concrete bridge deck 330345 (6N)
Location: Forsythe County, North Carolina
Purpose: Observe general characteristics

Sample ID: 6N C-3

Sample Description

Dimensions:	4-1/16 inches wide, 3 inches long
Top surface finish:	Grooves evident
Bottom surface finish:	Sawcut from full core sample
Reinforcement:	None in polished section
Cracks, Joints, Voids:	A few small voids and a few moderately sized voids where not fully consolidated.

Aggregates

Coarse aggregate:

Type:	Foliated granite, more mafic material than other granites observed in this study. Some quartz, some plagioclase feldspar, and some potassium feldspar. Typically dark gray and light gray with some pink.
Gradation and top size:	Well-graded ¾ inch max nominal size
Shape and distribution:	Larger particles subangular to subrounded. Smaller particles tend to be flatter and more elongated.

Fine aggregate:

Type:	Multi-colored natural silica, mainly white, clear, and light gray. Some tan and brown.
Gradation and top size:	Well-graded, 3/8 inch max nominal size.
Shape and distribution:	Subangular to subrounded

Paste

Color:	Medium gray
Luster:	Subvitreous
Hardness:	Moderately hard to hard
Supplementary cementitious matls:	Possibly contains fly ash, but not confirmed. Dark particles evident, which may be fly ash, but cenospheres not observed after acid etch. Mixture submittals not available.
Depth of carbonation:	Approx. 1/8 inch

Other observations

Paste-aggregate bond:	Good
Secondary deposits:	Trace amounts observed in a few small voids.
Air content:	Air-entrained, approx. 5-7%
Microcracking:	A few microcracks extending from top surface, mainly around aggregate perimeters but through some coarse aggregates. Typically within top 1 inch, one microcrack extends to a depth of approx. 2 inches.
Estimated water-cement ratio:	0.35-0.40 (with water-reducing admixture, assumed)

Notes

1. Samples 6N C-3 and 6N C-6B appear to contain more microcracks than 6L C-1 and 6L C-6A.
2. More white secondary deposits observed in 6L C-1 and 6L C-6A than observed in 6N C-3 and 6N C-6B.

Figure I-52: Datasheet for petrographic examination of sample 6N C-3.

MACROSCOPIC AND MICROSCOPIC OBSERVATION OF HARDENED CONCRETE – POLISHED SAMPLE

Project Name:	NCDOT 2011-06		
Client:	NCDOT	**Project No.:**	520180
Observations by:	Tara Cavalline	**Date:**	Spring / Summer 2012

Type of Structure: Concrete bridge deck 330345 (6N)
Location: Forsythe County, North Carolina
Purpose: Observe general characteristics

Sample ID: 6N C-6B

Sample Description

Dimensions:	4-1/16 inches wide, 3 inches long
Top surface finish:	Grooves evident
Bottom surface finish:	Sawcut from full core sample
Reinforcement:	None in polished section
Cracks, Joints, Voids:	A few small voids and one moderate sized void where not fully consolidated.

Aggregates

Coarse aggregate:

Type:	Foliated granite, more mafic material than other granites observed in this study. Some quartz, some plagioclase feldspar, and some potassium feldspar. Typically dark gray and light gray with some pink.
Gradation and top size:	Well-graded ¾ inch max nominal size
Shape and distribution:	Larger particles subangular to subrounded. Smaller particles tend to be flatter and more elongated.

Fine aggregate:

Type:	Multi-colored natural silica, mainly white, clear, and light gray. Some tan and brown.
Gradation and top size:	Well-graded, 3/8 inch max nominal size
Shape and distribution:	Subangular to subrounded

Paste

Color:	Medium gray
Luster:	Subvitreous
Hardness:	Moderately hard to hard
Supplementary cementitious matls:	Possibly contains fly ash, but not confirmed. Dark particles evident, which may be fly ash, but cenospheres not observed after acid etch. Mixture submittals not available.
Depth of carbonation:	Approx. 1 inch

Other observations

Paste-aggregate bond:	Good
Secondary deposits:	Trace amounts observed in a few small voids
Air content:	Air-entrained, approx. 5-7%
Microcracking:	A few microcracks extending from top surface, mainly around aggregate perimeters, typically within top ½ inch.
Estimated water-cement ratio:	0.35-0.40 (with water-reducing admixture, assumed)

Notes

1. Samples 6N C-3 and 6N C-6 B appear to contain more microcracks than 6L C-1 and 6L C-6A.
2. More white secondary deposits observed in 6L C-1 and 6L C-6A than observed in 6N C-3 and 6N C-6B.

Figure I-53: Datasheet for petrographic examination of sample 6N C-6B.

MACROSCOPIC AND MICROSCOPIC OBSERVATION OF HARDENED CONCRETE – POLISHED SAMPLE

Project Name:	NCDOT 2011-06		
Client:	NCDOT	**Project No.:**	520180
Observations by:	Tara Cavalline	**Date:**	Spring / Summer 2012

Type of Structure: Concrete bridge deck 330254 (6L)
Location: Forsythe County, North Carolina
Purpose: Observe general characteristics

Sample ID: 6L C-1

Sample Description

Dimensions:	4-1/16 inches wide, 2-7/8 inches long
Top surface finish:	Grooves evident
Bottom surface finish:	Sawcut from full core sample
Reinforcement:	None in polished section
Cracks, Joints, Voids:	A few small voids and a few moderately sized voids where not fully consolidated.

Aggregates

Coarse aggregate:

Type:	Manufactured lightweight aggregate, typically dark gray to medium gray
Gradation and top size:	Well-graded ¾ inch max nominal size
Shape and distribution:	Subangular to subrounded, some particles flatter and more elongated than others

Fine aggregate:

Type:	Multi-colored natural silica, mainly white, clear, and light gray. Some tan and brown.
Gradation and top size:	Well-graded, 3/8 inch max nominal size
Shape and distribution:	Subangular to subrounded

Paste

Color:	Medium gray
Luster:	Subvitreous
Hardness:	Moderately hard to hard
Supplementary cementitious matls:	Possibly contains fly ash, but not confirmed. Dark particles evident, which may be fly ash, but cenospheres not observed after acid etch. Mixture submittals not available.
Depth of carbonation:	Approx. ¼ inch

Other observations

Paste-aggregate bond:	Good
Secondary deposits:	Secondary deposits observed lining or filling many entrained air voids and some voids in coarse aggregate perimeters.
Air content:	Air-entrained, 6-8% some water voids
Microcracking:	One microcrack extending from the top surface extending ½ inch
Estimated water-cement ratio:	0.35-0.40 (with water-reducing admixture, assumed)

Notes

1. Significantly fewer water voids in 6L C-1 than in 6L C-6A.
2. Samples 6N C-3 and 6N C-6 B appear to contain more microcracks than 6L C-1 and 6L C-6A.
3. More white secondary deposits observed in 6L C-1 and 6L C-6A than observed in 6N C-3 and 6N C-6B.

Figure I-54: Datasheet for petrographic examination of sample 6L C-1.

MACROSCOPIC AND MICROSCOPIC OBSERVATION OF HARDENED CONCRETE – POLISHED SAMPLE

Project Name:	NCDOT 2011-06		
Client:	NCDOT	**Project No.:**	520180
Observations by:	Tara Cavalline	**Date:**	Spring / Summer 2012

Type of Structure: Concrete bridge deck 330254 (6L)
Location: Forsythe County, North Carolina
Purpose: Observe general characteristics

Sample ID: 6L C-6A

Sample Description

Dimensions:	4 inches wide, 2¾ inches long
Top surface finish:	Grooves evident
Bottom surface finish:	Sawcut from full core sample
Reinforcement:	None in polished section
Cracks, Joints, Voids:	A few very small voids where not fully consolidated.

Aggregates

Coarse aggregate:

Type:	Manufactured lightweight aggregate, typically dark gray to medium gray
Gradation and top size:	Well-graded ¾ inch max nominal size
Shape and distribution:	Subangular to subrounded, some particles flatter and more elongated than others. Tends to be more sparse in areas.

Fine aggregate:

Type:	Multi-colored natural silica, mainly white, clear, and light gray. Some tan and brown.
Gradation and top size:	Well-graded, 3/8 inch max nominal size.
Shape and distribution:	Subangular to subrounded

Paste

Color:	Medium gray
Luster:	Subvitreous
Hardness:	Moderately hard to hard
Supplementary cementitious matls:	Possibly contains fly ash, but not confirmed. Dark particles evident, which may be fly ash, but cenospheres not observed after acid etch. Mixture submittals not available.
Depth of carbonation:	Approx. 3/8 inch

Other observations

Paste-aggregate bond:	Good
Secondary deposits:	Secondary deposits typically limited to voids near microcracks.
Air content:	Air-entrained, approx. 7-9% plus a number of irregularly shaped water voids similar in size to air-entrained voids.
Microcracking:	Two microcracks observed extending from top surface to ½ inch.
Estimated water-cement ratio:	0.35-0.40 (with water-reducing admixture, assumed)

Notes

1. Inordinate number of water voids may contribute to weaker paste structure.
2. Some evidence of segregation.
3. Some areas of deteriorated paste at top surface, near microcracks and grooves.
4. Samples 6N C-3 and 6N C-6 B appear to contain more microcracks than 6L C-1 and 6L C-6 A.
5. More white secondary deposits observed in 6L C-1 and 6L C-6A than observed in 6N C-3 and 6N C-6B.

Figure I-55: Datasheet for petrographic examination of sample 6L C-6A.

MACROSCOPIC AND MICROSCOPIC OBSERVATION OF HARDENED CONCRETE – POLISHED SAMPLE

Project Name:	NCDOT 2011-06		
Client:	NCDOT	**Project No.:**	520180
Observations by:	Tara Cavalline	**Date:**	Spring / Summer 2012

Type of Structure: Concrete bridge deck 590541 (7N)
Location: Mecklenburg, North Carolina
Purpose: Observe general characteristics

Sample ID: 7N C-6

Sample Description

Dimensions: 4-1/16 inches wide, 3-1/16 inches long
Top surface finish: Grooves evident
Bottom surface finish: Sawcut from full core sample
Reinforcement: None in polished section
Cracks, Joints, Voids: A number of small to medium voids were not fully consolidated. Macrocrack extending from top surface to depth of approx. 1½ inches and propagates through coarse aggregates.

Aggregates

Coarse aggregate:
- Type: Granitic material, mainly plagioclase feldspar. Also some mafic material and some quartz material present (roughly equal). Some localized potassium feldspar present. Typically light gray, dark gray, and white, with some pink.
- Gradation and top size: ¾ inch max nominal size, sample is heavy on smaller sizes
- Shape and distribution: Subangular to subrounded relatively evenly distributed, some smaller sizes relatively elongated.

Fine aggregate:
- Type: Multi-colored natural silica, mainly white, clear, and light gray. Some tan and brown.
- Gradation and top size: Well-graded, 3/8 inch max nominal size.
- Shape and distribution: Subangular to subrounded

Paste

Color: Medium to light gray
Luster: Subvitreous
Hardness: Moderately hard to hard
Supplementary cementitious matls: Possibly contains fly ash, but not confirmed. Dark particles evident, which may be fly ash, but cenospheres not observed after acid etch. Mixture submittals not available.
Depth of carbonation: Approx. ¼ inch

Other observations

Paste-aggregate bond: Good
Secondary deposits: A few secondary deposits lining or filling some air-entrained air voids in localized areas. Not judged to be extensive.
Air content: Air-entrained, approx. 3-5%
Microcracking: One microcrack near top surface within top ¼ inch
Estimated water-cement ratio: 0.35-0.40 (with water-reducing admixture, assumed)

Notes

1. More secondary deposits observed in 7L C-5A and 7L C-7A than observed in 7N C-6 and 7N C-8.
2. Extent of microcracking in 7N C-6 and 7N C-8 appears to be similar to the extent of microcracking in 7L C-5A and 7L C-7A.

Figure I-56: Datasheet for petrographic examination of sample 7N C-6.

MACROSCOPIC AND MICROSCOPIC OBSERVATION OF HARDENED CONCRETE – POLISHED SAMPLE

Project Name:	NCDOT 2011-06		
Client:	NCDOT	**Project No.:**	520180
Observations by:	Tara Cavalline	**Date:**	Spring / Summer 2012

Type of Structure: Concrete bridge deck 590541 (7N)
Location: Mecklenburg, North Carolina
Purpose: Observe general characteristics

Sample ID: 7N C-8

Sample Description

Dimensions:	4 1/16 inches wide, 3 inches long
Top surface finish:	Grooves evident
Bottom surface finish:	Sawcut from full core sample
Reinforcement:	None in polished section
Cracks, Joints, Voids:	A few small voids where not fully consolidated.

Aggregates

Coarse aggregate:

Type:	Granitic material, mainly plagioclase feldspar. Also some mafic material and some quartz material present (roughly equal). Some localized potassium feldspar present. Typically light gray, dark gray, and white, with some pink.
Gradation and top size:	Well-graded, ¾ inch max nominal size
Shape and distribution:	Subangular to subrounded relatively evenly distributed, some smaller sizes relatively elongated.

Fine aggregate:

Type:	Multi-colored natural silica, mainly white, clear, and light gray. Some tan and brown.
Gradation and top size:	Well-graded, 3/8 inch max nominal size.
Shape and distribution:	Subangular to subrounded

Paste

Color:	Medium to light gray
Luster:	Subvitreous
Hardness:	Moderately hard to hard
Supplementary cementitious matls:	Possibly contains fly ash, but not confirmed. Dark particles evident, which may be fly ash, but cenospheres not observed after acid etch. Mixture submittals not available.
Depth of carbonation:	Approx. ¼ inch

Other observations

Paste-aggregate bond:	Good
Secondary deposits:	A few secondary deposits lining or filling some air-entrained air voids in localized areas. Not judged to be extensive.
Air content:	Air-entrained, approx. 3-5%
Microcracking:	One macrocrack
Estimated water-cement ratio:	0.35-0.40 (with water-reducing admixture, assumed)

Notes

1. More secondary deposits observed in 7L C-5A and 7L C-7A than observed in 7N C-6 and 7N C-8.
2. Extent of microcracking in 7N C-6 and 7N C-8 appears to be similar to the extent of microcracking in 7L C-5A and 7L C-7A.

Figure I-57: Datasheet for petrographic examination of sample 7N C-8.

MACROSCOPIC AND MICROSCOPIC OBSERVATION OF HARDENED CONCRETE – POLISHED SAMPLE

Project Name:	NCDOT 2011-06		
Client:	NCDOT	**Project No.:**	520180
Observations by:	Tara Cavalline	**Date:**	Spring / Summer 2012

Type of Structure: Concrete bridge deck 590363 (7L)
Location: Mecklenburg, North Carolina
Purpose: Observe general characteristics

Sample ID: 7L C-5A

Sample Description

Dimensions:	4 1/16 inches wide, 2 ½ inches long
Top surface finish:	Grooves evident
Bottom surface finish:	Sawcut from full core sample
Reinforcement:	None in polished section
Cracks, Joints, Voids:	A few very small voids where not fully consolidated.

Aggregates

Coarse aggregate:

Type:	Manufactured lightweight aggregate, typically dark gray to medium gray
Gradation and top size:	Well-graded, ¾ inch max nominal size
Shape and distribution:	Subangular to subrounded relatively evenly distributed

Fine aggregate:

Type:	Multi-colored natural silica, mainly white, clear, and light gray. Some tan and brown.
Gradation and top size:	Well-graded, 3/8 inch max nominal size.
Shape and distribution:	Subangular to subrounded

Paste

Color:	Medium Gray
Luster:	Subvitreous
Hardness:	Moderately hard to hard
Supplementary cementitious matls:	Possibly contains fly ash, but not confirmed. Dark particles evident, which may be fly ash, but cenospheres not observed after acid etch. Mixture submittals not available.
Depth of carbonation:	Approx. ½ inch

Other observations

Paste-aggregate bond:	Good
Secondary deposits:	Secondary deposits lining and filling many entrained air voids and some voids in coarse aggregates. Tends to be present in localized areas, mostly near surface and near microcracks. Upper 1 inch of sample.
Air content:	Air-entrained, approx. 5-7%
Microcracking:	Two microcracks extending from top surface typically within upper ½ inch.
Estimated water-cement ratio:	0.35-0.40 (with water-reducing admixture, assumed)

Notes

1. More secondary deposits observed in 7L C-5A and 7L C-7A than observed in 7N C-6 and 7N C-8.
2. Extent of microcracking in 7N C-6 and 7N C-8 appears to be similar to the extent of microcracking in 7L C-5A and 7L C-7A.

Figure I-58: Datasheet for petrographic examination of sample 7L C-5A.

MACROSCOPIC AND MICROSCOPIC OBSERVATION OF HARDENED CONCRETE – POLISHED SAMPLE

Project Name:	NCDOT 2011-06		
Client:	NCDOT	**Project No.:**	520180
Observations by:	Tara Cavalline	**Date:**	Spring / Summer 2012

Type of Structure: Concrete bridge deck 590363 (7L)
Location: Mecklenburg, North Carolina
Purpose: Observe general characteristics

Sample ID: 7L C-7A

Sample Description

Dimensions:	4-1/16 inches wide, 3-1/16 inches long
Top surface finish:	Grooves evident
Bottom surface finish:	Sawcut from full core sample
Reinforcement:	None in polished section
Cracks, Joints, Voids:	A few very small voids where not fully consolidated.

Aggregates

Coarse aggregate:

Type:	Manufactured lightweight aggregate, typically dark gray to medium gray
Gradation and top size:	Well-graded, ¾ inch max nominal size
Shape and distribution:	Subangular to subrounded relatively evenly distributed

Fine aggregate:

Type:	Multi-colored natural silica, mainly white, clear, and light gray. Some tan and brown.
Gradation and top size:	Well-graded, 3/8 inch max nominal size.
Shape and distribution:	Subangular to subrounded

Paste

Color:	Medium Gray
Luster:	Subvitreous
Hardness:	Moderately hard to hard
Supplementary cementitious matls:	Possibly contains fly ash, but not confirmed. Dark particles evident, which may be fly ash, but cenospheres not observed after acid etch. Mixture submittals not available.
Depth of carbonation:	Approx. 3/8 inch

Other observations

Paste-aggregate bond:	Good
Secondary deposits:	Secondary deposits lining and filling many entrained air voids and some voids in coarse aggregates. Tends to be present in localized areas, mostly near surface and near microcracks.
Air content:	Air-entrained, approx. 5-7%
Microcracking:	One microcrack extending from top surface to a depth of 1 ½ inches
Estimated water-cement ratio:	0.35-0.40 (with water-reducing admixture, assumed)

Notes

1. More secondary deposits observed in 7L C-5A and 7L C-7A than observed in 7N C-6 and 7N C-8.
2. Extent of microcracking in 7N C-6 and 7N C-8 appears to be similar to the extent of microcracking in 7L C-5A and 7L C-7A.

Figure I-59: Datasheet for petrographic examination of sample 7L C-7A.

MACROSCOPIC AND MICROSCOPIC OBSERVATION OF HARDENED CONCRETE – POLISHED SAMPLE

Project Name:	NCDOT 2011-06		
Client:	NCDOT	**Project No.:**	520180
Observations by:	Tara Cavalline	**Date:**	Spring / Summer 2012

Type of Structure: Concrete bridge deck 580160 (8N)
Location: McDowell County, North Carolina
Purpose: Observe general characteristics

Sample ID: 8N C-2

Sample Description

Dimensions: 4-1/16 inches wide, 3 inches long
Top surface finish: Grooves evident
Bottom surface finish: Sawcut from full core sample
Reinforcement: None in polished section
Cracks, Joints, Voids: A few small voids where not consolidated.

Aggregates

Coarse aggregate:

- Type: Mainly quartz, typically gray, white, and light gray. Some mafic gneiss, typically tan and brown with foliation.
- Gradation and top size: Well-graded ¾ inch max nominal size.
- Shape and distribution: Subangular relatively evenly distributed.

Fine aggregate:

- Type: Multi-colored natural silica, mainly white, clear, and light gray. Some tan and light brown.
- Gradation and top size: Well-graded, 3/8 inch max nominal size
- Shape and distribution: Subrounded to subangular

Paste

Color: Medium Gray
Luster: Subvitreous
Hardness: Moderately hard to hard. Areas of deteriorated paste along some near-surface microcracks.
Supplementary cementitious matls: Possibly contains fly ash, but not confirmed. Dark particles evident, which may be fly ash, but cenospheres not observed after acid etch. Mixture submittals not available.
Depth of carbonation: Approx. 1/8 inch

Other observations

Paste-aggregate bond: Good
Secondary deposits: Trace amounts observed in a few small voids.
Air content: Air-entrained, approx. 6-8%
Microcracking: A few microcracks extending from the top surface typically within top ½ inch. One microcrack extends down approximately 1 inch through coarse aggregate particle.
Estimated water-cement ratio: 0.35-0.40 (with water-reducing admixture, assumed)

Notes

1. Minimal secondary deposits observed in 8N C-2, 8N C-7, 8L C-4 and 8L C-8.
2. Extent of microcracking observed in 8N C-2, 8N C-7, 8L C-4 and 8L C-8 appears to be similar.
3. Construction date of this bridge is 2000. Based on NCDOT information, bridge decks constructed after June 2000 in this division should contain fly ash. Observations indicate that fly ash may be present in this concrete, but the presence of fly ash was not confirmed.

Figure I-60: Datasheet for petrographic examination of sample 8N C-2.

MACROSCOPIC AND MICROSCOPIC OBSERVATION OF HARDENED CONCRETE – POLISHED SAMPLE

Project Name:	NCDOT 2011-06		
Client:	NCDOT	**Project No.:**	520180
Observations by:	Tara Cavalline	**Date:**	Spring / Summer 2012

Type of Structure: Concrete bridge deck 580160 (8N)
Location: McDowell County, North Carolina
Purpose: Observe general characteristics

Sample ID: 8N C-7

Sample Description

Dimensions:	4-1/16 inches wide, 3 inches long
Top surface finish:	Grooves evident
Bottom surface finish:	Sawcut from full core sample
Reinforcement:	None in polished section
Cracks, Joints, Voids:	A few small voids where not consolidated.

Aggregates

Coarse aggregate:

Type:	Mainly quartz, typically gray, white, and light gray. Some mafic gneiss, typically tan and brown with foliation.
Gradation and top size:	Well-graded ¾ inch max nominal size.
Shape and distribution:	Missing some coarse aggregate in top 1½ inch.

Fine aggregate:

Type:	Multi-colored natural silica, mainly white, clear, and light gray. Some tan and light brown.
Gradation and top size:	Well-graded, 3/8 inch max nominal size
Shape and distribution:	Subrounded to subangular

Paste

Color:	Medium gray
Luster:	Subvitreous
Hardness:	Moderately hard to hard. Areas of deteriorated paste along some near-surface microcracks.
Supplementary cementitious matls:	Possibly contains fly ash, but not confirmed. Dark particles evident, which may be fly ash, but cenospheres not observed after acid etch. Mixture submittals not available.
Depth of carbonation:	Approx. ¼ inch

Other observations

Paste-aggregate bond:	Good
Secondary deposits:	Trace amounts observed in a few small voids.
Air content:	Air-entrained, approx. 4-6%
Microcracking:	A few microcracks extending from the top surface typically within top ½ inch.
Estimated water-cement ratio:	0.35-0.40 (with water-reducing admixture, assumed)

Notes

1. Minimal secondary deposits observed in 8N C-2, 8N C-7, 8L C-4 and 8L C-8.
2. Extent of microcracking observed in 8N C-2, 8N C-7, 8L C-4 and 8L C-8 appears to be similar.
3. Construction date of this bridge is 2000. Based on NCDOT information, bridge decks constructed after June 2000 in this division should contain fly ash. Observations indicate that fly ash may be present in this concrete, but the presence of fly ash was not confirmed.

Figure I-61: Datasheet for petrographic examination of sample 8N C-7.

MACROSCOPIC AND MICROSCOPIC OBSERVATION OF HARDENED CONCRETE – POLISHED SAMPLE

Project Name:	NCDOT 2011-06		
Client:	NCDOT	**Project No.:**	520180
Observations by:	Tara Cavalline	**Date:**	Spring / Summer 2012

Type of Structure: Concrete bridge deck 430120 (8L)
Location: Haywood County, North Carolina
Purpose: Observe general characteristics

Sample ID: 8L C-4

Sample Description

Dimensions:	4-1/16 inches wide, 2-7/8 inches long
Top surface finish:	Grooves evident
Bottom surface finish:	Sawcut from full core sample
Reinforcement:	None in polished section
Cracks, Joints, Voids:	A few voids where not consolidated

Aggregates

Coarse aggregate:

Type:	Manufactured lightweight aggregate, typically dark gray to medium gray
Gradation and top size:	Well-graded, ¾ inch max nominal size
Shape and distribution:	Subrounded to subangular

Fine aggregate:

Type:	Multi-colored natural silica, mainly white, clear, light gray and tan and light brown.
Gradation and top size:	Well-graded, 3/8 inch max nominal size
Shape and distribution:	Subangular to subrounded

Paste

Color:	Light gray
Luster:	Subvitreous
Hardness:	Moderately hard to hard
Supplementary cementitious matls:	May or may not contain fly ash. Fewer dark particles observed in paste, and cenospheres not observed after acid etch.
Depth of carbonation:	Approx. 1/8 inch

Other observations

Paste-aggregate bond:	Good
Secondary deposits:	Trace amounts observed in a few small voids.
Air content:	Air-entrained, approx. 4-6%
Microcracking:	Several microcracks extending from top surface, typically within top ½ inch. One microcrack extends down approximately 1 inch from top surface.
Estimated water-cement ratio:	0.35-0.40 (with water-reducing admixture, assumed)

Notes

1. Minimal secondary deposits observed in 8N C-2, 8N C-7, 8L C-4 and 8L C-8.
2. Extent of microcracking observed in 8N C-2, 8N C-7, 8L C-4 and 8L C-8 appears to be similar.
3. May or may not contain fly ash. Fewer dark particles observed in paste, and cenospheres not observed after acid etch.

Figure I-62: Datasheet for petrographic examination of sample 8L C-4.

MACROSCOPIC AND MICROSCOPIC OBSERVATION OF HARDENED CONCRETE – POLISHED SAMPLE

Project Name:	NCDOT 2011-06		
Client:	NCDOT	**Project No.:**	520180
Observations by:	Tara Cavalline	**Date:**	Spring / Summer 2012

Type of Structure: Concrete bridge deck 430120 (8L)
Location: Haywood County, North Carolina
Purpose: Observe general characteristics

Sample ID: 8L C-8

Sample Description

Dimensions:	4-1/16 inches wide, 2-15/16 inches long
Top surface finish:	Grooves evident
Bottom surface finish:	Sawcut from full core sample
Reinforcement:	None in polished section
Cracks, Joints, Voids:	Macrocrack extending to approximately 1 ½ inches.

Aggregates

Coarse aggregate:

Type:	Manufactured lightweight aggregate, typically dark gray to medium gray
Gradation and top size:	Well-graded, ¾ inch max nominal size,
Shape and distribution:	Subrounded to subangular, tends to be sparse in some areas of sample.

Fine aggregate:

Type:	Multi-colored natural silica, mainly white, clear, light gray and tan and light brown.
Gradation and top size:	Well-graded, 3/8 inch max nominal size
Shape and distribution:	Subangular to subrounded

Paste

Color:	Medium gray
Luster:	Subvitreous
Hardness:	Moderately hard to hard
Supplementary cementitious matls:	May or may not contain fly ash. Fewer dark particles observed in paste, and cenospheres not observed after acid etch.
Depth of carbonation:	Approx. 1/8 inch

Other observations

Paste-aggregate bond:	Good
Secondary deposits:	Trace amounts observed in a few small voids.
Air content:	Air-entrained, approx. 4-6%
Microcracking:	Several microcracks extending from top surface, typically within top ½ inch.
Estimated water-cement ratio:	0.35-0.40 (with water-reducing admixture, assumed)

Notes

1. Minimal secondary deposits observed in 8N C-2, 8N C-7, 8L C-4 and 8L C-8.
2. Extent of microcracking observed in 8N C-2, 8N C-7, 8L C-4 and 8L C-8 appears to be similar.
3. May or may not contain fly ash. Fewer dark particles observed in paste, and cenospheres not observed after acid etch.

Figure I-63: Datasheet for petrographic examination of sample 8L C-8.

MACROSCOPIC AND MICROSCOPIC OBSERVATION OF HARDENED CONCRETE – POLISHED SAMPLE

Project Name:	NCDOT 2011-06		
Client:	NCDOT	**Project No.:**	520180
Observations by:	Tara Cavalline	**Date:**	Spring / Summer 2012

Type of Structure: Concrete bridge deck 580153 (9N)
Location: McDowell County, North Carolina
Purpose: Observe general characteristics

Sample ID: 9N C-3

Sample Description

Dimensions:	4-1/16 inches wide, 2-7/8 inches long
Top surface finish:	Grooves evident
Bottom surface finish:	Sawcut from full core sample
Reinforcement:	None in polished section
Cracks, Joints, Voids:	A few small voids where not consolidated.

Aggregates

Coarse aggregate:

Type:	Mainly quartz, typically gray, white, and light gray. Some mafic gneiss, typically tan and brown with foliation.
Gradation and top size:	Fairly well-graded, ¾ inch max nominal size. Missing larger sizes in some areas.
Shape and distribution:	Larger particles tended to more subangular to subrounded and smaller particles tending to be flatter and more elongated.

Fine aggregate:

Type:	Multi-colored natural silica, mainly white, clear, and light gray. Some tan and light brown.
Gradation and top size:	Well-graded, 3/8 inch max nominal size
Shape and distribution:	Subrounded to subangular

Paste

Color:	Medium Gray
Luster:	Subvitreous
Hardness:	Moderately hard to hard. Areas of deteriorated paste along some near-surface microcracks.
Supplementary cementitious matls:	Possibly contains fly ash, but not confirmed. Dark particles evident, which may be fly ash, but cenospheres not observed after acid etch. Mixture submittals not available.
Depth of carbonation:	Approx. 1/8 inch

Other observations

Paste-aggregate bond:	Good
Secondary deposits:	Trace amounts observed in a few small voids.
Air content:	Air-entrained, approx. 6-8%
Microcracking:	Several microcracks within ¾ inch, some of the microcracks propagates through some of the coarse aggregates.
Estimated water-cement ratio:	0.35-0.40 (with water-reducing admixture, assumed)

Notes

1. More microcracking observed in 9N C-3and 9N C-5 than observed in 9L C-5 and 9L C-8.
2. More secondary deposit material observed in 9L C-5 and 9L C-8 than observed in 9NC-3 and 9N C-5.
3. Construction date of this bridge is 2000. Based on NCDOT information, bridge decks constructed after June 2000 in this division should contain fly ash. Observations indicate that fly ash may be present in this concrete, but the presence of fly ash was not confirmed.

Figure I-64: Datasheet for petrographic examination of sample 9N C-3.

MACROSCOPIC AND MICROSCOPIC OBSERVATION OF HARDENED CONCRETE – POLISHED SAMPLE

Project Name:	NCDOT 2011-06		
Client:	NCDOT	**Project No.:**	520180
Observations by:	Tara Cavalline	**Date:**	Spring / Summer 2012

Type of Structure: Concrete bridge deck 580153 (9N)
Location: McDowell County, North Carolina
Purpose: Observe general characteristics

Sample ID: 9N C-5

Sample Description

Dimensions:	4-1/16 inches wide, 3 inches long
Top surface finish:	Grooves evident
Bottom surface finish:	Sawcut from full core sample
Reinforcement:	None in polished section
Cracks, Joints, Voids:	A few small voids where not consolidated.

Aggregates

Coarse aggregate:

Type:	Mainly quartz, typically gray, white, and light gray. Some mafic gneiss, typically tan and brown with foliation.
Gradation and top size:	Well-graded, ¾ inch max nominal size.
Shape and distribution:	Subrounded to subangular

Fine aggregate:

Type:	Multi-colored natural silica, mainly white, clear, and light gray. Some tan and light brown.
Gradation and top size:	Well-graded, 3/8 inch max nominal size
Shape and distribution:	Subrounded to subangular

Paste

Color:	Medium Gray
Luster:	Subvitreous
Hardness:	Moderately hard to hard. Areas of deteriorated paste along some near-surface microcracks.
Supplementary cementitious matls:	Possibly contains fly ash, but not confirmed. Dark particles evident, which may be fly ash, but cenospheres not observed after acid etch. Mixture submittals not available.
Depth of carbonation:	Approx. 1/8 inch

Other observations

Paste-aggregate bond:	Good
Secondary deposits:	Trace amounts observed in a few small voids.
Air content:	Air-entrained, approx. 6-8%
Microcracking:	A few microcracks near top surface approx. 1/8 inch.
Estimated water-cement ratio:	0.35-0.40 (with water-reducing admixture, assumed)

Notes

1. More microcracking observed in 9N C-3 and 9N C-5 than observed in 9L C-5 and 9L C-8.
2. More secondary deposit material observed in 9L C-5 and 9L C-8 than observed in 9NC-3 and 9N C-5.
3. Construction date of this bridge is 2000. Based on NCDOT information, bridge decks constructed after June 2000 in this division should contain fly ash. Observations indicate that fly ash may be present in this concrete, but the presence of fly ash was not confirmed.

Figure I-65: Datasheet for petrographic examination of sample 9N C-5.

MACROSCOPIC AND MICROSCOPIC OBSERVATION OF HARDENED CONCRETE – POLISHED SAMPLE

Project Name:	NCDOT 2011-06		
Client:	NCDOT	**Project No.:**	520180
Observations by:	Tara Cavalline	**Date:**	Spring / Summer 2012

Type of Structure: Concrete bridge deck 580146 (9L)
Location: McDowell County, North Carolina
Purpose: Observe general characteristics

Sample ID: 9L C-5

Sample Description

Dimensions:	4-1/16 inches wide, 2-15/16 inches long
Top surface finish:	Grooves evident
Bottom surface finish:	Sawcut from full core sample
Reinforcement:	None in polished section
Cracks, Joints, Voids:	A number of small to medium size voids where not fully consolidated.

Aggregates

Coarse aggregate:

Type:	Manufactured lightweight aggregate, typically dark gray to medium gray
Gradation and top size:	Well-graded, ¾ inch max nominal size
Shape and distribution:	Subangular to subrounded

Fine aggregate:

Type:	Multi-colored natural silica, mainly white, clear, and light gray. Some tan and light brown.
Gradation and top size:	Well-graded, 3/8 inch max nominal size
Shape and distribution:	Subrounded to subangular

Paste

Color:	Medium gray
Luster:	Subvitreous
Hardness:	Moderately hard to hard.
Supplementary cementitious matls:	Possibly contains fly ash, but not confirmed. Dark particles evident, which may be fly ash, but cenospheres not observed after acid etch. Mixture submittals not available.
Depth of carbonation:	Approx. ¼ inch

Other observations

Paste-aggregate bond:	Good
Secondary deposits:	Some secondary deposits present in a few voids in paste and coarse aggregates.
Air content:	Air-entrained, approx. 5-7%
Microcracking:	None observed
Estimated water-cement ratio:	0.35-0.40 (with water-reducing admixture, assumed)

Notes

1. More microcracking observed in 9N C-3 and 9N C-5 than observed in 9L C-5 and 9L C-8.
2. More secondary deposit material observed in 9L C-5 and 9L C-8 than observed in 9NC-3 and 9N C-5.

Figure I-66: Datasheet for petrographic examination of sample 9L C-5.

MACROSCOPIC AND MICROSCOPIC OBSERVATION OF HARDENED CONCRETE – POLISHED SAMPLE

Project Name:	NCDOT 2011-06		
Client:	NCDOT	**Project No.:**	520180
Observations by:	Tara Cavalline	**Date:**	Spring / Summer 2012

Type of Structure: Concrete bridge deck 580146 (9L)
Location: McDowell County, North Carolina
Purpose: Observe general characteristics

Sample ID: 9L C-8

Sample Description

Dimensions:	4 1/16 inches wide, 3 inches long
Top surface finish:	Grooves evident
Bottom surface finish:	Sawcut from full core sample
Reinforcement:	None in polished section
Cracks, Joints, Voids:	Macrocrack of approximately 0.005 inch width at one inch present through full thickness of sample, a few small voids where not fully consolidated.

Aggregates

Coarse aggregate:

Type:	Manufactured lightweight aggregate, typically dark gray to medium gray
Gradation and top size:	Well-graded, ¾ inch max nominal size
Shape and distribution:	Subangular to subrounded

Fine aggregate:

Type:	Multi-colored natural silica, mainly white, clear, and light gray. Some tan and light brown.
Gradation and top size:	Well-graded, 3/8 inch max nominal size
Shape and distribution:	Subrounded to subangular

Paste

Color:	Medium gray
Luster:	Subvitreous
Hardness:	Moderately hard to hard. Some deteriorated paste near top of macrocrack.
Supplementary cementitious matls:	Possibly contains fly ash, but not confirmed. Dark particles evident, which may be fly ash, but cenospheres not observed after acid etch. Mixture submittals not available.
Depth of carbonation:	Undetermined due to macrocrack through full thickness of sample. Sample encapsulated in hardened resin.

Other observations

Paste-aggregate bond:	Good
Secondary deposits:	Secondary deposits lining or partially filling a number of air-entrained voids in localized areas.
Air content:	Air-entrained, approx. 5-7%
Microcracking:	None observed
Estimated water-cement ratio:	0.35-0.40 (with water-reducing admixture, assumed)

Notes

1. More microcracking observed in 9N C-3 and 9N C-5 than observed in 9L C-5 and 9L C-8.
2. More secondary deposit material observed in 9L C-5 and 9L C-8 than observed in 9NC-3 and 9N C-5.

Figure I-67: Datasheet for petrographic examination of sample 9L C-8.